

ISSN: 2067-3809



ACTA TECHNICA CORVINIENSIS

– Bulletin of
Engineering

Tome XIV [2021]

Fascicule 4

[October – December]



EDITURA POLITEHNICA



Edited by:

UNIVERSITY POLITEHNICA TIMISOARA



with kindly supported by:

THE GENERAL ASSOCIATION OF ROMANIAN ENGINEERS (AGIR)
– branch of HUNEDOARA



Editor / Technical preparation / Cover design:

Assoc. Prof. Eng. KISS Imre, PhD.
UNIVERSITY POLITEHNICA TIMISOARA,
FACULTY OF ENGINEERING HUNEDOARA

Commenced publication year:

2008



ASSOCIATE EDITORS and REGIONAL COLLABORATORS

MANAGER & CHAIRMAN

ROMANIA Imre KISS, University Politehnica TIMISOARA, Faculty of Engineering HUNEDOARA



EDITORS from:

ROMANIA Dragoş UTU, University Politehnica TIMIŞOARA – TIMIŞOARA



Vasile ALEXĂ, University Politehnica TIMIŞOARA – HUNEDOARA

Sorin Aurel RAȚIU, University Politehnica TIMIŞOARA – HUNEDOARA

Vasile George CIOATĂ, University Politehnica TIMIŞOARA – HUNEDOARA

Emanoil LINUL, University Politehnica TIMIŞOARA – TIMIŞOARA

Virgil STOICA, University Politehnica TIMIŞOARA – TIMIŞOARA

Simona DZIȚAC, University of Oradea – ORADEA

Valentin VLĂDUȚ, Institute of Research-Development for Machines & Installations – BUCUREȘTI

Mihai G. MĂTACHE, Institute of Research-Development for Machines & Installations – BUCUREȘTI

Dan Ludovic LEMLE, University Politehnica TIMIŞOARA – HUNEDOARA

Gabriel Nicolae POPA, University Politehnica TIMIŞOARA – HUNEDOARA

Sorin Ștefan BIRIȘ, University Politehnica BUCUREȘTI – BUCUREȘTI

Stelian STAN, University Politehnica BUCUREȘTI – BUCUREȘTI

Dan GLĂVAN, University “Aurel Vlaicu” ARAD – ARAD

REGIONAL EDITORS from:

SLOVAKIA Juraj ŠPALEK, University of ŽILINA – ŽILINA



Peter KOŠTÁL, Slovak University of Technology in BRATISLAVA – TRNAVA

Tibor KRENICKÝ, Technical University of KOŠICE – PREŠOV

Peter KRÍŽAN, Slovak University of Technology in BRATISLAVA – BRATISLAVA

Vanessa PRAJOVA, Slovak University of Technology in BRATISLAVA – TRNAVA

Beata SIMEKOVA, Slovak University of Technology in BRATISLAVA – TRNAVA

Ingrid KOVAŘÍKOVÁ, Slovak University of Technology in BRATISLAVA – TRNAVA

Miriám MATÚŠOVÁ, Slovak University of Technology in BRATISLAVA – TRNAVA

Erika HRUŠKOVÁ, Slovak University of Technology in BRATISLAVA – TRNAVA

HUNGARY Tamás HARTVÁNYI, Széchenyi István University – GYŐR



József SÁROSI, University of SZEGED – SZEGED

György KOVÁCS, University of MISKOLC – MISKOLC

Zsolt Csaba JOHANYÁK, John von Neumann University – KECSKEMÉT

Gergely DEZSŐ, University of NYÍREGYHÁZA – NYÍREGYHÁZA

Árpád FERENCZ, Pallasz Athéné University – KECSKEMÉT

Loránt KOVÁCS, Pallasz Athéné University – KECSKEMÉT

Sándor BESZÉDES, University of SZEGED – SZEGED

Csaba Imre HENCZ, Széchenyi István University – GYŐR

Zoltán András NAGY, Széchenyi István University – GYŐR

László GOGOLÁK, University of SZEGED – SZEGED

Krisztián LAMÁR, Óbuda University BUDAPEST – BUDAPEST

Valeria NAGY, University of SZEGED – SZEGED

Ferenc SZIGETI, University of NYÍREGYHÁZA – NYÍREGYHÁZA

SERBIA Zoran ANIŠIĆ, University of NOVI SAD – NOVI SAD



Milan RACKOV, University of NOVI SAD – NOVI SAD

Igor FÜRSTNER, SUBOTICA Tech – SUBOTICA

Eleonora DESNICA, University of NOVI SAD – ZRENJANIN

Ljiljana RADOVANOVIĆ, University of NOVI SAD – ZRENJANIN

Blaža STOJANOVIĆ, University of KRAGUJEVAC – KRAGUJEVAC

Slobodan STEFANOVIĆ, Graduate School of Applied Professional Studies – VRANJE

Sinisa BIKIĆ, University of NOVI SAD – NOVI SAD

Živko PAVLOVIĆ, University of NOVI SAD – NOVI SAD

CROATIA Gordana BARIC, University of ZAGREB – ZAGREB



Goran DUKIC, University of ZAGREB – ZAGREB

BULGARIA  Krasimir Ivanov TUJAROV, “Angel Kanchev” University of ROUSSE – ROUSSE
Ivanka ZHELEVA, “Angel Kanchev” University of ROUSSE – ROUSSE
Atanas ATANASOV, “Angel Kanchev” University of ROUSSE – ROUSSE

BOSNIA & HERZEGOVINA  Tihomir LATINOVIC, University in BANJA LUKA – BANJA LUKA
Sabahudin JASAREVIC, University of ZENICA – ZENICA
Stevo BOROJEVIĆ, University in BANJA LUKA – BANJA LUKA

POLAND  Jarosław ZUBRZYCKI, LUBLIN University of Technology – LUBLIN
Maciej BIELECKI, Technical University of LODZ – LODZ

TURKEY  Önder KABAŞ, Akdeniz University – KONYAAALTI/Antalya

GREECE  Apostolos TSAGARIS, Alexander Technological Educational Institute of THESSALONIKI – THESSALONIKI
Panagiotis KYRATSIS, Western Macedonia University of Applied Sciences – KOZANI

SPAIN  César GARCÍA HERNÁNDEZ, University of ZARAGOZA – ZARAGOZA



The Editor and editorial board members do not receive any remuneration. These positions are voluntary. The members of the Editorial Board may serve as scientific reviewers.

We are very pleased to inform that our journal **ACTA TECHNICA CORVINIENSIS – Bulletin of Engineering** is going to complete its ten years of publication successfully. In a very short period it has acquired global presence and scholars from all over the world have taken it with great enthusiasm. We are extremely grateful and heartily acknowledge the kind of support and encouragement from you.

ACTA TECHNICA CORVINIENSIS – Bulletin of Engineering seeking qualified researchers as members of the editorial team. Like our other journals, **ACTA TECHNICA CORVINIENSIS – Bulletin of Engineering** will serve as a great resource for researchers and students across the globe. We ask you to support this initiative by joining our editorial team. If you are interested in serving as a member of the editorial team, kindly send us your resume to redactie@fih.upt.ro.



ISSN: 2067-3809

copyright © University POLITEHNICA Timisoara,
Faculty of Engineering Hunedoara,
5, Revolutiei, 331128, Hunedoara, ROMANIA
<http://acta.fih.upt.ro>

INTERNATIONAL SCIENTIFIC COMMITTEE MEMBERS and SCIENTIFIC REVIEWERS

MANAGER & CHAIRMAN

ROMANIA Imre KISS, University Politehnica TIMISOARA, Faculty of Engineering HUNEDOARA



INTERNATIONAL SCIENTIFIC COMMITTEE MEMBERS & SCIENTIFIC REVIEWERS from:

ROMANIA Viorel–Aurel ȘERBAN, University Politehnica TIMIȘOARA – TIMIȘOARA



Teodor HEPUȚ, University Politehnica TIMIȘOARA – HUNEDOARA

Ilare BORDEAȘU, University Politehnica TIMIȘOARA – TIMIȘOARA

Liviu MARȘAVIA, University Politehnica TIMIȘOARA – TIMIȘOARA

Ioan VIDA-SIMITI, Technical University of CLUJ-NAPOCA – CLUJ-NAPOCA

Csaba GYENGE, Technical University of CLUJ-NAPOCA – CLUJ-NAPOCA

Sorin VLASE, “Transilvania” University of BRASOV – BRASOV

Horatiu TEODORESCU DRĂGHICESCU, “Transilvania” University of BRASOV – BRASOV

Maria Luminița SCUTARU, “Transilvania” University of BRASOV – BRASOV

Carmen ALIC, University Politehnica TIMIȘOARA – HUNEDOARA

Liviu MIHON, University Politehnica TIMIȘOARA – TIMIȘOARA

SLOVAKIA Ervin LUMNITZER, Technical University of KOŠICE – KOŠICE



Miroslav BADIDA, Technical University of KOŠICE – KOŠICE

Juraj ŠPALEK, University of ŽILINA – ŽILINA

Karol VELIŠEK, Slovak University of Technology BRATISLAVA – TRNAVA

Imrich KISS, Institute of Economic & Environmental Security – KOŠICE

Vladimir MODRAK, Technical University of KOSICE – PRESOV

CROATIA Drazan KOZAK, Josip Juraj Strossmayer University of OSIJEK – SLAVONKI BROD



Predrag COSIC, University of ZAGREB – ZAGREB

Milan KLJAJIN, Josip Juraj Strossmayer University of OSIJEK – SLAVONKI BROD

Antun STOIĆ, Josip Juraj Strossmayer University of OSIJEK – SLAVONKI BROD

Ivo ALFIREVIĆ, University of ZAGREB – ZAGREB

HUNGARY Imre DEKÁNY, University of SZEGED – SZEGED



Cecilia HODŰR, University of SZEGED – SZEGED

Béla ILLÉS, University of MISKOLC – MISKOLC

Imre RUDAS, Óbuda University of BUDAPEST – BUDAPEST

István BIRÓ, University of SZEGED – SZEGED

Tamás KISS, University of SZEGED – SZEGED

Imre TIMÁR, University of Pannonia – VESZPRÉM

Károly JÁRMAI, University of MISKOLC – MISKOLC

Ádám DÖBRÖCZÖNI, University of MISKOLC – MISKOLC

György SZEIDL, University of MISKOLC – MISKOLC

Miklós TISZA, University of MISKOLC – MISKOLC

József GÁL, University of SZEGED – SZEGED

Ferenc FARKAS, University of SZEGED – SZEGED

Géza HUSI, University of DEBRECEN – DEBRECEN

BULGARIA Kliment Blagoev HADJOV, University of Chemical Technology and Metallurgy – SOFIA



Nikolay MIHAILOV, “Anghel Kanchev” University of ROUSSE – ROUSSE

Stefan STEFANOV, University of Food Technologies – PLOVDIV

SERBIA Sinisa KUZMANOVIC, University of NOVI SAD – NOVI SAD



Zoran ANIŠIĆ, University of NOVI SAD – NOVI SAD

Mirjana VOJINOVIĆ MILORADOV, University of NOVI SAD – NOVI SAD

Miroslav PLANČAK, University of NOVI SAD – NOVI SAD

ITALY Alessandro GASPARETTO, University of UDINE – UDINE



Alessandro RUGGIERO, University of SALERNO – SALERNO

Adolfo SENATORE, University of SALERNO – SALERNO

Enrico LORENZINI, University of BOLOGNA – BOLOGNA

- BOSNIA & HERZEGOVINA**  Tihomir LATINOVIC, University of BANJA LUKA – BANJA LUKA
Safet BRDAREVIĆ, University of ZENICA – ZENICA
Zorana TANASIC, University of BANJA LUKA – BANJA LUKA
Zlatko BUNDALO, University of BANJA LUKA – BANJA LUKA
Milan TICA, University of BANJA LUKA – BANJA LUKA
Strain POSAVLJAK, University of BANJA LUKA – BANJA LUKA
- MACEDONIA**  Valentina GECEVSKA, University “St. Cyril and Methodius” SKOPJE – SKOPJE
Zoran PANDILOV, University “St. Cyril and Methodius” SKOPJE – SKOPJE
- GREECE**  Nicolaos VAXEVANIDIS, University of THESSALY – VOLOS
- PORTUGAL**  João Paulo DAVIM, University of AVEIRO – AVEIRO
Paulo BARTOLO, Polytechnique Institute – LEIRIA
José MENDES MACHADO, University of MINHO – GUIMARÃES
- SLOVENIA**  Janez GRUM, University of LJUBLJANA – LJUBLJANA
Štefan BOJNEC, University of Primorska – KOPER
- POLAND**  Leszek DOBRZANSKI, Silesian University of Technology – GLIWICE
Stanisław LEGUTKO, Polytechnic University – POZNAN
Andrzej WYCISLIK, Silesian University of Technology – KATOWICE
Antoni ŚWIĆ, University of Technology – LUBLIN
Aleksander SŁADKOWSKI, Silesian University of Technology – KATOWICE
- AUSTRIA**  Branko KATALINIC, VIENNA University of Technology – VIENNA
- SPAIN**  Patricio FRANCO, Universidad Politecnica of CARTAGENA – CARTAGENA
Luis Norberto LOPEZ De LACALLE, University of Basque Country – BILBAO
Aitzol Lamikiz MENTXAKA, University of Basque Country – BILBAO
- CUBA**  Norge I. COELLO MACHADO, Universidad Central “Marta Abreu” LAS VILLAS – SANTA CLARA
José Roberto Marty DELGADO, Universidad Central “Marta Abreu” LAS VILLAS – SANTA CLARA
- USA**  David HUI, University of NEW ORLEANS – NEW ORLEANS
- INDIA**  Sugata SANYAL, Tata Consultancy Services – MUMBAI
Siby ABRAHAM, University of MUMBAI – MUMBAI
- TURKEY**  Ali Naci CELIK, Abant Izzet Baysal University – BOLU
Önder KABAŞ, Akdeniz University –KONYAAALTI/Antalya
- ISRAEL**  Abraham TAL, University TEL-AVIV, Space & Remote Sensing Division – TEL-AVIV
Amnon EINAIV, University TEL-AVIV, Space & Remote Sensing Division – TEL-AVIV
- NORWAY**  Trygve THOMESSEN, Norwegian University of Science and Technology – TRONDHEIM
Gábor SZIEBIG, Narvik University College – NARVIK
Terje Kristofer LIEN, Norwegian University of Science and Technology – TRONDHEIM
Bjoern SOLVANG, Narvik University College – NARVIK
- LITHUANIA**  Egidijus ŠARAUSKIS, Aleksandras Stulginskis University – KAUNAS
Zita KRIAUCIŪNIENĖ, Experimental Station of Aleksandras Stulginskis University – KAUNAS
- FINLAND**  Antti Samuli KORHONEN, University of Technology – HELSINKI
Pentti KARJALAINEN, University of OULU – OULU
- UKRAINE**  Sergiy G. DZHURA, Donetsk National Technical University – DONETSK
Heorhiy SULYM, Ivan Franko National University of LVIV – LVIV
Yevhen CHAPLYA, Ukrainian National Academy of Sciences – LVIV
Vitalii IVANOV, Sumy State University – SUMY



The Scientific Committee members and Reviewers do not receive any remuneration. These positions are voluntary.

We are extremely grateful and heartily acknowledge the kind of support and encouragement from all contributors and all collaborators!

ACTA TECHNICA CORVINIENSIS – Bulletin of Engineering is dedicated to publishing material of the highest engineering interest, and to this end we have assembled a distinguished Editorial Board and Scientific Committee of academics, professors and researchers.

ACTA TECHNICA CORVINIENSIS – Bulletin of Engineering publishes invited review papers covering the full spectrum of engineering. The reviews, both experimental and theoretical, provide general background information as well as a critical assessment on topics in a state of flux. We are primarily interested in those contributions which bring new insights, and papers will be selected on the basis of the importance of the new knowledge they provide.

ACTA TECHNICA CORVINIENSIS – Bulletin of Engineering encourages the submission of comments on papers published particularly in our journal. The journal publishes articles focused on topics of current interest within the scope of the journal and coordinated by invited guest editors. Interested authors are invited to contact one of the Editors for further details.

ACTA TECHNICA CORVINIENSIS – Bulletin of Engineering accept for publication unpublished manuscripts on the understanding that the same manuscript is not under simultaneous consideration of other journals. Publication of a part of the data as the abstract of conference proceedings is exempted.

Manuscripts submitted (original articles, technical notes, brief communications and case studies) will be subject to peer review by the members of the Editorial Board or by qualified outside reviewers. Only papers of high scientific quality will be accepted for publication. Manuscripts are accepted for review only when they report unpublished work that is not being considered for publication elsewhere.

The evaluated paper may be recommended for:

- **Acceptance without any changes** – in that case the authors will be asked to send the paper electronically in the required .doc format according to authors' instructions;
- **Acceptance with minor changes** – if the authors follow the conditions imposed by referees the paper will be sent in the required .doc format;

— **Acceptance with major changes** – if the authors follow completely the conditions imposed by referees the paper will be sent in the required .doc format;

— **Rejection** – in that case the reasons for rejection will be transmitted to authors along with some suggestions for future improvements (if that will be considered necessary).

The manuscript accepted for publication will be published in the next issue of **ACTA TECHNICA CORVINIENSIS – Bulletin of Engineering** after the acceptance date.

All rights are reserved by **ACTA TECHNICA CORVINIENSIS – Bulletin of Engineering**. The publication, reproduction or dissemination of the published paper is permitted only by written consent of one of the Managing Editors.

All the authors and the corresponding author in particular take the responsibility to ensure that the text of the article does not contain portions copied from any other published material which amounts to plagiarism. We also request the authors to familiarize themselves with the good publication ethics principles before finalizing their manuscripts.



ISSN: 2067-3809

copyright © University POLITEHNICA Timisoara,
Faculty of Engineering Hunedoara,
5, Revolutiei, 331128, Hunedoara, ROMANIA
<http://acta.fih.upt.ro>

Fascicule 4

[October – December]

t o m e

[2021] **XIV**

ACTA Technica CORVINIENSIS
BULLETIN OF ENGINEERING



ISSN: 2067-3809

copyright © University POLITEHNICA Timisoara,
Faculty of Engineering Hunedoara,
5, Revolutiei, 331128, Hunedoara, ROMANIA
<http://acta.fih.upt.ro>

TABLE of CONTENTS

| | | |
|-----|---|----|
| 1. | Goran JANJIĆ, M. RADAKOVIĆ, Zorana TANASIĆ, Borut KOSEC, Danijela KARDAŠ ANČIĆ – BOSNIA & HERZEGOVINA / SLOVENIA STRATEGIC ANALYSIS OF THE POSSIBILITY OF STARTING THE PRODUCTION OF FAST-GROWING PAULOWNIA TREE | 11 |
| 2. | Mustefa JIBRIL, Messay TADESE, Nuriye HASSEN – ETHIOPIA POSITION CONTROL OF A THREE DEGREE OF FREEDOM GYROSCOPE USING OPTIMAL CONTROL | 17 |
| 3. | Jameel Al-NAFFAKH, Mohammed R. Al-QASSAB – IRAQ DATASET THE ANNUAL GROWTH GENERATED OF RENEWABLE ENERGY BETWEEN TURKEY, IRAN AND IRAQ | 21 |
| 4. | Adebola ADEKUNLE, Iheoma ADEKUNLE, Ayokunle O. FAMILUSI, Mohammed ADAMU – NIGERIA ANALYSIS OF FLOW IN WATER DISTRIBUTION NETWORK USING NUMERICAL AND EXPERIMENTAL MODELLING | 25 |
| 5. | Branislav SREDANOVIĆ, Đjordje ČIČA, Stevo BOROJEVIĆ, Saša TEŠIĆ, Davorin KRAMAR – BOSNIA & HERZEGOVINA / SLOVENIA ANALYSIS OF CUTTING FORCES IN HYBRID TURNING AIDED BY GAS COMBUSTION HEATING OF WORKPIECE | 29 |
| 6. | Nghien Nguyen BA – VIETNAM FUSION OF SOFT COMPUTING AND CHAOS THEORY TO BUILD A MODEL FOR PREDICTION QUALITY OF WASTEWATER IN INDUSTRIAL ZONES | 35 |
| 7. | Ayanniyi M. AYANSHOLA, A.A. ALAO, Adebayo Wahab SALAMI, Solomon O. BILEWU, A.A. MOHAMMED, Oluwafemi O. ADELEKE, Oluwatosin O. OLOFINTOYE – NIGERIA MODELLING OF TURBIDITY VARIATION IN A WATER TREATMENT PLANT | 41 |
| 8. | Abass I. TAIWO, Timothy O. OLATAYO – NIGERIA OPTIMAL AND EFFICIENT MODEL SELECTION CRITERIA FOR PARAMETRIC SPECTRAL ESTIMATION | 45 |
| 9. | Zorana TANASIĆ, A. JOKIĆ, Goran JANJIĆ, Miljko BOBREK, Borut KOSEC – BOSNIA & HERZEGOVINA / SLOVENIA BUSINESS PROCESS IMPROVEMENT IN THE AUTOMOTIVE INDUSTRY - QUALITY METHODS AND TOOLS | 49 |
| 10. | Olutola Olaide FAGBOLU, Chukwunonso Stanley EDU, Adekunle Joseph ADEWALE – SIERRA LEONE / UGANDA / NIGERIA MULTILINGUAL SOCIAL MEDIA PLATFORM-BASED TOURISM OPERATIONS IN UGANDA | 55 |
| 11. | Anna YEHOROVA, Ervin LUMNITZER – SLOVAKIA ANALYSIS OF METHODOLOGIES IN THE FIELD OF OBJECTIVE EVALUATION OF ACOUSTIC DRONE DESCRIPTORS | 61 |
| 12. | Kenechi NWOSU-OBIEOGU, Goziya DZARMA, Linus CHIEMENEM – NIGERIA ANFIS PREDICTION OF ANTIOXIDANTS YIELD FOR LUFFA OIL | 65 |
| 13. | Mulualem Bekele NORA, Jiratu Wundessa GERBI, Basavaraj PARUTI – ETHIOPIA ANALYSIS OF CONSTRUCTION WASTE IN PUBLIC BUILDINGS USING REGRESSION METHOD: A CASE STUDY OF AMBO TOWN | 69 |
| 14. | Tajudeen Kolawole AJIBOYE, Sulyman Age ABDULKAREEM, Olusegun Samuel BALOGUN – NIGERIA ANALYSIS OF SLIDING PARAMETERS ON WEAR BEHAVIOUR OF BRAKE LINING MATERIALS | 77 |
| 15. | Sakina TOUZARA, Abdelilah CHTAINI, Amina AMLIL, Olivier F.A.B. KOFFI – MOROCCO ELECTROANALYSIS OF COPPER IONS BY SENSOR BASED ON CARBON PASTE AND EDTA | 83 |
| 16. | Precious EHIOMOGUE, Israel I. AHUCHAOGU, Isiguzo Edwin AHANEKU – NIGERIA REVIEW OF ADSORPTION ISOTHERMS MODELS | 87 |

| | | |
|-----|--|-----|
| 17. | Zoran PANDILOV – NORTH MACEDONIA COMPUTER SOFTWARE FOR INTERACTIVE DESIGN OF CNC MACHINE TOOLS MAIN SPINDLE DRIVES | 97 |
| 18. | Abhishek Kumar MEENA, Abhishek VAISHNAV, Akshat GOVIL, Ekta SHARMA, Mohd. IMRAN – INDIA VEHICLE NUMBER PLATE RECOGNITION SYSTEM USING MATLAB: A HISTOGRAM BASED APPROACH | 101 |
| 19. | Suleiman I. SALAWU, A.M. SALIU – NIGERIA CHARACTERIZATION AND BENEFICIATION OF OBAJANA IRON ORE, KOGI STATE, NIGERIA | 105 |
| 20. | Mustefa JIBRIL, Messay TADESE, Reta DEGEFA – ETHIOPIA DESIGN & CONTROL OF A GANTRY CRANE SYSTEM WITH LIMITED PAYLOAD ANGLE USING ROBUST & STATE FEEDBACK CONTROLLERS | 109 |
| *** | MANUSCRIPT PREPARATION – General guidelines | 115 |

The **ACTA TECHNICA CORVINIENSIS – Bulletin of Engineering, Tome XIV [2021], Fascicule 4 [October – December]** includes original papers submitted to the Editorial Board, directly by authors or by the regional collaborators of the Journal.

Also, the **ACTA TECHNICA CORVINIENSIS – Bulletin of Engineering, Tome XIV [2021], Fascicule 4 [October – December]**, includes scientific papers presented in the sections of:

— **DEMI 2021 – The 15th INTERNATIONAL CONFERENCE ON ACCOMPLISHMENTS IN MECHANICAL AND INDUSTRIAL ENGINEERING**, organized by Faculty of Mechanical Engineering, University of Banja Luka, BOSNIA & HERZEGOVINA, co-organized by Faculty of Mechanical Engineering, University of Niš, SERBIA, Faculty of Mechanical Engineering Podgorica, University of Montenegro, MONTENEGRO and Faculty of Engineering Hunedoara, University Politehnica Timisoara, ROMANIA, in Banja Luka, BOSNIA & HERZEGOVINA, in 28–29 May 2021. The current identification numbers of the selected papers are the #1, #5 and #9, according to the present contents list.



ISSN: 2067–3809

copyright © University POLITEHNICA Timisoara,
Faculty of Engineering Hunedoara,
5, Revolutiei, 331128, Hunedoara, ROMANIA
<http://acta.fih.upt.ro>

¹Goran JANJIĆ, ²M. RADAKOVIĆ, ¹Zorana TANASIĆ,
³Borut KOSEC, ¹Danijela KARDAŠ ANČIĆ

STRATEGIC ANALYSIS OF THE POSSIBILITY OF STARTING THE PRODUCTION OF FAST-GROWING PAULOWNIA TREE

¹ University of Banja Luka, Faculty of Mechanical Engineering, Banja Luka, BOSNIA & HERZEGOVINA

² University of Banja Luka, Faculty of Architecture, Civil Engineering and Geodesy, Banja Luka, BOSNIA & HERZEGOVINA

³ University of Ljubljana, Faculty of Natural Sciences and Engineering, Ljubljana, SLOVENIA

Abstract: Increasing energy needs and demands to reduce environmental impact have expanded interest in exploring sustainable alternative energy sources. The purpose of the article is to analyse the cost-effectiveness of starting the production of fast-growing Paulownia tree, which is characterized by low concentration of ash, sulphur, and nitrogen, as well as high calorific value and absorption of CO₂ from the air. Also, Paulownia is suitable for carving and insulation and it is an excellent raw material for ethanol production. Through the given strategic analysis, it is necessary to observe all-important external and internal factors that affect the success of the production of a quality product and its placement on the market. The paper also provides an assessment of the risks of identified threats arising from the environment and weaknesses related to the observed product.

Keywords: strategic analysis, paulownia, profitability

INTRODUCTION

Wood production through the planting of fast-growing energy crops leads to the preservation of natural ecosystems that are partly disturbed by unsustainable deforestation. Among many fast-growing woody crops, Paulownia is considered a “magic tree” because of its fast-growing rate and a large amount of wood mass delivered in such a short time [1]. Each part of the Paulownia plant, as an energy source, can be exploited for the production of pellets [2].

Paulownia, because of its high percentage of cellulose, can be used for the production of ethanol [3]. In addition to renewable energy, Paulownia has found its purpose in building construction, furniture manufacturing, musical instruments and veneers production, and etc. because of its good insulating characteristics and natural fire resistance.

Additionally, the Paulownia plant has the following characteristic: lightness, firmness, dry quickly, pleasant unchangeable colour, ease to process, and resistance to diseases and insect attacks.

It dries naturally for about 35 to 45 days and does not require storage to dry. Paulownia wood can be installed alone or mixed with particles of other materials (e.g., in plywood production to improve their strength properties) [4].

Paulownia has a low concentration of sulphur, nitrogen, and ash during combustion (by burning one cubic meter of wood, which is about 280 kilograms, as low as half a kilogram of ash will occur) [5]. Paulownia uses highly efficient photosynthesis to fix carbon [6] where one adult tree absorbs an average of about 22 kilograms of CO₂ and emits 6 kilograms of O₂ in a year [7]. After cutting, plants regenerate quickly. The estimated lifespan of the roots is about 70 years, and they can support about 8 to 9 cuttings with a vegetative cycle of 8 years [1]. After the third year of growth tree almost does not require any care.

One of the crucial factors that benefit the Paulownia wood production is the *European Green Deal* from 2014 related to

climate change and the energy framework. This document sets ambitious goals for the European Union countries by 2030, whose legislation in this area country Bosnia and Herzegovina accepted through the *Stabilisation and Association Agreement* which came into force in 2015. To this date, the given objectives, to a certain extent, have been revised. These objectives are as follows [8]:

≡ At least 40 % reduction of greenhouse gases emission compared to the 1990 level (the European Commission proposed in September 2020 the goal of reducing greenhouse gases emissions by 2030 by raising it to at least 55 %),

≡ At least 32 % share of renewable energy sources,

≡ Improve energy efficiency by at least 32,5 %.

The cost-benefit analysis of the production of the fast-growing Paulownia trees in Bosnia and Herzegovina, used as raw material for different types of products, was analysed in this paper.

The external environment, in which complex changing factors operate, imposes on the company the obligation of a strategic way of thinking and timely decision making. It is necessary to establish the firm's and its business units' strategic positions and their environmental factors. Strategic management is a continuous process whose purpose is to optimally prepare the organization for responding to changes coming from the surroundings. Its task is to create a solid strategic position in those markets in which the organization has decided to operate.

PHASES OF STRATEGIC MANAGEMENT

There are no large differences in defining the phases of strategic management among well-known authors in this field. In his book *Strategic Management in Action*, Coulter talks about situational analysis, formulation, implementation, and evaluation of strategy as phases of strategic management whose result is a series of strategies that an organization applies in its business (Figure 1.) [9].

A well-known researcher in the strategic management field, called Ansoff, suggests that environmental variability and dynamism, strategic and firms open-mindedness to conditions of the environment represent the essence of strategic management. The relationship between listed components of strategic management determines the strategic position of the organization. According to Ansoff, strategic management includes strategic planning (strategic analysis and strategic choice) and strategic action (strategic implementation and control) [10].

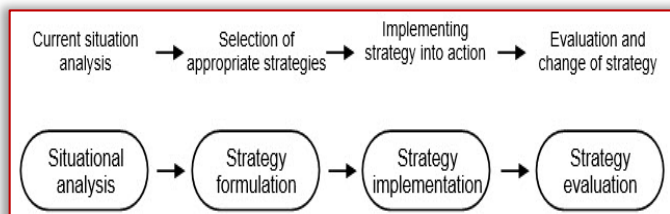


Figure 1. Phases of strategic management

Defining the company's strategy implies setting strategic goals and measures for their realization. It includes the development of long-term plans for managing opportunities and threats from the environment concerning the strengths and weaknesses of the company. There are several types of strategy, according to its design for appropriate hierarchical level: for an entire organization (basic strategy), for the business unit (which is independent within budgeting, target market, marketing mix), and the level of products and services (lowest level of strategy). Above mentioned strategies of the company should be implemented and shaped in compliance with the principle of hierarchical superiority. The product and service strategy, often called the product marketing strategy, should be in with the business unit strategy, and it should be in line with the company strategy.

The marketing strategy, above all, must take into account the needs of the market and the potential of the company to create competitive advantages and overcome the competition strategy. It requires a detailed strategic analysis of the external environment and internal factors of the company.

STRATEGIC ANALYSIS

The strategic analysis includes the following (Figure 2) [11]:

≡ the forecasting of various trends and events in the external environment in which the company should operate. Analysis of external factors involves customers, markets and competition analysis, and a wide range of other environmental factors, and,

≡ analysis of the internal factors that affect the company's agility and ability to respond to environmental changes.

— External environment analysis

≡ *Customer analysis*. Customer satisfaction with parallel profit-making is the fundamental imperative of every company. The aim of the customer analysis is to provide market segmentation on relatively homogeneous groups of customers, identify customer's profiles (number of customers, their needs, behavior patterns, loyalty levels), and to detect unsatisfied needs.

≡ *Market analysis*. This type of analysis aims to determine the market potential (maximum demand estimation) and the size of the market, or total sales.

≡ *Competition analysis*. The competition analysis should determine who are the leading competitors and which part of the target market they capture, the strengths and weaknesses of the competition, their goals, sales volume, product quality, technologies used, development intentions and opportunities, etc.

≡ *PEST(EL)*. This environment contains a wide range of social forces, which significantly affect the organization and consist of demographic, natural, technological, economic, legal-political, and socio-cultural factors.

— Internal environment analysis

Internal environment analysis aims to identify the strengths and weaknesses of the company. It includes financial analysis (like the total sale and profitability measured by ratios such as return on sales, return on assets, etc. to decide whether or not to launch a new product). Internal environment analysis considers staff, organizational structure, information system, crucial business portfolio process and the allocation of, potentially, successful and unsuccessful products.

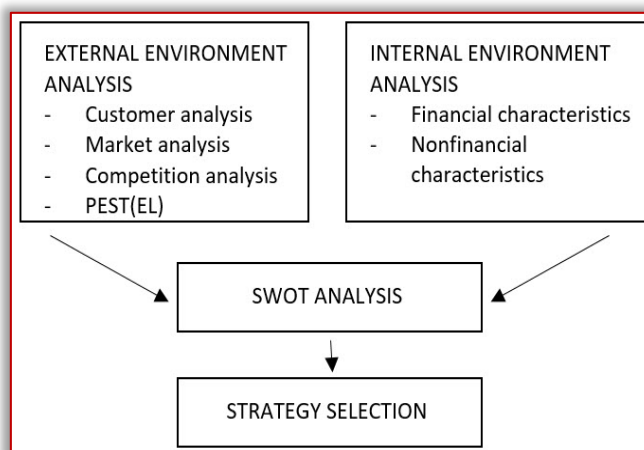


Figure 2. The process of developing and designing marketing strategy

FEASIBILITY ANALYSIS OF LAUNCHING THE PRODUCTION OF FAST-GROWING PAULOWNIA TREES

“M&M PAULOWNIA” LLC, the company for the production of fast-growing trees, plans to produce Paulownia plants for sale. Sales range includes quarterly seedlings (obtained by “in vitro” technology), sawmill wood products (uses in construction and wood industry for furniture production), wood biomass as a heating fuel (biomass can be used by other companies for the production of pellets and briquettes) and investment cultivation on an area of one hectare. An additional product, coming from the production process, is biomass generated mainly from the waste during the shredding of leaves and branches after pruning trees, which can be used to heat buildings or make briquettes and pellets. The planned location of the plantation - Aleksandrovac, the municipality of Laktaši in Bosnia and Herzegovina.

— **Analysis of the external environment of the company**

The market research process identifies potential buyers and competitors, as well as possibilities of market expansion.

≡ *Customer analysis.* On the domestic market, there is not a dominant presence of Paulownia plant culture. This culture can replace most of our woody species in terms of quality, so a gradual increase of new customers is expected. The most important identified buyers of the company's products (seedlings, biomass, sawmill wood, investment cultivation packages) are those from sector of wood processing (sawmills, furniture factories, and other companies engaged in primary and final wood processing), and companies for the production of pellets and briquettes in the Banja Luka region (thirty companies have been identified of which eleven companies have expressed their interest in business cooperation). There is a possibility of selling products to construction companies (in the form of rafters, slats, planks, beams, etc.), to individual buyers and sales intermediaries.

≡ *Market analysis.* The forestry sector is very significant for the Republic of Srpska and includes the business of the company “M&M PAULOWNIA” LLC. This sector employs 3,11 % of the total working population of the Republic of Srpska [12]. At the annual level, about 1.958.000,00 cubic meters of various wood assortments produced in the forests of the Republic of Srpska. The production of forest assortments in 2019 was lower by 19,81 % compared to the year 2018 according to the Agency for Statistics of Bosnia and Herzegovina.

Some of the main problems in the forestry sector are forest fires and illegal logging. Insect damage and plant diseases did not have a growth trend for a long-time period. Market segmentation has done according to territorial criteria (Table 1):

Table 1. Market segmentation

| Market segment | Area |
|---|--------|
| Banja Luka region | Area 1 |
| Bosnia and Herzegovina except for the Banja Luka region | Area 2 |
| Region except Bosnia and Herzegovina | Area 3 |

≡ *Competition analysis.* In the Banja Luka region and the whole of Bosnia and Herzegovina, there are no Paulownia plantations, but there are only trial plantations on very small areas. There is significant competition in companies that places other types of wood that can be used for the same purposes as Paulownia. The most significant competitors on the main market of the company (Area 1 – Banja Luka region) are PFE “Šume Republike Srpske” (Forests of the Republic of Srpska) and the owners of private forests. In this market, the company “M&M PAULOWNIA” LLC should be able to position itself due to the high demand for wood assortments. Besides that, the company would be able to take advantage of reduced transportation costs due to the proximity of customers.

In Area 2, there is greater competition due to the import of wood assortments from neighbouring countries, especially

in border municipalities, but in this market, the company has great opportunities. There is a lot of competition in the regional market (Area 3) and positioning can be a real challenge. The Republic of Serbia and the Republic of Croatia have the most modern Paulownia plantations and the most modern technology in the region.

The company “M&M PAULOWNIA” LLC seeks to single out and primarily be better than the competition through the offer of investment cultivation, through several sales packages, on a plot of one hectare on which would be planted 500 seedlings of fast-growing Paulownia trees obtained “in vitro” technology of high genetic quality. The presence of strong competition in the region tells us that the market in Bosnia and Herzegovina will experience an expansion of Paulownia trees production.

≡ *PEST(EL).* Population migrations to Western Europe harmed the number of inhabitants, the number of customers, and the choice of the labour force.

The economy in Bosnia and Herzegovina is far behind the economy of neighbouring countries and European Union countries. In recent years, banks have eased the conditions for obtaining loans, and now it is easier for companies to get more favourable loans. Due to the bad rating of the state, the insurance system is quite expensive.

The company has no problems in procuring seedlings and equipment for its products.

In recent years, the weather conditions have been very changeable.

— **Internal Analysis of the company**

≡ *Purchase.* Due to the insufficient presence of fast-growing Paulownia trees in our area, the supplier choice is small. The company decided to buy seedlings from supplier “AGROPLAN” nursery garden located in the City of Bijeljina for 6,50 BAM per piece with VAT included (5,60 BAM without VAT). If a larger quantity of seedlings is taken, it is possible to agree on a discount, when for purchase of 1.500,00 seedlings the supplier gives a price of 4,00 BAM per piece without VAT. The distance between our company and the supplier is 220,00 kilometres, which should be taken into account when agreeing on the delivery of purchased seedlings.

≡ *Finances.* After the establishment of the company “M&M PAULOWNIA” LLC, the key focus will be to purchase: high-quality planting material, drip irrigation system, purchase ten hectares of land (after production stabilise buy additional ten hectares of land), three containers for offices with associated furniture and equipment, connections to electricity grid and water supply network. Previous activities follow terrain preparation works, installation of irrigation systems, planting, procurement of system for hail protection, weather conditions, insects, and purchase of a stationary chipboard machine with a protective canopy, for what is estimated to provide a total of 145.700,00 BAM. This amount of money includes equipment that is not completely necessary for launching the business. According to this, the sum of 132.300,00 BAM is enough to start a business.

After three years of growth from its planting, one Paulownia tree reaches a market value from 40,00 to 60,00 euro. After eight years of growing the Paulownia tree (when the tree is best for lumbering), it can provide from 0,50 to 0,70 cubic meters of usable material worth from 140,00 to 500,00 euro depending on its quality.

The company plans to plant 1.500,00 seedlings every year, and to do lumbering according to the recommended periods. After three years of production, after planting the first seedlings, we can expect plant growth to value between 60.000,00 and 90.000,00 euros, depending on the quality. Every following year company would have the arrival of new 1.500,00 three-year-old trees. In the income statement (Table 2), the total projected revenues after eight years of company operation are 956.550,00 BAM with total expenses for the same period of 627.982,40 BAM.

Table 2. Income statement

| | YEAR | | | |
|-------------------|-----------|-----------|-----------|-----------|
| | 1. | 2. | 3. | 4. |
| NET PROFIT “+“ | -25.069,4 | -29.109,0 | 14.661,9 | 32.031,9 |
| (NET LOSS „-“) | | | | |
| BUSINESS REVENUE | 18.750,0 | 51.100,0 | 98.200,0 | 120.000,0 |
| BUSINESS EXPENSES | 43.819,4 | 80.209,0 | 81.909,0 | 84.409,0 |
| | YEAR | | | |
| | 5. | 6. | 7. | 8. |
| NET PROFIT “+“ | 45.711,9 | 59.301,9 | 79.731,9 | 113.031,9 |
| (NET LOSS „-“) | | | | |
| BUSINESS REVENUE | 135.200,0 | 150.300,0 | 173.000,0 | 210.000,0 |
| BUSINESS EXPENSES | 84.409,0 | 84.409,0 | 84.409,0 | 84.409,0 |

Table 3. Income statement the payback period of investment (economic flow)

| Year | Total investment | Net receipts | | |
|------|------------------|--------------|------------|---------------------------|
| | | By years | Cumulative | Uncovered investment part |
| 1 | 2 | 3 | 4 | 5 (4-2) |
| 1 | 132.300,00 | 0 | 0 | -132.300,00 |
| 2 | 132.300,00 | 0 | 0 | -132.300,00 |
| 3 | 132.300,00 | 10.346,90 | 10.346,90 | -121.953,10 |
| 4 | 132.300,00 | 27.716,90 | 38.063,80 | -94.236,20 |
| 5 | 132.300,00 | 41.396,90 | 79.460,70 | -52.839,30 |
| 6 | 132.300,00 | 54.986,90 | 134.447,60 | 2.147,60 |
| 7 | 132.300,00 | 75.416,90 | 209.864,50 | 77.564,50 |
| 8 | 132.300,00 | 108.716,90 | 318.581,40 | 186.281,40 |

The payback period of investment, determined according to economic flow, is estimated to be at five years and 143 days (Table 3). Also, a net present value represents a positive value.

≡ *Employees.* A team of young and dedicated people with the required level of expertise makes up the company “M&M PAULOWNIA” LLC. The director manages the company. The operational section of the company includes forestry and agricultural technician who is in charge of the preparation, planting, and maintenance of the plantation.

Besides him, the company needs two wood technicians for felling and chopping of wood.

— SWOT analysis

By analyzing the internal and external environment of the company, key elements are determined and classified: strengths, weaknesses, opportunities, and threats (Table 4)

Table 4. SWOT analysis matrix

| SWOT analysis matrix | |
|--|---|
| <p>Strengths</p> <ul style="list-style-type: none"> - Low product prices - Sale of investment cultivation – an innovative product - Experience and qualification of workers - Quality of equipment - Seed quality - Market potential - Cheap labour - Providing technical support to customers from the moment of planting to felling | <p>Weaknesses</p> <ul style="list-style-type: none"> - Low information about the product by customers - Exploitation period - Satisfying market demand - Relatively long investment repayment period - Insufficient experience in growing Paulownia trees |
| <p>Opportunities</p> <ul style="list-style-type: none"> - Lack of Paulownia plantations in the Banja Luka region (Area 1), which is the primary market - Weak competition in Bosnia and Herzegovina - Subsidies - Availability of skilled labour - Quality of the finished product - High demand for wood assortments - In Bosnia and Herzegovina and the region, there is a large number of companies for final wood processing - In recent years, banks have eased the conditions for obtaining loans | <p>Threats</p> <ul style="list-style-type: none"> - Big competition in the region, especially in the Republic of Croatia - Occurrence of pests (insects) - Uncontrolled import of wood assortments - Entry of new competitors - Weather trouble - Presence of coronavirus pandemic (COVID-19) - Small number of suppliers in Bosnia and Herzegovina - Population decline in Bosnia and Herzegovina and the region due to migrations - Due to the bad rating of the state, the insurance system is quite expensive |

— Vision and mission of the company

“M&M PAULOWNIA” LLC company vision is to become a leader in Bosnia and Herzegovina in the production of quarterly seedlings of fast-growing Paulownia trees, raw materials for the sawmills, and the sale of investment cultivation with the ambition to expand the product range and increase production in each subsequent year.

To grow from good roots into a firm and stable organization. “M&M PAULOWNIA” LLC company mission is to provide the more affordable offer of raw materials for the sawmills, which would affect the prices of final products in economic branches with which the company cooperates. Special emphasis is dedicated to stimulating the use of land suitable for planting the Paulownia trees in Bosnia and Herzegovina. The company will have a special aspect of monitoring customer satisfaction, market demand, attracting new customers and retaining existing ones, continuous

improvement of technologies and personnel in order to obtain higher quality products compared to the competition.

— **Strategy of the company**

The strategy of the company “M&M PAULOWNIA” LLC is based on the idea that by combining resources and existing opportunities, with a view to the challenges and environment limitations, find the best way for achieving the strategic goals, mission, and vision of the company.

Strategic goal 1: Offer of innovative products – purchase of investment cultivation.

Measures:

- ≡ At the plantation in Aleksandrovac, parcel the land intended for investment sale on plots of one hectare with a capacity for planting about 500 seedlings of fast-growing Paulownia trees obtained by “in vitro” technology.
- ≡ As part of the business, the company will offer several sales packages on one-hectare plots:
 - PACKAGE 1: Purchase of investment cultivation after three years of growth and independent continuation of work and maintenance until the moment suitable for logging (next 4-5 years);
 - PACKAGE 2: Purchase of investment cultivation after three years of growth with continued maintenance by the company “M&M PAULOWNIA” LLC (irrigation, pruning, and all other actions prescribed by the profession);
 - PACKAGE 3: Independent work on the formation of the plot from planting, through plucking after the first year of growth, and further monitoring of growth until the moment suitable for logging. As part of this packaging company “M&M PAULOWNIA” LLC offers a plot of one hectare, all its knowledge and skills and transfers it to the investor for necessary education. The acquired knowledge and skills can later be used by the investor for independent cultivation and starting a business;
 - PACKAGE 4: Giving the investor opportunity to create the contents of the package where all combinations of the Package 1, 2 and 3, which are already mentioned, are allowed with the possibility of adding new elements (e.g., between rows of Paulownia trees other plant species can be planted [13]; usage for beekeeping during the flowering of Paulownia trees [1] and other).

Strategic goal 2: Strengthening marketing activities

Measures:

- ≡ Create a company's website to improve the visibility in the market, better inform customers, and reach new customers easier,
- ≡ In addition to on-site sales, the company will offer the possibility of selling through the online store on the company's official website,
- ≡ Developing a network of distributors in strategic locations in the country (and later in the region) to deliver products faster to customers.

Strategic goal 3: Placing products on the European Union market

Measures:

- ≡ After gaining the necessary experience and work references, the company plans to expand the scope of its activities to the market of the European Union countries,
- ≡ To achieve this ambitious strategic goal, it is necessary for planting material and other products of the company to pass all strict phytosanitary inspections and successfully meet all the required conditions for export to the European Union countries.
- ≡ To find an adequate business partner and exclusive distributor for our company's products in the European Union.
- ≡ Find new suppliers to ensure a constant supply of planting material and better prices.

— **Risk assessment**

Table 5 provides an excerpt of the risk analysis for the identified hazards coming from the environment and weaknesses of the company with the necessary risk mitigation measures.

Table 5. Excerpt from the risk assessment for identified hazards and weaknesses

| RISK | RISK ASSESSMENT | | |
|---------------------------|---------------------|---|---|
| | POSSIBILITY | CONSEQUENCES | MEASURES |
| Insect appearance | Low, to 10 % | Partial or complete damage to seedlings; Repeated planting | Application of insecticides from verified manufacturers |
| Natural disasters | Unable to determine | Partial or complete damage to seedlings; Repeated planting | Installation of protective structure |
| Irrigation system failure | Low, to 5 % | Slow plant growth | Preventive control and regular maintenance |
| Theft on plantation | Low, to 5 % | Reduced sales; Repeated planting | Hiring security worker |
| Low demand for products | Low, to 8 % | Reduced sales; Financial problems | Appropriate promotion and advertising |

CONCLUSION

The production of fast-growing energy crops, which includes Paulownia trees observed through this paper, can play a major role in increasing the share of renewable energy sources in the Republic of Srpska and Bosnia and Herzegovina. Also, their impact on reducing global warming by absorbing greenhouse gases should not be ignored. Before starting the production of Paulownia trees all-important external and internal factors, that may have an impact on the placement of products on target markets should be considered because all areas where the Paulownia tree production is present have a specific business environment. The analysis that has been done for starting the production of Paulownia trees in the Banja Luka region showed good

profitability and great opportunities for its placement on the Bosnia and Herzegovina market. It is necessary to strengthen product innovation and marketing activities in order for the customer to become better acquainted with its characteristics and advantages.

Note:

This work is based on the paper presented at DEMI 2021 – The 15th INTERNATIONAL CONFERENCE ON ACCOMPLISHMENTS IN MECHANICAL AND INDUSTRIAL ENGINEERING, organized by Faculty of Mechanical Engineering, University of Banja Luka, BOSNIA & HERZEGOVINA, co-organized by Faculty of Mechanical Engineering, University of Niš, SERBIA, Faculty of Mechanical Engineering Podgorica, University of Montenegro, MONTENEGRO and Faculty of Engineering Hunedoara, University Politehnica Timisoara, ROMANIA, in Banja Luka, BOSNIA & HERZEGOVINA, in 28–29 May 2021.

References

- [1] Icka, P., Damo, R., Icka, E. (2016). Paulownia Tomentosa, a Fast-Growing Timber. *Annals "Valahia" University of Targoviste – Agriculture*, vol. 10, no. 1, p. 14-19
- [2] Rodríguez-Seoanea, P., Beatriz Díaz-Reinosob, B., Mourea, A., Domínguez, H. (2020). Potential of Paulownia sp. for biorefinery. *Industrial Crops & Products*, vol. 155, p. 1-15
- [3] Woods, V. (2008). Paulownia as a novel biomass crop for Northern Ireland?: a review of current knowledge, Hillsborough, Co. Down: Agri-Food and Biosciences Institute, Global Research Unit, Occasional Publication, no. 7
- [4] Nelis, P., Michaelis, F., Krause, K., Mai, C., (2018). Kiri wood (Paulownia tomentosa): can it improve the performance of particleboards? *European Journal of Wood and Wood Products*, vol. 76, p. 445–453
- [5] Qi, Y., Yang, C., Hidayat, W., Jang, J. H., & Kim, N. H. (2016). Solid bioenergy properties of Paulownia tomentosa grown in Korea. *Journal of the Korean Wood Science and Technology*, vol. 44, no. 6, p. 890-896
- [6] Ferreira, A., Paiva, J. Evaluation of Paulownia's biomass in a pelletized form, 23rd ABCM International Congress of Mechanical Engineering, December 6-11, 2015, Rio de Janeiro
- [7] Angelov, B., (2010). "Paulownia the tree of future", Velboy Ltd. Bulgaria
- [8] https://ec.europa.eu/clima/policies/strategies/2030_en, accessed on: March 31, 2021.
- [9] Coulter, M. (2008). *Strategic Management in Action*. Prentice Hall, Upper Saddle River, New Jersey
- [10] Martinović, S., Nićin, N. (1995). *Menadžment danas, Ulixes marketing*, Novi Sad
- [11] Kukić, S. (2007). *Marketing*, Ekonomski fakultet Sveučilišta u Mostaru, Mostar
- [12] The Republic of Srpska Institute of Statistics, <http://www3.rzs.rs.ba:8080/rzs/faces/indicators.xhtml>, accessed on: March 31, 2021.
- [13] Yin, R., & He, Q. (1997). The spatial and temporal effects of paulownia intercropping: the case of northern China. *Agroforestry Systems*, vol. 37, no. 1, p. 91-109.



ISSN: 2067-3809

copyright © University POLITEHNICA Timisoara,
Faculty of Engineering Hunedoara,
5, Revolutiei, 331128, Hunedoara, ROMANIA
<http://acta.fih.upt.ro>

¹Mustefa JIBRIL, ¹Messay TADESE, ¹Nuriye HASSEN

POSITION CONTROL OF A THREE DEGREE OF FREEDOM GYROSCOPE USING OPTIMAL CONTROL

¹ School of Electrical & Computer Engineering, Dire Dawa Institute of Technology, Dire Dawa, ETHIOPIA

Abstract: In this paper, a 3 DOF gyroscope position control have been designed and controlled using optimal control theory. An input torque has been given to the first axis and the angular position of the second axis have been analyzed while the third axis are kept free from rotation. The system mathematical model is controllable and observable. Linear Quadratic Integral (LQI) and Linear Quadratic State Feedback Regulator (LQRY) controllers have been used to improve the performance of the system. Comparison of the system with the proposed controllers for tracking a desired step and random angular position have been done using Matlab/Simulink Toolbox and a promising results has been analyzed.

Keywords: Gyroscope, Linear Quadratic Integral, Linear Quadratic State Feedback Regulator

INTRODUCTION

A gyroscope is a system used for measuring or accordance angular position and angular velocity. It is a spinning wheel in which the axis of rotation (spin axis) is free to assume any tendency by itself. When rotating, the tendency of this axis is unaffected by inclining or rotation of the mounting, according to the conservation of angular momentum. Gyroscopes based on other operating precept also exist, such as the microchip-packaged MEMS gyroscopes found in electronic devices and the extremely sensitive quantum gyroscope. A gyroscope is a wheel mounted in two or three gimbals, which are pivoted supports that allow the rotation of the wheel roughly a single axis. The axle of the spinning wheel defines the spin axis. The rotor is constrained to spin closely an axis, which is always perpendicular to the axis of the inner gimbal. So the rotor possesses three degree of rotational freedom and its axis possesses two. The wheel responds to a torque applied to the input axis by a response torque to the output axis.

MATHEMATICAL MODELING OF THE GYROSCOPE

The gyroscope system is shown in Figure 1 below.

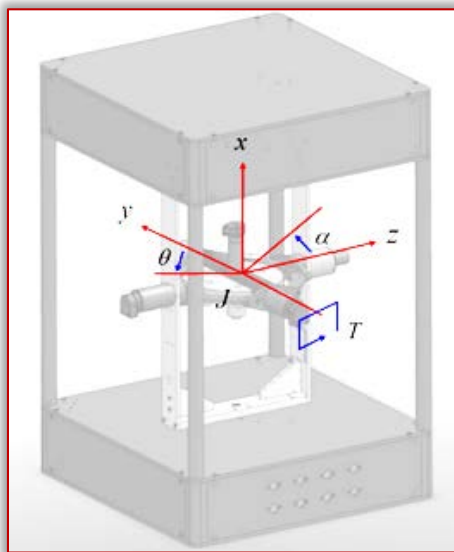


Figure 1. Gyroscope system

The equations of motion representing the angular rate of the Z axis α and the y axis θ are

$$J_y \ddot{\theta} + B_y \dot{\theta} + I_g \dot{\alpha} = T \quad (1)$$

$$J_z \ddot{\alpha} + B_z \dot{\alpha} - I_g \dot{\theta} = 0 \quad (2)$$

where

J_y moment of inertia about the y-axis

J_z moment of inertia about the z-axis

B_y damping friction about the y-axis

B_z damping friction about the z-axis

I_g moment of inertia of the gyroscope rotor about its own axis and its velocity.

Taking the Laplace transfer of Equation (1) and Equation (2) yields

$$J_y \theta(s) s^2 + B_y \theta(s) s + I_g \alpha(s) s = T(s) \quad (3)$$

$$J_z \alpha(s) s^2 + B_z \alpha(s) s - I_g \theta(s) s = 0 \quad (4)$$

The only actuated axis is the y-axis and the control input in the single-input single-output (SISO) system is the torque applied in the y-axis, T . The transfer function of the system becomes

$$G(s) = \frac{\alpha(s)}{T(s)} = \frac{1}{J_y J_z s^3 + (B_z + B_y J_z) s^2 + (B_y B_z + I_g^2) s}$$

The parameters of the system are shown in Table 1 below.

Table 1. System parameter

| No | Parameter | Symbol | Value |
|----|---|--------|------------------------------|
| 1 | Moment of inertia about the y-axis | J_y | 0.00429 kg.m ² |
| 2 | Moment of inertia about the z-axis | J_z | 0.02453 kg.m ² |
| 3 | damping friction about the y-axis | B_y | 0.01584 Nms |
| 4 | damping friction about the z-axis | B_z | 0.018756 Nms |
| 5 | Moment of inertia of the gyroscope rotor about its own axis and its velocity. | I_g | 0.00484 kg.m ² /s |

The transfer function becomes

$$G(s) = \frac{\alpha(s)}{T(s)} = \frac{9503}{s^3 + 182s^2 + 3.05s}$$

PROPOSED CONTROLLERS DESIGN

— Linear Quadratic Integral Controller Design

LQI computes an optimal state-feedback control law for the tracking loop. Block diagram of a quarter vehicle electromagnetic suspension system with LQI controller is shown in Figure 2 below.

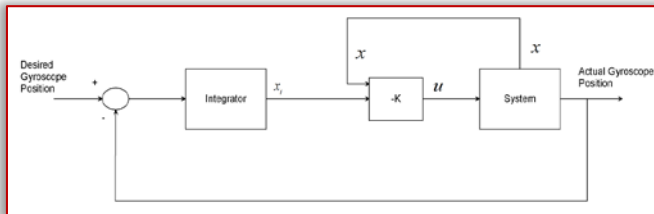


Figure 2. Block diagram of a quarter vehicle electromagnetic suspension system with LQI controller

For a plant sys with the state-space equations

$$\dot{x} = Ax + Bu \quad (5)$$

$$y = Cx + Du$$

The state-feedback control is of the form

$$u = -K[x, x_i] \quad (6)$$

Where x_i is the integrator output. This control law ensures that the output y tracks the reference command r . For MIMO systems, the number of integrators equals the dimension of the output y . LQI calculates the optimal gain matrix K , given a state-space model SYS for the plant and weighting matrices Q, R, N .

The value of Q, R and N is chosen as

$$Q = \begin{bmatrix} 5 & 0 & 0 & 0 \\ 0 & 5 & 0 & 0 \\ 0 & 0 & 5 & 0 \\ 0 & 0 & 0 & 5 \end{bmatrix}; R = 10 \text{ and } N = \begin{bmatrix} 1 \\ 0 \\ 0 \\ 1 \end{bmatrix}$$

The LQI optimal gain matrix becomes

$$K = [0.3030 \quad 5.4075 \quad 33.7473 \quad -0.7071]$$

— Linear Quadratic State Feedback Regulator Control

Linear quadratic state feedback regulator control is a manipulate scheme that gives the pleasant feasible performance with respect to a few given degree of performance. The overall performance degree is a quadratic feature composed of state vector and manage input. Linear quadratic state feedback regulator is the top of the line principle of pole placement method. Linear quadratic state feedback regulator algorithm defines the gold standard pole place primarily based on two main feature. To find the finest gains, one need to define the most advantageous performance index first of all and then clear up algebraic Riccati equation. Linear quadratic state feedback regulator does now not have any unique strategy to outline the value feature to attain the most suitable gains and the cost function need to be described in iterative manner.

Linear quadratic state feedback regulator is a manipulate scheme that offers the quality feasible overall performance

with respect to a few given measure of overall performance. The linear quadratic state feedback regulator design hassle is to design a state comments controller K such that the index performance J is minimized. In this method a remarks gain matrix is designed which minimizes the objective feature so as to achieve some compromise between the usage of control attempt, the importance, and the speed of reaction a good way to assure a stable system. Designer pick the correct cost of Q, R and N to discover the perfect benefit matrix K the usage of MATLAB. The state variable configuration is shown below in Figure 3.

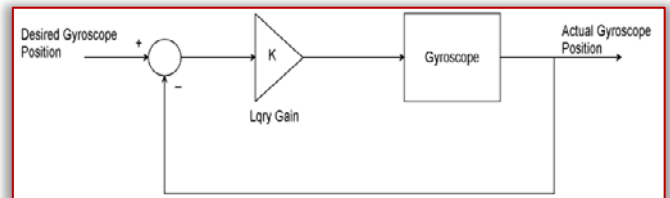


Figure 3. State variable feedback configuration

In this paper, the value of Q, R and N is chosen as

$$Q = 54 \quad R = 10 \quad N = 1$$

The value of obtained feedback gain matrix K of lqry is given by

$$K = (0.1190 \quad 11.2860 \quad 172.5233)$$

RESULT AND DISCUSSION

— Controllability and Observability of the Pendulum

A system (state space representation) is controllable iff the controllable matrix $C = [B \ AB \ A^2B \ \dots \ A^{n-1}B]$ has rank n where n is the number of states in the system,

In our system, the controllable matrix $C = [B \ AB \ A^2B]$ has rank 3 which the number of degree of freedom of the system. So, the system is controllable.

A system (state space representation) is Observable if the Observable Matrix $D = [C \ CA \ CA^2 \ \dots \ CA^{n-1}]^T$ has a full rank n .

In our system, the Observable Matrix $D = [C \ CA \ CA^2]^T$ has a full rank of 3 which the number of states of the system. So, the system is Observable.

— Comparison of the Gyroscope with LQI and LQRY Controllers for Tracking a Desired Angular Position using Step Input Signal

The comparison simulation of the gyroscope with LQI and LQRY controllers for tracking a desired step change from 0-35-degree angular position is shown in Figure 4 below.

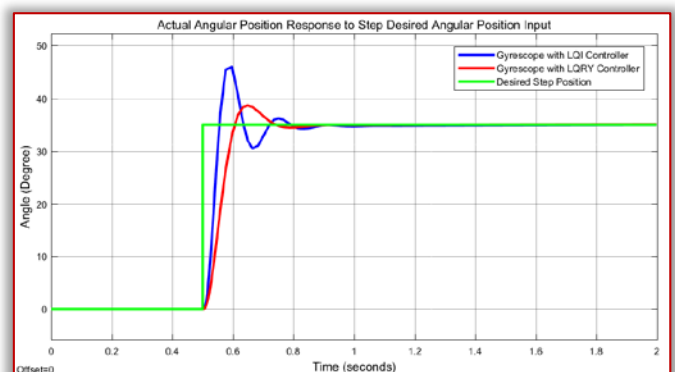


Figure 4. Step response result

The corresponding torque input for the gyroscope with LQI and LQRY controllers is shown in Figure 5 and Figure 6 respectively.

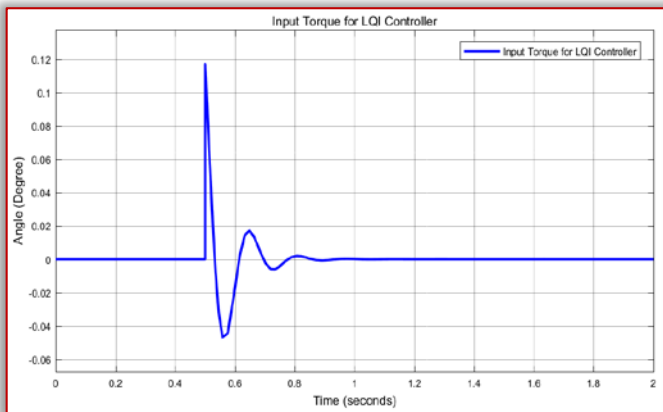


Figure 5. Torque input for the gyroscope with LQI controller

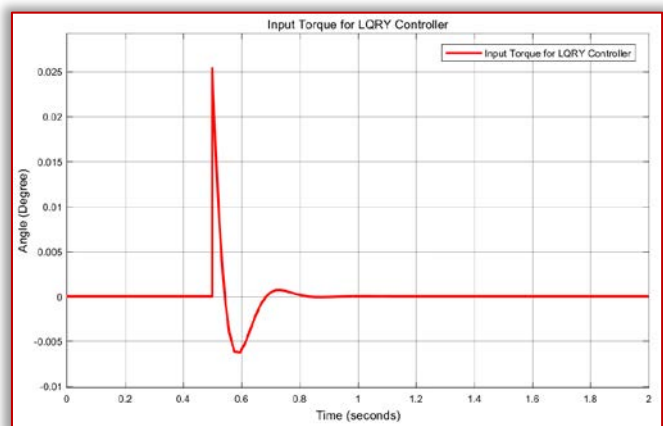


Figure 6. Torque input for the gyroscope with LQRY controller
The data of the rise time, percentage overshoot, settling time and peak value is shown in Table 2.

Table 2. Step response data

| No | Performance Data | LQRY controller | LQI controller |
|----|------------------|-----------------|----------------|
| 1 | Rise time | 0.56 sec | 0.54 sec |
| 2 | Per. overshoot | 8.57 % | 34.2 % |
| 3 | Settling time | 0.75 sec | 0.88 sec |
| 4 | Peak value | 37 Degree | 47.3 Degree |

As Table 2 shows that the gyroscope with LQRY controller improves the performance of the system by minimizing the percentage overshoot and settling time.

— Comparison of the Gyroscope with LQI and LQRY Controllers for Tracking a Desired Angular Position using Random Input Signal

The comparison simulation of the gyroscope with LQI and LQRY controllers for tracking a desired random change between 3 and 35-degree angular position is shown in Figure 7 below.

The corresponding torque input for the gyroscope with LQI and LQRY controllers is shown in Figure 8 and Figure 9 respectively.

As we seen from Figure 7, the gyroscope with LQRY controller improves the performance of the system by minimizing the percentage overshoot and settling time.

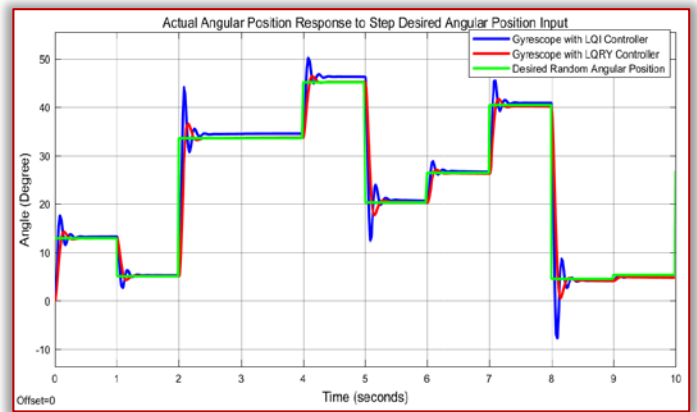


Figure 7. Random response result

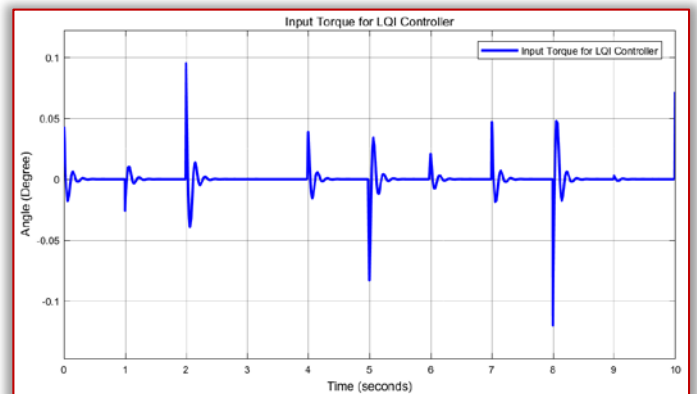


Figure 8. Torque input for the gyroscope with LQI controller

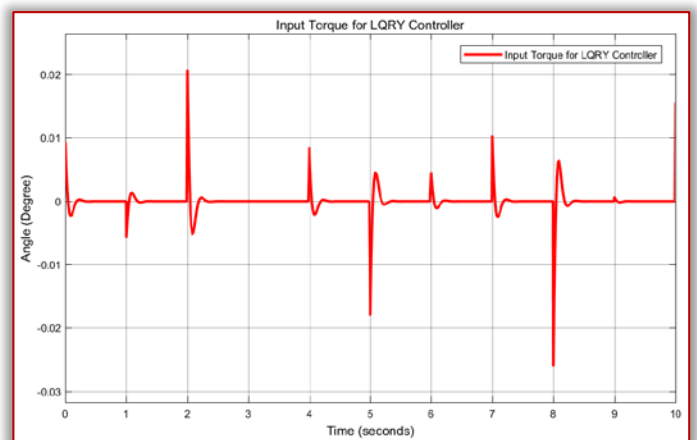


Figure 9. Torque input for the gyroscope with LQRY controller

CONCLUSION

This study aims to improve the performance of a 3 DOF gyroscope position control using Linear Quadratic Integral (LQI) and Linear Quadratic State Feedback Regulator (LQRY) controllers. The comparison simulation results of the system with the proposed controllers for tracking a desired step and random angular position shows that in both inputs the gyroscope with LQRY controller improves the performance of the system by minimizing the percentage overshoot and settling time.

Reference

[1] Ryspek U. et al. "Inertial Forces Acting on a Gyroscope" Journal of Mechanical Science and Technology, Vol. 32, Issue 1, pp. 101-108, 2018.

- [2] P.J.W. Koelewijn et al. “LPV Control of a Gyroscope with Inverted Pendulum Attachment” IFAC-PapersOnline, Vol. 51, Issue 26, pp. 49-54, 2018.
- [3] Mohammed R. et al. “Comparison of Position Control of a Gyroscopic Inverted Pendulum using PID, Fuzzy Logic and Fuzzy PID Controllers” International Journal of Fuzzy Logic and Intelligent Systems, Vol. 18, Issue 2, pp. 103-110, 2018.
- [4] Sinan B. et al. “Composite Adaptive Control of Single Gimbal Control Moment Gyroscope Supported by Active Magnetic Bearings” Journal of Aerospace Engineering, Vol. 30, Issue 1, 2017.
- [5] Talha M. et al. “Design of Fuzzy Tuned PID Controller for Anti Rolling Gyro (ARG) Stabilizer in Ships” International Journal of Fuzzy Logic and Intelligent Systems, Vol. 17, pp. 210-220, 2017.
- [6] Vittorio M. N. Passaro et al. “Gyroscope Technology and Applications: A Review in the Industrial Perspectives” Sensors (Basel), Vol. 17, Issue 10, 2017.



ISSN: 2067-3809

copyright © University POLITEHNICA Timisoara,
Faculty of Engineering Hunedoara,
5, Revolutiei, 331128, Hunedoara, ROMANIA
<http://acta.fih.upt.ro>

¹Jameel Al-NAFFAKH, ²Mohammed R. Al-QASSAB

DATASET THE ANNUAL GROWTH GENERATED OF RENEWABLE ENERGY BETWEEN TURKEY, IRAN AND IRAQ

^{1,2}Mechanical power Department, AL-Furat Al-Awsat Technical University, Najaf Technical engineering college, Najaf, IRAQ

Abstract: The consumption of fossil fuels has risen to be the main source of energy generation in most countries since the start of the industrial revolution around the world. The greenhouse gases generated from this use produce significant negative effects on the environment and human health. As a result of these disadvantages, the world needs to search for alternative energy sources that are low in carbon. The article focused on the amount of renewable energy generation in Turkey, Iran and Iraq from the collection of statistical data for the period from 2010-2020. Turkey occupied the clear progress to benefit from renewable energy sources, followed by Iran and Iraq. Where the percentage of annual growth of power generation based on hydropower in Turkey, Iran and Iraq (71.4%, 28.5% and 0.1%) respectively. With regard to other sources of renewable energy, Turkey had the largest share in generating energy from wind and solar energy, with an annual growth rate of (88.03%, 98.22%), respectively. Finally, renewable energy can be considered as a promising source of energy for future generations when correct planning policies are determined by countries.

Keywords: renewable energy, solar energy, wind energy, hydropower energy

INTRODUCTION

Fossil fuels have become dominant in energy production after the start of the Great Industrial Revolution in most countries of the world, which led to significant negative effects on human health and the global climate as a result of the emission of greenhouse gases resulting from burning fossil fuels. In order to reduce the emissions of pollutants resulting from burning fossil fuels, the world needs to switch to using renewable energy sources that are low in carbon and environmentally friendly. The International Renewable Energy Agency indicated in its report that 66% of the total energy should be from renewable energy by 2050, through the promotion, development and use of internationally concerted efforts [1]. The use of various renewable energy sources is widely considered beneficial, such as wind energy, solar energy, geothermal energy, hydropower in the face of crises from the use of fossil energy, and they are considered as clean energy sources[2], [3]. Clean energy has led to an increase in global awareness to reach a climate free from the problems of global warming and environmental pollution, which can cover the needs of local energy requirements, part of which is the traditional dependence on fossil fuels [4]. The great demand for energy has led to a global trend to exploit remote and mountainous areas to implement international commitments and agreements to use renewable energy sources as an alternative to traditional energy sources[5]. There are many challenges facing future generations in exploring and promoting the use of renewable energy sources, through setting policies and increasing public opinion education towards a clean climate. Where it can be used to direct increasing global awareness by focusing on various global social networking sites, and reaching useful insights into the advantages of using renewable energy technology as an alternative future energy plan[6]. China is the main player in the field of renewable energy globally, accounting for half of the global production of solar and wind energy, with a growth of nearly 800 gigawatts, which

is equivalent to an average annual increase of 18% between the period 2015-2020. A plan has also been drawn up to increase the percentage of wind and solar energy use in China at an annual rate of 14% and 18%, respectively, over the next ten years. The indicator is that China is on the right track in using renewable energy resources[7]. Turkey is one of the poor countries in the production of fossil fuels, as nearly 80% of the total energy requirements are imported from other countries. Where the amount of energy consumption was 230 thousand kilotons of oil, while the average energy production was 35 thousand kilotons of oil for the year 2016. This leads to the fact that Turkey relied on renewable energy sources to meet the requirements and reduce the expenditures required to import fossil energy types from abroad[8], [9]. Oil was discovered in Iran in 1908, thus becoming one of the countries with oil production in the Middle East. Reliance on fossil fuels, especially oil, represents a major source of income for Iran. Then, the share of crude oil consumption in energy sources decreased from 91% to 43% from 1980-2018[10]. In contrast, the rate of natural gas extraction increased from 7% to 56% between 1980-2018, to be a major source of energy in Iran[10]. This country has not given great importance to the use of renewable energy sources to provide alternative sources, although it has a diverse resource environment to diversify its energy mix due to various economic and technical constraints. Therefore, various techniques and policies must be applied to exploit the natural sources of renewable energy in Iran[11]. Iraq is characterized as one of the countries with high oil productivity and is one of the members of the Organization of Petroleum Exporting Countries, so it depends on fossil fuels for domestic consumption for energy production[12]. Also, the geographical location gives it the privilege to benefit from solar radiation (one of the renewable energy sources), which reaches 1899 kilowatts/m², especially in central and southern Iraq. Despite that, there are no serious attempts to adopt

renewable energy sources to be a parallel line to the production of fossil energy in the country. Where Iraq suffers from a severe shortage of energy as a result of the rapid growth in energy consumption, especially electric power plants as a result of the destruction of various wars from 1980 until now. Therefore, the Iraqi government must rely on tangible programs and policies to build renewable energy plants to fill the shortage. Research centers in Iraqi universities discussed presenting plans to exploit renewable energy of various kinds, such as solar distillation of non-potable water or the use of solar cells to generate electricity and increase its efficiency[13], [14]. In this statistical article, data on renewable energy technologies and the rate of consumption and production in Iraq, Iran and Turkey are considered. These countries have a variety of renewable energy resources that can be used in addition to fossil fuel energy, with the extent of the change in the share of renewable energy for the period from 2010-2020.

MAIN RENEWABLE ENERGY SOURCES

- **Solar Energy:** Solar energy is one of the most, cheapest and cleanest renewable energy sources that can be directly accessed. The amount of solar radiation received varies according to several factors, including geographical location, the degree of clarity of the atmosphere, and others. Where the intensity of the incident solar radiation ranges from 50 to 1500 W/m². Several techniques have been developed to take advantage of this large source to obtain energy that can be exploited in different fields (converting solar energy to thermal or photovoltaic)[15].
- **Wind Energy:** One of the fastest growing types of renewable energy as an alternative to fossil fuels, it is abundant and renewable. It is classified as a type of electromechanical energy, and the production capacity to benefit from wind energy has increased at a growth rate of 25% annually, from 8.25 GW in 2000 to 570 GW in 2020, according to the statistics of the International Renewable Energy Agency. Wind energy systems can be used in open areas, and it is not preferable to use them in the center of cities because of the obstacles that prevent the benefit from wind speed, which is the basis in the generation process[16].
- **Hydropower:** Energy generated from the movement of flowing water at dams or reservoirs to move turbine blades to generate hydroelectric power. Many countries have taken advantage of this technology in building hydroelectric power stations, as Norway relies on this technology to generate 99% of the coverage of the need for electricity. China has also built the largest hydroelectric power station with a generation rate of 80-100 TW.h/year. The benefits of hydropower lie as an environmentally friendly fuel source, as well as associated benefits such as flood control, irrigation methods, water supply, and drought reduction[17].

DATASETS RENEWABLE ENERGY

A study of the share of consumption of renewable energy of all kinds (solar energy, wind energy, hydro energy and

others) in Iraq, Iran and Turkey. Turkey took the lead in benefiting from the use of renewable energy, with a rate of more than 12%, compared with Iraq and Iran, with small percentages that did not exceed 3%, as shown in Figure 1[18].

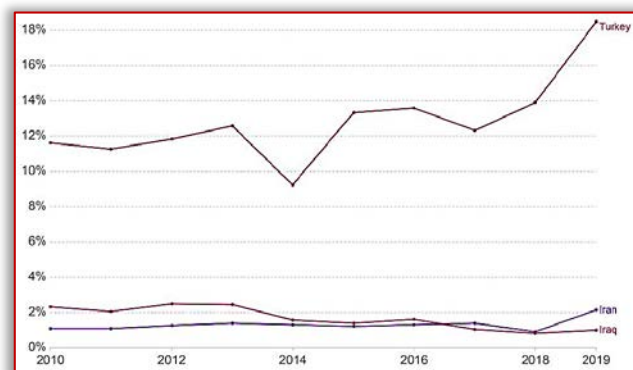


Figure 1. The share of primary energy from renewable sources

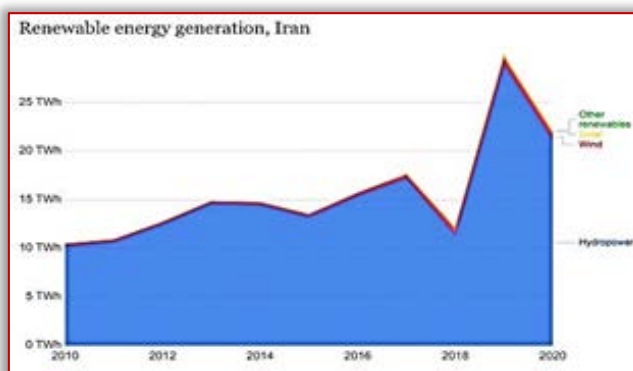
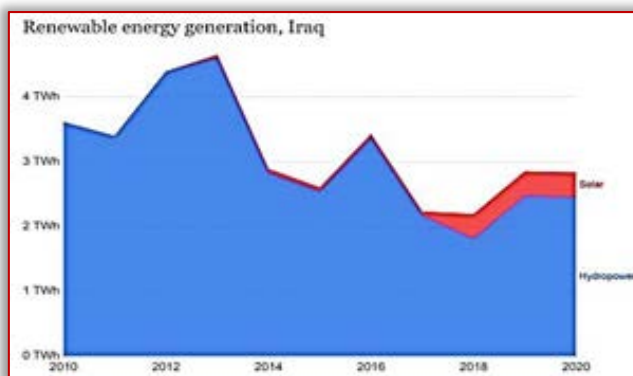
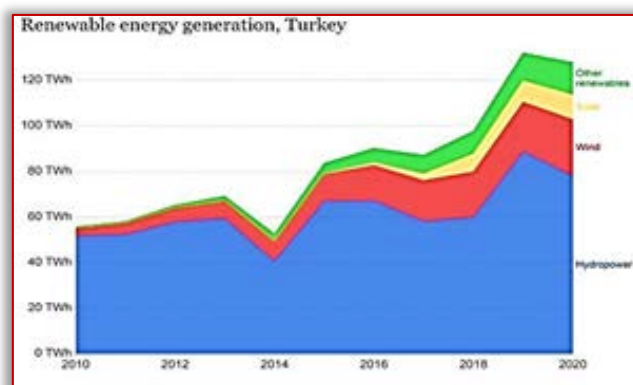


Figure 2. Renewables energy mix

Figure 2 showed a stacked areal chart of the mix of renewable energy technologies according to their types and the relative annual contribution of each. Where we note that

hydropower is the largest renewable source of energy generation in the study area, and Turkey's share of the largest benefit from the renewable energy mix, followed by Iran and finally Iraq[18].

Hydropower is the largest renewable energy source with low carbon and used globally. Figure 3 shows that 60% of renewable energy is generated from hydropower. The amount of hydroelectric energy varies clearly according to the contribution and exploitation of each country in the study area. Where the annual birth rate of Turkey, Iran and Iraq were (53.9TWh, 12.79 TWh and 1.52 TWh) respectively[18].

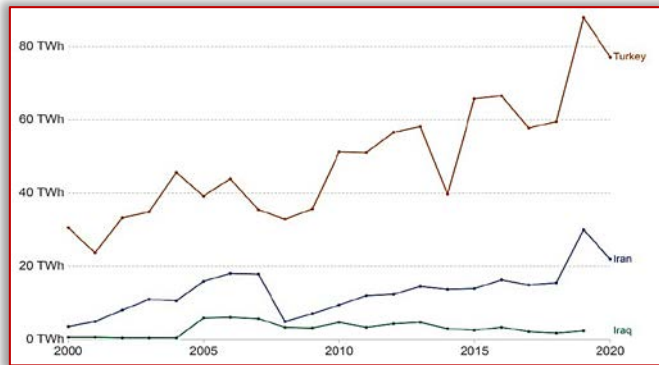


Figure 3. Annual hydropower generation is measured in terawatt-hours (TWh)

Wind power generation is one of the renewable energy technologies used in some countries of the world to generate the energy needed to meet their needs. Figure 4 shows Turkey's uniqueness in exploiting wind energy generated from onshore and offshore wind farms, with a large difference from Iraq and Iran. The growth rate during 10 years increased by 912 percent in Turkey, on the other hand, wind energy was not exploited in Iraq and Iran despite the availability of the appropriate environment for it[18].

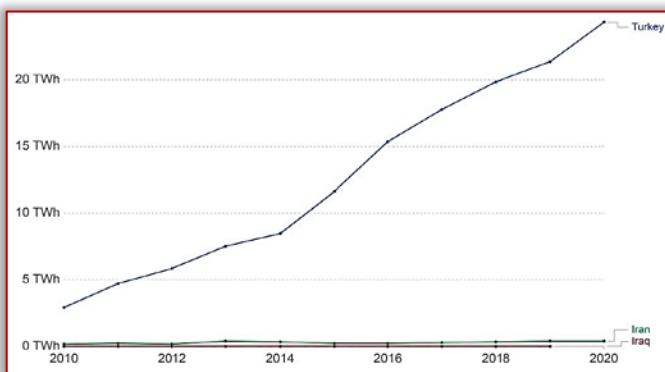


Figure 4. Annual wind power generation

The technologies for using solar energy are diverse, but it is worth noting that only a small part of the available solar energy has been used in our lives. Electrical energy is generated from solar energy by heat engines or photovoltaic converters. Among the applications that are made using solar energy are heating and cooling systems during architectural designs that depend on the exploitation of solar energy, potable water during distillation and disinfection, the exploitation of daylight, water heating, solar cooking, and high temperatures for industrial

purposes. Figure 5 shows the amount of energy generated from solar energy each year and the amount of accelerating growth in each country.

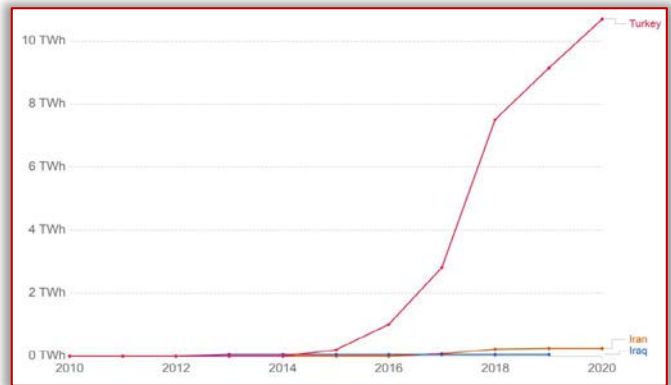


Figure 5. Annual solar energy generation

CONCLUSIONS

Renewable energy is the amount of energy generated from natural resources that are continuously renewed, such as wind, sun and water, and which do not produce greenhouse gases that are harmful to the climate. The world is heading towards benefiting from renewable energy to face environmental challenges and provide resources and economic returns that help in facing external shocks with regard to energy production and consumption. Some countries lacked real policies to spread and develop the use of renewable energy of various kinds, so in this paper, the rates of renewable energy generation in Turkey, Iran and Iraq for the past decade were concluded. The share of primary energy consumption resulting from alternative energy sources in Figure 1 showed Turkey's progress in the exploitation of alternative resources by 15.05% within 10 years, compared to the lowest decrease in 2014 by 9.22%. As for Iraq and Iran, there is no tangible economic policy in the field of renewable energy generation, as their percentage did not exceed 2% for the same period, due to their dependence on fossil fuels as a main source of energy production. It was found that despite the diversity of renewable energy sources with the availability of the appropriate environment for their exploitation, the share of hydropower acquired the largest share of the average amount of energy produced, as it reached in Turkey, Iran and Iraq (64.32, 15.69 and 3.58) TWh, respectively from 2010-2020, as shown in Figure 2. While the share of production from the rest of the renewable energy sources was very small and untapped in Iraq and Iran, unlike Turkey, where the production rate was 16.24 TWh. With regard to wind energy, noticed a linear and accelerated growth in Turkey, where its production in 2020 reached 24.32 TWh, as shown in Figure 4. The geographical location of the study area has an abundance of solar radiation to be utilized in generating energy, but Figure 5 shows that the policies of hard work have started recently, as Turkey achieved a great leap in the production rate from 0.19 TWh in 2010 to 10.71 TWh in 2020 with Iraq and Iran remaining below the acceptable level. Finally, this article revealed the lack of seriousness of relying on renewable energy sources in the study area compared to the global growth in the

development and use of clean energies with the availability of all climatic conditions and the abundance of natural resources. Rather, it relied on fossil fuels, despite the negatives that regional agreements on the environment and climate warned.

References

- [1] A. Jahid, M. S. Islam, M. S. Hossain, M. E. Hossain, M. K. H. Monju, and M. F. Hossain, "Toward energy efficiency aware renewable energy management in green cellular networks with joint coordination," *IEEE Access*, vol. 7, pp. 75782–75797, 2019.
- [2] A. Ashfaq and A. Ianakiev, "Features of fully integrated renewable energy atlas for Pakistan; wind, solar and cooling," *Renew. Sustain. Energy Rev.*, vol. 97, pp. 14–27, 2018.
- [3] D. C. Momete, "Analysis of the potential of clean energy deployment in the European Union," *IEEE Access*, vol. 6, pp. 54811–54822, 2018.
- [4] H. Lucas, S. Pinnington, and L. F. Cabeza, "Education and training gaps in the renewable energy sector," *Sol. Energy*, vol. 173, pp. 449–455, 2018.
- [5] M. R. Borovik and J. D. Albers, "Participation in the Illinois solar renewable energy market," *Electr. J.*, vol. 31, no. 2, pp. 33–39, 2018.
- [6] R. Thonig *et al.*, "Does ideology influence the ambition level of climate and renewable energy policy? Insights from four European countries," *Energy Sources, Part B Econ. Planning, Policy*, vol. 16, no. 1, pp. 4–22, 2021.
- [7] X. Xu, Z. Wei, Q. Ji, C. Wang, and G. Gao, "Global renewable energy development: Influencing factors, trend predictions and countermeasures," *Resour. Policy*, vol. 63, p. 101470, 2019.
- [8] K. Kaygusuz, "Hydropower as clean and renewable energy source for electricity generation," *J. Eng. Res. Appl. Sci.*, vol. 5, no. 1, pp. 359–369, 2016.
- [9] K. Kaygusuz, M. S. Guney, and O. Kaygusuz, "Renewable energy for rural development in Turkey," *J. Eng. Res. Appl. Sci.*, vol. 8, no. 1, pp. 1109–1118, 2019.
- [10] S. Solaymani, "A Review on Energy and Renewable Energy Policies in Iran," *Sustainability*, vol. 13, no. 13, p. 7328, 2021.
- [11] F. Atabi, "Renewable energy in Iran: Challenges and opportunities for sustainable development," *Int. J. Environ. Sci. Technol.*, vol. 1, no. 1, pp. 69–80, 2004.
- [12] J. Al-naffakh, M. R. Al-qassab, and Z. M. H. Al-makhzoomi, "Share of CO₂ emissions in Iraq, Saudi Arabia and Kuwait from the combustion of fossil fuels: A statistical study," vol. 2, no. 3, pp. 114–120, 2021.
- [13] M. R. Al-Qasab, Q. A. Abed, W. A. Abd Al-wahid, and J. T. Al-Naffakh, "Comparative Investigation for Solar Thermal Energy Technologies System," in *Journal of Physics: Conference Series*, 2019, vol. 1362, no. 1, p. 12116.
- [14] M. R. Alqasaab, Q. A. Abed, and W. A. Abd Al-wahid, "Enhancement the solar distiller water by using parabolic dish collector with single slope solar still," *J. Therm. Eng.*, vol. 7, no. 4, pp. 1000–1015, 2021.
- [15] S. R. G. Weliwaththage, "The Review of Innovation in Renewable Energy Sector in the World," vol. 1, no. 4, pp. 117–147, 2020.
- [16] F. Altuntas and M. Ş. Gök, "Technological evolution of wind energy with social network analysis," *Kybernetes*, 2020.
- [17] Y. Yao and Y. Xiuyuan, "A Summary of Research on Benefit Distribution in Coordinated Operation of Wind Power and

Hydropower," *Power Gener. Technol.*, vol. 39, no. 5, pp. 469–474, 2018.

- [18] B. Looney, "Statistical Review of World Energy globally consistent data on world energy markets . and authoritative publications in the field of energy," *Rev. World Energy data*, vol. 70, pp. 8–20, 2021.



ISSN: 2067-3809

copyright © University POLITEHNICA Timisoara,
Faculty of Engineering Hunedoara,
5, Revolutiei, 331128, Hunedoara, ROMANIA
<http://acta.fih.upt.ro>

¹Adebola ADEKUNLE, ²Iheoma ADEKUNLE, ³Ayokunle O. FAMILUSI, ⁴Mohammed ADAMU

ANALYSIS OF FLOW IN WATER DISTRIBUTION NETWORK USING NUMERICAL AND EXPERIMENTAL MODELLING

^{1,3,4}Department of Civil Engineering, Federal University of Agriculture Abeokuta, NIGERIA

²Department of Chemistry, Federal University Otuoke, NIGERIA

Abstract: Several studies have focused on addressing the challenges posed by increasing level of complexity and interdependence of water and other infrastructure systems to reliable design and optimal control, hence the need for such issues to be supported with insights generated beyond the traditional engineering disciplines. This work investigates the modelling techniques used in the analysis of water distribution networks. The analysis of the distribution network studied showed the similarities and disparities of the results obtained in the application of the Hardy Cross method and the Newton Raphson method. The distribution network analysed is that of a water distribution network layout of a University Campus in South West Nigeria. For simplicity purpose, only the mains of the network were analysed and emphasis was placed on the analysis of the loops the network was made up of. The flow rate of the Hardy Cross model and that of the Newton Raphson model for the pipe network was found to be 0.0536 m³/s for both at the start of the analysis but the final flow rates in each pipes differ for both models on completion of the analysis. The results observed were compared using correlation analysis.

Keywords: Distribution, analysis, head loss, modelling, iteration

INTRODUCTION

Modern society is highly dependent on the reliable performance of critical infrastructures such as those of water, energy and transport systems. The increasing level of complexity and interdependence of such systems poses numerous challenges to reliable design and optimal control, hence the need for such issues to be supported with insights generated beyond traditional engineering disciplines (Yazdani and Jeffrey, 2020). Water distribution network analysis has gained more importance in Civil Engineering in recent years since the optimization of water distribution network has become a focus of current research (Basha and Kassab, 1996).

Ramalingam, Lingireddy and Wood (2009) highlighted the computational advantages of the wave characteristics method for transient modelling of water distribution networks. Pipe networks are composed of a number of constant diameter pipe sections containing pumps and fittings. Hydraulic performance of pipe networks is based on mass continuity and energy conservation. Generally, the hydraulic analysis of water distribution network is performed by considering the steady state situation (Tezcan, Gokkims & Sinir, 1998) and for the solution, one of the three methods containing generally the Hardy Cross, the Linear Theory and the Newton Raphson method is preferred to find the pressure and velocity at any point in the network (Tezcan et al., 1998).

— Review of Hardy Cross & Newton Raphson Methods

□ Hardy Cross Method

The Hardy Cross is an iterative method, that is, it is a method that utilizes successive corrections of obtained values during analysis. Today, most engineers use the most improved version of Hardy Cross method (Sereshki, Saffari & Elahi, 2016) for delta p, which analyses the entire loop network of pipes simultaneously (Brkic & Praks, 2019). Hardy Cross's famous equation is as follows and can be used to estimate the flow rate error in each loop:

$$\begin{aligned}
 Q &= Q_0 + \Delta \\
 \Delta P &= RQ^n \\
 RQ^n &= R(Q_0 + \Delta)^n \\
 RQ^n &= R(Q_0^n + n\Delta Q_0^{n-1} + \dots) \cong RQ_0^n + nR\Delta Q_0^{n-1} \\
 \sum RQ^n &= \sum RQ_0^n + \Delta \sum nRQ_0^{n-1} \\
 \sum RQ^n &= 0 \\
 \sum RQ_0^n &= -\Delta \sum nRQ_0^{n-1} \\
 \Delta &= -\frac{\sum RQ_0^n}{\sum nRQ_0^{n-1}} \xrightarrow{n=2} \Delta = -\frac{\sum RQ_0^2}{2 \sum RQ_0} \\
 \Delta &= -\frac{\sum \pm \Delta P_i}{2 \sum R_i Q_i} = -\frac{\sum \pm R_i Q_i^2}{2 \sum R_i Q_i}
 \end{aligned}$$

where: Q = Actual flow rate (m³/s); Q₀ = Assumed flow rate (m³/s); Δ = Flow rate error in loop (m³/s); R = Flow resistance in each branch; Δp = Pressure loss for each branch (mm of water)

□ Newton Raphson Method

Newton Raphson technique is one of the methods that is useful for solving numerical computations. This technique is based on the definition on the definition of the derivative and the correction of it. In this technique, the initial guess of error value for the solution of the equation is estimated and then iteratively corrected (Sereshki et al., 2016). The mathematical expression can be expressed as follows;

$$\begin{aligned}
 f(x) = 0 &\rightarrow f'(x_1) = \frac{f(x_2) - f(x_1)}{x_2 - x_1} \\
 \Rightarrow x_2 &= x_1 - \frac{f(x_1)}{f'(x_1)}
 \end{aligned}$$

where: x₁: Initial guess. x₂: Answer of the next step. f(x₁): Value of the function on the basis of initial guess. f(x₂): Value of the function on the basis of the final answer. f'(x₁): The value of the derivative of the function. Various complex problems that arise in hydraulics and water resources in general have been solved using evolution based programs and their hybrids. The applications of these techniques yield remarkable results when dealing with

respect to the number of possible solutions an engineer may be faced with dealing with the design and management of hydraulic systems (Savic and Walters, 1995). Basha and Kassab (1996) in their analysis of water distribution systems by perturbation method concluded that the method may prove advantageous when a water distribution network solver is needed as part of a larger model or program as in optimization or water quality modelling. They further concluded that the system process is fast and efficient, which could prove useful in the optimization of water distribution systems wherein the network is solved for every trial set of design parameters.

However, it is very important that a realistic assessment of the network structure, efficiency or vulnerability should avoid attempting an exclusive characterization of network structure of function by using only single or even few network measurements or ultimate indicators (Yazdani and Jeffrey, 2020). The aim of this research is to improve understanding of the modelling techniques used in the analysis of water distribution networks.

MATERIALS AND METHODS

The following software packages and flow measuring devices were used for the flow analysis:

- ≡ Microsoft Excel Spreadsheet.
- ≡ Pipe Flow Expert 2016 Version 6.39 is a window based software application manufactured by Pipe Flow Software.
- ≡ Venturi Tube Meter.
- ≡ Typical Water Distribution Network.

The pipe flow expert software described above was used to analyse the flow characteristics of a typical water distribution network and the several flow results or flow characteristics of the software was compared. The distribution network analysed was the water distribution network layout of a University Campus in South West Nigeria. For simplicity purpose, only the mains of the network were analysed and emphasis placed on the analysis of the loops the network was made up of. The results of the Hardy Cross model and that of the Newton Raphson model were compared using correlation analysis.

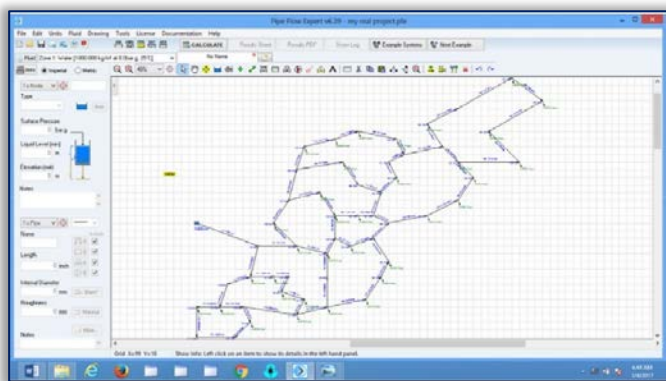


Figure 1: Graphical user interface of the pipe flow expert software for the Newton Raphson model

The Microsoft Excel spreadsheet carried out its calculations using the Hardy Cross method and the Pipe Flow Expert software employed the Newton Raphson model of analysis

to obtain the final flow rates in each pipe (as represented in Figure 1) after several iterations.

The following assumptions were made before the analysis was carried out:

- ≡ All nodes have same elevation.
- ≡ The diameter for each pipe was selected based on the purpose of making the initial flows uniform before iteration.
- ≡ The distribution systems receive 4.6 million litres of water daily which is equivalent to 1 million gallons daily.
- ≡ Piping components such as fittings, valves, bends and their losses were neglected.
- ≡ The pressure at each node was analysed and only the final flow rate in pipe after iteration was considered.

The final results from both models, the number of iterations, change in flow uniformity based on the velocity of flow were observed on completion of the analysis and the flow rates of both models were compared using the correlation method of descriptive statistics.

— Flow Analysis using a Venturi meter

The methodology applied here was the use of the Venturi effect, that is, the reduction in fluid pressure that results when a fluid flows through a constricted section of a pipe. The flow rate was now determined by measuring the change in pressure in the Venturi meter as shown in Figures 1 and 2. The Venturi effect was applied for flowing water in the Venturi meter at varying temperature with all other factors kept constant.

This was to obtain how significantly varying temperatures of an incompressible fluid such as water affect the flow rate. Flow rate was obtained for varying temperatures of 20°C, 30°C, 40°C, 50°C and 60°C. Finally, a graph of temperature against flow rate was plotted to obtain the equation of the line and a mathematical relationship between the two variables was generated.



Figure 2: Fluid Friction Factor Board Set Up for Venturi Tube Meter

RESULTS AND DISCUSSION

— Results of Numerical Analysis

The results of the final flow rate of the numerical analysis were obtained by solving a typical water distribution network using the Hardy Cross (HC) method and the Newton-Raphson (NR) method and they are as shown below in Table 1. The final flow rate was obtained after three iterations from the initial flow rate guessed.

Table I: Result of Numerical Analysis

| Pipe | Inner Diameter (mm) | Length (m) | Flow Rate (m ³ /s) | |
|------|---------------------|------------|-------------------------------|----------|
| | | | HC Model | NR Model |
| 1 | 200 | 700 | 0.054 | 0.054 |
| 2 | 140 | 300 | 0.031 | 0.031 |
| 3 | 100 | 700 | 0.017 | 0.018 |
| 4 | 70 | 367 | 0.004 | 0.002 |
| 5 | 70 | 400 | 0.004 | 0.002 |
| 6 | 100 | 500 | 0.012 | 0.009 |
| 7 | 90 | 100 | 0.01 | 0.009 |
| 8 | 95 | 230 | 0.011 | 0.01 |
| 9 | 100 | 300 | 0.005 | 0.012 |
| 10 | 100 | 160 | 0.012 | 0.012 |
| 11 | 105 | 330 | 0.014 | 0.013 |
| 12 | 140 | 400 | 0.023 | 0.023 |
| 13 | 90 | 400 | 0.008 | 0.009 |
| 14 | 90 | 460 | 0.008 | 0.009 |
| 15 | 60 | 360 | 0.002 | 0.002 |
| 16 | 65 | 650 | 0.003 | 8E-04 |
| 17 | 80 | 240 | 0.005 | 0.003 |
| 18 | 55 | 500 | 0.004 | 0.002 |
| 19 | 65 | 500 | 0.003 | 0.001 |
| 20 | 40 | 400 | 0.002 | 1E-04 |
| 21 | 30 | 100 | 0.001 | 0.001 |
| 22 | 120 | 260 | 0.019 | 0.018 |
| 23 | 90 | 267 | 0.011 | 0.011 |
| 24 | 80 | 267 | 0.009 | 0.009 |
| 25 | 55 | 340 | 0.003 | 0.002 |
| 26 | 65 | 320 | 0.005 | 0.003 |
| 27 | 70 | 300 | 0.006 | 0.004 |
| 28 | 75 | 600 | 0.007 | 0.005 |
| 29 | 100 | 450 | 0.013 | 0.012 |
| 30 | 95 | 253 | 0.013 | 0.011 |
| 31 | 40 | 180 | 0.013 | 0.002 |
| 32 | 30 | 260 | 0.002 | 0.001 |
| 33 | 75 | 220 | 0.008 | 0.008 |
| 34 | 75 | 284 | 0.008 | 0.008 |
| 35 | 75 | 180 | 0.008 | 0.007 |
| 36 | 60 | 167 | 0.005 | 0.004 |
| 37 | 100 | 200 | 0.012 | 0.011 |
| 38 | 85 | 330 | 0.01 | 0.009 |
| 39 | 50 | 460 | 0.003 | 0.002 |
| 40 | 35 | 300 | 0.002 | 0.001 |
| 41 | 30 | 200 | 0.001 | 0.001 |
| 42 | 95 | 233 | 0.013 | 0.011 |
| 43 | 75 | 200 | 0.008 | 0.007 |
| 44 | 65 | 360 | 0.007 | 0.005 |
| 45 | 65 | 300 | 0.005 | 0.005 |
| 46 | 100 | 150 | 0.012 | 0.012 |
| 47 | 95 | 100 | 0.012 | 0.011 |
| 48 | 95 | 100 | 0.012 | 0.011 |
| 49 | 50 | 150 | 0.004 | 0.003 |
| 50 | 55 | 300 | 0.005 | 0.004 |
| 51 | 110 | 200 | 0.016 | 0.014 |
| 52 | 75 | 353 | 0.008 | 0.007 |
| 53 | 55 | 332 | 0.003 | 0.003 |
| 54 | 65 | 460 | 0.005 | 0.049 |
| 55 | 27 | 400 | 0.005 | 0.006 |
| 56 | 75 | 150 | 0.073 | 0.007 |
| 57 | 80 | 200 | 0.008 | 0.007 |
| 58 | 65 | 300 | 0.005 | 0.004 |
| 59 | 65 | 360 | 0.005 | 0.004 |
| 60 | 45 | 340 | 0.002 | 0.002 |
| 61 | 70 | 460 | 0.006 | 0.001 |
| 62 | 50 | 360 | 0.004 | 0.003 |
| 63 | 80 | 333 | 0.009 | 0.008 |

□ Comparison of Hardy Cross and Newton Raphson Model

The Hardy Cross model uses an incremental change in flow rate to correct the initial guess work made when channelling the flow through the pipes while the Newton Raphson method attempts to solve all concerned equations simultaneously and iterations are used to solve the non-linear equations by finding the roots of the equations. This difference in methodical approach but similarity in flow principles created the interest in observing how the final flow rates calculated using these models correlate as shown in Figure 3. The correlation coefficient was calculated using the equation below

$$r = \frac{[N(\sum xy)(\sum x)(\sum y)]}{\sqrt{[N\sum x^2 - (\sum x)^2][N\sum y^2 - (\sum y)^2]}}$$

The values of X and Y represents final flow rate for the Hardy Cross method and the Newton Raphson method respectively where N represents the number of pipes which turns out to be 63. The value of the correlation coefficient ends up giving r = 0.54 which gives a positive but weak correlation between both methods. The number of iterations carried out by both models on the studied distribution network was the same; the weak correlation could be as a result of the difference in methodical approach. Although the final values of flow rates in each pipe were correct for both models based on their conformation to the principles governing the flow equations, the methodical approach is the cause if the discrepancies observed.

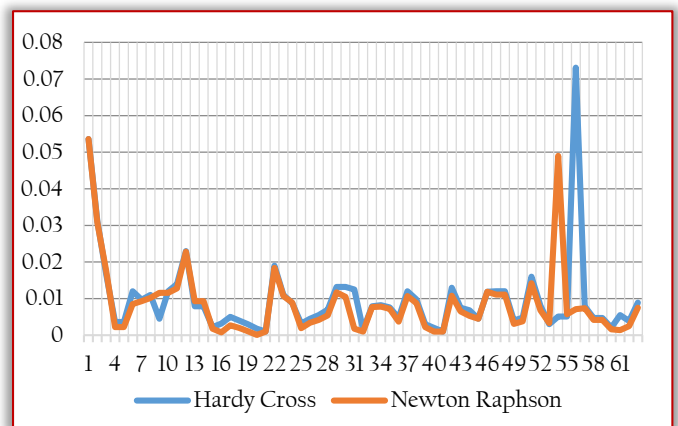


Figure 3: Image of the Correlation Plot between the Hardy Cross Model Result and the Newton Raphson Model Result

— Venturi Meter

The objective of the experiment carried out with the venturi meter was to observe the effect of temperature of water on its flow rate. This is carried out by checking for a change in the differential pressure at the manometer when water passes through the venturi tube from the divergent point to the convergent point. The temperature of the fluid rise varied between 20°C and 60°C and as the water flowed through the venture tube, the various differential pressure for each temperature was recorded from the differential pressure obtained, the flow rate for each temperature of water was obtained through the formula shown in the equation below:

$$Q = C_d \left[\frac{2d_p}{\rho} \right] \left[\frac{A_a}{\sqrt{\left(\frac{A_a}{A_b} \right)^2 - 1}} \right]$$

The results of the experiment are presented in Table 2:

Table 2: Flow Rate for Varying Temperature

| Temperature (°C) | Pressure Difference (mmH ₂ O) | Flow Rate (m ³ /s) | Velocity (m/s) | Viscosity 10 ⁻⁶ (m ² /s) |
|------------------|--|-------------------------------|----------------|--|
| 20 | 137 | 0.00042 | 0.522 | 1.01 |
| 30 | 170 | 0.00046 | 0.572 | 0.81 |
| 40 | 206 | 0.00051 | 0.572 | 0.67 |
| 50 | 245 | 0.00056 | 0.696 | 0.56 |
| 60 | 310 | 0.00063 | 0.784 | 0.45 |

The Table 2 above shows the flow rate obtained by varying temperature for the experiment carried out using a venturi tube. It was observed that as the temperature of the fluid increased, the velocity increased accordingly, which indicates there was an increase in the flow rate of the fluid. This increase in flow rate due to temperature could be attributed to the reduction in viscosity of the fluid as temperature increased. Although, the change or increase in flow rate was not significant, the little change signifies that temperature had an effect on the velocity of flow even if it is less significant in flow models for water due to its minimal effects. From the table it can be observed that there is a 0.0000052 m³/s average in the flow rate of water per degree rise in temperature for turbulent flow regimes in a venturi meter.

CONCLUSIONS

The study carried out here showed the similarities and discrepancies in results obtained in the application of the Hardy Cross method and the Newton Raphson method. The final flow in each of the pipe was governed by the Continuity equations and the Bernoulli equations, which was the reason the sum of head loss in each loop gives zero and the sum of flow into each junction equalled the sum flow exiting the junction.

The weak correlation in the final flow rates obtained from both methods after analysis has to do with the methodical approach towards analysing the network. It was also observed that as a result of the iterations carried out during the analysis, the final velocities changed from the initial uniform flow assumed before iteration.

The experiment carried out using the venturi meter indicates that there was an increase in velocity as a result of increase in temperature which in turn increases the overall flow rate of the water. This increase was as a result of the reduction in kinematic viscosity of the fluid due to temperature increase as this creates less resistance to shearing forces in order to enable flow.

References

- [1] Basha, H. and Kassab, B.: Analysis of Water Distribution Systems Using Perturbation Method, Applied Mathematical Modelling, 20, pp. 290-297, 1996.
- [2] Brkic, D. and Praks, P.: Short Overview of Early Developments of the Hardy Cross Type Methods for

Computation of Flow Distributed in Pipe Networks, Journal of Applied Sciences, pp. 1-15, 2019.

- [3] Ramalingam, D., Lingireddy, S. and Wood, D. J.: Using the WCM for Transient Modelling of Water Distribution Networks, Journal of American Works Association, 101 (2), pp. 75-89, 2009.
- [4] Savic, D. A. and Walters, G. A.: Generate Algorithm Techniques for Calibrating Network Models, A Report by Centre for Systems and Control Engineering, University of Exeter, North Park Road, Exeter, EX4 4QF, Davon United Kingdom, 1995.
- [5] Sereshki, F., Saffari, A. and Elahi, E.: Comparison of Mathematical Approximation Methods for Mine Ventilation Network Analysis, International Journal of Mining Science 2 (1), pp. 1-14, 2016.
- [6] Tezcan, T., Gokkms, U. and Sinir, G.: Analysis of Unsteady Flow in Complex Pipe Systems by the Method of Characteristics, Mathematical and Computational Applications 3 (1), pp. 27-36, 1998.
- [7] Yazdani, A. and Jeffrey, P.: Complex Network Analysis of Water Distribution Systems, School of Applied Sciences, Cranfield University, MK43 0AL, United Kingdom. <https://arxiv.org/pdf/1104.0121.pdf> Accessed: 15th May 2020.



ISSN: 2067-3809

copyright © University POLITEHNICA Timisoara,
Faculty of Engineering Hunedoara,
5, Revolutiei, 331128, Hunedoara, ROMANIA
<http://acta.fih.upt.ro>

¹Branislav SREDANOVIĆ, ¹Đjordje ČIČA, ¹Stevo BOROJEVIĆ,
¹Saša TEŠIĆ, ²Davorin KRAMAR

ANALYSIS OF CUTTING FORCES IN HYBRID TURNING AIDED BY GAS COMBUSTION HEATING OF WORKPIECE

¹University of Banjaluka, Faculty of Mechanical Engineering, Banja Luka, BOSNIA & HERZEGOVINA

²University of Ljubljana, Faculty of Mechanical Engineering, Ljubljana, SLOVENIA

Abstract: The global industry development is also reflected in the development of special engineering materials. These materials usually have special properties at high temperatures, such are tensile high strength and hardness. Due to this special properties, this materials usually have low machinability. Consequently, it is necessary to develop technologies for machining of mentioned materials, such are hybrid cutting processes. In this paper, the alloy steel X210Cr12 was turned, whereby the workpiece was heated. Heating, as secondary process, was performed by gas combustion, directly in point next to the point of the cutting tool action. Cutting forces were measured in the two cases: without heating, and by heating of workpiece. Effects analysis and process modeling were performed using Taguchi's experiment design, by combining the cutting parameters of primary process. The analysis showed significant reduction in cutting forces, but also poorer quality of machined surface. Conclusions were made about the possibilities of using this hybrid machining process in material machining.

Keywords: hybrid turning, heating, machinability, alloy steel

INTRODUCTION

The increasing of using engineering materials with special properties (alloyed structural and tool steels, special titanium and nickel alloys, ceramics, glass, sintered hard metals, composites, and etc.) in industrial, has led to the neediness to develop of the advanced machining methods [1]. Due to chemical content and structure (crystalline or amorphous) of these types of materials, special properties are reflected in increased tensile strength and hardness, durability on high temperatures, chemical resistance, and etc. Machining of these materials is very difficult regard to mentioned properties. There are difficulties in achieving the machined surface quality and dimensional accuracy, due to high cutting forces, high cutting temperatures, intensive cutting tool wear, unacceptable chip shape, vibrations, and etc. Consequently, there are difficulties to achieve adequate economic, productivity and operate safety, and process sustainability at least.

The development of hybrid processes, as advanced machining processes, is one of the directions to successfully machining of materials with special properties [2, 3]. Hybrid process combines basically processes regard to improved machining efficiency (Figure 1). CIRP definition of hybrid processes is that hybrid process combines two or more machining process in new one, where advantage of each of them can be used synergistically [2].

There are two types of hybrid processes: aided and mixture. In aided, only one of the combined processes, noted as primary process, directly removes the material, while the other process, noted as secondary, only helps to remove the material by positively affecting the material removal mechanism. In mixture, all involved processes are directly involved in material removal. Hybrid process can involve thermal, mechanical or electrochemical secondary process. In hybrid cutting processes aided by thermal process, the workpiece material softening due to its heating was used.

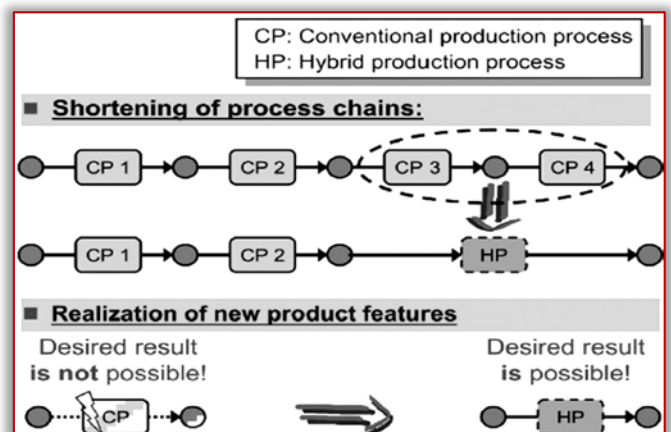


Figure 1. Principle of hybrid process introduction [2]

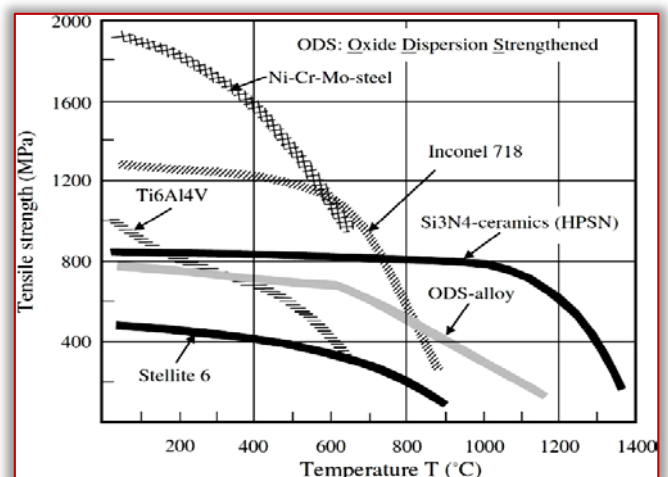


Figure 2. Tensile strength on different temperatures [3]

By increase of temperature, the workpiece material tensile strength and hardness decrease (Figure 2). It can be utilize with cutting by mechanical cutting tool, turning primarily, with aim to decrease cutting force and cutting tool wear. Other cutting processes (milling and drilling) have

constructive limitations, in terms of heat source action point and cutting tool tip relative positioning and orientation.

As the heat source of secondary process in thermal assisted machining, can be used: laser, plasma, electrical induction, and gas combustion. Laser and plasma are more commonly used due to the ability to focus heat on a small area, and relatively higher temperatures [4-7]. In other hand, laser and plasma devices must be mobile. This types of heat sources often have a high cost, and very high maintenance costs. Devices for electrical induction and gas combustion are much cheaper, and more available in production facilities. Disadvantage of this heating methods are the great heat dissipation and lower temperature [8].

In this study, workpiece was heated by gas combustion. The effect of using this type of heating on the cutting forces was analysed. The standard turning process without heating and the hybrid process were compared, and the machinability indicators were analysed.

EXPERIMENTAL SETUP

Experimental research was performed by turning. Machining system was consist lathe Prvomajska assembled with equipment for gas combustion (Figure 3). In addition, the risk of fire and the possible effect of flame and heat on machine parts, measuring devices and operator were taken into account.

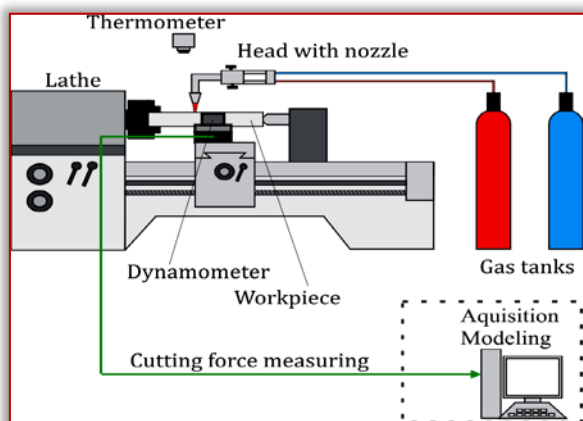


Figure 3. Schematic of machining system



Figure 4. Experimental measuring

Equipment for gas combustion was consist operating head, with gas nozzle, and gas flow adjustment valves. Head is connected to the two gas tanks via two hoses. As burning mixture, acetylene and oxygen are stored in the tanks. Point of heating was placed in front of point of cutting tool, on non-machined surface (Figure 4). Horizontal distance was between mentioned two point was 15 mm. Gas head was placed above of workpiece surface, on vertical distance of 15 mm. Workpiece materials was tool alloy steels X210Cr12. Its tensile strength on room temperature is $R_m = 600$ MPa. Workpiece was cylinder rod, diameter 50 mm and length 450 mm. This steel contains a relative large percentage of chromium, so it is one of the harder to cutting materials, due to high cutting force, pressures and intensive cutting tool wear. Cutting tool insert was SNMG 12 04 08, grade GC4525, manufactured by Sandvik. Tool holder was PSDNN 2525 M12.

Taguchi L9 plan of experiment was used. In experiment plan was combined primary process parameters, cutting parameters of turning, as follow: depth of cut was a_p of 1, 2 and 3 mm; feed rate f_n was 0.082, 0.164, and 0.330 mm/rev; and cutting speed v_c was 35, 60, and 106 m/min. By Taguchi plan, there was nine combinations made by mentioned tree cutting parameters (Table 1). Same sets of parameter combinations was used in two types turning: turning without heating and turning with heating. Resultant cutting force component: cutting force F_c (N), feed force F_f (N) and passive force F_p (N) was measured for each combination. Kistler measuring chain was used for cutting force measuring. It consisted of Kistler dynamometer Kistler 9259A, amplifier, A/D converter PC card, and analysing PC software.

Table 1. Taguchi plan combinations

| Exp no. | Depth of cut a_p (mm) | Cutting speed v_c (m/min) | Feed rate f_n (mm/rev) |
|---------|-------------------------|-----------------------------|--------------------------|
| 1 | 1.0 | 35 | 0.082 |
| 2 | 1.0 | 60 | 0.164 |
| 3 | 1.0 | 106 | 0.330 |
| 4 | 2.0 | 35 | 0.164 |
| 5 | 2.0 | 60 | 0.330 |
| 6 | 2.0 | 106 | 0.082 |
| 7 | 3.0 | 35 | 0.330 |
| 8 | 3.0 | 60 | 0.082 |
| 9 | 3.0 | 106 | 0.164 |

Workpiece surface temperatures during research was checked by remote point laser thermometer. Workpiece non machined surface temperature was from 460°C to 560°C. It was depended on feed rate (feed per tooth and cutting speed), because this parameter affects the retention time on the observed workpiece surface area. But, temperatures are not modelled in this part of study.

RESULTS AND DISSCUSION

Results of cutting force measuring without and with heating of workpiece are shown on Figure 5. Can be concluded that cutting forces depends on cutting parameters. The highest value is obtained for $a_p = 3$ mm, $f_n = 0.330$ mm/rev and $v_c = 35$ m/min. Cutting forces in case of workpiece heating showed

same tendency, but was lowest compare to forces without heating.

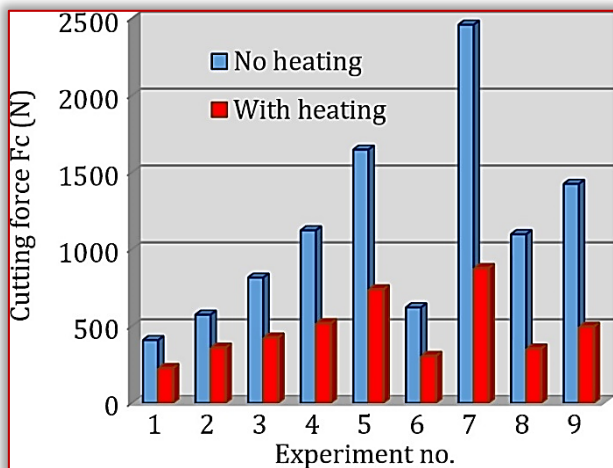


Figure 5. Cutting forces for two cases of turning

On Figure 6 and 7 are shown measured feed and passive forces for two cases of turning, without and with heating of workpiece. Based on combination and measured values, can be concluded that feed and passive force increase with increasing of cutting parameters. The higher values was obtained by using of higher values of depth of cut and feed rate, but the lowest value of cutting speed.

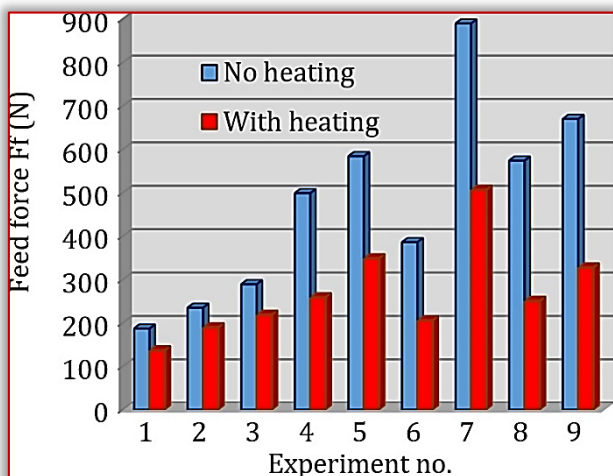


Figure 6. Feed forces for two cases of turning

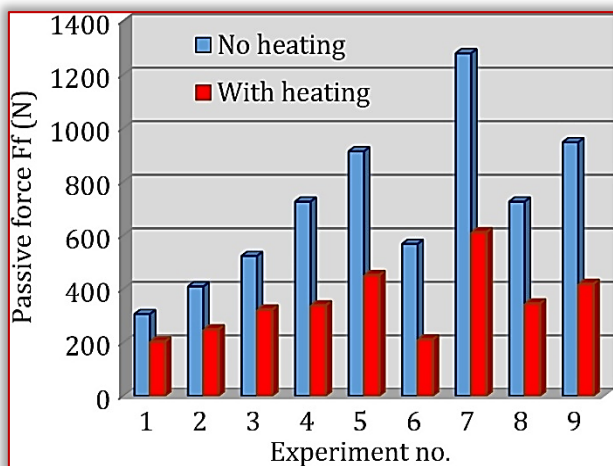


Figure 7. Passive forces for two cases of turning

Also, values of feed and passive forces in case of heating workpiece were lower in compare to the values obtained by turning without heating. On Figure 8, the percentage decrease in the value of the forces is shown. Minimum decreasing is obtained for feed forces on turning with cutting parameters $a_p = 1 \text{ mm}$, $f_n = 0.164 \text{ mm/rev}$ and $v_c = 60 \text{ m/min}$. Maximum value decreasing is obtained for cutting forces with cutting parameters $a_p = 3 \text{ mm}$, $f_n = 0.330 \text{ mm/rev}$ and $v_c = 35 \text{ m/min}$. However, the highest value of force was measured in this combination in case without heating. Higher percentages of reductions due workpiece heating were obtained in combinations with higher cutting parameter values. Higher percentages of were obtained for cutting forces in comparing with other two resultant cutting force components, also.

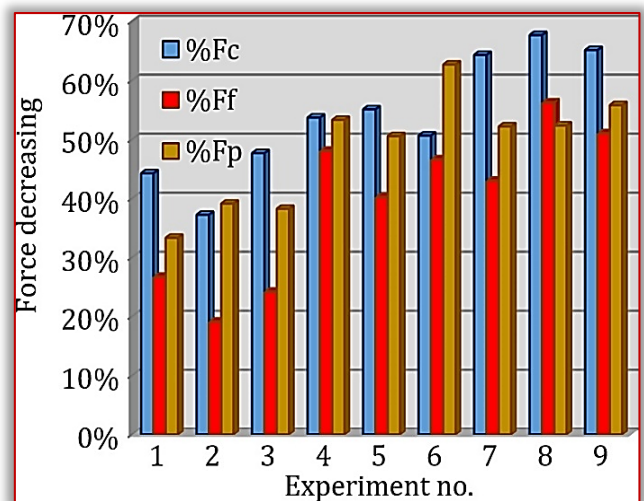


Figure 8. Percentages decreasing of cutting forces

Modelling and analysing of measured values was performed in DesigExpert 7.1 software. In modelling procedures, each cutting force components were analysed and modelled. Based on initial statistical parameters of F-value and P-value, for: model, each input parameters individually, and combination of input parameters, the software suggested the form of model function. Analyse of variance (ANOVA) was performed on each sets of measured values and adopted models.

In case of turning without workpiece heating, for cutting force model software suggested the linear model with all tree input parameters, but without their interactions:

$$F_c = -309.7 + 528.7 \cdot a_p - 5.0 \cdot v_c + 3751.2 \cdot f_n \quad (1)$$

Based on values and model mean value $\bar{x} = 1131.78$ and standard deviation $SD = 128.03$ was calculated. Signal to noise ratio was $S/N = 23.3$, and regression coefficient was $R^2 = 0.98$.

For feed and passive force, in case of turning without workpiece heating, software suggested the linear models with two input parameters depth of cut and feed rate, and without their interactions, follow as next:

$$F_f = -151 + 237.2 \cdot a_p + 812.4 \cdot f_n \quad (2)$$

$$F_p = -142.8 + 286 \cdot a_p + 1468.1 \cdot f_n \quad (3)$$

For feed force and passive force mean values are $\bar{x} = 479.3$ and $\bar{x} = 711.1$, respectively. Standard deviation is $SD = 49.5$ for feed force and $SD = 76.8$ for passive force. For feed force signal to noise ratio is $S/N = 23.6$, and regression coefficient $R^2 = 0.96$. For passive force $S/N = 21.1$, and $R^2 = 0.95$. Based on statistical analyse can be concluded that presented models are adequate. Model response for cutting force components in case of turning without workpiece heating are shown on Figure 9.

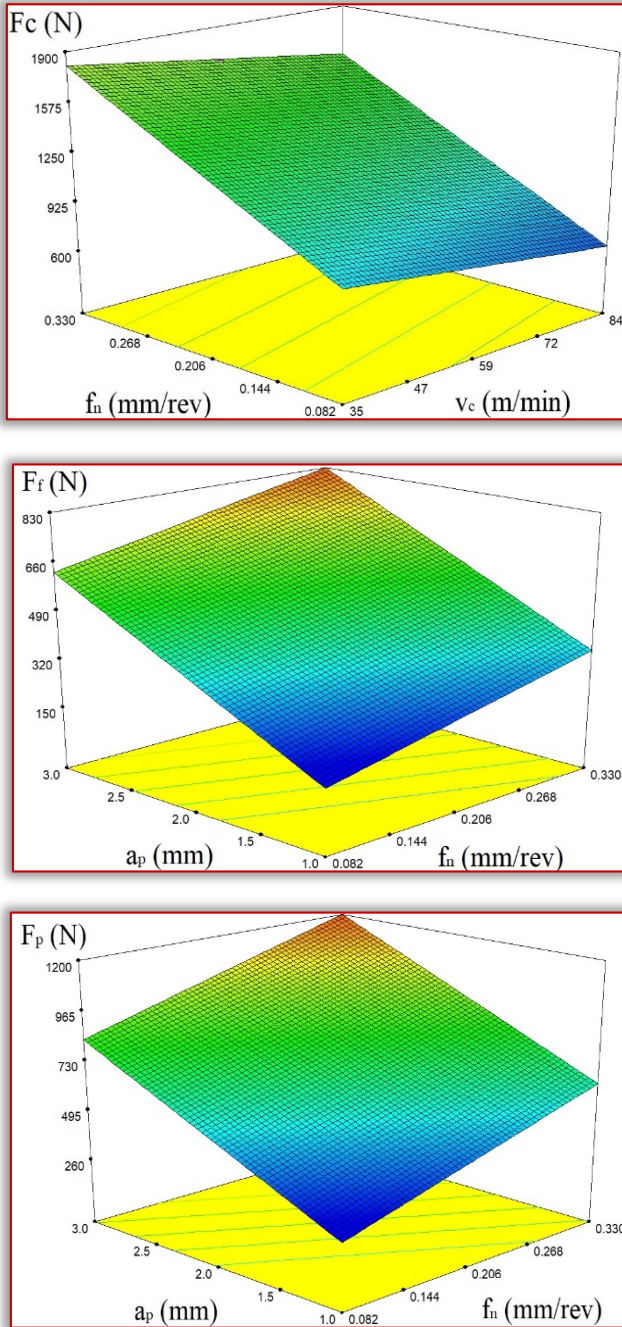


Figure 9. Model responses for turning without heating
For cutting and feed force in turning with workpiece heating, software suggested linear models with all tree input parameters, and their interactions. For passive force model, there was suggested linear model without parameter interaction. The mentioned models functions are listed below, while their responses are shown in Figure 10.

$$F_c = -72.5 + 78.3 \cdot a_p + 1.5 \cdot v_c + 2696.3 \cdot f_n - 17.6 \cdot v_c \cdot f_n \quad (4)$$

$$F_f = -60.2 + 69.3 \cdot a_p + 1.1 \cdot v_c + 1234.8 \cdot f_n - 8.91 \cdot v_c \cdot f_n \quad (5)$$

$$F_p = -52.3 + 100.2 \cdot a_p - 0.9 \cdot v_c + 828.9 \cdot f_n \quad (6)$$

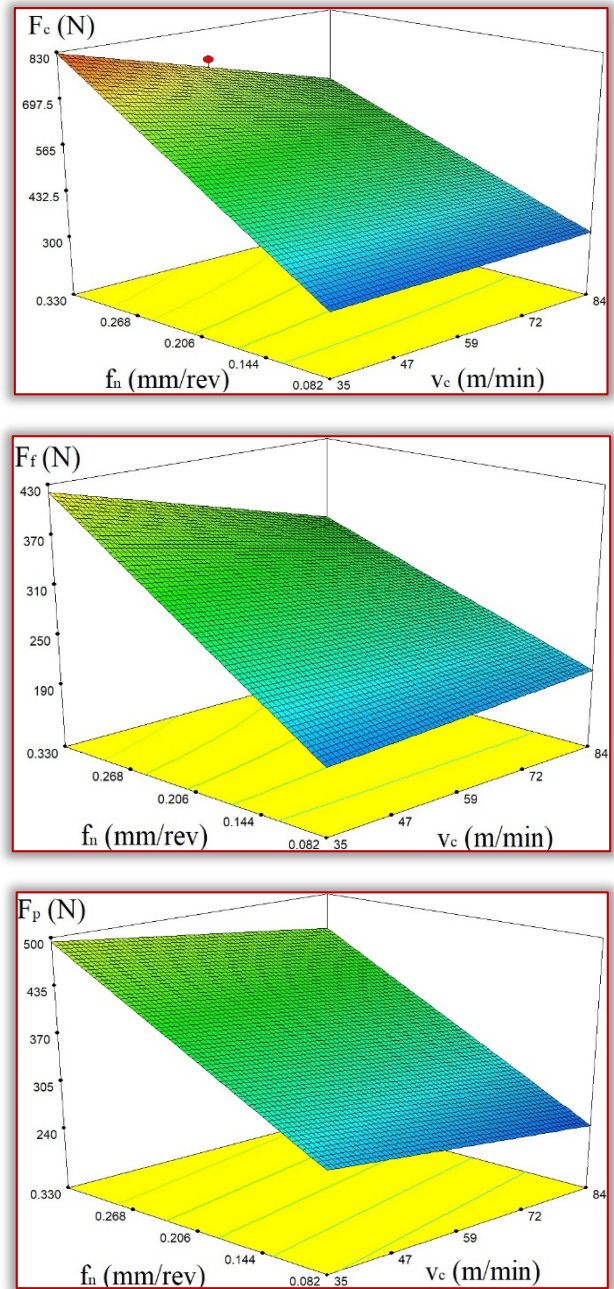


Figure 10. Model responses for turning with heating
Based on experimental obtained values and model responses, statistical parameters calculation is performed. For cutting force with workpiece heating data, mean value is $\bar{x} = 479.2$, and standard deviation is $SD = 37.8$. Signal to noise ratio was $S/N = 23.9$, and regression coefficient was $R^2 = 0.98$. For feed force with workpiece heating data, mean value is $\bar{x} = 271.8$, and standard deviation is $SD = 21.9$. Signal to noise ratio was $S/N = 22.5$, and regression coefficient was $R^2 = 0.98$. For passive force with workpiece heating data, mean value is $\bar{x} = 350.7$, standard deviation is $SD = 23.5$, signal to noise ratio is $S/N = 25.9$, and regression coefficient is $R^2 = 0.97$. Based on

calculated statistical parameters, there was concluded that previous presented linear models are adequate. Based on analysed data and model responses can be concluded that depth of cut and feed rate have high influence on cutting force components. As the values of these two parameters increase the values of the forces increase. Cutting speed has relative lower influence on cutting force component. Influence of cutting speed is often neglected in cutting force components models. In most cases, with increasing cutting speed, there is a decrease in cutting forces components. In the case of turning assisted by heating the workpiece, the cutting speed has a greater impact, especially in its interaction with the feed rate. The reason for this can be time and position of the heating flame action point. With higher speeds and steps, the workpiece heats up less.

CONCLUSIONS

From other research in this field, can be concluded that hard-to-machining materials are machined by lasers and plasma assisting, but these devices can be expensive and difficult to maintenance. However, laser and plasma have many advantages. In other hand, gas combustion heating devices are much cheaper and available.

Presented research in this paper shows possibility of reducing the cutting forces component in turning, by assisting with gas combustion heating of non-machined workpiece surface. The analysis is showed a significant difference in the values of the cutting forces components. Also, the models have shown that it is possible to adequately describe process and cutting forces. The value of the cutting forces components is significantly reduced. The reduction averages about 50%.

Additionally, the effect of heat on the machined surface was observed. There was poor machined surface, with visible burnt places. These facts could be investigated in future research, where the penetration of heat through the workpiece would be studied. Future research will directed on optimizing the heater head construction regard flame focusing. Examinations of the influence of its position relative to the cutting edge will be performed. Also, an analysis of the processing of different materials will be carried out, using different methods of workpiece heating.

Note:

This work is based on the paper presented at DEMI 2021 – The 15th INTERNATIONAL CONFERENCE ON ACCOMPLISHMENTS IN MECHANICAL AND INDUSTRIAL ENGINEERING, organized by Faculty of Mechanical Engineering, University of Banja Luka, BOSNIA & HERZEGOVINA, co-organized by Faculty of Mechanical Engineering, University of Niš, SERBIA, Faculty of Mechanical Engineering Podgorica, University of Montenegro, MONTENEGRO and Faculty of Engineering Hunedoara, University Politehnica Timisoara, ROMANIA, in Banja Luka, BOSNIA & HERZEGOVINA, in 28–29 May 2021.

References

[1] Gresik, W. (2008). *Advanced Machining Processes of Metallic Materials: Theory, Modelling and Application*. Elsevier, Amsterdam.

- [2] Klocke, F., Roderburg, A., Zeppenfeld, C., (2011). Design methodology for hybrid production processes. *Procedia Engineering*, vol. 9, pp. 417-430.
- [3] Virginia, G., et al. (2013). Mechanisms involved in the improvement of Inconel 718 machinability by laser assisted machining (LAM). *International journal of machine tools and manufacture*, vol. 74, pp. 19-28.
- [4] Tian, Yinggang, T., et al. (2008). Laser-assisted milling of silicon nitride ceramics and Inconel 718. *Journal of manufacturing science and engineering*. vol. 130, no. 3, pp. 3-10.
- [5] Dumitrescu, P., Koshy, P., Stenekes, J., Elbestawi, M.A. (2006). High-power diode laser assisted hard turning of AISI D2 steel. *International journal of advance manufacturing technology*, vol. 46, pp. 2009-2016.
- [6] Ding, H., Yung C. Shine, Y. C (2010), Laser-assisted machining of hardened steel parts with surface integrity analysis. *International journal of advance manufacturing technology*, vol. 50, pp. 106-114.
- [7] Masood, S.H., Armitage K., Brandt, M. (2011). An experimental study of laser-assisted machining of hard-to-wear white cast iron. *International journal of advance manufacturing technology*, vol. 51, pp. 450-456.
- [8] Mohammed, K. A., et al. (2020). Experimental Analysis of Hot Machining Parameters in Surface Finishing of Crankshaft. *Journal of Mechanical Engineering Research and Developments*, vol. 43, no. 4, pp. 105-114.



ISSN: 2067-3809

copyright © University POLITEHNICA Timisoara,
Faculty of Engineering Hunedoara,
5, Revolutiei, 331128, Hunedoara, ROMANIA
<http://acta.fih.upt.ro>

Fascicule 4

[October – December]

t o m e

[2021] XIV

ACTA Technica CORVINIENSIS
BULLETIN OF ENGINEERING



ISSN: 2067-3809

copyright © University POLITEHNICA Timisoara,
Faculty of Engineering Hunedoara,
5, Revolutiei, 331128, Hunedoara, ROMANIA
<http://acta.fih.upt.ro>

FUSION OF SOFT COMPUTING AND CHAOS THEORY TO BUILD A MODEL FOR PREDICTION QUALITY OF WASTEWATER IN INDUSTRIAL ZONES

¹ Department of the Information Technology, Hanoi university of Industry, Bac Tu Liem Distric, Ha Noi, VIETNAM

Abstract: In this paper, we present a novel method for detecting environmental pollution of waste-water in industrial zones. Firstly, the quality of waste-water data is filtered by an adaptive filter. After that, the false nearest neighbor and average mutual information algorithms are applied to find embedding dimension space and time delay of waste-water quality time series to form training and testing set for the model. Finally, the Support Vector Regression and Fuzzy logic is implemented to build model for prediction quality of waste-water in industrial zones. Four main parameters at the waste-water processing station of Nittoku paper factory in the Kim Bang district, Ha Nam province, Vietnam have been used to test proposed method. The experimental results show that the proposed model is high accuracy and short training time, to helps waste-water processing station operators take early action and avoid environmental pollution.

Keywords: Support Vector Regression, Fuzzy logic, pollution, waste water, time delay, embedding dimension space

INTRODUCTION

According to Circular 24 of the Vietnamese Ministry of Natural Resources and Environment, all industrial zones that is discharged waste into the environment with a flow rate is greater than 1000 m³ per day must be installed an automatic monitoring system for waste-water quality. At the waste-water processing station of an industrial zone, the operator based on certain measurement and monitoring values, must take proper action when any criterion of waste-water is over the permitted threshold value. Therefore, waste-water that does not satisfy this standard that has already discharged to environment lead to environment pollution. Hence, to avoid the environmental pollution, we can build a model based on historical data collected by data-loggers to predict future quality of the waste water; the model could help operators of the waste water processing stations take early action to make sure that the quality of the waste water always satisfies the standard requirements.

Predicting future time series values from the past is applied in many fields, such as the following: economics where forecasting stock price helps investors choose the best time to invest in the stock market to get the highest profit; predicting exchange rates which helps import-export businesses choose appropriate times to import or export products (Wang, Y. F., 2002; Castillo, Oscar Melin, Patricia, 2002); energy, where predicting the wind speed of a wind farm and the electrical load helps energy policymakers give a best plan to meet the requirement of clients (Lanzhen, L., Tan, S. et al., 2010; Hua, X., Zhang, D., Leung, S.C., et al., 2010), and so on.

Due to the importance of predictive work, scientists have successfully used a number of techniques in recent years to build a data series predictive model. In (Hua, X., Zhang, D., Leung, S.C., 2010) authors combined Kernel Regression (KR) and Function Link Artificial Neural Network (FLANN) to predict exchange rates from USD to GBP, INR and JPY. KR played role in filtering and FLANN was a model for

prediction. The authors in (Hanas, M.P., Curtis, P.G., 2008) used chaos theory and reconstructed state space for predicting the exchange rates between USD and EUR. Fan-Yong Liu (et al. 2010) used a hybrid Discrete Wavelet Transform (DWT) and Support Vector Regression (SVR) to predict the exchange rates between CNY and USD. Firstly, he used DWT to decompose the time series data to a different time scale and then he chose an appropriate kernel function for SVR and prediction corresponding with each time scale. Finally, he synthesized the prediction result from different predicted time scale results. The authors in (Iokibe, T., Murata, S., Koyama, M et al. 1995) used a local fuzzy reconstruction method to predict exchange rates between JPY, USD and CAN. The authors in (Božić, J., Vukotić, S., Babić, D. et al. 2011) used a successful wavelet transform to filter noise in the exchange rate time series before using it for training and prediction based on Multi-Layer Feed Forward Neural Network. Weiping Liu (2018) used hybrid of neuron and fuzzy logic to predict exchange rates between JPY and USA.

Recently, scientific literature (Nghien Nguyen Ba and Ricardo Rodriguez Jorge et al. 2019) has been used SVR and Fuzzy logic to build model for prediction quality of waste-water in industrial zone. To specify number of the inputs for the model they used embedding dimension space. They used default time delay is one. The drawback of their proposed method is using original data time series that is contaminated by noise so the embedding dimension space of time series data is high and time delay is one so it is hard to distinguish two data points next to each other. This phenomenon caused not only the model's complexity but also loose accuracy prediction. Authors in [18] used SVR to build model to predict surface roughness in hole turning process of 3X13steel. They reported that SVR model is better accuracy prediction than response surface method (RSM). Authors in [19] used SVR for prediction the sorption

capacity of lead (II) ions. They statement that SVR model is more accurate and generalized for prediction of the sorption capacity of lead (II) ions than multiple linear regression does. Authors in [20] compares the classical regression with SVR using some dataset base on root mean square error (RMSE) and R^2 . They report that SVR achieves more accuracy prediction than classical model.

In this paper, the author proposes a fusion method to build model for prediction quality of waste-water in industrial zones. Firstly, he uses Hilbert – Huang transform as an adaptive filter to filter out noise from the original time series data. Next, the proposed method used false nearest neighbor and mutual information of cleaned time series data to find embedding dimension space and time delay. After that, forming input – output training pair from cleaned time series data and found embedding dimension space and time delay. Finally, method builds a model base on SVR and Fuzzy logic for prediction quality of the waste-water. Our proposed method not only decrease system's complexity but also increase accuracy of prediction.

RELATED WORK

— Finding the time delay

According to the literature review (Abarbanel, H.D., Brown, R., Sidorowich, J.J., Tsimring, L.S., 1993). If we select the time delay T too small, then two data points $s(n+jT)$ and $s(n+(j+1)T)$ will be so close to each other that we can not distinguish them from each other. Similarly, if we choose T so large, then $s(n+jT)$ and $s(n+(j+1)T)$ are completely independent of each other in a statistical sense. To determine proper time delay of a time series we can base on average mutual information. Assume we have two systems called A and B, and measured values from those system denoted by a_k , b_k . The mutual information between a_k and b_k is specified as equation (1) below:

$$I_{AB}(a_i, b_k) = \log_2 \left[\frac{P_{AB}(a_i, b_k)}{P_A(a_i)P_B(b_k)} \right] \quad (1)$$

where, $P_A(a)$ is probability of observing a out of the set of all A, and the probability of finding b in a measurement of B is $P_B(b)$, and the joint probability of the measurement of a and b is $P_{AB}(a, b)$.

The average mutual information between measurements of any value a_i from a system A, and b_k from a system B is average over all possible measurements of $I_{AB}(a_i, b_k)$ and can be calculated by equation (2) below:

$$I_{AB}(T) = \sum_{a_i, b_k} P_{AB}(a_i, b_k) I_{AB}(a_i, b_k) \quad (2)$$

To apply this definition into time series data $s(n)$ which is measured from a physical system. We consider set of measurements $s(n)$ as the set A and measurements a time lag T , $s(n+T)$, as the B set. The average mutual information between time series $s(n)$ and $s(n+T)$ can be evaluated as equation (3).

$$I(T) = \sum_{i=1}^n P[s(n), s(n+T)] \log_2 \left[\frac{P[s(n), s(n+T)]}{P[s(n)]P[s(n+T)]} \right] \quad (3)$$

Hence, the average mutual information is a function of time lag T and T can be specified as the first min of the $I(T)$. If $I(T)$ has not a minimum, then T will be chosen as 1.

— Finding the embedding dimension space

The number of inputs for predictor is embedding dimension or can be thought as windows size (Frank, R.J., Davey, N.,

Hunt, S.P.). To valuate this parameter (Abarbanel, H.D., Brown, R., Sidorowich, J.J., Tsimring, L.S.) present the implementation of false nearest neighbors to find the minimum embed dimension. Assume we have a data time series, $s(n)$, the idea of the algorithm to combine sequence values of series together to form a set of vectors V of dimension d ($d=1, 2, 3, \dots$). For example, vector $v(k)=[s(k), s(k+T), s(k+2T), \dots, s(k+(d-1)T)]$, where T is time lag of time series. We use Euclidean distance to calculate the distance between two vectors. Formula (4) calculates the distance between vectors $v(k)$ and $v(m)$.

$$D(d)_{km} = \sqrt{\sum_{i=0}^{d-1} [s(k+i) - s(m+i)]^2} \quad (4)$$

For any $v(k)$ we can find its nearest neighbor $v(m)$ with distance $D(d)_{km}$, increase the dimension to $d+1$ to calculate $D(d)_{km}$, and check expression (5) to determine if the distance meets, which is then a false nearest neighbor.

$$\frac{|D(d)_{km} - D(d+1)_{km}|}{D(d)_{km}} > D_{th} \quad (5)$$

where D_{th} is the threshold. According to Abarbanel, H.D., Brown, R., Sidorowich, J.J., Tsimring, L.S. the D_{th} lies in the range 10 to 50. In our case we choose D_{th} to be 15. We repeat this procedure from $d = 1$. After each iteration, we increase d by 1 until the percent of false nearest neighbors is approaching zero or a small value in case of increasing d but the percent of false nearest neighbor decreases slowly or is unchanged.

— Building the model based on Support Vector Regression (SVR)

The goal of a Support Vector Machine (SVM) is to find the optimal hyper plane (Hyper plane may be plane or curve) to classify data into two separate regions so that the distance between the closest point and the hyper plane is at maximum. This is also called the margin. Figure 1 illustrates a hyper plane and a margin.

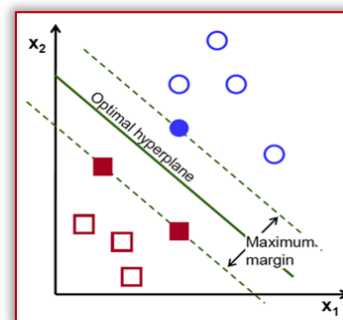


Figure 1. Illustration of the hyper plane and the margin.

Source: Data Mining Map https://www.saedsayad.com/support_vector_machine_reg.htm

Assume, the equation of a hyper plane is $w \cdot x + b = 0$. The goal for the SVM algorithm is to find w and b to maximize the margin. The SVM algorithm not only applies to solving classification problems but also to finding solutions to regression subjects. The SVR algorithm is based on a loss function, which is tolerant of error for points distant from the true value with in a small epsilon. This means that this function gives zero error for all the points in training set that lie in the epsilon range. Figures 2 and 3 illustrate linear and nonlinear regression within the epsilon range.

For SVR, the input x is mapped into m dimension feature space by a nonlinear mapping function first, and then the linear model is built, which is based on this dimension feature space by equation (6):

$$f(x, w) = \sum_{i=1}^m w_i \cdot g_i(x) + b \quad (6)$$

where: $g_i(x)$, $i = 1, 2, 3, \dots, m$ is a set of nonlinear mapping functions.

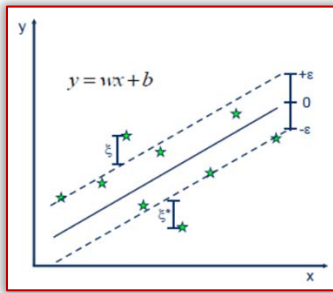


Figure 2. Linear regression with the epsilon range.
Source: Data Mining Map https://www.saedsayad.com/support_vector_machine_reg.htm

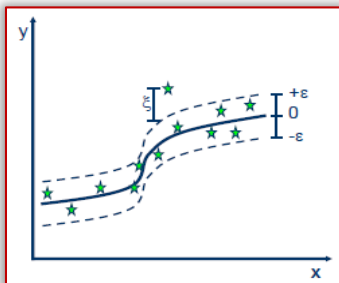


Figure 3. Nonlinear regression with the epsilon range.
Source: Data Mining Map https://www.saedsayad.com/support_vector_machine_reg.htm

The accuracy of the estimate is evaluated by loss function $L(y, f(x, w))$. SVR uses a loss function called epsilon – an insensitive loss function which proposed by Vapnik:

$$L = \begin{cases} 0 & \text{if } |y - f(x, w)| \leq \varepsilon \\ |y - f(x, w)| & \text{otherwise} \end{cases} \quad (7)$$

Thus, SVR is performs linear regression in multi dimension feature space using function L and minimizing $\|w\|^2$ for decreasing complexity of the model. This problem can be solved by introducing slug variables ξ_i and ξ_i^* with $i = 1, 2, 3, \dots, n$, to measure the deviation of the training samples which lie outside of the epsilon range. Therefore, SVR is minimized by the function below:

$$\min \frac{1}{2} \|w\|^2 + C \sum_{i=1}^n (\xi_i + \xi_i^*) \quad (8)$$

with constraints:

$$\begin{cases} y_i - f(x_i, w) \leq \varepsilon + \xi_i^* \\ f(x_i, w) - y_i \leq \varepsilon + \xi_i \\ \xi_i, \xi_i^* > 0 \forall i = 1, \dots, n \end{cases} \quad (9)$$

Applying the duality theorem for minimizing problems, we finally obtain the function $f(x)$:

$$f(x) = \sum_{i=1}^{n_{SV}} (\alpha_i - \alpha_i^*) \cdot K(x_i, x) + b \quad (10)$$

$$0 \leq \alpha_i, \alpha_i^* \leq C$$

where: n_{SV} is the number of support vector, and $K(x_i, x)$ is the kernel function which can be defined as

$$K(x_i, x) = \sum_{j=1}^m g_j(x_i) \cdot g_j(x) \quad (11)$$

— Building a model bases on fuzzy logic

Assume that we have a data time series that was collected from a system at equal time intervals denoted by $s(1), s(2), s(3), \dots, s(n)$. The task of the prediction time series to find a mapping from $[s(k-(d-1)T), s(k-(d-2)T), \dots, s(k)]$ to $s(k+T)$, where d and T are constant positive integer numbers, and d is the number of inputs to the predictor, T is time lag of time series data. For simple case, we assume $d = 2$ and $T = 1$. Figure 4 below shows the block diagram of the system for prediction. According to the algorithm presented by L. Wang (Li, W., 1994), we first form $n - 2$ input – output pairs: $(s(1), s(2) \rightarrow s(3)), (s(2), s(3) \rightarrow s(4)), \dots, (s(n-2), s(n-1) \rightarrow s(n))$. Next, we find the maximum and minimum of the time series and divide this domain interval into $2 * R + 1$ regions (R is a positive integer number), denoted by $T_1, T_2, \dots, T_{2 * R + 1}$ and then we assign each region with a fuzzy membership function. In our case, we choose the shape of membership function as a triangle wave. Figures 4 and 5 illustrate the fuzzy system and membership function of the input and output with $R = 3$.

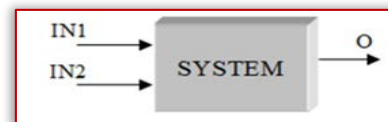


Figure 4. Fuzzy system with 2 input and 1 output.
Source: authors' research

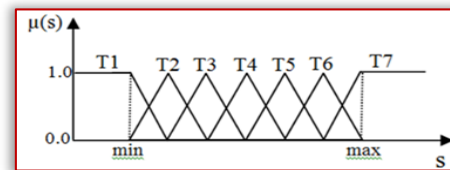


Figure 5. Membership function for input and output.
Source: authors' research

In the next step we calculate the degree of given input-output pairs in different regions, assign it to the region with maximum degree, and then form an IF – THEN rule. For example, IN_1 has a max degree 0.85 in region T_1 , IN_2 has a max degree 0.7 in region T_3 and O has a max degree 0.8 in region T_7 . Hence, we form the rule: IF IN_1 is T_1 AND IN_2 is T_3 THEN O is T_7 . Repeating this procedure for each input – output pair gives a set of rules. To avoid conflict rule (two rules have same IF part but different THEN part), we only accept the rule from the conflict group that has a maximum degree. To do so we use table – lookup to present a fuzzy rule base. The cells of the rule base are filled by the rules. If there is more than one rule on one cell of the fuzzy rule base, then the rule that has highest degree is used. The degree of the rule is calculated by formula (12) below:

$$D(\text{rule}) = \mu_A(IN_1) \times \mu_B(IN_2) \times \mu_C(O) \quad (12)$$

So far, we obtain the fuzzy rule base corresponding to all input-output pairs. The next task is calculating output O when we have a new input sample IN_1 and IN_2 . Firstly, calculate the degree of output control of the k -th rule combined with the fuzzy rule base corresponding to the new input IN_1 and IN_2 according to formula (13) below:

$$\mu_{O^k} = \mu_{1k}(IN_1) \times \mu_{2k}(IN_2) \quad (13)$$

where O^k denotes the output region of rule k , and I_j^k denotes the input region of rule k for the j -th component. Finally, we use the centre average defuzzification formula to determine the output.

$$o = \frac{\sum_{k=1}^N \mu_{O^k}^k \times o^k}{\sum_{k=1}^N \mu_{O^k}^k} \quad (14)$$

where O^k denotes the center value of region O^k and N is number of rules in the combined fuzzy rule base.

— The Empirical Mode Decomposition method (EMD)

The EMD method is developed from the simple assumption that any non-stationary and non-linear signal consists of number of intrinsic mode of oscillations. In this way, any signal can decomposition into a number of intrinsic mode function (IMF) which has two interesting properties (N. E. Huang, et al., 1998). The first one is in the whole dataset, the number of extrema and the number of zero-crossings must either equal or differ at most by one. The second one is at any point, the mean value of the envelope defined by the local maxima and, the envelope defined by the local minima is zero.

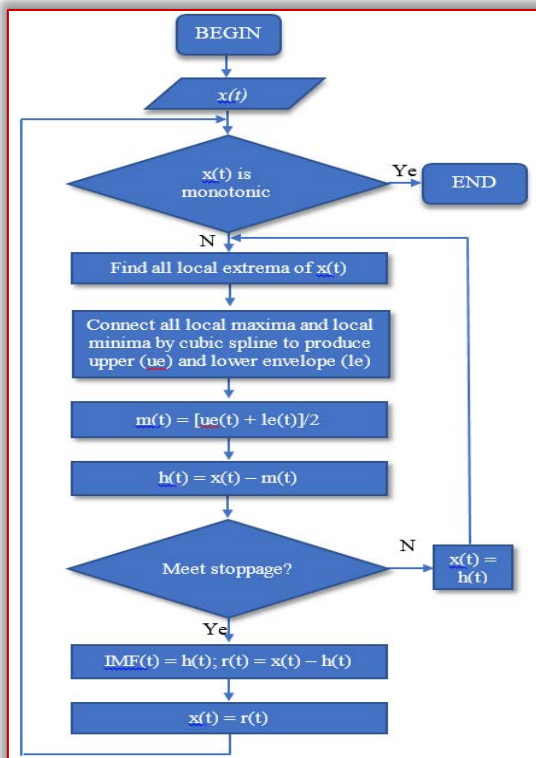


Figure 6. Flowchart of EMD algorithm.

Source: authors' research

With the above definition for the IMF, the algorithm to decompose any data set $x(t)$ into IFM as flowchart in figure 6.

In figure 6 we should make some clearly describe. The monotonic function is function that has maximum two extrema. The stoppage was used by doctor Huang (Huang et al. 1998). This stoppage criterion is determined by using a Cauchy type of convergence test. Specifically, the test requires the normalized squared difference between two successive sifting operations defined as:

$$SD_k = \frac{\sum_{t=0}^T |h_{k-1}(t) - h_k(t)|^2}{\sum_{t=0}^T h_{k-1}(t)^2} \quad (15)$$

If this squared difference SD_k is smaller than a predetermined value, the sifting process will be stopped.

Summing up all IMFs and residue we obtain:

$$x(t) = \sum_{i=1}^n IMF_i + r_n \quad (16)$$

Thus, one achieves a decomposition of the data into n -empirical IMF modes, plus a residue, r_n .

PRINCIPLES OF OUR PROPOSAL

Principal of our proposed method is illustrated by Figure 7.

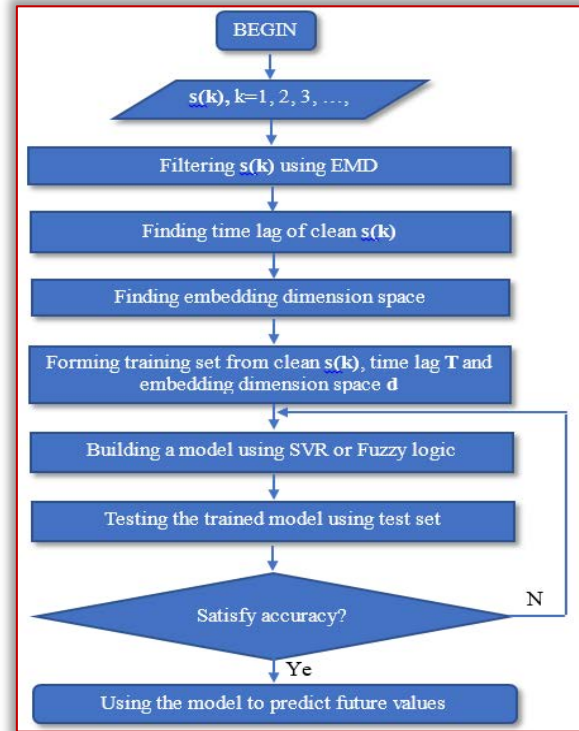


Figure 7. Principles of our proposed method.

Source: authors' research

The first step, we clean the original signal by using EMD. To do so, we decompose original signal into a number of IMFs. After that, we calculate correlation between original signal and each IMF. Finally, we synthesis signal without low correlation and high frequency IMFs. The second step, we find time lag of clean data. The next step, we find embedding dimension space of clean data. After that, forming training set from clean $s(k)$, time lag T and embedding dimension space d . Then, we train the model is built by fuzzy logic or SVR. Next, we test the trained model using testing data and check the accuracy criterion. If it meets the criterion then, we use the model for predicting future values. Otherwise, we change model's parameters and go back to the training model step.

EXPERIMENTAL RESULTS

To assess the performance of our proposal we use four time series data consisting of PH, temperature, TSS and COD. These data sets are collected from 0 AM of 25th February 2019 to 2 PM of 26th February 2019 with the sampling period set to five minutes at the waste water processing station of Nittoku paper factory in the Kim Bang district, Ha Nam province, Vietnam. The total data length is 451 points for

each parameter. We use the first 40l points as training set and use the remaining 50 points as the test set. Firstly, each time series data is decomposed into IMFs by the EMD algorithm, and then synthesis signal (clean signal) from IMF and residue without high frequency and low correlation IMF. Figure 8, 9 demonstrate EMD and synthesis for PH time series. After that, time lag and embedding dimension space of clean signal are found. Finally, the models have been built by fuzzy logic or SVR.

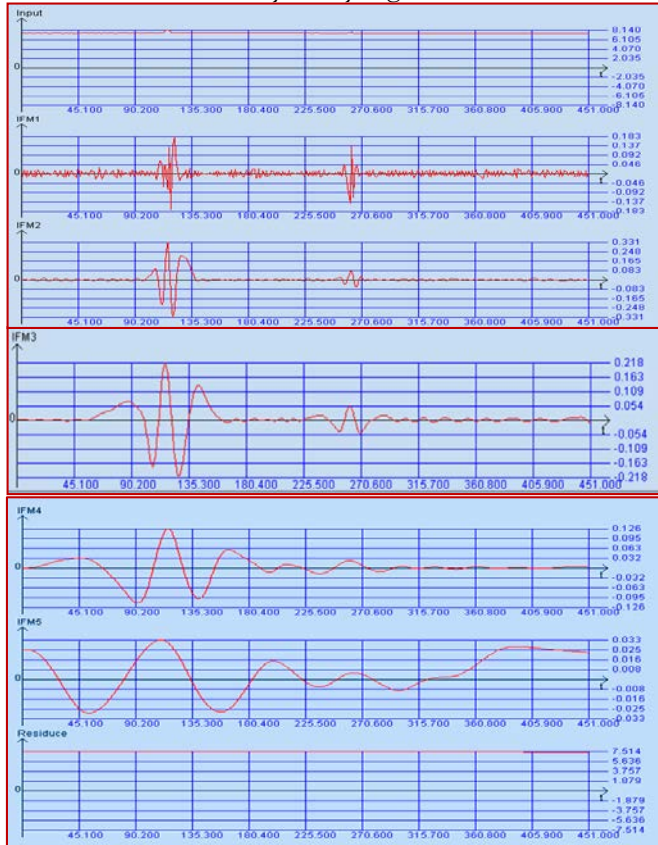


Figure 8. The IMFs of PH signal.
Source: authors' research



Figure 9. The synthetical PH signal.
Source: authors' research

With the PH parameter we find that the time lag is one and embedding dimension space is four. This means that we use four points' data from the past to predict one point in the future, or the model has four inputs and one output. Figure 10 shows prediction results by the SVM model vs the fuzzy logic model. The mean square error of SVR is 0.000074, while fuzzy logic is 0.0002.

For the temperature parameter, we found the time lag is two and the embedding dimension space of the time series is four. Figure 11 shows prediction results by the SVM model vs the fuzzy logic model. The mean square error of SVR is 0.008, while fuzzy logic is 0.03.

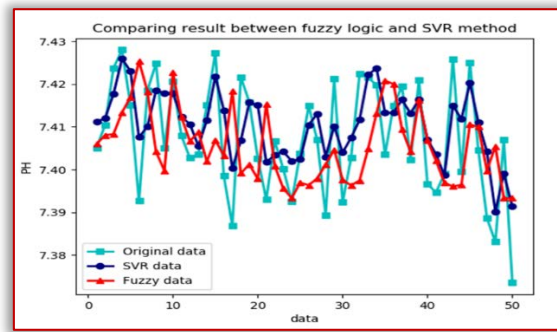


Figure 10. The prediction result for PH parameter.
Source: authors' research

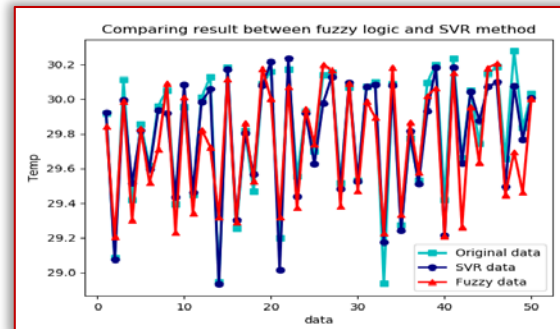


Figure 11. The prediction result for temperature parameter.
Source: authors' research

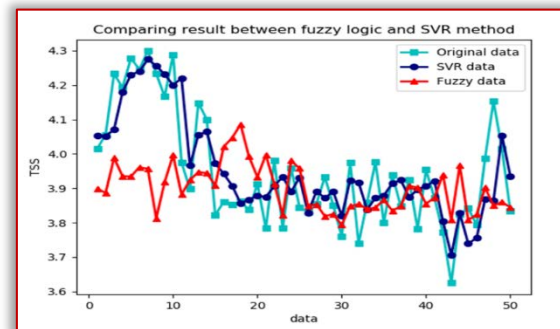


Figure 12. The prediction result for TSS parameter.
Source: authors' research

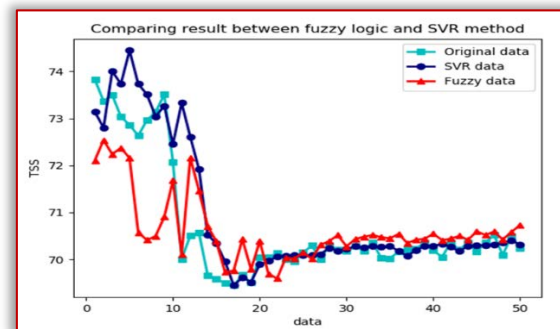


Figure 13. The prediction result for COD parameter.
Source: authors' research

For the TSS, we found the time lag is 12 and the embedding dimension space of the time series is four. Figure 12 shows prediction results by the SVM model vs the fuzzy logic model. The mean square error of SVR is 0.008, while fuzzy logic is 0.051.

For the COD, we found the time lag is 2 and the embedding dimension space of the time series is five. Figure 13 shows

prediction results by the SVM model vs the fuzzy logic model. Mean square error of SVR is 0.018, while fuzzy logic is 0.77.

Table 1 compares the performance between a previous proposed method and the author' novel method.

Table 1. Comparison performance between previous and novel method

| Method | Embed. dim. space | Time lag | MSE | |
|----------|-------------------|----------|-------|----------|
| | | | Fuzzy | SVR |
| Previous | 9 | 1 | 0.003 | 0.000077 |
| Novel | 4 | 1 | 0.002 | 0.000074 |

| Method | Embed. dim. space | Time lag | MSE | |
|----------|-------------------|----------|-------|-------|
| | | | Fuzzy | SVR |
| Previous | 11 | 1 | 0.09 | 0.04 |
| Novel | 4 | 2 | 0.03 | 0.008 |

| Method | Embed. dim. space | Time lag | MSE | |
|----------|-------------------|----------|-------|-------|
| | | | Fuzzy | SVR |
| Previous | 9 | 1 | 0.07 | 0.06 |
| Novel | 4 | 12 | 0.051 | 0.008 |

Source: author' research

CONCLUSIONS

In this paper, author present the fusing of empirical mode decomposition, average mutual information, false nearest neighbor algorithm to clean, find time lag and embedding dimension space for time series, fuzzy logic and SVR to build model for predicting quality of waste water in industrial zone. EMD plays adaptive filter role to clean data time series helps decreasing embedding dimension. From the results of experiment show that the proposed method not only decreases complexity of the model but also increases accuracy of prediction. In addition, the experimental results also show that the SVR model obtains the results are more accurate than fuzzy model for all case study. However, training fuzzy logic model spend smaller time than SVR model because training fuzzy logic model we only need to travel training data set one time while training SVR model we need to travel training data set many times. Therefore, we can apply fuzzy logic model for real time and least accurate parameter. Otherwise, we apply SVR model.

References

[1] According to Circular 24 of the Vietnamese Ministry of Natural Resources and Environment: 24/2017/TT-BTNMT, 1st September 2017, Ha Noi, Vietnam, 2017

[2] Abarbanel, H.D., Brown, R., Sidorowich, J.J., Tsimring, L.S., (1993). The analysis of observed chaotic data in physical systems. *Reviews of modern physics*. 1993 Oct 1;65(4):1331.

[3] Božić, J., Vukotić, S., Babić, D., (2011). Prediction of the RSD exchange rate by using wavelets and neural networks. In 2011 19th Telecommunications Forum (TELFOR) Proceedings of Papers 2011 Nov 22 (pp. 703-706). IEEE.

[4] Castillo, O., Melin, P. (2002). Hybrid intelligent system for time series prediction using neural networks, fuzzy logic, and fractal theory. *IEEE transactions on neural network* Vol.13, No.6, November 2002

[5] Frank, R.J., Davey, N., Hunt, S.P., (2001). Time series prediction and neural networks. *Journal of intelligent and robotic systems*. 2001 May 1;31(1-3):91-103.

[6] Haniias, M.P., Curtis, P.G. (2008). Time series prediction of dollar/euro exchange rate index. *International Research Journal of finance and economics*. 2008;15:232-9.

[7] Hua, X., Zhang, D., Leung, S.C. (2010). Exchange rate prediction through ANN Based on Kernel Regression. In 2010

Third International Conference on Business Intelligence and Financial Engineering 2010 Aug 13 (pp. 39-43). IEEE

[8] Iokibe, T., Murata, S., Koyama, M., (1995). Prediction of foreign exchange rate by local fuzzy reconstruction method. In 1995 IEEE International Conference on Systems, Man and Cybernetics. Intelligent Systems for the 21st Century 1995 Oct 22 (Vol. 5, pp. 4051-4054). IEEE

[9] Wang, Y.-F. (2002). Predicting stock price using fuzzy grey prediction system. *Expert system with application* 22 (2002) 33-39

[10] Lanzhen, L., Tan, S. (2010). The study on short-time wind speed prediction base on time-series neural network algorithm. Power and energy engineering conference (APPEEC), 2010 Asia-Pacific

[11] Liu, F-Y., (2010). Exchange Rate Based on Wavelet and Support Vector Regression. *Advanced Computer Control (ICACC), 2010 2nd International Conference*.

[12] Liu, W., (2008). Forecasting Exchange Rate Change between USD and JPY Using Dynamic Adaptive Neuron-Fuzzy Logic System. *Asia Pacific Journal of Finance and Banking Research*. 2008 Jul 4;2(2)

[13] Li, W., (1994). *Adaptive Fuzzy Systems and Control Design and Stability Analysis*. Prentice Hall International, 1994, pp. 65-69.

[14] N. E. Huang, et al., (1998). The empirical mode decomposition and the Hilbert spectrum for non-linear and non-stationary time series analysis, *Proceedings of the Royal Society of London Series A—Mathematical Physical and Engineering Sciences*, 1998, 454: 903-995.

[15] Nghien Nguyen Ba, Ricardo Rodriguez Jorge, (2019). Building an Early Warning Model for Detecting Environmental Pollution of Wastewater in Industrial Zones. *Advances on P2P, Parallel, Grid, Cloud and Internet Computing, Proceedings of the 14th International Conference on P2P, Parallel, Grid, Cloud and Internet Computing (3PGCIC-2019 pp. 828-837)*

[16] Support Vector Regression - Data Mining Map <http://www.saedsayad.com/>

[17] Thiang, Y.K. (2010) Electrical load time series data forecasting using interval type 2 Fuzzy logic system. In 2010 3rd International Conference on Computer Science and Information Technology, vol. 5, pp. 527-531. IEEE, 2010

[18] T. Do Duc, N. Nguyen Ba, C. Nguyen Van, T. Nguyen Nhu, D. Hoang Tien (2020) Surface Roughness Prediction in CNC Hole Turning of 3X13 Steel using Support Vector Machine Algorithm, *Tribology in Industry*, <http://www.tribology.rs/journals/aips/940.pdf>,

[19] NusratParveen, SadafZaidi, MohammadDanish (2016), Support vector regression model for predicting the sorption capacity of lead, *Perspectives in Science: Volume 8, September 2016, Pages 629-631*

[20] Muthukrishnan. R, Maryam Jamila. S (2020), Predictive Modeling Using Support Vector Regression, *International Journal of Scientific & Technology Research* volume 9, issue 02, february 2020, <http://www.ijstr.org/final-print/feb2020/Predictive-Modeling-Using-Support-Vector-Regression.pdf>.



ISSN: 2067-3809

copyright © University POLITEHNICA Timisoara,
Faculty of Engineering Hunedoara,
5, Revolutiei, 331128, Hunedoara, ROMANIA
<http://acta.fih.upt.ro>

¹Ayanniyi M. AYANSHOLA, ²A.A. ALAO, ³Adebayo Wahab SALAMI, ⁴Solomon O. BILEWU,
⁵A.A. MOHAMMED, ⁶Oluwafemi O. ADELEKE, ⁷Oluwatosin O. OLOFINTOYE

MODELLING OF TURBIDITY VARIATION IN A WATER TREATMENT PLANT

^{1,3,4,7}Department water Resources and Environmental Engineering, University of Ilorin, Ilorin, NIGERIA

²Kwara State Water Corporation, Ilorin, Kwara State, NIGERIA

⁵National Centre for Hydropower Research and Development, University of Ilorin, Ilorin, NIGERIA

⁶Department of Civil Engineering, University of Ilorin, Ilorin, NIGERIA

Abstract: Runoff is one of the principal factors that determine the level of surface water turbidity. The determination of optimum coagulant dose for the turbidity removal by the traditional method, jar tests is expensive, it takes time and may not be effective in the response to the changes in raw water quality in real time. These issues can therefore be alleviated with the use of modelling. This work made use of Multiple Linear Regression (MLR) and Artificial Neural Network (ANN) models to predict treated water turbidity. Precipitation and Water Treatment Plant (WTP) data was analyzed and the treated water turbidity was predicted using. The aim was to find out which variables affect and create simple and reliable prediction models which can be used in an early warning system. Both ANN and MLR models accuracy of were compared. Results showed that it is possible to predict the baseline level of treated water turbidity in drinking water treatment plants with a simple model. Precipitation, variation in raw water turbidity, coagulant dosage and retention time are variables that mostly affect the amount of treated water turbidity. The accuracies of MLR and ANN models were found to be almost the same.

Keywords: Artificial Neural Network, Rainfall, Turbidity, Water Treatment Plant

INTRODUCTION

Water has been identified as one of the most abundant natural resources on earth, being 75% of the earth surface [1]. The need for water is universal and without water, life will simply cease to exist. Earth's water is constantly in motion, passing from one state to another and from one location to another, which makes its rational planning and management a very complex and difficult task.

Water quality standards set limits on the concentrations of impurities allowed in water. Standards also affect the selection of raw water sources and the choice of treatment processes. The development of water quality standards began in the United States in the early 20th century [2]. The contaminant of most concern is high turbidity, especially rapid increases in turbidity, due to erosion and sediment runoff. Turbidity is the measure of water clarity and transparency and it is one of the primary pollutants regulated in finished drinking water under the Safe Drinking Water Act [3].

Goransson et al. [4] investigated the influence of rainfall, surface runoff and river flow on the temporal and spatial variability of turbidity in a regulated river system. A six year time series data on precipitation, discharge and turbidity from six stations along the river were examined using linear correlation and regression analysis, combined with nonparametric tests. The results showed that there is no simple relationship between discharge, precipitation and turbidity. Mozejko and Gniot [5] applied ANN for time series modeling of total phosphorous concentrations in the Odra River. Data from the monitoring site was used for training, validating and testing of the model. The result showed a high ability of the model to predict the parameter.

Samira et al. [6] modelled total dissolved solid (TDS) at the Simineh River in northwest Iran using ANN. The input parameters to the model were Calcium (Ca^{2+}), Chloride (Cl^-), Magnesium (Mg^{2+}), Sodium (Na^+), Bicarbonate (HCO_3^-), Sulfate (SO_4^{2-}) and water discharge (Q) from 1993 to 2011. The results revealed that Mg^{2+} and Ca^{2+} concentrations were the most and least influential parameters with approximate values of 18 and 12 % respectively. Leon-Luque et al. [7] developed a model of Artificial Neural Network (ANN) that, when faced with real time variations of turbidity is able to calculate an indicated dose of coagulant, with the aim of achieve effective coagulation in the trial water and avoid excessive or insufficient presence of coagulant, minimize the need to make jars test continuously and reduce economic losses due to inadequate spending of coagulant, while the input parameters are turbidity, pH, conductivity, alkalinity and temperature. Modelling of the water turbidity using some water parameter to develop useful models for the determination of turbidity was also carried out by some authors, but the work did not consider the effect of precipitation variation as one of the factors that determines the level of turbidity in surface water [8,9].

An ANN typically consists of three layers: an input layer, one or more hidden layers and an output layer. External inputs of the network are received by neurons in the input layer. Inputs are multiplied by interconnection weights and sent forward to the hidden layer where they are summed and processed by a nonlinear transfer function. The Multilayer Perceptron (MLP) and Radial Basis Function (RBF) are the commonly used neural network model. MLP and RBF are feed forward ANN which utilizes a supervised learning technique called back propagation for training a network. Neural networks are trained by examples using historical

data. Back-error propagation, or back propagation, is widely and successfully used in Neural Network paradigms because it is easy to understand [7]. Performance of ANN models can be evaluated for example using Root Mean Square Error (RMSE), Mean Relative Error (MRE) and coefficient of determination (R^2). MRE can be used to determine whether model predictions are suitable for process control. R^2 value can be used to compare the relative performance of the models [10].

MATERIALS AND METHODS

— The study area

Asa reservoir as shown in Figure 1 [11] is located in Ilorin, Kwara state, Nigeria. Although the water quality is still good, erosion, degradation, negative influence of toxic pollution from heavy metals and human activities at the upstream of Asa River threaten its water quality. It is located on longitude $4^{\circ}35'E$ and latitude $8^{\circ}30'N$. The population of Ilorin from 2006 censuses is estimated to be 781,934 [12]. Ilorin metropolis presently occupies an area of about 89 Km^2 while three main rivers that flow through the city are Oyun, Asa, and Moro [13].

— Data collection

Turbidity data, coagulant dose and retention time were obtained from Asa dam water treatment plant. The turbidity data obtained are daily turbidity data for a period of five consecutive years ranging from 2014 to 2018 for both raw and treated water. Daily coagulant dose data (mg/l) were also obtained from 2014 to 2018 and retention time at the sedimentation tanks were obtained through measurement and calculation.

Precipitation data obtained from the Nigerian Meteorological Agency (NIMET), Abuja, Nigeria which includes rainfall data from Ilorin, Ibadan, Ogbomosho and Oshogbo gauging stations for the five consecutive years ranging from 2014 to 2018. The data obtained were daily precipitation data which are measured in (mm)

DATA ANALYSIS

— Estimation of precipitation data for asa dam site

Precipitation data from Ilorin, Ibadan, Ogbomosho and Oshogbo gauging stations were used to determine the rainfall responsible for the runoff in the Asa River (Figs 2 and 3).

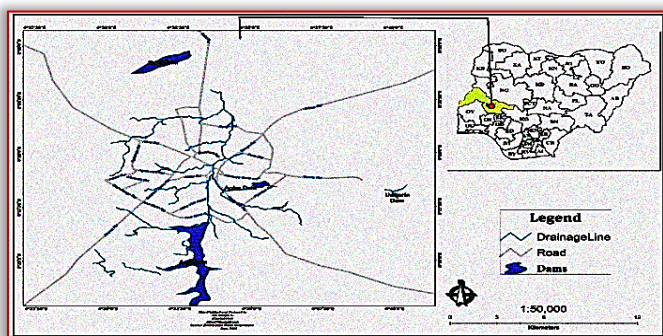


Figure 1. Map of Ilorin showing the location of the lake dams.

Inset: map of Nigeria showing the states [10].

The mathematical expression for weighted average method is presented in equation (1)

$$P_1 = \frac{\frac{P_2}{d_2^2} + \frac{P_3}{d_3^2} + \frac{P_4}{d_4^2} + \frac{P_5}{d_5^2}}{\frac{1}{d_2^2} + \frac{1}{d_3^2} + \frac{1}{d_4^2} + \frac{1}{d_5^2}} \quad (1)$$

where P_1, P_2, P_3, P_4 and P_5 is the precipitation at Asa dam site, Ogbomosho, Oshogbo, Ibadan and Ilorin respectively while d_2, d_3, d_4 and d_5 is the respective distance from Ogbomosho, Oshogbo, Ibadan and Ilorin to the watershed centroid.

— Coagulant dose and retention time

The coagulant dose varies directly with turbidity of the raw water quality. The daily alum consumption between 2014 and 2018 were analysed and the monthly mean was established while the retention time in the sedimentation tank was calculated from equation 2.

$$\text{Retention time} = \frac{\text{flowrate of the intake(s)pump}}{\text{volume of the clarifier}} \quad (2)$$

— Multiple regression models

Multiple Regression Models are statistical tool for modeling variables with one dependent and two or more independent variables. Equation (3) is a multiple regression model that can be used to assess the performance of typical water treatment plant.

$$Y = a_1 + b_1X_1 + b_2X_2 + b_3X_3 + \dots + b_nX_n + C \quad (3)$$

where: X_1, X_2, \dots, X_n =set of independent; Y = dependent variable; a_1, b_1, \dots, b_n = constant; c = error term (negligible). However, for this study, Y = treated water turbidity (NTU); X_1 = Coagulant dose (ml/g); X_2 = Rainfall (mm); X_3 = Retention time (t) and; X_4 = Raw water turbidity (NTU)

Two ANN modeling approaches; that is Multilayer Perceptron Neural Network (MLPNN) and Radial Basic Function Neural Network (RBFNN) in Statistical Package for Social Science (SPSS) software version 16.0 were used to model treated water turbidity at Asa dam WTP as a function of raw water turbidity, retention time, coagulant dose and precipitation. Over 80% and less than 20% of the data set were used for model training and testing. The performance evaluation of the models was carried out using RMSE, MRE and correlation coefficient (r).

RESULTS AND DISCUSSION

— Rainfall trends

It was observed that rainfall and raw water turbidity followed similar trend pattern, hence raw water turbidity varies with amount of rainfall. After treatment, it was noticed that the water turbidity reduced drastically (Figure 4). The turbidity increases from April through September and reduces as the rainfall reduces as shown in Figure 4. It was also observed that rainfall increases from 50 mm in April to above 100 mm in May and slightly decrease in June and reach the peak of 250 mm in August. It was also revealed that the variations in the rainfall trend at the observed locations are the same. The study also revealed that coagulant dosage varied with the raw water turbidity. This pattern was probably due to the amount of runoff entering the Asa dam reservoir at that time of year. The turbidity of the raw water reduces at the end of filtration and disinfection resulting in lower levels of suspended and dissolved solids washed by the run-off due to rainfall. It is evident that turbidity levels reduce considerably along the treatment process units due to settlement of flocs formed during coagulation process.

The turbidity removal by the flocculation process can be directly attributed to improved coagulant dosage. The Nigerian Drinking Water Standards (NDWS) recommends a turbidity of an upper limit of 5 NTU. The result of the study also show clearly that the average coagulant dose is effective coagulation of the raw water. Hence there is significant change in levels of raw and treated water turbidity and this is as a result of the coagulation properties of the alum which is able to settle most of the particles in the raw water within a short time.

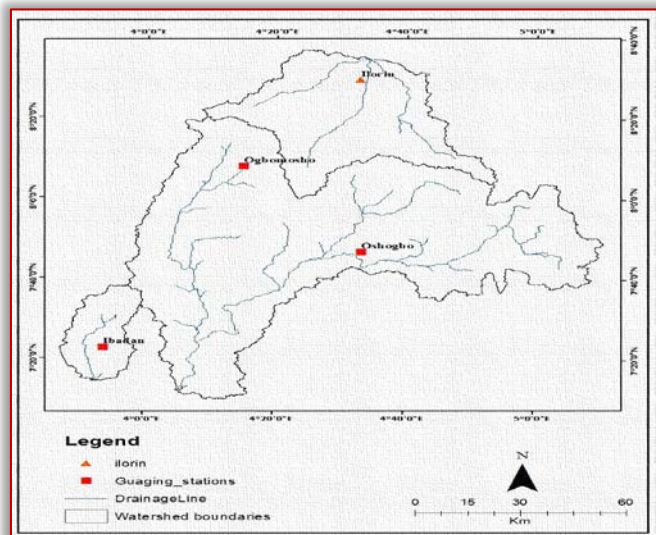


Figure 2. Gauging stations and Asa watershed

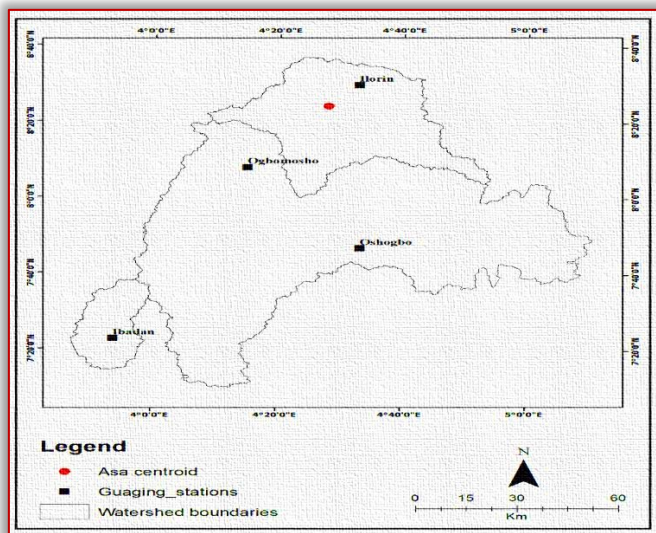


Figure 3. Centriod and the rainfall gauging stations

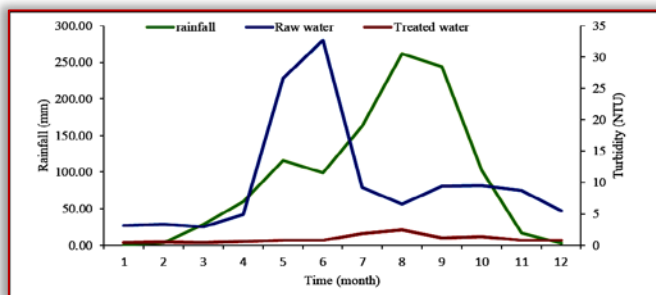


Figure 4: Trends of rainfall, raw and treated water turbidity (NTU)

REGRESSION STATISTICS

Tables 1 and 2 show the Summary of Regression Statistics Model and the Analysis of Variance (ANOVA) respectively. The Multiple regression analysis (MRA) showed a high R^2 value of 73.1% (Table 1). The all-inclusive model generated from the stepwise regression analysis which is a useful approach to understand how the output of water treatment processes are affected by some parameters such as rainfall, raw water turbidity, coagulant dosage and retention time. These three component parameters are strong predictors for determining the treated water turbidity which can be refer to as the plant efficiency. The model derived is valid at 95% level of significance. Coagulant dosage, rainfall and raw water turbidity made significant contribution to the prediction of treated water turbidity. Coagulant dosage is positively related to the treated water turbidity. This could be as a result of effectiveness of Alum. Rainfall is positively related to the treated water turbidity. This could be as a result of climate change that affects the pattern of rainfall. The retention time of water at the sedimentation basin is not significant at 5%. This implies that it did not make much significant contribution to the treated water turbidity. The multiple correlation coefficient of 0.85 indicates that the correlation among independent and dependent variables is positive. The coefficient of determination, R^2 , is 73.1%, which implies that close to 73% of the variation in the dependent variable is explained by the independent variables. The standard error of the regression is 0.40, which is the estimate of the variation of the observed treated water turbidity about the regression. The regression model formulated is presented in Equation 4.

$$Y = -1.5491 + 0.0764X_1 + 0.0047X_2 - 2.2408X_3 - 0.0463X_4 \quad (4)$$

The treated water turbidity was modelled for Asa dam WTP using MLPNN and RBFNN models. The percentage of data used for model training and testing was 83.3% and 16.7%. The correlation coefficients (r) for treated water turbidity using MLPNN is 0.87 while that of RBFNN is 0.97. The plots of the actual and modelled treated water turbidity using MLPNN and RBFNN are presented in Figs. 5 and 6 which indicate strong relationships between the actual and modelled treated water turbidity at the station. RMSE and MRE for training and testing using MLPNN approach are 1.0242, 0.2665 and 0.4827, 1.0208 respectively while that of RBFNN were 0.8735, 0.4669 and 1.6352, 0.6213 respectively. The RMSE for the training and testing using the two NN approaches at the station varied between 0.2665 and 1.0242 while the MRE for training and testing ranged between 0.4827 and 1.6352. The results obtained for RMSE and MRE for treated water turbidity modeling are comparable with what was obtained in similar study as reported by Mozejko and Gniot [5].

Table 1: Summary of Regression Statistics Model

| Multiple R | R Square | Adjusted R ² | Standard Error | Observation |
|------------|----------|-------------------------|----------------|-------------|
| 0.85 | 0.73 | 0.58 | 0.40 | 12 |

Table 2: Variance Analysis (ANOVA) treated water turbidity

| Sample | DF | SS | MS | F | SF |
|------------|----|------|------|------|------|
| Regression | 4 | 3.09 | 0.77 | 4.75 | 0.04 |
| Residual | 7 | 1.14 | 0.16 | | |
| Total | 11 | 4.23 | | | |

DF=Degree of freedom, SS=Sum of square, MS= Mean of square, F=F-test statistic, F Significance = p-value

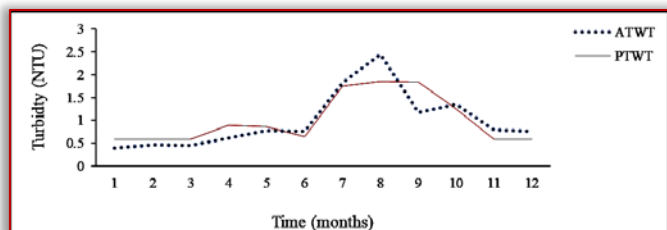


Figure 5: Actual and predicted treated water turbidity using MLPNN

Note: actual treated water (ATWT) and predicted treated water turbidity (PTWT)

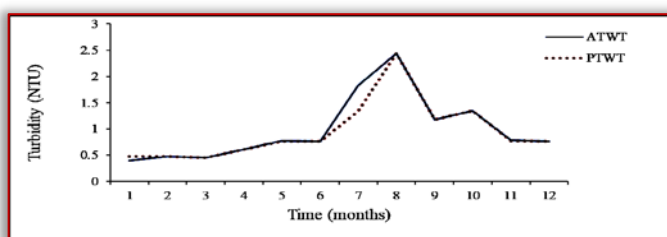


Figure 6: Actual and predicted treated water turbidity RBFNN

Note: actual treated water (ATWT) and predicted treated water turbidity (PTWT)

CONCLUSIONS

The important objective WTP is its effective physical removal of colloidal particles, microorganisms and other particulate materials. Because of low concentration of suspended material in drinking water, turbidity has traditionally been the main water quality parameter for assessing particle removal in water treatment facility. The comparison of the water quality before and after the treatment revealed that Physico-chemical and microbial constituents were below the Nigerian Drinking Water Standards (NDWS). The regression analysis showed that the regression equation for treated water turbidity is good. It was found that coagulant dosage, rainfall and raw water turbidity are significant at 5% level. However, retention time in the sedimentation tanks is not significant at 5% level. Modeling the treated water turbidity using MLPNN and RBFNN approaches revealed that the two modeling methods were able to simulate the parameter adequately with correlation coefficients varying between 0.87 and 0.97. The performance evaluation of the model using correlation coefficients, MRE and RMSE showed that the application of the two NN approaches to simulate treated water turbidity gives satisfactory results for the two NN modeling approaches. Hence the two NN modeling approaches are efficient tools and useful alternatives for simulation of water quality parameters. It is very important to mention that this study can serve as baseline information for further research to help in the monitoring the turbidity removal and other water quality parameters at WTP before supplying potable

water for domestic use. The modeling results indicated that reasonable prediction accuracy was achieved for both the regression analysis and ANN models.

The prediction of the aerodynamic coefficients of the investigated projectiles shown in Fig. 1 was carried using the methods and the computer programme described above. The effects of forebody and afterbody shapes on the aerodynamics at supersonic speeds are analysed in this paper.

References

- [1] Sule, B. F. (2003). Water security: now and the future. The Sixty-fifth Inaugural Lecture, University of Ilorin, Published by Library and Publications Committee, University of Ilorin, Unilorin Press, Nigeria.
- [2] Riyanto, E. (2009). A heuristic revamp strategy to improve operational flexibility of water networks based on active constraints. *Chemical Engineering Science Journal*, 65(9), 2758-2770.
- [3] Seeds, J. (2010). Turbidity analysis for Oregon Public Water Systems. *Water Quality in Coast Range Drinking Water Source Areas*. Oregon Department of Environmental Quality, Portland.
- [4] Goransson, G.; Larson, M.; and Bendz, D. (2013). Variation in turbidity with precipitation and flow in a regulated river system. *Hydrology and Earth System Sciences Journal*, 17, 2529-2542.
- [5] Mozejko, J.; and Gniot, R. (2008). Application of neural networks for the prediction of total phosphorus concentrations in surface waters. *Polish Journal of Environmental Study*, 17(3), 363-368.
- [6] Samira N.; Leila N.; and Mohammad, H. (2014). Artificial neural network modeling of total dissolved solid in the Simineh River. *Iran Journal of Civil Engineering and Urbanism*, 4(1), 8-14.
- [7] León-Luque, A. J.; Barajas, C. L.; and Peña-Guzmán, C. A. (2016). Determination of the optimal dosage of aluminum sulfate in the coagulation-flocculation process using an Artificial Neural Network. *International Journal of Environmental Science and Development*, 7(5), 346-350.
- [8] Ezemagu, I.G., Ejimofor, M.I., Menkiti, M.C. and Nwobi-Okoye, C.C. (2020), Modelling and optimization of turbidity removal from produced water using response surface methodology and artificial neural network, *South African Journal of Chemical Engineering, ScienceDirect*, 35: 78-88
- [9] Kovo, A.S. (2005): Modelling of water turbidity parameters in water treatment plant, *Leonardo Journal of Sciences, AcademicDirect Publishing House*, 6: 68-77
- [10] Tomperi J.; Pelo, M.; and Leivisk, K. (2013). Predicting the residual aluminum level in water treatment process. *Journal of Drinking Water Engineering Science*, 6, 39-46.
- [11] Ogunkunle, C.O.; Mustapha, K.; Oyediji, S.; and Fatoba, P.O. (2016). Assessment of metallic pollution status of surface water and aquatic macrophytes of earthen dams in Ilorin, north-central of Nigeria as indicators of environmental health. *Journal of King Saud University - Science*, 28(4), 324-331.
- [12] Brinkhoff, T. (2011). National Population Commission of Nigeria (web): Accessed from <http://www.citypopulation.de/php/nigeria-admin.php?admlid> (accessed on 19/06/2016).
- [13] Ayanshola, A. M., Sule, B. F. and Mandal, K. (2015) Evaluation of Supply Variability of Household Water Use in Ilorin Metropolis North Central

¹Abass I. TAIWO, ¹Timothy O. OLATAYO

OPTIMAL AND EFFICIENT MODEL SELECTION CRITERIA FOR PARAMETRIC SPECTRAL ESTIMATION

¹Department of Mathematical Sciences, Olabisi Onabanjo University, Ago-Iwoye, NIGERIA

Abstract: Traditional Parametric spectral estimation methods have been widely used to obtain spectral estimate, resolution and variance distribution in signals or time series data across several fields. But the challenges of how to select an optimal and efficient model order were often encountered. In this research work, modified forms of Final Prediction Error, Akaike Information Criteria, Bayesian Information Criteria and Minimum Description Length which involved the replacement of variance error with sample autocorrelation function that has capabilities of detecting non-randomness in time series data were used to select the optimal model order. In order to determine the efficiency of the modified criteria, Autoregressive model, AR(11) was selected based on all the modified information criteria while AR(7) was selected based on all the traditional information criteria as the optimal model orders. Using the AR spectral estimation method, AR(11) and AR(7) models were used to analyse 1000 points Heartbeat readings. The results indicated that the spectral estimate and resolution of AR(11) were better than that of AR(7). Conclusively, the optimal model order selected using the modified information criteria gives a better result when compared to the traditional information criteria based on the spectral estimate and resolution of the Autoregressive spectral estimation method.

Keywords: Parametric Spectral estimation, Information Criteria, Heart-beat readings, Optimal model order, Autocorrelation function

INTRODUCTION

There are many criteria that has been used to determine model order selection in parametric spectral estimation. The final prediction error (FPE) criterion was the first of two tools proposed by Akaike for the purpose of model order selection (Akaike, 1969; Akaike, 1970; Akaike, 1971). Since, the second one, presented several years later and known as the Akaike's information criterion (AIC) (Akaike, 1974) has deeper statistical justification and wider range of applicability than FPE, it is much more frequently used and referred to. Both criteria were derived for time-invariant systems/signals operated under stationary conditions and whenever both can be applied they asymptotically yield the same results. Schwartz, 1974 went ahead to propose Akaike's Bayesian Information criteria (BIC) and this was an improvement over AIC. The penalties in BIC are there to reduce the effects of overfitting and it is of note that the penalty is stronger in BIC than AIC for any reasonable sample size. BIC as well generally comes across only true models and penalizes free parameters more strongly with more accuracy but in practice it often overfit the data (Cruz-Ramírez *et al.*, 2006).

In another vain, minimum description length (MDL) proposed in (Rissanen, 1978) and further discussed in (Rissanen, 1983) is a formalization of Occam's razor in which the best hypothesis (a model and its parameters) for a given set of data is the one that leads to the best compression of the data. Despite the abilities of this criteria it is computationally difficult and in practice it often leads to overfit of data (Cruz-Ramírez *et al.*, 2006).

Over the years, several other criteria and algorithms has been developed and these included Criterion Autoregressive Transfer (CAT) (Parzen, 1974), Residual Variance (RV)

(Box and Jenkins, 1970), Hannan and Quinn (HQ) (Hannan and Quinn, 1979), Generic algorithm (Palanippan, 2006), Particle swarm optimization (PSO) (Bijaya, 2010) and many more. But these model selection methods are not completely outlined here since vast amount of techniques for solving the problem of selecting model order may have not being mentioned. The main goal of this research article is to improve the method of selecting the optimal and efficient model order in parametric spectral estimation. This will be done by modifying some existing traditional information criteria (Final prediction error, Akaike, Schwartz Bayesian and Minimum Description length information criteria) for selecting optimal order. The modification will involve the replacement of variance of error with sample autocorrelation function which has the capabilities of detecting non-randomness, help in identifying an appropriate model for non-randomness time series data and instead of estimating the error variance that required minimization of the log-likelihood function of the given model.

MATERIALS AND METHODS

— Final prediction error (FPE)

This is the first criteria proposed by (Akaike, 1969) and it is based on minimizing one step ahead predictor error. It is denoted by

$$FPE_{(k)} = \left(1 + \frac{k}{N}\right) \hat{\sigma}_k^2 \quad (1)$$

where $\hat{\sigma}_k^2$ is the unbiased estimate of σ_k^2 after fitting the k^{th} order model.

— Akaike information criteria

This is the most well-known and mostly used criteria and it was proposed by (Akaike, 1970). It is denoted by

$$AIC(k) = N \ln \hat{\sigma}_k^2 + 2k \quad (2)$$

where N is the number of observation and $\hat{\sigma}_k^2$ is the maximum likelihood estimation of the residual after fitting the k^{th} order model.

— **Schwartz's SBC criteria**

Similar to Akaike's, Bayesian criteria, (Akaike, 1971) suggest the Bayesian criteria defined as

$$SBIC(k) = N \ln \hat{\sigma}_k^2 + M \ln N \quad (3)$$

where $\hat{\sigma}_k^2$ is the maximum likelihood estimate of σ_k^2 , M is the number of parameters in the model and N is the number of observations.

— **Minimum description length criteria**

Based on the work of (Akaike, 1974), it was proved that the Akaike information criteria is inconsistent and it tends to overestimate the order. Schwartz, 1974, proposed a modified Akaike information criteria by replacing the term $2k$ by a term which increases more rapidly. This criterion was named minimum description length (MDL) and is of the form

$$MDL = N \ln |\hat{\sigma}_k^2| + k \ln(N) \quad (4)$$

— **Modified final prediction error (MFPE)**

This is the first criteria proposed by (Akaike, 1969) and it is modified by replacing the variance of error by sample autocorrelation function. It is denoted by

$$FPE_{(k)} = \frac{|N+k|}{N-k} |\hat{\rho}_k| \quad (5)$$

where $\hat{\rho}_k = \hat{\gamma}_k(0) + \sum_{i=1}^k \hat{\alpha}_i \hat{\gamma}_{kk}(1)$ is the power of the prediction error that decreases with k while the term $\frac{N+k}{N-k}$ increases with k .

— **Modified Akaike information criteria**

This is the most well-known criteria and it was proposed by (Akaike, 1970) and was modified by replacing the variance of error by sample autocorrelation function. It is denoted by

$$AIC(k) = N \ln |\hat{\rho}_k| + 2k \quad (6)$$

This criterion is more general than final prediction error and it can be applied to determine the order of the moving average part of an autoregressive moving average model.

— **Schwartz's SBC criteria**

Similar to Akaike's, Bayesian criteria, Akaike, 1971 suggest the Bayesian criteria model that is modified by replacing variance of error with sample autocorrelation function and it is defined as

$$SBC(k) = k \ln |\hat{\rho}_k| + N \ln k \quad (7)$$

where $\hat{\rho}_k$ is an estimate of ρ_k , k is the number of parameters in the model and N is the number of observations.

— **Minimum description length criteria**

Based on the work of Kashyap (Akaike, 1974), it was proved that the Akaike information criteria is inconsistent and it tends to overestimate the order. Schwartz, 1974 proposed a modified Akaike information criteria by replacing the term $2k$ by a term which increases more rapidly. This criterion is named minimum description length (MDL) and is of the form

$$MDL = N \ln |\hat{\rho}_k| + k \ln(N) \quad (8)$$

— **Spectral density function of AR(1) Process**

Given an autoregressive model AR(1),

$$y_t = \phi_0 + \phi_1 y_{t-1} + \varepsilon_t \quad (9)$$

Using the backshift operator gives

$$\Phi(B)y_t = \varepsilon_t, \text{ where } \Phi(B) = (1 - \phi_1 B)$$

since $y_t = \Phi^{-1}(B)\varepsilon_t$, then

$$\gamma_k = E(y_t y_{t-k}) = \sigma_\varepsilon^2 \left(\frac{1}{(1 - \phi B)(1 - \phi B^{-1})} \right) \quad (10)$$

Equation (10) is written in spectral representation as

$$f(\omega) = \frac{\sigma_\varepsilon^2}{2\pi} \left[\frac{1}{|\Phi(e^{-i\omega})|^2} \right] \quad (11)$$

$$\text{Since } |1 - \Phi(e^{-i\omega})|^2 = 1 - \phi_1 e^{i\omega} - \phi_1 e^{-i\omega} + \phi_1^2 = 1 - \phi_1 (e^{i\omega} + e^{-i\omega}) + \phi_1^2$$

and using a standard trigonometric form given as

$$\cos \omega = \frac{e^{i\omega} + e^{-i\omega}}{2}$$

$$|1 - \Phi(e^{-i\omega})|^2 = 1 - 2\phi_1 \cos \omega + \phi_1^2$$

Then, equation (11) becomes

$$f(\omega) = \frac{\sigma_\varepsilon^2}{2\pi} \left[\frac{1}{1 - 2\phi_1 \cos \omega + \phi_1^2} \right] \quad (12)$$

— **Spectral density function of AR(2) Process**

The Yule Walker process is given by

$$y_t = \phi_0 + \phi_1 y_{t-1} + \phi_2 y_{t-2} + \varepsilon_t \quad (13)$$

Using the backshift operator to obtain

$$\Phi(B)y_t = \varepsilon_t,$$

where $\Phi(B) = (1 - \phi_1 B - \phi_2 B^2)$

Since $y_t = \Phi^{-1}(B)\varepsilon_t$

$$\gamma_k = \sigma_\varepsilon^2 \left(\frac{1}{(1 - \phi_1 B - \phi_2 B^2)(1 - \phi_1 B^{-1} - \phi_2 B^{-2})} \right) \quad (14)$$

Equation (14) is written in spectral representation as

$$\begin{aligned} f(\omega) &= \frac{\sigma_\varepsilon^2}{2\pi} \left[\frac{1}{|1 - \phi_1(e^{-i\omega}) - \phi_2(e^{-2i\omega})|^2} \right] \\ &= \frac{\sigma_\varepsilon^2}{2\pi} \left[\frac{1}{|1 - \phi_1(\cos \omega - i \sin \omega) - \phi_2(\cos 2\omega - i \sin 2\omega)|^2} \right] \\ &= \frac{\sigma_\varepsilon^2}{2\pi} \left[\frac{1}{(1 - \phi_1 e^{-i\omega} - \phi_2 e^{-2i\omega})(1 - \phi_1 e^{i\omega} - \phi_2 e^{2i\omega})} \right] \\ &= \frac{\sigma_\varepsilon^2}{2\pi} \left[\frac{1}{1 - \phi_1 e^{i\omega} - \phi_2 e^{2i\omega} - \phi_1 e^{-i\omega} + \phi_1^2 + \phi_1 \phi_2 e^{i\omega} - \phi_2 e^{-2i\omega} + \phi_2 \phi_1 e^{-i\omega} + \phi_2^2} \right] \end{aligned}$$

Using a standard trigonometric form given as

$$\cos \omega = \frac{e^{-i\omega} + e^{i\omega}}{2}$$

Equation (14) can be expressed as

$$f(\omega) = \frac{\sigma_\varepsilon^2}{2\pi} \left[\frac{1}{1 + \phi_1^2 + \phi_2^2 - 2\phi_1 \cos \omega - 2\phi_2 \cos 2\omega + 2\phi_1 \phi_2 \cos \omega} \right] \quad (15)$$

RESULT AND DISCUSSIONS

In order to identify the optimal model, autocorrelation and partial autocorrelation functions were used to identify tentative models AR(3), AR(5), AR(7), AR(9) and AR(11) for 1000 heart-beat readings observed at equal space and time of 0.05 second. To validate these models, modified and traditional information criteria were obtained.

From table 1 and figure 2, the lowest values of all the modified information criteria occurred at AR(11) while the lowest values for the traditional information criteria occurred at AR(7) in table 2. The performance of both information criteria were determined based on spectral estimate and resolution of Autoregressive spectral

estimation using modified covariance autoregressive estimator. Based on figure 3, the spectral estimate of AR(7), AR(9) and AR(11) indicated a relatively fast oscillation. This was explained by the two sinusoidal components in all autoregressive order but AR(11) is better since it has a dominant peak, better spectral estimate and resolution when compared to AR(7) and AR(9). AR(11) depict the general oscillation better than AR(7) and AR(9). Thus the modified information criteria that is, modified final prediction error, Akaike, Schwartz Bayesian and Minimum Description length information criteria gives an optimal and efficiency model selection as against the most frequently used traditional information criteria.

Table 1: Modified information criterion for 1000 heartbeat readings

| NUMBER | FPE | AIC | BIC | MDL |
|--------|----------|------------|-----------|------------|
| 1 | 45.74546 | -1.45679 | -0.06914 | 0.45524 |
| 2 | 19.42644 | -4.61658 | 34.31270 | -0.79254 |
| 3 | 16.46170 | -8.77227 | 54.04428 | -3.03620 |
| 4 | 14.04178 | -12.50380 | 67.67442 | -4.85569 |
| 5 | 11.93420 | -16.31390 | 77.84051 | -6.75377 |
| 6 | 9.63539 | -22.57740 | 85.43868 | -11.10530 |
| 7 | 7.23339 | -32.35490 | 90.80581 | -18.97080 |
| 8 | 5.00028 | -46.11840 | 94.03314 | -30.82220 |
| 9 | 3.18856 | -63.76340 | 95.14381 | -46.55520 |
| 10 | 1.79256 | -87.53610 | 93.62203 | -68.41590 |
| 11 | 0.59493 | -137.46600 | 84.81228 | -116.43400 |
| 12 | 0.50280 | -140.43800 | 84.78019 | -117.49400 |
| 13 | 1.38346 | -84.13700 | 99.61185 | -59.28070 |
| 14 | 1.95248 | -60.92240 | 107.05460 | -34.15410 |
| 15 | 2.22812 | -47.98480 | 112.00710 | -19.30440 |
| 16 | 2.28275 | -40.02700 | 115.58080 | -9.43460 |
| 17 | 8.28499 | -35.61560 | 117.99140 | -3.11123 |
| 18 | 1.89294 | -34.28410 | 119.21630 | 0.13236 |
| 19 | 1.56426 | -35.18040 | 119.41340 | 1.14806 |
| 20 | 1.24642 | -36.87910 | 119.03500 | 1.36134 |

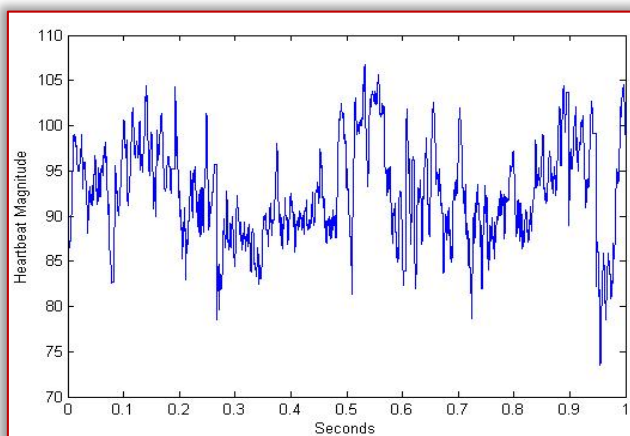


Figure 1: Heartbeat readings in time

Table 2. Traditional information criterion values for 1000 heartbeat readings

| NUMBER | FPE | AIC | BIC | MDL |
|--------|---------|---------|---------|---------|
| 3 | 1.84691 | 1.99214 | 1.99214 | 1.85246 |
| 5 | 1.43891 | 1.56250 | 1.56250 | 1.43891 |
| 7 | 1.18234 | 1.47838 | 1.47838 | 1.18234 |
| 9 | 1.34821 | 1.29929 | 1.71723 | 1.34821 |
| 11 | 1.41245 | 1.86863 | 1.86863 | 1.41245 |

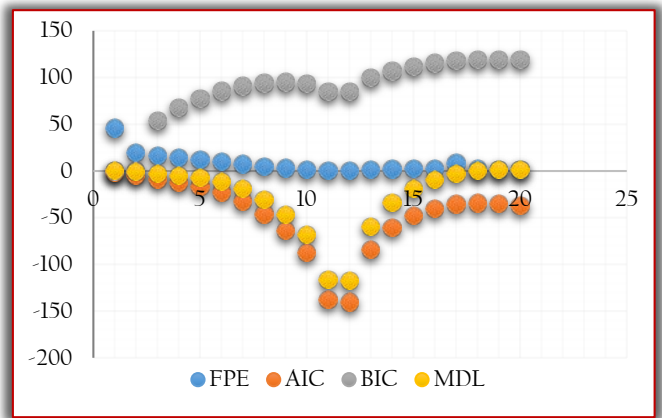


Figure 2: Graphical representation of modified information criteria

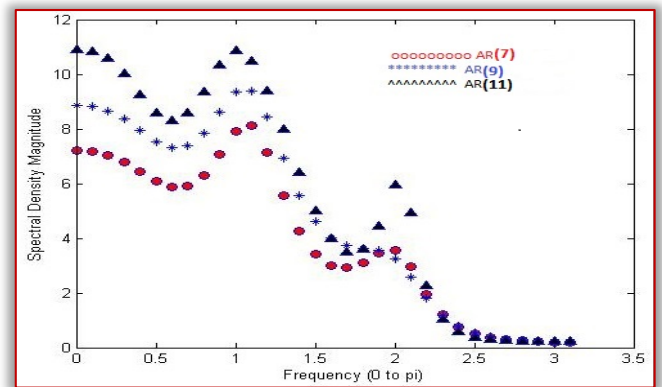


Figure 3: Spectral estimates for AR(7), AR(9) and AR(11)

CONCLUSION

This paper was used to propose improved and modified methods that can be used to select optimal model order in parametric spectral estimation. This was done by modifying the traditional information criteria and from the results obtained, AR(11) and AR(7) were the optimal model selected using modified and traditional information criteria.

The spectral estimate and resolution of AR(11) were better than AR(7). Conclusively, the modified information criteria outperformed the traditional information criteria when analysing the spectral estimate of 1000 heart beat readings, with lower parameters than the traditional methods.

References

- [1] Abdul-Majeeb, H, A., Mohammed, Q. A. and Wadhah, S. I.: Estimating the Spectral Power density function of Non-Gaussian Second order Autoregressive model., Journal of Asian Scientific Research, 4, 513 – 521, 2014.
- [2] Andrea, F., Arianna, P., Laura, S. and Massimilland, M.: Fourier analysis for Demand Forecasting in a Fashion Company. International Journal of Engineering Business Mngements, 5, 1 – 10, 2013.
- [3] Akaike, H.: Fitting autoregressive models for prediction, Ann. Inst. Statist. Math., 21, 243–247, 1969.
- [4] Akaike, H.: Statistical predictor identification, Ann. Inst. Statist. Math., 22, 203–217, 1970.
- [5] Akaike, H.: Autoregressive model fitting for control, Ann. Inst. Statist. Math., 23, 163–180, 1971.

- [6] Akaike, H.: A new look at the statistical model identification,” IEEE Trans. Automat. Contr., 19, 716–723, 1974.
- [7] Andrew, J. G. and Barry, G. Q.: Parametric Spectral Discrimination, Journal of Time series Analysis, 38, 1 – 27, 2017.
- [8] Batorova, I.: Spectral Techniques for Economic Time series, Ph.D. Thesis Dissertation, Cornenius University, Bratislava, Slovakia, 2012.
- [9] Beheshti, S.: A New Approach to Order Selection and Parametric Spectrum Estimation, Acoustics, Speech and Signal Processing, Proceedings of ICASSP, Toulouse, France, 2006
- [10] Bijaya, G.: Spectral Estimation of Electroencephalogram signal using ARMAX model and Particle Swarm Optimization, M.Sc. Dissertation. Lamar University, Texas, 2010.
- [11] Box, G. E. P. and Jenkins, G. M.: Time Series Analysis; forecasting and control, Holden Day, San Francisco, California, 125 – 135, 1970.
- [12] Cruz-Ramírez, N., Acosta-Mesa, H. G., Barrientos-Martínez, R. E., Nava-Fernández, L. A.: How Good Are the Bayesian Information Criterion and the Minimum Description Length Principle for Model Selection? A Bayesian Network Analysis. In: Gelbukh, A., Reyes-García, C. A. (eds) MICAI 2006: Advances in Artificial Intelligence. MICAI. Lecture Notes in Computer Science, 4293. Springer, Berlin, Heidelberg 494 – 504, 2006.
- [13] Hannan, E. J. and Quinn, B. G. 1979, The determination of the order of an Autoregression, Journal of the Royal Statistical Society, 41, 190 – 195, 1979.
- [14] Schwartz, G.: Estimating the Dimension of a model. Annal of Statistics, 6, 461 – 464, 1974.
- [15] Palanippa, R.: Towards Optimal model order Selection for Autoregressive Spectral Analysis of Mental Tasks using Genetic Algorithm. International Journal of Computer Science and Network Security, 6, 153 – 161, 2006.
- [16] Parzen, E.: Some recent advances in Time series modeling. IEEE Trans. Automat. Contr., 19, 723-730, 1974.
- [17] Rissanen, J.: Modeling by shortest data description, Automatica. 14(5), 465 – 658, 1978.
- [18] Rissanen, J.: A Universal prior for the Integers and Estimation by Minimum Description Length Annal of Statistics, 11, 417 – 431, 1983.
- [19] Rossi, G. B., Crenna, F., Piscopo, V. and Scamardella, A.: Comparison of Spectrum Estimation Methods for the Accurate Evaluation of Sea State Parameters, Sensors, 20, 1 –15, 2020.
- [20] Taiwo, A. I.: Spectral and Fourier Parameter Estimation of Periodic Autocorrelated Time Series Data, Department of Mathematical Sciences, Ph.D. Thesis, Olabisi Onabanjo University, Ago-Iwoye, Nigeria, 2017.
- [21] Taiwo, A. I. and Olatayo, T. O.: Performance of an Autoregressive Spectral estimation method based on Signal Length, Annals Computer Science Series Tibiscus, 17(1), 252 – 257, 2019.
- [22] Thanagasundran, S. and Schindwein, F. S.: Autoregressive order selection for Rotating Machinery, International Journal of Acoustics and Vibration, 11, 1 – 11, 2006.



ISSN: 2067-3809

copyright © University POLITEHNICA Timisoara,
Faculty of Engineering Hunedoara,
5, Revolutiei, 331128, Hunedoara, ROMANIA
<http://acta.fih.upt.ro>

¹Zorana TANASIĆ, ²A. JOKIĆ, ¹Goran JANJIĆ,
¹Miljko BOBREK, ³Borut KOSEC

BUSINESS PROCESS IMPROVEMENT IN THE AUTOMOTIVE INDUSTRY - QUALITY METHODS AND TOOLS

¹ Faculty of Mechanical Engineering, University of Banja Luka, Banja Luka, BOSNIA & HERZEGOVINA

² MAHLE Electric Drives Bosnia, Laktaši, BOSNIA & HERZEGOVINA

³ Faculty of Natural Sciences and Engineering, University of Ljubljana, Ljubljana, SLOVENIA

Abstract: The development of global economy has forced many companies to introduce and apply modern approaches, models, and initiatives for rapid and long-term business improvement. Achieving business excellence and creating world-class products and services are a basic prerequisite for the survival, growth, and development of the company. It is not the job of just one organizational unit, but the result of synchronized action of all processes in the organization according to clearly defined business goals. This paper includes and elaborates tools and methods of a quality management system in the automotive industry. As statistical process control and the occurrence of non-compliance are indispensable, only organizations that continuously improve the level of product quality and reduce costs survive in the market. Therefore, it is very important to establish an efficient system for managing the quality of processes and products, which means the efficient application of quality tools and the commitment of all employees in the organization.

Keywords: quality standards, automotive industry, quality tools

INTRODUCTION

The automotive industry has made a huge contribution to the overall development of mankind, especially in the area of quality. It was the first to realize that in order to achieve the development and improvement of the competitive position on the market, it is not enough to be good, but it is necessary to be in the group of the best, where those who are equal in terms of technology compete. [1].

In order to assure that the desired quality of the products is achieved, there are several standards that are used in the automotive industry. ISO 9000 defines the quality standards and general rules on quality management for all industries. QMS is based on five pillars of quality, which are [2].

- ≡ Advanced Product Quality Planning (APQP) and Control Plans
- ≡ Failure Mode and Effect Analysis (FMEA)
- ≡ Statistical Process Control (SPC)
- ≡ Measurement System Analysis (MSA)
- ≡ Production Part Approval Process (PPAP).

However, ISO/TS 16949 is specific for the automotive industry in terms of quality management systems.

Today, the world's leading companies are increasingly using the term "business excellence", which claims that providing high quality is a unique and right path to efficiency and effectiveness.

APQP is a structured method for defining and executing the steps necessary to ensure that the product meets the requirements of the customer /consumer. APQP is a team approach required of all systems, subsystems, production processes, and suppliers. This method was first applied by Ford, to be later integrated as a major element of ISO / TS 16949. Compared to earlier systems, the progressive quality plan covers several influencing factors, systematizes them and prescribes clear rules.

The goal of the quality system according to ISO / TS 16949 is the development of a quality management system that provides continuous improvement, failure prevention, and reduction of variations and defects in the supply chain. It is applied in the design (development), production, assembly, and servicing of products in the automotive industry and represents the harmonization of the requirements of the European (German, French, and Italian), American (GM, Ford, and Dodge / Chrysler) and Japanese automotive industries [2, 3].

Figure 1 shows the historical development of the quality management system (QMS) standard from 1970, until the establishment of the ISO / TS 16949: 2002 standard and its revision in 2009.

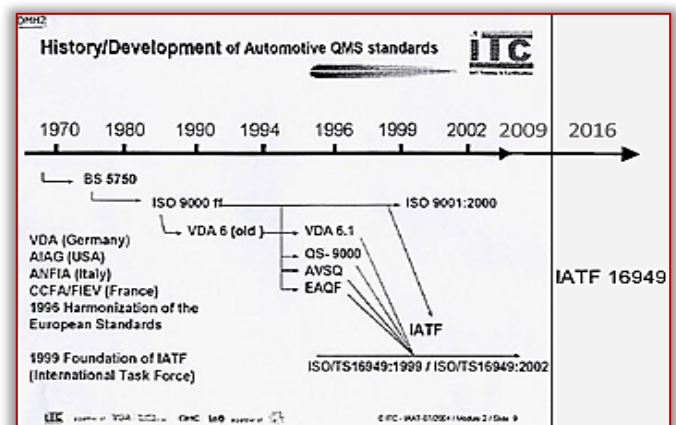


Figure 1. Development of standards for the quality management system in the automotive industry
From October 2016, ISO / TS 16949 became IATF 16949, based on the ISO 9000 standard. Nevertheless, IATF declares in the History chapter of IATF 16949:2016 that „The IATF maintains strong cooperation with ISO by continuing liaison committee status ensuring continued alignment with

ISO 9001” (IATF, 2016). IATF 16949:2016 is linked with ISO 9001:2015, and cannot be considered a standalone QMS standard. It is a supplement to ISO 9001:2015 and must be used in conjunction with [3].

METHODS AND TOOLS OF THE QUALITY SYSTEM

Tools for improving quality in the automotive industry are known as: concepts, techniques, methods, studies, tools, or, more generally, all efforts aimed at improving quality. Quality policy covers the basic directions and goals of the organization in terms of quality, so it is one of the elements of the general policy of the company and must be in accordance with the strategy, goals, and mission of the organization. Also, the full effect of the application of quality tools (the tools of the quality management system), requires the correct choice of tools and their mutual coordination.

This paper presents only some of the quality tools used in the observed company, namely:

1. PPAP analysis,
2. Process flow chart,
3. FMEA analysis,
4. Control plan, and
5. MSA/SPC analysis.

— PPAP and MSA/SPC analysis

PPAP in the automotive industry represents a process that is required to ensure mutual trust between the customer and the supplier. The buyer / customer is the one who sets out his requirements, and the supplier needs to find the most favourable and easiest way to meet the requirements set by the customer.

Every supplier aims to conquer new markets and make a profit in the most competitive way possible. Therefore, the proper process of approving the first samples is paramount for ensuring deliveries for serial production with risks, in terms of quality, minimized, but also ensuring the delivery of the required quantity of products.

The customer submits to the supplier the technical documentation of the requested product / part, with defined dimensions and permitted deviations. The key characteristics and potential places (positions) where the risks of failure may occur are the positions that are processed in MSA/SPC analysis. According to the customer's requirements, the supplier must submit the first samples, DFMEA analysis, flow chart as well as control plans with MSA / SPC analysis. PPAP ensures that the supplier can meet the customer's requirements in terms of production and quality, engineering design as well as the requirements and specifications defined in the technical documentation. Also, the analysis shows that the selected technological process of production can produce a part that complies with all the set requirements. Through PPAP analysis the customer requires a detailed process of analysis of his requirements and needs from the supplier. This analysis involves making the first samples and sending them to the customer for approval.

The PPAP analysis process is quite complex and long lasting, but, as such, it defined requirements that must be provided in order to confirm that the production process will produce a quality product. The elements that are required depend

exclusively on the customer, which is most often defined in the offer for the production of a certain product [4].

The PPAP process is detailed and time consuming, but, as such, it provides customers with adequate information and confirmation that all processes from design to production and control will be inspected in detail and, thus, ensure that only high quality products will always be delivered.

— FMEA analysis

The FMEA methodology was developed to systematically monitor and analyze process failures. This method belongs to the methodology of building business processes, and was developed in the 1950s. FMEA is one of the most reliable methodologies for monitoring and analyzing failures in management systems and it includes many factors to identify failures and their causes.

Today, many methodologies are used in business process management and construction systems, for example: IDEFO (International Definition for Function Modelling), SIPOC (Supplier Input Process Output Customer), UML (Unified Modelling Language) and others. All of the above methodologies are useful for a quality management system. The FMEA was first used in the U.S. military industry and at the NASA. Due to good results it has shown, it has started to be applied in other areas of industry as well.

— The Control plan

The control plan defines the method of assessing functional characteristics throughout the entire process of manufacturing semi-finished products and products, in order to meet the specific requirements of the process.

The process of making a control plan implies a detailed analysis of the process and place of occurrence of risks that affect the quality of products through the definition of control characteristics (control-points). Defining control points implies:

- ≡ Determining the type of quality characteristics (numerical or attributive), the form and specifications of failures, the availability of means and methods for measurement as well as the importance of quality characteristics,
- ≡ Defining the scope and frequency of quality control,
- ≡ Determining the holder of control (worker, process controller, or leader).

The results of the measurements are entered in the form “Taking over the process” on the basis of which it is possible to identify the deviation of the controlled measure from the measure prescribed by the control plan.

APPLICATION OF QUALITY METHODS AND TOOLS

– a case study

The company was founded in 1994, and its main activity is the production of stator windings for motors and starters for customers of the automotive industry, Figure 2. The production line combines winding elements with soldering, which are impregnated with electrical insulating varnish immersion process. The installation of the protective layer elements takes place on an automatic line with dedicated devices.



Figure 2. The finished product

In accordance with the procedures of the company that is under research, specific data (numerical values) will not be visible in this paper because they are secret, but they can always be available and presented to a potential customer.

— PPAP – customer requirements

This paper presents a part of the PPAP analysis that is performed in the observed company, as a process of approving the first parts for a specific project of production and assembly of the final product.

In order to make the first parts and send them for approval, all the requirements stated in the technical documentation must first be realized. The first step in accepting and developing the first PPAP samples is to form a team, which will follow and support the whole process of making the first parts and develop an APQP plan, based on their knowledge and skills. This plan facilitates communication between all participants in the process and ensures that all required steps are implemented on time. The benefits expected from the application of the APQP are:

- ≡ directing resources to achieve customer satisfaction,
- ≡ enabling early identification of necessary changes,
- ≡ avoiding delayed changes,
- ≡ providing a quality product, on time, with minimal costs [3].

As shown in Figure 3, the customer submits a request stating all the necessary analysis, or specific requirements, for the first product samples to be approved, which are:

- ≡ three reference samples,
- ≡ the dimensions of the samples must be within the tolerances shown in the drawing,
- ≡ performing analysis of materials that are part of the stator,
- ≡ FMEA process analysis,
- ≡ a process flow diagram, and
- ≡ a control plan.

Also, the request provides key measures:

- ≡ inner diameter (during further installation, this dimension is one of the key functional characteristics),
- ≡ breakdown (100% control, value >2s/ 750V),
- ≡ water resistance (air release test), etc.

Figure 4. shows the measurement report. The analysis and production of the first samples is given on the example of stator assembly.

| | | | |
|--|--|---|--------------------------------------|
| PPAP - REQUIREMENTS PSW | | Številka naročila: 22/20 | |
| | | Datum naročila: | |
| DOBAVITELJ | | | |
| Naziv: | | Kontaktna: | |
| Naslov: | | Tel.: | |
| | | e-mail: borisa.radovic@ba.mahle.com | |
| PROIZVOD 16.286.995.599 | | | |
| Naziv proizvoda: stator z nosilcem krtačk | | Mahle Dobavitelj | |
| Vzrok vzorčenja: | | Ident.št. proizvoda | |
| <input type="checkbox"/> Nov dobavitelj | | Št.obvestil/datum | |
| <input type="checkbox"/> Nov proizvod | | Standard | |
| <input type="checkbox"/> Sprememba konstrukcije | | Kataloška št. | |
| <input type="checkbox"/> Sprememba materiala | | Ostale zahteve Mahle: | |
| <input type="checkbox"/> Sprememba tehnologije | | | |
| <input type="checkbox"/> Sprememba lokacije proizvodnje | | | |
| <input type="checkbox"/> Dajlja prekinitov proizvodnje | | | |
| <input type="checkbox"/> Zamenjava nabavnega vira ali poddobavitelja | | | |
| <input checked="" type="checkbox"/> Ostalo: Projekt Scania | | Odgovorni SQE: Andrej Jerkič | |
| PPAP ZAHTEVE | | | |
| | Pojasnila | Zahtevk | Prejeto |
| 1. Vzorci | Zahtevana količina: 3 | <input checked="" type="checkbox"/> | <input type="checkbox"/> |
| 2. Risba | <input checked="" type="checkbox"/> Mahle <input type="checkbox"/> Dobaviteljeva | <input checked="" type="checkbox"/> | <input type="checkbox"/> |
| 3. Merilne dimenzije | | <input checked="" type="checkbox"/> | <input type="checkbox"/> |
| 4. Analize materialov | <input checked="" type="checkbox"/> Kem. <input checked="" type="checkbox"/> Meh. <input type="checkbox"/> Metal. <input type="checkbox"/> Elek. | <input checked="" type="checkbox"/> | <input type="checkbox"/> |
| 5. Rezultati preizkusov | | <input type="checkbox"/> | <input type="checkbox"/> |
| 6. FMEA konstrukcije | | <input checked="" type="checkbox"/> | <input type="checkbox"/> |
| 7. FMEA procesa | | <input checked="" type="checkbox"/> | <input type="checkbox"/> |
| 8. Diagram poteka proiz. procesa | | <input checked="" type="checkbox"/> | <input type="checkbox"/> |
| 9. Analize sposobnosti procesa | Ppk ≥ 1,67 Cpk ≥ 1,67 | <input type="checkbox"/> | <input type="checkbox"/> |
| 10. Analize sposobnosti merilnega sistema MSA | | <input type="checkbox"/> | <input type="checkbox"/> |
| 11. Načrt nadzora kakovosti | Control plan | <input checked="" type="checkbox"/> | <input type="checkbox"/> |
| 12. Podatki o laboratorjih | | <input type="checkbox"/> | <input type="checkbox"/> |
| 13. Poročilo o zunanjem ogledu | | <input checked="" type="checkbox"/> | <input type="checkbox"/> |
| 14. Zapis o skladnosti s posebnimi kupčevimi zahtevami | | <input type="checkbox"/> | <input type="checkbox"/> |
| 15. Izjava o skladnosti materialov z okoljskimi zahtevami | | <input checked="" type="checkbox"/> | <input type="checkbox"/> |
| 16. IMDS | | <input checked="" type="checkbox"/> | <input type="checkbox"/> |
| 17. Drugo: | | <input type="checkbox"/> | <input type="checkbox"/> |
| POTRDITEV PREDLOŽITVE | | | |
| Odgovorna oseba (tiskano): Njegoslav Đokic, Aleksandra Jokic | | Podpis: | Teža (kg): |
| | | Naziv: IZUMIRNA KVALIFIKACIJA e-mail: njegoslav.dokic@ba.mahle.com Tel.: 00387 51 535 480 | Datum predložitve vzorcev: 10/7/2020 |
| Opombe: Prvi vzorci | | | |
| ODLOČITEV MAHLE: | | | |
| <input type="checkbox"/> ODOBRENO | | | |
| <input type="checkbox"/> ZAČASNO ODOBRENO | | | |
| <input type="checkbox"/> ZAVRNJENO | | | |
| Odgovorna oseba: | | Opombe: | |
| Datum: | | | |
| Podpis: | | | |

Figure 3. PPAP requirements

| | | | | | |
|----------------------------|--------------------------------|---|-----------|--------------|--------------|
| PPAP - MEASUREMENT RESULTS | | Številka naročila: 22/20 | | | |
| | | Datum naročila: | | | |
| Dobavitelj: | | Naziv proizvoda: stator z nosilcem krtačk | | | |
| | | Ident.št. Mahle: | | | |
| | | List 1 od 1 | | | |
| REZULTATI MERITEV | | | | | |
| Poz. | Predpisana vrednost | Izmerjena vrednost | | Nespregledno | Spremenljivo |
| | | DOBAVITELJ | MAHLE EDS | | |
| 1. | MIN ϕ | | | | |
| 2. | MIN 2 x MIN | | | | |
| 3. | MIN | | | | |
| 4. | MIN | | | | |
| 6. | MIN | | | | |
| 7. | PRIVIJALNI MOMENT ZA POZ 4. JE | | | | |

Figure 4. A measurement report

— MSA/SPC analysis

Since most customers have certain dimensions on their products that are defined as key process characteristics (KPC), for such dimensions / measures during the production process, continuous statistical monitoring is performed.

Figure 5 shows the samples on which the measurement was performed. Measurement results can be presented in two

forms, a process under statistical control and a process not under statistical control. A total of fifty samples were tested, of which forty-nine are within the prescribed limits, while sample number twelve goes beyond the set limits, which means that the samples meet the set tolerance limits. It is crucial that the process is under statistical control, if 2/3 of the values of the controlled parameters are within the central third of the control chart, in a width $\pm \sigma$ around the central line. The values of C_g and C_{gk} are indicators of the process ability, and as $C_g = 2.01$ and is in the range $(1.62 < 2.01 < 2.41)$, the results show that the possibility of scrap is reduced.



Figure 5. MSA analysis for the product (winding)

This ensures that the most important measures are under constant control and that potential errors are detected as soon as possible, which allows us to stabilize the process and reduce production costs.

Figure 6 shows the SPC analysis of the windings and based on a hundred values tested, they were all in the prescribed tolerance field. Process capability index $C_p = 3.45$ as well as long-term study of a stable process $C_{pk} = 1.56$.

Figure 6 shows us that the process is stable, as shown in the diagram, both parameters are green and are within the allowable limits ($C_p \rightarrow 2.95 < 3.42 < 3.90$); ($C_{pk} \rightarrow 1.33 < 1.56 < 1.79$).

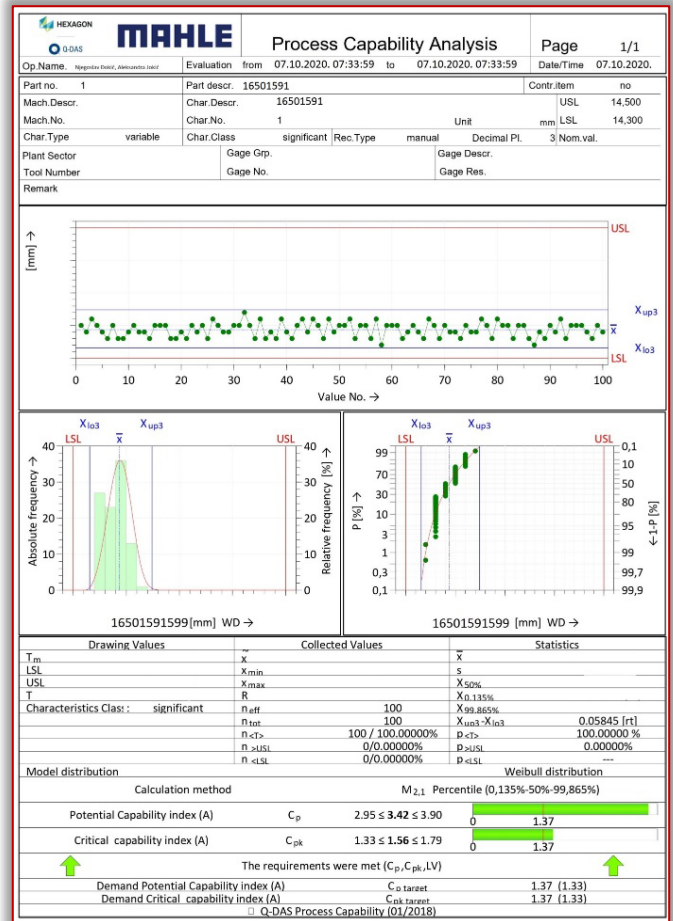


Figure 6. Statistical monitoring of critical measures (winding)

— The control plan

To ensure good traceability, the most important thing is to create a good control plan. At the workplace, there are forms called "Process takeover", which define the measurements to be performed, and which are prescribed by control plans. The control plan clearly follows the technological process of product development and provides support in ensuring the control of measures to comply with the prescribed tolerances, Figure 7.

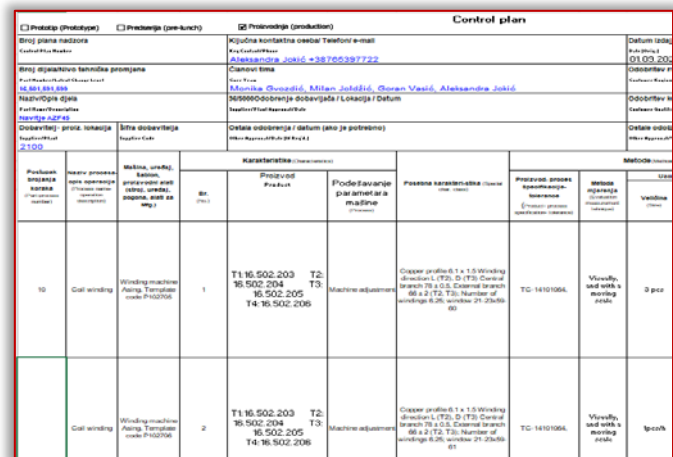


Figure 7. The control plan – extract

In case of deviations, it is prescribed how to act in order to avoid poor product quality. It is very important to

distinguish and abide by the methods of control that are also prescribed, and relate to:

- ≡ **PP (taking over the process)** - performed by the person responsible for adjusting the machine, which confirms that the first three pieces are good, both as visually and in terms of metrology, and meet the requirements prescribed by the control plan, after which production can begin.
- ≡ **NP (process control)** – performed by a line or process controller, at the beginning of the process and during the production process.
- ≡ **AK (auto-control)** – performed by a worker at his workplace, who has a defined procedure when he should perform the measurement, while confirming that the production is going according to plan, i.e. there are no deviations.

— **FMEA analysis**

As shown in the form in Figure 8, the parts supplier should perform a failure risk analysis based on the flowchart and control plan. It is necessary to have a systematic approach to operations and to perform an analysis of the entire production process, in order to reduce the risk of failures and minimize them.

Figure 8 shows part of the conducted FMEA analysis. Based on the defined functional requirement of the process, the team determines the potential forms of failure and the potential consequences of the fault failure. Evaluation performed on the basis of a defined procedure for performing FMEA analysis (RPN = SxOxD).

| Process operation / Function (F) | Functional process requirement (R) | Potential form of the fault (C) | Potential consequences of the fault (E) | Potential causes of fault mechanism (C) | Prevention (P) | Detection (D) |
|---|--|--|---|---|---|---------------------|
| S20 Shipping accuracy of the winding | Shipping accuracy of the winding (R20) | Winding position of the added part on the winding | Irregularity of insulation (assembly) | Winding position during winding | Welding device visual inspection, operating instructions, qualification cards | 100% visual control |
| | | Change in winding components (cables, brushes, jumper, tube and connecting elements) | Breakthrough | Winding manipulation | Facilitating lessons Learned, operating manual, competency matrix | 100% visual control |
| | | Bad winding of the winding | Irregularity of insulation (assembly), breakthrough | Insufficient height of connection of the winding in the current | Adaptation process, operator on call, matrix management, AutoControl, operating instructions, qualification cards | 100% visual control |
| | | Low winding | Breakthrough | Human factor | Behavior of operator according to technological instructions, operating instructions, training matrix | 100% visual control |

Figure 8. FMEA analysis – extract

CONCLUSION

In today's turbulent business environment, organizations can successfully achieve and direct defined goals only by establishing the right strategies and policies, finding the right methods and their implementation, and constantly monitoring the effects achieved.

In the automotive industry, in addition to multiple requirements for meeting standards, both basic quality standards such as ISO standards and required standards specific to the automotive industry IATF 16949, VDA 6.3, AIAG quality tools, CQI standards still need to meet

customer specific requirements. Very often, IATF 16949 is called the customer standard, since the specific requirements of the customer have priority over the requirements of the standard itself. The links between the requirements of the standard and the customer specific requirements must also be harmonized with the existing technologies of manufacturing individual components, whereby new technologies are often approached and applied in order to achieve competitiveness in the market. New technologies, new suppliers, and projects represent a huge set of risks for the successful placement of products on the market while achieving appropriate competitiveness.

The revision of the standard, ISO / TS 16949: 2009 and the transition to IATF 16949: 2016 aims to develop a quality management system that provides continuous improvement highlighting the lack of prevention and reduction of waste and variation in the supply chain. The incorporation of ISO 9001: 2015 and IATF 16949 requirements includes specific requirements: employee competence (awareness and training), design, development, production and provision of services, control and monitoring of measuring devices and measurements, analysis, and improvement. All of this aims to get products and services that satisfy customers.

Quality control is performed by process controllers at all stages of production. In order to make a product of satisfactory quality, it is important that the production process is stable.

Constant investment in new technologies, modernization of production, education, and training of employees at all levels improve the quality system in the company

Continuous improvement of the quality of the production process, based on increasing the productivity and knowledge of each employee in the organization, is crucial for the realization of the mentioned preconditions. Competition and the globalization of all flows are forcing companies to find increasingly successful management approaches using quality management tools in all business processes. The main goal of every company is to strive to always deliver improved value to the customer and user, as a result of improving the overall performance of the business system as well as capabilities and success in the market.

Note:

This work is based on the paper presented at DEMI 2021 – The 15th INTERNATIONAL CONFERENCE ON ACCOMPLISHMENTS IN MECHANICAL AND INDUSTRIAL ENGINEERING, organized by Faculty of Mechanical Engineering, University of Banja Luka, BOSNIA & HERZEGOVINA, co-organized by Faculty of Mechanical Engineering, University of Niš, SERBIA, Faculty of Mechanical Engineering Podgorica, University of Montenegro, MONTENEGRO and Faculty of Engineering Hunedoara, University Politehnica Timisoara, ROMANIA, in Banja Luka, BOSNIA & HERZEGOVINA, in 28–29 May 2021.

References

- [1] Tanasić Z., Janjić G., Bobrek M. (2016). Organizacija i menadžment. Univerzitet u Banjoj Luci, Mašinski fakultet, Banja Luka.
- [2] Kušar, K., Rihar, L., Duhovnik, J., Starbek, M. (2014). Concurrent realisation and quality assurance of products

- in the automotive industry. Concurrent engineering: Research and Applications. Sage Publications. vol. 22 (2), p. 162-171.
- [3] <https://www.researchgate.net/publication/320356880>
Quality Management Requirements in the Automotive Sector a Structured System, accessed on: March 20, 2021.
- [4] Bobrek, M., Sokovic, M. (2005). Implementation of APQP concept in design of QMS. Journal of Materials Processing Technology, vol. 162-163. p. 718-724.
- [5] Ebrahimi, M., Baboll, A., Rother, E. (2019). The Evolution of World Class Manufacturing Toward Industry 4.0: A Case Study in the Automotive Industry, IFAC-Papers On Line, vol. 52, p. 188-194.
- [6] IATF 16949:2016 - Automotive Quality Management System. International Organization for Standardization. Geneva.
- [7] <https://www.svijet-kvalitete.com/index.php /upravljanje-kvalitetom/878-fmea-metodologija>
- [8] Belu, N., Ali, A., Khassawneh, N. (2013). Application of Control Plan – PPAP Tool in Automotive Industry. Production QUALITY access to success, vol. 14 (136), p. 5-12.
- [9] Doshi Jigar A., Desai Darshak A. (2018). Role of Production Part Approval Process in Continuous Quality Improvement and Customer Satisfaction. International Journal of Engineering Research in Africa, vol. 22, p. 174-183
- [10] Chiarini, A., Vagnoni, E. (2018). Can IATF 16949 certification facilitate and foster Lean Six Sigma implementation? Research from Italy, Total Quality Management & Business Excellence. ISSN: 1478-3363 (Print) 1478-3371 (Online), vol. 31, Issue 7-8, p. 887-906



ISSN: 2067-3809

copyright © University POLITEHNICA Timisoara,
Faculty of Engineering Hunedoara,
5, Revolutiei, 331128, Hunedoara, ROMANIA
<http://acta.fih.upt.ro>

¹Olutola Olaide FAGBOLU, ²Chukwunonso Stanley EDU, ³Adekunle Joseph ADEWALE

MULTILINGUAL SOCIAL MEDIA PLATFORM-BASED TOURISM OPERATIONS IN UGANDA

¹Department of Mathematics and Statistics, Fourah Bay College University of Sierra Leone, Freetown, SIERRA LEONE

²Department of Computer Science, School of Computing & Information Technology, Kampala International University, Kampala, UGANDA

³Department of Multimedia Technology, Faculty of Communication & Information Technology Osun State, College of Technology Esa-Oke, NIGERIA

Abstract: Tourism is travelling for pleasure to places outside the usual environment and it is an important source of revenue in Africa which has not been properly harnessed to generate expected income in Uganda hence the need to develop a social media app called TourIt. TourIt will showcase landscapes, rich history of ancient and cultural heritages, water bodies (such as lakes and rivers), wild safari expeditions, artefacts. It is user-centred design, interactive information-sharing, interoperability, and collaboration on tourism with multi-languages including Luganda, English, Swahili, Yoruba, Ibo for now while other languages can be added as the app evolves. The app was developed using Android Studio XML for the graphical user interface, Firebase for database, Java, and XML for coding while Javascript handles several modules including functions in the database and automatic restoration of multiple languages were done with MBL (Memory-Based Learning), CRF (Conditional Random Field) and rule expressions which were implemented in UML class of Python Programming Language with NLTK (Natural Language Tool Kit). This social media app will create and co-create tourism-based content, edit the content, determine the ratings of its content. Comments, commentaries and narrations are handled by the multilingual social media platform whenever it is necessary, contents of the social media platform are discussed, shared, tagged, organized and mashed with other contents to promote rich cultural values, natural endowments, tourist centres, and other attractive places in Uganda.

Keywords: Social Media, Mobile App, TourIt, Android Studio XML, Multilingual, Information Technology, Tourists

INTRODUCTION

Most of the African countries are naturally endowed with vast human and natural resources that are populated in a wide variety of points of interest. There are diverse cultural heritages and great numbers of landscapes that were left untapped or underutilized. In Uganda, more revenue would have been generated if all these natural and cultural resources are adequately publicized. Lesser revenues are obtained from her tourism than the expectation because prospective tourists or explorers were not aware of the abundance of tourist resources and attractive centres that are found in the Pearl of Africa [3] [7]. The continent of Africa can be divided into three categories relative to tourism: countries with the developed tourism industry (such as Egypt, South Africa, Morocco, and Tunisia); countries with developing tourism industry (such as Kenya, Mauritius, and Botswana); and countries with the evolving tourism industry (such as Algeria, Burundi, and Uganda)[4] [7].

Uganda has a magnificent piece of land whose diverse landscape is encompassing a snow-capped Mountain Rwenzori and other mountains such as Elgon, Mufumbiro, Stanley, Kiyanja, Speke, Gessi, Baker, Muhabura, Moroto, Toroto Rock, Zulia, Imatong, Wati, Morungole, Emin and so on. The nation's 40 percent landmass is covered with water bodies that are rivers, lakes, and wetlands as it is the home of the world's longest river, the River Nile [7]. This country has well over 1,000 species of birds, that is 68 percent of the Africa continent birds are domiciled in Uganda and 12 percent of the total population of the world birds are found

in this nation. Uganda is one of the few countries in the world where the imaginary line that divides the earth into two half passes (Northern and Southern hemispheres). The equator which is a magnetic needle-like found on the compass where sunrises and falls rapidly with no gravitational pull that invariably reduces weight with about 3 percent.

There are numerous cultural sites and heritage of which some are recognized by UNESCO to preserve the rich culture of different ethnicities in the country, conserve historical values of events, commemorate incidents, hold treasure, and symbolize slavery. Some of the examples are Kasubi tombs, Namugongo Shrine, Baker's Fort, Bigo bya Mugenyi, Sezibwa Falls, Nakayima Tree, Nyero Rock Paintings, Naggalabi-Buddo Coronation Site, Itaaba Kyabanyoro, and other National parks. Its abundant wildlife includes Chimpanzees, Giraffes, Gorillas, Hippopotamus that littered all these National Parks and there is a plan to make Uganda an Africa's premier birdwatching destination. The growth of social media is an added advantage in terms of connectivity which means people from all over the world can connect with one another [2], it represents a movement away from static web pages to dynamic and shareable content with social networking for example Facebook has evolved from what was college friend's network to host users that are more than U.S residents [13]. Nearly 4 or 5 people participate in one or more online communities or social networks. TourIt (social media app) is a tool that facilitates user-centered design, interactive information-sharing, interoperability, and collaboration on tourism with multi-

languages such as Luganda, English, Swahili, Ibo, Yoruba for a start while other languages can be added as the app evolves [8] [10].

Social media and its tools have become a focal point for many people to connect around the world, extend to reach more people, new and diverse audiences meet for feedback mechanism and this app brings audiences who may share the same interest in an excursion, holiday, travelling and tour to bridge the geographical boundaries [1] [5]. The multilingual feature of this app will enhance free flow of communication between individuals of different backgrounds, languages, and other social status, these multiple languages, and compartmentalization of their interest is done based on their language of choice [8] [9] [11].

RESEARCH OBJECTIVES

The objective of this research is to design social media app for prospective explorers and tourists in multiple languages [6] which will serve as a guide. It will typify how tourism businesses are to be conducted with the advent of ICT, increase the level of awareness, and explore untapped resources (tangible and intangible benefits) in Uganda.

- ≡ To develop social media tourism app (TourIt) that can guide and provide vital information about places of interests
- ≡ To implement the social app in (a)
- ≡ To test and prototype the social media app in the tourism industry.

METHODOLOGY

To achieve all these objectives, an appropriate blueprint that represents all the necessary requirements were done with FIGMA and Adobe Photoshop as graphic editors to plan and document this project, Graphical User Interface (GUI) was designed using Android Studio XML which is an official IDE for Google's Android OS built with JetBrains' IntelliJ IDEA software and available for download on Windows, MacOS and Linux.

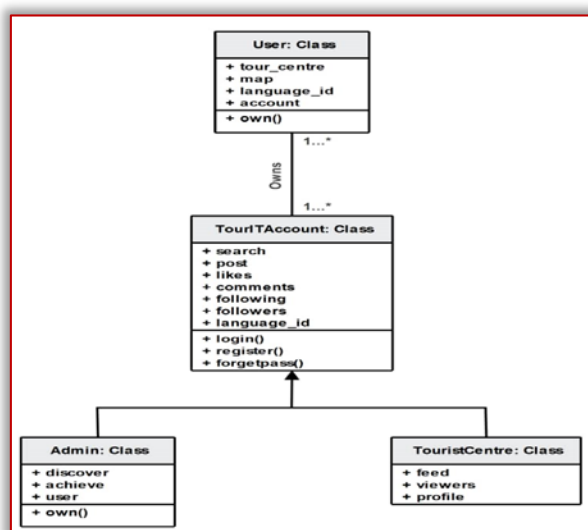


Figure 1. Class diagram for TourIt App

There are 14 different UML diagrams that can model the social media platform entities and their attributes but the class diagram is selected to serve as a building block for Object-Oriented solutions within expected classes, its

attributes and expected operations, and the existing relationship between classes. The Figure 1 typifies how the class diagram is applied to the development of a multilingual social media platform for tourism operations in Uganda.

— Mathematical Model

In the development of a multilingual social media platform for tourists the variable changes in discrete-time which starts whenever a user creates any query into the platform through the graphical user interface provided. If the current variable is a_n then the predicted value of the variable will be a_{n+1} . A mathematical model for the evolution of the social media platform a_n will take the form of equation 1.

$$a_{n+1} = \alpha a_n + \beta \quad (1)$$

where the α is a scalar multiple of the social media platform by constant β . This model can be amended to make the dependence depend on more terms and include the possibility that every iteration in social media for tourists can be depicted as shown in equation 2.

$$a_{n+1} = \alpha_1 a_n + \alpha_2 a_n^2 + \beta \quad (2)$$

which corresponds to the population model of visitors to the social media platform where the number of views changes every time.

— Database Design

The database was designed using firebase (it is a real-time database). Firebase is a mobile and web application development platform developed by Firebase, Inc. in 2011, then acquired by Google in 2014. As of October 2018, the firebase platform has 18 products, which are used by 1.5million apps [15] and list of firebase services used are firebase AUTH, firebase Database(real-time), cloud messaging, firebase functions

— Multilingual approach

A computational model with the probabilistic and deterministic component for automatic restoration of multiple languages is required which will use Memory-Based Learning (MBL), Conditional Random Field (CRF), and rule expressions.

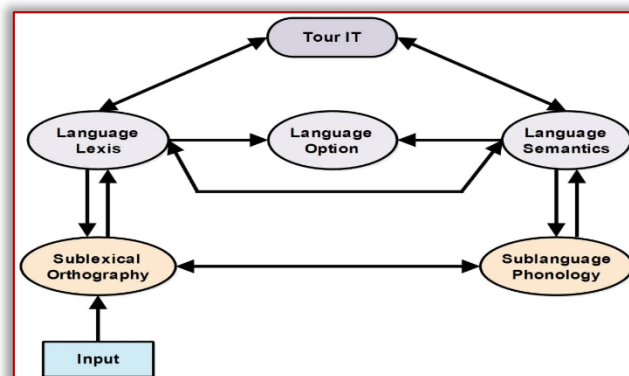


Figure 2. The multimodal representation of languages

The multilingual aspect of this app was handled with a UML class diagram and implemented using Python Programming Language with Natural Language ToolKit (NLTK). Distillation-based approach to boost the multilingual machine translation in which individual models are first trained and regarded as teachers and then the multilingual model is trained to fit the training data and match the

outputs of individual models simultaneously through knowledge distillation and experimented in Ted Talk Translation [14].

— Programming languages

Java and XML were used for most of the coding, Javascript handles several modules and were used to write functions like notifications in the firebase database. The choice was made based on the platform-independent, security features, high-performance of JIT compilers, and excellent for handling any complexities in data and its structure. Advantages and Disadvantages of the System.

Advantages.

- ≡ Lower costs.
- ≡ Improved integrity.
- ≡ Promotes confidentiality.
- ≡ Covers a wide area/vastness (the whole of Uganda).

Disadvantages.

- ≡ Requires network connection (Data Charges).
- ≡ Limited access/only accessible on the mobile device (an Android phone).
- ≡ Requires prior knowledge about the system.

— System Requirements

It comprises of functional requirements and non-functional requirements. A functional requirement describes what the software will do that is, the main services the system should provide and how it will respond to inputs while non-functional requirement describes the criteria that can be used to judge the operation (behaviour) of the system such as usability requirement, efficiency requirement, performance requirement, space requirement, reliability requirement and portability requirement [12]. The hardware required is itemized as Phone with Android OS version 5.0 Lollipop and above, for system testing Computer system with 512MB RAM, Monitor with a minimum resolution of 1024X768, Keyboard, Mouse, HDD with NTFS format system is needed. The use-case diagram list parameters and values of the requirements as depicted in Figure 3.

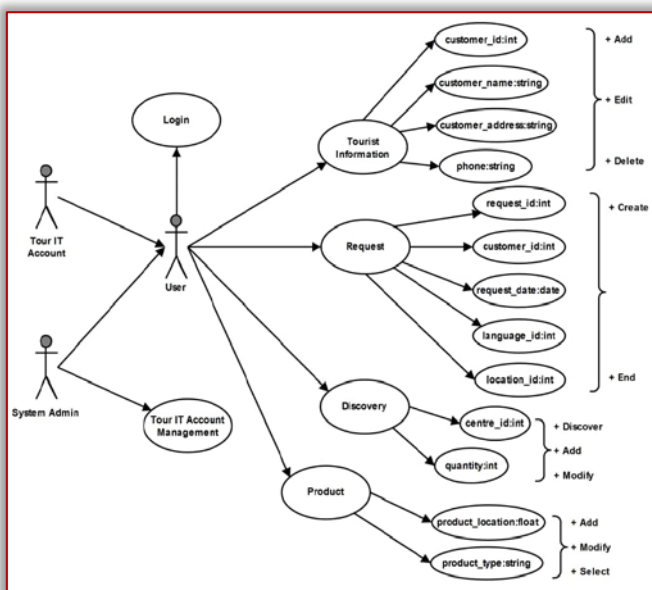


Figure 3. Use-case for social media App

— Basic concept of the System

The developed app contains detailed texts, pictures, videos and other guiding information about tourist centres visited by any individual or intending centres to be visited. It is a value-added media for those interested in visiting some places while some people may have their interest arising for having a fair and better understanding of the tourist attractions that existed and make decisions objectively.

The Modules in the System.

- ≡ Find the current location
- ≡ Locate in map
- ≡ Calculate the distance between two cities
- ≡ Location of different tourist sites

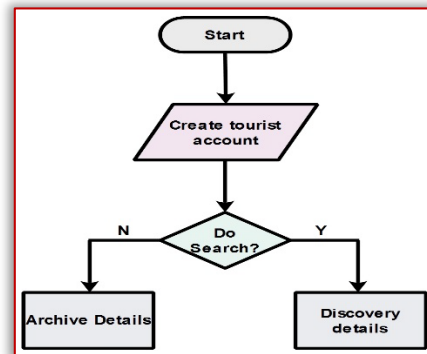


Figure 4. Annotated flowchart of TourIT

The annotated flowchart of TourIT that show how an account is created and what can be done once a particular tourist centre is looked for in Uganda

IMPLEMENTATION

This app offers an opportunity for users and a platform where potential tourists will be able to post pictures and videos of the places they are currently visiting or intend to tour in any of the prototyped languages. This platform will guide the prospective users and inform them about different tourist centres and attractions at the location he or she is currently, or check different districts within Uganda for tourist attractions, cultural heritage sites, and other places of interest from anywhere in the world. It is patterned after Instagram social media where tourists can view different activities through another tourist’s post and the typical screenshots of the app are depicted in different Figures and explicitly described. In Figure 5, the following notations are found:

- ≡ Search icon
- ≡ Following post icon
- ≡ Change the language icon
- ≡ Newsfeed posts from users
- ≡ User’s profile picture
- ≡ Number of users that view the post
- ≡ Liked posts (where user like others post)
- ≡ Comment on post
- ≡ Newsfeed
- ≡ Map icon
- ≡ Profile icon
- ≡ Upload post

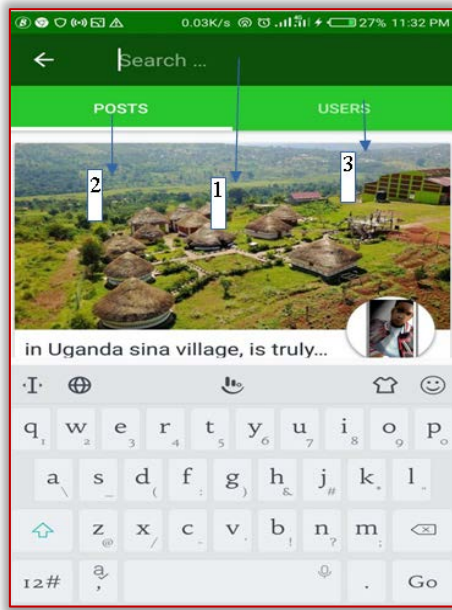


Figure 5. Home page of TourIt app

Once the app is launched, Figure 6 automatically pop-up as the first page while the search icon look for different users' post or new user that are making use of the app and this can be accessed from the homepage as shown in pop-up Figure 6 List of activities in Figure 6 are:

- ≡ Search(search on post based on what tab you choose)
- ≡ Post(click on the post tab to search for user post)
- ≡ User(click on the user tab to search for user post)

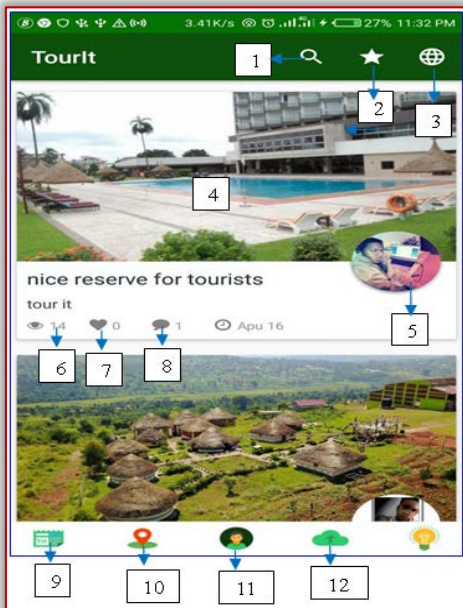


Figure 6. The search page of TourIt app

The map interface shows different tour attractions near your current location and direction as represented in Figure 7 coupled with other information about the nearest hotels, restaurants, shopping malls etc.

List of activities in Figure 7:

- ≡ Search(search for any location on map)
- ≡ Search for nearest (restaurant, attraction, and hotel near your current location)

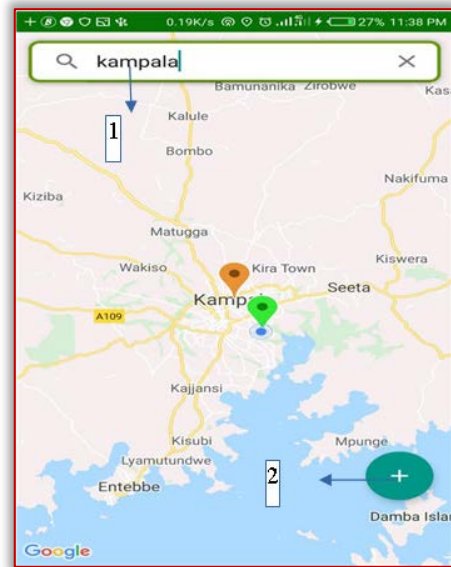


Figure 7. Map interface page

In Figure 8, we have the user's current profile page with different posts the users have made, the number of likes, people that the user follows, others that are following the user coupled with other personal details.

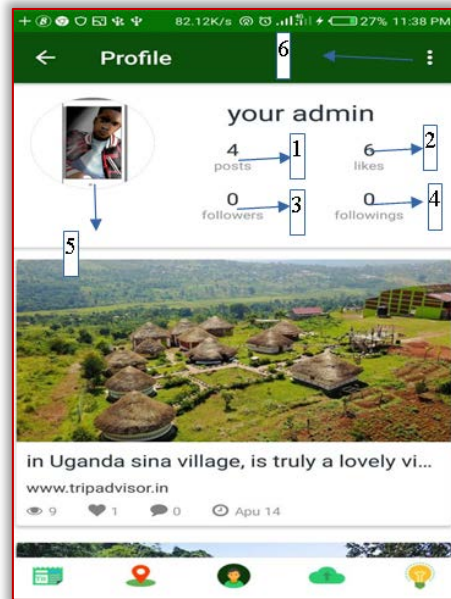


Figure 8. Profile page

List of activities/modules in Figure 8:

1. Post(how many posts the user have posted)
2. Likes(accumulated likes the user have gotten from all the post only the user can see this)
3. Followers(who is following the user)
4. Following (who is the user following)
5. Profile picture
6. Tab-bar(create a post, edit a post, and sign out)

CONCLUSIONS

In conclusion, the development of social media apps for prospective tourists in Uganda will promote tourism as an industry as well as increase internally generated revenue. More employment opportunities, enrich business scopes and build Uganda's brand, image, and identity that will make the nation more famous and wealthier than it is. It will

encourage more people to visit the pearl of Africa, promote cultural diversity, and international connections and take the country to the category of countries with developed tourism such as South Africa, Morocco and Egypt. This app will offer exceptional tourism services to both users and the nation to solve problems of practice, application of new technology, and other sundry matters of tourism and travel. Any user or tourist that may wish to explore Uganda will be properly guided with the app.

This research work brought about Mobile application (android based application) that solve envisaged problems of the visitors, tourists or travellers by strengthening the tourism industry, enhance the social status of the nation and bring about economic transformation, the richer the nation, the more the quality of life of the citizenry. The ease of use and ICT adoption is part of the scope covered by this research.

This app accommodates a high number of users from different locations within and outside Uganda without redundancy and high-performance mobile computing are catered for with embedded fault-tolerant systems to prevent both expected and unexpected errors which will increase usability and acceptability of TourIt. Although there are few limitations, not all languages are catered for in the social media app but the more the languages the better the acceptability. The usability testing was done within the university campus and efficiently gathered statistically valid data on the TourIt, it includes twenty (20) questions which the user answered and Software Usability Scale (SUS) is 75 which attest to the priority given to users on the usability of tourism-based operation in Uganda. The future work is to include all languages of the world for the convenience of users and ease of use of any intending travellers to Uganda and possibly deploy the app for all nations of the world that are developing or have developed their tourism sector.

References

- [1] Abuhashesh, M.Y. (2014). Integration of Social Media in Businesses, International Journal of Business and Social Science Vol 5, No. 8 July 2014.
- [2] Advanced Android Tutorial Simply Easy Learning by tutorialspoint.com.
- [3] Alhroot, A.H.H. and Al-Alak, B.A.M. (2009). Tourism roots and destination marketing bridging civilizations, cultural heritage and tourism theories. Asian Journal of Marketing, 3: 108-116
- [4] Brown, B. and Chalmers, M. (2003). Tourism and Mobile Technology, Proceedings of the Eighth European Conference on Computer-supported cooperative work, Kluwer Academic Publishers, Netherlands.
- [5] Cheverst, K. Davies, N. Mitchell, K. Friday, A. and Efstratiou, C. (2000). Developing a Context-aware Tourist Guide: Some Issues and Experiences, The Guide Project, Distributed Multimedia Research Group, Lancaster University, UK.
- [6] De Pauw, G., de Schryver, G.-M. and Wagacha, Peter Waignjo. (2009)a. A corpus-based survey of four electronic Swahili-English bilingual dictionaries. Lexikos, 19, p. 340-352.

- [7] Lepp, A. (2002). Uganda's Bwindi Impenetrable National Park: Meeting the challenges of conservation and community development through sustainable tourism.
- [8] Inversini, A. and Sykes, E. (2013). An Investigation into the use of Social Media Marketing and Measuring its Effectiveness in the Event Industry, Information and Communication Technologies in Tourism 2014, pp 131-144.
- [9] Oinas-Kukkonen, H. and Kurkela, V. (2003). Developing Successful Mobile Mobile Applications, IASTED International Conference on Computer Science and Technology, 19-21 May 2003, pp. 50-54.
- [10] Owaied, H.H., Farhan, H.A., Al-Hawamdeh, N. and Al-Okialy, N. (2011). A model for intelligent Tourism Guide System. Journal of Applied Sciences, 11: 324-347.
- [11] Papineni, K., Roukos, S., Ward, T. and Zhu, W. (2002). BLEU: A method for automatic evaluation of machine translation. ACL-2002:40th Annual Meeting of the Association for Computational Linguistics, Philadelphia, July 2002; pp311-318
- [12] Bochmann, G. (2009). Non-Functional Requirements, University of Ottawa based on powerpoint slides by Gunter Mussbacher (2009).
- [13] Xiang, Z. and Gretzel, U. (2010). Role of Social Media in Online Travel Information Search- Tourism Management, 31(2), 179-188.
- [14] Tan et al. (2019). Multilingual Neural Machine Translation with Knowledge Distillation, International Conference on Learning Representation, USA.
- [15] www.wikipedia.org/wiki/firebase accessed Apr,2019.



ISSN: 2067-3809

copyright © University POLITEHNICA Timisoara,
Faculty of Engineering Hunedoara,
5, Revolutiei, 331128, Hunedoara, ROMANIA
<http://acta.fih.upt.ro>

Fascicule 4

[October – December]

t o m e

[2021] XIV

ACTA Technica CORVINIENSIS
BULLETIN OF ENGINEERING



ISSN: 2067-3809

copyright © University POLITEHNICA Timisoara,
Faculty of Engineering Hunedoara,
5, Revolutiei, 331128, Hunedoara, ROMANIA
<http://acta.fih.upt.ro>

¹Anna YEHOVA, ²Ervin LUMNITZER

ANALYSIS OF METHODOLOGIES IN THE FIELD OF OBJECTIVE EVALUATION OF ACOUSTIC DRONE DESCRIPTORS

¹ Technical University of Košice, Faculty of Mechanical Engineering, Department of Environmental Engineering, Košice, SLOVAKIA

Abstract: Drones are currently used for various purposes. The ever-increasing number of professionally or amateurly used drones is causing an ever-increasing noise load in the area. Those sources of noise that occur historically in the environment (for example railways) are currently perceived by people as less disturbing. On the contrary, new noise sources are perceived as significantly disturbing (various types of industrial noise) and people are not able to tolerate them. Drone is a completely new and so far not explored source of noise, which is characterized by a specific spectral composition of noise and often subjectively felt a high degree of interference. At present, there are no clear national or international methodologies for assessing the impact of drones on the population. For this reason, we have started research in this area in order to develop a methodology for assessing this specific noise source. We also consider it important that this period of drone growth in some countries is crucial for the accelerated implementation of methodological procedures for dealing with noise issues. The paper proposes a basic methodology for assessing the impact of drones on humans and performed noise measurements at different flight speeds for two types of drones.

Keywords: Drone, quadcopter, noise, human impact, field measurements

INTRODUCTION

In nowadays, the number of applications for small unmanned aerial vehicles (UAVs) is growing rapidly. Relatively new consumer markets for drones include forestry, agriculture and road management, energy and communications, oil and gas production and transportation, safety and environmental protection, and so on. The widespread use of drones, in addition to the undoubtedly positive aspects, has brought a number of noise problems. According to US scientists from NASA, the disturbing sound caused by drones hinders people more than the current noise of cars and trucks. The paper seeks to advance research in the field of drone acoustics and to improve the acoustic quality of the environment in which we live, work, and relax. It is necessary to realize that in the horizon of several years there will be a significant development of the user sector of drones (scanning of terrain, buildings, stands, delivery service, filming and, last but not least, amateur use as a hobby).

DRONE LAWS AND REGULATIONS

Flying with drones, most often in the form of a compact quadcopter with a camera, have in increasing popularity in both the recreational and professional spheres. According to Chapter 7 of the Aviation Act 143/1998 Coll. drones are distinguished between autonomous aircraft, remotely piloted aircraft and flight models.

The latest European Regulations, EU 2019/947 and 2019/945, provide a framework for the safe operation of civilian drones in the European sky (EU Member States and EASA). They consider the weight and technical parameters of the drone and the operation to be performed.

Implementing Regulation (EU) 2019/947 [1] regulates the operating rules for drones, divides the operation of drones by type and place of use, and evaluate their level of risk. Delegated Regulation (EU) 2019/945 [2] describes the building regulations and the characteristics of drones in

different categories. It defines three categories "open", "specific" and "certified".

We consider the following to be the most important conclusions of the analysis of the legislative framework:

- ≡ based on the class (C0 - C4), the drones will be marked with a corresponding label,
- ≡ the drone operator will be required to register with the Civil Aviation Authority - thus obtaining a 12-digit personal identification number,
- ≡ the operator will have to mark all his drones with a personal identification number,
- ≡ the minimum age of the drone pilot is set at 16 years,
- ≡ the maximum drone flight is reduced to 120 meters above the ground, even outside operating areas and controlled areas.

All these measures concern pilots, operators and the drones themselves. But still there is no detailed specification of the effects of drones on inhabited areas and human-inhabitants. As mentioned, Delegated Regulation (EU) 2019/945 includes a standard assessment of drone noise. This is an indication of the guaranteed sound power level. This level should be determined according to STN EN ISO 3744: 2010 Acoustics.

The operation of the drone as a source of noise in accordance with Decree MzSR 549/2006 Coll., which lays down details on permissible values of noise, infrasound and vibration and requirements for objectification of noise, infrasound and vibration in the environment, corresponds to the category "Noise from other sources" according to tab. 1 of the said Decree. For this reason, the basic quantity for assessing compliance with the legislation is the equivalent A-weighted sound level for the relevant time interval $L_{Aeq,T}$, which is binding in the external environment for the relevant categories of territory.

Due to the nature of the sound of drones, which very often contains a significant tonal component, it is also possible to apply a correction for specific noise according to tab. 2 of the said Decree. We currently classify drones as "noise from other sources". According to a study of the available literature and analyzes of the perception of drone noise by the population, this classification often does not correspond to its operational character (random, aeronautical). It is clear that further legislation will be needed in this area.

DESIGN OF DRON NOISE MEASUREMENT METHODOLOGY

The process of elaboration of the methodology suitable for solving the problem of drone noise consists of the following steps:

- ≡ analysis of the requirements and objectives of the methodology,
- ≡ draft methodology,
- ≡ analysis and selection of appropriate technical equipment,
- ≡ selection of measuring objects - drones,
- ≡ verification of the methodology by trial measurement.

Among the basic recommended measuring principles that can be used to assess the acoustic quality of drones we advise:

- ≡ sound visualization by acoustic camera,
- ≡ acoustic compass,
- ≡ sound level meter system,
- ≡ sound intensity measuring device,
- ≡ 3D visualization.

— Sound level meter measurements

For testing the principles of measurement as well as verification of the proposed methodology, classical measurements were performed with a system of sound level meters. The measurement of acoustic properties using a system of sound level meters was performed on the area of the Faculty of Aviation of the Technical University in Košice. The measuring points were located in an isolated zone, which eliminated interfering effects on the measurement.

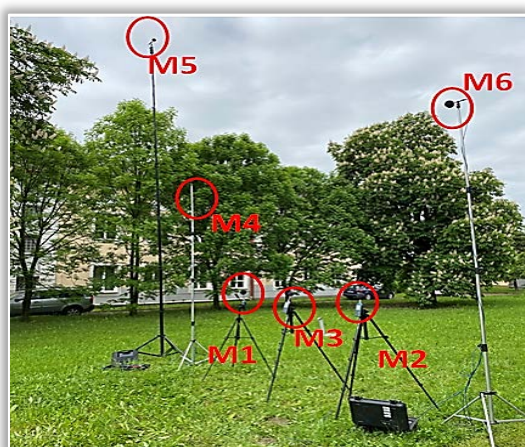


Figure 1. Scene of the measuring points

Figure 1 shows a scene of the measuring points and the arrangement of the measuring devices. The location of the measuring points was chosen so that it was possible to

characterize the acoustic properties of individual typical drone operations. The measuring microphones were arranged in a way, that we could assess the effect of a flying drone on a person who is at ground level (1.5 m above ground level) and at several heights (the effect of drones on protected objects at level 2 to 3 above ground). The task of the placement and setting of the instruments was to analyze the individual acoustic events in terms of time domain (time record) and frequency domain (frequency spectrum).

Drones have a wide range of different noise characteristics. The main components of noise are the noise of the flow when the propeller moves and the noise from the engine. The nature of the noise is very closely related to the drone flight mode and flight speed. For the initial testing of the methodology, we decided to focus on the individual flights of two different quadcopters at different speeds. Said quadcopters and their characteristics are shown in Figure 2. The nature of drone noise is also affected by the current air flow rate, load and acceleration.

For the needs of the initial analysis, which we present in this work, 2 types of drones were selected.

≡ Quadcopter No.1

The manufacturer of this quadcopter operates at the Faculty of Aviation of the Technical University in Košice, it is his own design and construction, printed on a 3D printer. Look at this quadcopter and its characteristics are shown in Figure 2 and in tab. 1.



Figure 2. Quadcopter no.1 and no.2

Table 1. Characteristics of the quadcopter no.1 and no.2

| Quadcopter number | No.1 | No. 2 |
|--------------------|-------------------|---------------------|
| Power supply: | 3S LiPo, 4500 mAh | 2S Li-ion, 2400 mAh |
| Propellers: | GWS EP 9050x3 | 4,7x2,6x2 |
| Weight: | 1350 g | 249 g |
| Shoulder length ** | 225 mm | 107 mm |

≡ Quadcopter No.2 DJI Mavic Mini

This quadcopter is a Professional one that excels in its compactness and performance. It is a popular model for those who want to operate a professional drone at a relatively low price. Look at the quadcopter no. 2 and its characteristics are shown in Figure 2 and in table 1.

— Measurement results

During our research, 4 sets of measurements were made. Each quadcopter flew back and forth at low and high speeds. Figure 3 shows the time record of the equivalent A-weighted sound level when flying at a low speed by the quadcopter no. 1 through the vertical microphone system.

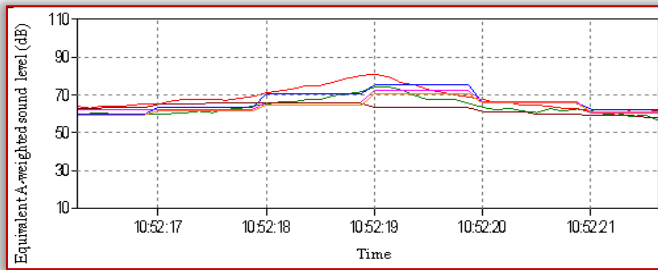


Figure 3. Time record from all measuring points, low speed flight of the quadcopter no. 1

Legend: measuring point M1 – red colour, M2 – green, M3 – blue, M4 – pink, M5 – burgundy, M6 – orange colour.

From the time course it is clear:

- ≡ changes in the equivalent A-weighted sound level as the drone approaches and departs from the measuring system,
- ≡ scattering of equivalent A-weighted sound level for individual measuring microphones, which depend on the height above ground level and the distance from the flying drone.

This analysis also shows the scatter of the equivalent A-weighted sound level of the individual measuring microphones during the flight.

Figure 4 shows the frequency spectrum of the low speed flight of the quadcopter no.1 at the measuring point M1.

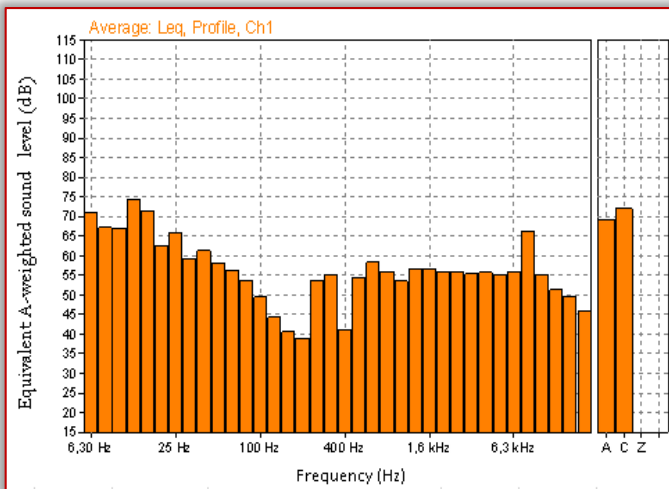


Figure 4. Frequency spectrum from measuring point M1, low speed flight of the quadcopter no. 1

Figure 5 shows the time record of the equivalent A-weighted sound level when flying at a high speed by the quadcopter no. 1 through the vertical microphone system.

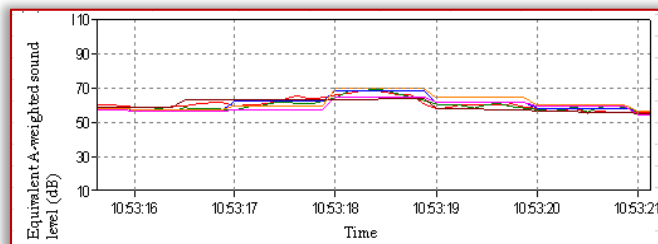


Figure 5. Time record from all measuring points, high speed flight of the quadcopter no. 1

Figure 6 shows the frequency spectrum of the high speed flight of the quadcopter no.1 at the measuring point M1.

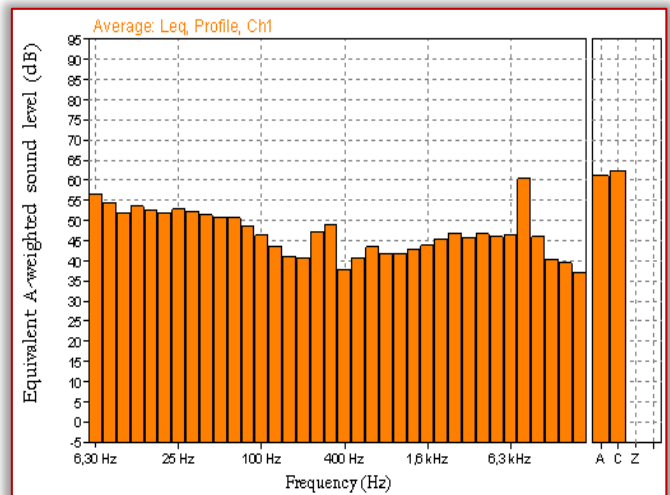


Figure 6. Frequency spectrum from measuring point M1, high speed flight of the quadcopter no. 1

A comparison of the frequency spectra of high and low speed flights shows that significant tonal components appeared at different frequencies at low flight speed, but at 250 and 315 Hz they disappear at high speed, on the contrary, at 8.0 kHz the tone component is still more pronounced.

It should be noted that in the case of a low speed flight, higher noise levels were measured, as is evident from the above records. This is due to the smaller drone flight distance, as the operator did not dare fly at close distances from the microphones at higher speeds. This is another of the problems that need to be addressed in the further processing of the topic.

Figure 7 shows a time record of the equivalent A-weighted sound level when flying low speed of quadcopter no. 2 through a vertical microphone system.

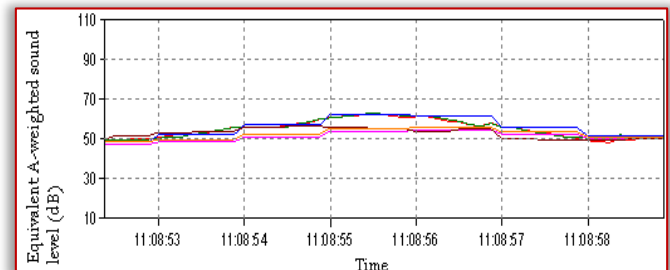


Figure 7. Time record from all measuring points, low speed flight of the quadcopter no. 2

Figure 8 shows the frequency spectrum of the low speed flight of the quadcopter no.2 at the measuring point M1.

It is clear from the frequency spectrum that the emitted noise does not have a significant tonal character. In this case, it is a professional product of one of the renowned manufacturers (DJI Mavic Mini). It is clear that the manufacturer dealt with acoustic optimization, which results in the frequency spectrum. In further proposals, it would be appropriate to address the situation in the range of 250-315 Hz, as there are more significant anomalies (deviations from the smooth frequency spectrum).

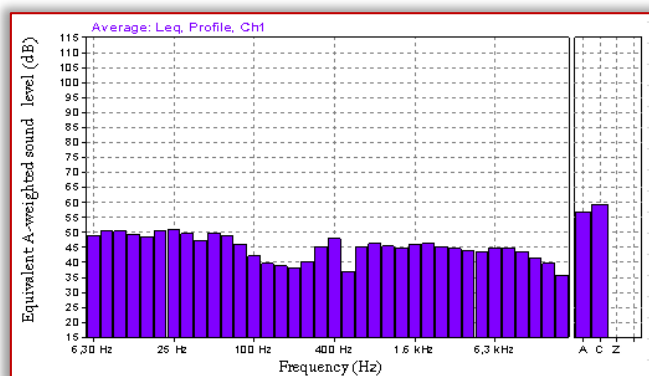


Figure 8. Frequency spectrum from measuring point M1, low speed flight of the quadcopter no. 2

Figure 9 shows the time record of the equivalent A-weighted sound level when flying at a high speed of the quadcopter no. 2 through the vertical microphone system.

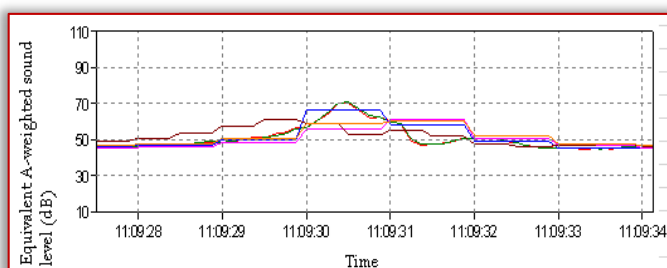


Figure 9. Time record from all measuring points, high speed flight of the quadcopter no. 2

Figure 10 shows the frequency spectrum of the high speed flight of the quadcopter no.2 at the measuring point M1.

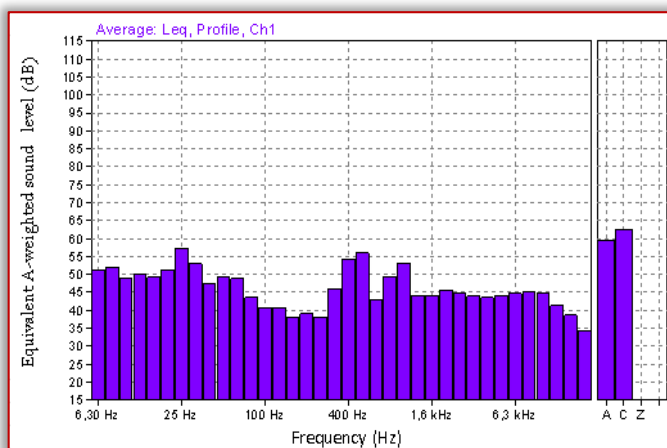


Figure 10. Frequency spectrum from measuring point M1, high speed flight of the quadcopter no. 2

A comparison of the frequency spectra of high and low speed flights for quadcopter no. 2 shows that when flying at a higher speed, there are more tonal components at different frequencies, namely at 25 Hz, 400 Hz, 500 Hz, 800 Hz and 1000 Hz, with which is associated with a significant increase in the disruption of the population. In this case, the pilot was able to follow the same drone flight paths at both speeds, as evidenced by the achieved noise values.

CONCLUSION

The measurements that were performed and described in this paper were the first step in the design of a methodology

for measuring drone noise and its effects on humans. In addition to the described measurements when flying through the vertical system of microphones, other measurements were performed, measurements with the horizontal system of microphones, measurements with an acoustic camera, which will be gradually incorporated into the new methodology.

Acknowledgments

This paper was created within the project KEGA 011TUKE-4/2021.

References

- [1] Commission Implementing Regulation (EÚ) 2019/947 of 24 May 2019 on the rules and procedures for the operation of unmanned aircraft.
- [2] Commission Delegated Regulation (EU) 2019/945 of 12 March 2019 on unmanned aircraft systems and on third-country operators of unmanned aircraft systems.
- [3] Lumnitzer, E. et al.: Evaluation of the effects of physical factors on human health. TU, 2014.159
- [4] Yehorova, A. et al.: Methodology for increasing the quality of technical equipment In: Acta Technica Corviniensis : Bulletin of Engineering. Roč. 13, č. 4 (2020), s. 13-18
- [5] Lumnitzer, E; Yehorova, A: Acoustic properties of washing machines in terms of customer expectations. In: Fyzikálne fakulty prostredia = FFP. - Košice (Slovakia): IbSolve Roč. 10, č. 1 (2020), s. 16-21
- [6] Lumnitzer, E; Badida, M; Polačeková, J. Akustika. Základy psychoakustiky, 2012, Košice – ISBN 978-80-8086-182-8, str.51-73
- [7] Abagnali, V; Fabbri, G. Sound Waves: Propagation, Frequencies and Effects. Hauppauge: Nova Science Publishers, 2012. ISBN 9781614701699.
- [8] Kloet, N. Drone on: a preliminary investigation of the acoustic impact of unmanned aircraft systems (UAS). 24th International congress of sound and vibration, 2017.
- [9] Perron, S. Review of the effect of aircraft noise on sleep disturbance in adults. Noise and Health, 2012.
- [10] Yongcho, T. Characterizing sources of small DC motor noise and vibration. Micromachines 2018;84(9):1-16.
- [11] Sinibaldi, G. Experimental analysis on the noise of propellers for small UAV. Applied Acoustics 74 (2013).



ISSN: 2067-3809

copyright © University POLITEHNICA Timisoara,
Faculty of Engineering Hunedoara,
5, Revolutiei, 331128, Hunedoara, ROMANIA
<http://acta.fih.upt.ro>

¹Kenechi NWOSU-OBIEOGU, ²Goziya DZARMA, ³Linus CHIEMENEM

ANFIS PREDICTION OF ANTIOXIDANTS YIELD FOR *LUFFA* OIL

^{1,3}Chemical Engineering Department, Faculty of Engineering, Michael Okpara University of Agriculture, Umudike, Abia, NIGERIA

Abstract: In this study, an Adaptive neuro-fuzzy inference system (ANFIS) was applied in predicting the optimum yield of terpineol and polyphenol for *luffa cylindrica* seed oil. The experiment was conducted at a temperature (60-80°C), time (4-6 hours) and solvent/seed ratio (8-12 ml/g). Fourier transform infrared spectroscopy (FTIR) confirmed the presence of terpineol and polyphenol at peaks of 1461.1cm⁻¹ and 3008.0cm⁻¹, respectively. Parametric analysis showed that time and solvent/seed ratio had the most effect on terpineol yield, while time and temperature affected polyphenol yield significantly. The ANFIS prediction indices are thus; terpineol (R²= 0.95614, MSE=1.11179) and polyphenol (R²= 0.8258, MSE= 0.4253). This proves that the ANFIS technique is a reliable approach for predicting antioxidants from *luffa cylindrica* seed oil.

Keywords: *luffa cylindrica*, antioxidant, ANN, ANFIS, polyphenol, terpineol

INTRODUCTION

Antioxidants are naturally present in plants; they convert free radicals produced during the oxidation process to less reactive species at a low concentration. Thus, it plays a physiological role in the body defence system [1]. Antioxidants are primarily found in fruits and vegetables. Studies revealed that food rich in antioxidants positively impacts health; hence, their regular consumption reduces the risk of chronic diseases [2,3].

Luffa cylindrica is a non-edible plant commonly found in the tropics, a member of the family *Cucurbitaceae*; the fruits, leaves, flowers, and seeds draw considerable attention from researchers to harness its potentials [4]. However, phytochemicals in seed oils have been revealed to offer interesting nutritional and economic possibilities due to the high levels of polar antioxidants [5].

Reports have shown that *luffa* based derivatives contain antioxidants such as terpineol, polyphenol which are present in our food, employed in treating a various health condition, cosmetics and antiseptics production [6-12]. Extraction and analysis of polyphenols and terpineol from plants have been researched extensively [12,13]. However, the relationship between input extraction process parameters and measurable output (polyphenol/terpineol yield) is imprecise, blur, non-linear and vague, as reported by earlier researchers [14-16].

Recent reports show the capability and efficiency of soft-computational models such as artificial neural network (ANN), Adaptive neuro-fuzzy inference system (ANFIS), Support Vector Machine (SVM), Non-Linear Multilinear Regression (NLMLR), Genetic Algorithm (GA) and Particle Swarm Optimization (PSO) for modelling intricate and complex processes [17,18]. Earlier studies on estimation and prediction of extraction process have been based on linear regression techniques [19,20]. Nonetheless, the relationship between extraction and dependent process variables cannot be elucidated and explained linearly. Therefore, neural network and fuzzy inference systems have gained increasing applications in modelling and controlling the relationship among process variables [17,18,21,22]

ANFIS seems to be an excellent model to map the interaction of process parameters on antioxidant yield. Yue et al [9] employed ANFIS to model biodiesel production from castor oil, and ANFIS proved superior compared to other predictive models in the literature. Roy et al [23] predicted maximum oil yield from almond seed considering pressure, temperature, heating time, and moisture content as input parameters and type-2 fuzzy logic predicted and improved the process parameters during extraction. Khoshnervisan et al. [24] predicted wheat grain yield based on energy inputs using the ANFIS model compared with ANN models; the result illustrated that the ANFIS model predicted the product more precisely. ANFIS has been widely applied as an efficient predictive model for a highly non-linear relationship due to its learning capability [25]. Thus, this study predicted polyphenol and terpineol yield from *luffa cylindrica* seed oil using the ANFIS model.

MATERIALS AND METHODS

— Sample preparation

Luffa cylindrica fruits, a natural precursor, were procured at Michael Okpara University of Agriculture Umudike, Abia State, Nigeria. Both matured and dried fruit of this tree was harvested in bulk quantity. First, the seed was winnowed, husks and dirt removed, after which it was sun-dried for easy removal of the shell and was also oven-dried at 60°C to constant weight before grinding to increase the surface area for oil extraction.

— Experimental procedure

The extraction of the *luffa* oil was carried out at the Department of Chemical Engineering laboratory, Michael Okpara University of Agriculture Umudike, Abia State, Nigeria, using the solvent extraction method reported by Afolabi et al. [26]. It was done with the Soxhlet apparatus of 250 cm³ capacity using *n*-hexane of analytical grade as the solvent. The parameters were 40 g of grounded *luffa* seed, extraction time of 4 to 6 h, extraction temperature between the ranges of 60°C to 80°C and the ratio of the solvent (*n*-hexane) to solute (biomass) from 8 to 12ml/g. The solvent used was recovered at every interval. The oil obtained was weighed; the experiment was repeated for other parameters,

and the percentage yield was calculated using the equation below.

$$Y = \frac{M_o}{M_s} \times 100 \quad (1)$$

where: Y = oil yield (%), M_o = mass of oil extracted (g), M_s = mass of luffa seed (g)

— Terpeneol Concentration Determination

The terpeneol concentration was determined using a method modified by Narayan et al. [27]. 0.1g of the luffa oil was introduced into a test tube, 1ml of methanol was added, placed in a water bath, it was stirred for 30minutes at a temperature of 100°C, the mixture was removed, and 1ml of sulphuric acid was introduced, the colour turned to reddish-brown, it was allowed to stand for 30minutes then the absorbance was taken in a UV spectrophotometer, the standard curve was generated by treating the linalool as the sample with serial dilution

— Polyphenol yield determination

The total polyphenol content was determined using the Folin Ciocalteu method (Singleton and Rossi [28]). About 0.1g of the oil extract was weighed into a test tube, 1ml of methanol was introduced and was taken into a water bath and shaker, where it was allowed to shake for 30minutes at 40°C. Next, the sample was removed, and 1ml of Folin-Ciocalteu and 2ml of 20% Na_2CO_3 were introduced; the mixture was allowed to stand for 10 minutes before it was stirred in a centrifuge 20minutes at 400rpm. The absorbance was taken using a UV spectrophotometer at 625nm. The standard curve was generated by preparing different concentration ranging from 10mg/l of Gallic acid.

— FT-IR analysis

The pure luffa seed oil was characterized using Fourier Transform Infrared (FTIR) Spectroscopy Technique to determine surface functional groups. The FTIR analyses were carried out on the samples using Shimadzu FT-IR-8400S Spectrophotometer with a resolution of 4 cm^{-1} in the range of 4000 - 500 cm^{-1} .

— ANFIS Modelling Development

Artificial neural network (ANN) and Fuzzy Inference System (FIS) are integrated to form an Adaptive Neuro-Fuzzy Inference System (ANFIS) for solving and explaining imprecise and uncertainty problems.

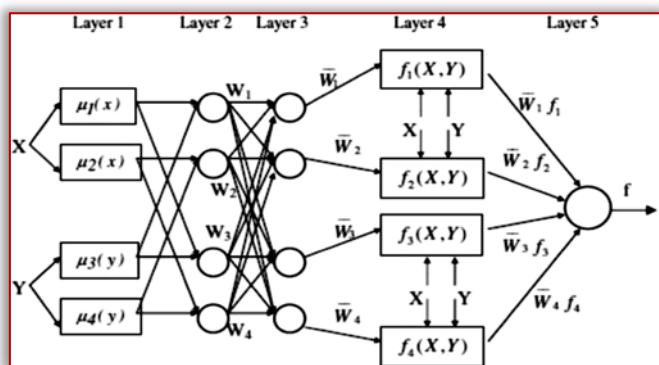


Figure 1: A basic structure of the ANFIS

The “exhsrch” function in MATLAB 8.4 (R2014b) software environment was implemented in an exhaustive search within the available inputs of the extraction process

(temperature, time and solvent/seed ratio) to select the set of one and two variable input combinations that has the maximum influence on the terpeneol/polyphenol yield. The ‘exhsrch’ function built an ANFIS model for each input variable and trained it for one thousand epoch reporting the performance achieved.

— Performance Evaluation of the Developed Models

Statistical parameters were applied to determine the performance of the proposed model for the prediction of the extraction process. MSE (Root Mean Square Error) and the R^2 value (Correlation Coefficient) were used as considered below:

$$R^2 = 1 - \frac{\sum_{p=1}^p (DP - O_p)^2}{\sum_{p=1}^p (O_p)^2} \quad (2)$$

$$MSE = \frac{1}{p} \sum_{p=1}^p (d_p - O_p)^2 \quad (3)$$

The MSE value close to zero and the R^2 values close to one show the models' predictability and reliability. Li et al. [29] claimed that Soft-computing Model's evaluation should be based on ranges of RMSE as given in Table 1.

Table 1: Ranges of MSE for models performance

| Ranges of MSE | Performance |
|--------------------|-------------------------------|
| < 0.009 | Excellent prediction accuracy |
| 0.009 < MSE < 0.09 | Good prediction accuracy |
| 0.09 < MSE < 0.5 | Reasonable prediction |
| > 0.5 | Inaccurate prediction |

Source: Li et al. [29]

RESULT AND DISCUSSION

— FTIR Result

The FT-IR result of the oil yield from *luffa cylindrica* is shown in figure 2, the peak at 3008.0 cm^{-1} can be ascribed to -OH stretching, which indicates the presence of polyphenol, two sharp-pointed peaks at 2922.2 cm^{-1} and 2855.1 cm^{-1} indicated alkane group, another sharply pointed peak with value 1744 cm^{-1} indicates the presence of esters (6-membered lactone) with the structure C=O, hence the oil has high saponification value and could be recommended for soap production.

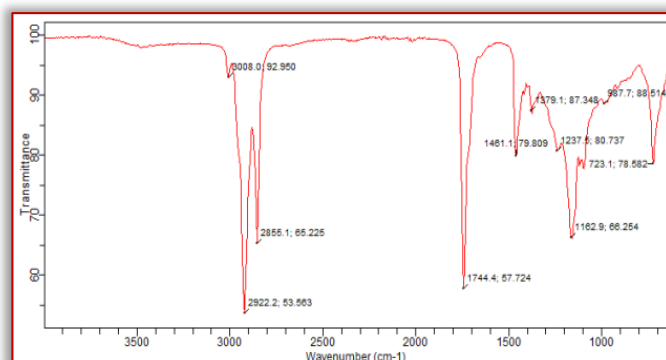


Figure 2: FT-IR result of the oil yield

The shorter, smaller pointed peak with a vibrational mode at 1461.1 cm^{-1} indicates the presence of terpeneol (Agatonovic-kustrum et al. 2020), while a medium sharp peak was observed with a value of 1379 cm^{-1} , indicating an alkane of the gem dimethyl group. The peak at 1237.5 cm^{-1} indicates an alkyl aryl ether with structure C - O - C, while 987.7 cm^{-1} and 723.1 cm^{-1} peak indicated alkene compounds. The presence of the unsaturated hydrocarbons makes the oil suitable for plastic and paint industries, as a drying agent in the

production of cosmetics and maybe edible for animal feed [30].

— ANFIS simulation results

To obtain the best prediction of antioxidant yield, the developed ANFIS structure was simulated at various membership functions (MF) such as gauss mf, gauss2 mf, gbell mf, tri mf, trap mf, psig mf and dsig mf. The correlation coefficient (R^2) and the root mean square error (RMSE) were used as statistical criteria to evaluate the degree of reliability of the network. Table 2 and 3 summarizes the ANFIS results for terpineol and polyphenol yield of different input membership function types for linear and constant output mf, respectively. In Table 2, for linear output, the optimum value of R^2 (0.95614), MSE (1.4059) was obtained at tri mf, for the constant output mf, the trap of had the best prediction for R^2 (0.94799), with its corresponding MSE value (1.11179) obtained at tri mf, for polyphenol yield prediction in Table 3 trap and dsig mf has the best R^2 projection of (0.8150), (0.8258). In contrast, tri mf had the best MSE prediction of (0.4253), (13.9715) for linear and constant output, respectively; this affirms that optimum yield for terpineol was predicted by tri mf. In contrast, polyphenol yield was predicted by dsig and tri mf.

Table 2: Prediction efficiency of ANFIS model for terpineol yield

| Input membership function | MSE (linear) | R^2 (linear) | MSE (constant) | R^2 (constant) |
|---------------------------|--------------|----------------|----------------|------------------|
| Gauss | 19.5374 | 0.94628 | 1.15111 | 0.94646 |
| Gauss2 | 69.9386 | 0.94623 | 1.11491 | 0.94641 |
| Gbell | 77.2027 | 0.94631 | 1.1178 | 0.94164 |
| Tri | 1.4059 | 0.95614 | 1.11179 | 0.94628 |
| Trap | 7.67826 | 0.91321 | 1.11537 | 0.94799 |
| Pi | 90.0508 | 0.94312 | 1.11356 | 0.94634 |
| Design | 77.2027 | 0.90315 | 1.11779 | 0.94164 |
| Psig | 40.106 | 0.93215 | 1.13363 | 0.94622 |

Table 3: Prediction efficiency of ANFIS model for polyphenol yield

| Input membership function | MSE (linear) | R^2 (linear) | MSE (constant) | R^2 (constant) |
|---------------------------|--------------|----------------|----------------|------------------|
| Gauss | 1.611 | 0.71012 | 15.1564 | 0.8093 |
| Gauss2 | 6.3827 | 0.710135 | 36.2802 | 0.80104 |
| Gbell | 6.9954 | 0.71021 | 37.9403 | 0.82461 |
| Tri | 0.4253 | 0.71301 | 13.9715 | 0.82077 |
| Trap | 7.1824 | 0.8150 | 39.082 | 0.81567 |
| Pi | 8.9391 | 0.71019 | 42.988 | 0.79811 |
| Dsig | 6.9954 | 0.7314 | 37.9403 | 0.8258 |
| Psig | 3.0278 | 0.71013 | 21.8584 | 0.799955 |

— Exhaustive search result

Exhaustive search result for one input and two-input variable ANFIS model for antioxidant yields.

The ANFIS models using different input variable combinations were investigated with the exhaustive search method to determine the input variable that has the most significant effect on the antioxidant yield using RMSE as the performance indicator. Table 4 shows an exhaustive ANFIS model result with single/double input variables for terpineol yield. It was observed for single input, time had the least RMSE. In contrast, a combination of time and solvent/seed ratio had the least RMSE for double input; for polyphenol

yield in table 5, temperature possessed the least RMSE. In contrast, a combination of temperature and time maintained the least RMSE; this indicated that time and solvent/seed ratio were the most relevant variable for terpineol yield. In contrast, time and temperature had a more significant effect on polyphenol yield.

Table 4: Exhaustive search result of one / two- input variable ANFIS model for terpineol yield

| Input variable | RMSE training | RMSE Checking | Input variable | RMSE training | RMSE checking |
|--------------------|---------------|---------------|---------------------------|---------------|---------------|
| Temperature | 3.6582 | 3.5683 | Temperature, time | 1.86295 | 1.84745 |
| Time | 2.29572 | 2.29572 | Temperature, solvent/seed | 2.6176 | 2.6599 |
| Solvent/seed ratio | 2.9658 | 2.893121 | Time, solvent/seed ratio | 1.31504 | 1.327939 |

Table 5: Exhaustive search result of one/two-input variable ANFIS model for polyphenol yield

| Input variable | RMSE training | RMSE Checking | Input variable | RMSE training | RMSE checking |
|--------------------|---------------|---------------|---------------------------|---------------|---------------|
| temperature | 0.9077 | 0.89961 | Temperature, time | 0.556 | 0.5713 |
| Time | 0.930231 | 0.880086 | Temperature, solvent/seed | 0.7621 | 0.7412 |
| Solvent/seed ratio | 1.03552 | 0.98705 | Time, solvent/seed ratio | 0.8424 | 0.79106 |

CONCLUSIONS

This study has successfully developed an ANFIS model to optimize the process parameters for antioxidants (terpineol and polyphenol) yield from *luffa cylindrica* seed oil using statistical indicators (RMSE, R^2). The parametric analysis using exhaustive search showed that time, temperature and solvent/seed ratio significantly affected the antioxidants yield. The model developed can be used for process behaviour prediction, optimization and a learning tool for operators in the chemical industry.

References

- [1] Yadav A, Kumari RI, Mishra JP, Srivtva S, Prabha SI, Antioxidants and its functions in human body- A review, 2016. Res. Environ. Life Sci. 9(11): 1328-1337
- [2] Ohlsson T, Bengtsson N, Minimal processing technologies in the food industry, 2002
- [3] Liyana-Pathirana CM, Shahidi F, Alasalvar C, Antioxidant activity of cherry laurel fruit (*Laurocerasus officinalis Roem.*) and its concentrated juice. Food Chemistry, 2006. 99: 121-128.
- [4] Oboh IO, Aluyor EO, *luffa cylindrica*- an emerging cash crop, African Journal of Agricultural Research, 2009. 4(8):684-688.
- [5] Oyetayo FL, Ojo BA, Food value and phytochemical composition of *luffa cylindrica* seed flour. American journal of biochemistry, 2012. 2(6):98-103.
- [6] Shendge PN, Belemkar S, Therapeutic potential of *luffa rectangular*: A review on its traditional uses, phytochemistry, pharmacology and toxicological aspects. Frontiers in pharmacology, 2018. 9(1177).
- [7] Park S, Lin YK, Friere OM, Cho E, Jin D, Kook J, Antimicrobial effect of linalool and α -terpineol against periodontopathic and cariogenic bacteria, Anaerobe, 2012. 18(3): 369-372.

- [8] Akinsanmi AO, Oboh G, Akinyemi JA and Adefagha AS, Assessment of the nutritional, antinutritional and antioxidant capacity of unripe, ripe and overripe plantain (*Musa paradisiaca*) peels, 2015. International journal of advanced research. 3(2):63-72.
- [9] Yu L, Jin I, Li X, Zhang Y, Optimization of bioactive ingredient extraction from Chinese herbal medicine *Glycyrrhiza glabra*: a comparative study of three optimization models, Evidence-based complementary and alternative medicine, 2018.1(2): 122-135.
- [10] Okla K M, Alamri SA, Salem MZM, Ali HM, Behiry IS, Nasser AR, Alaraidh IA, Al-Ghtani SM, Yield, Phytochemical Constituents, and Antibacterial Activity of Essential Oils from the Leaves/Twigs, Branches, Branch Wood, and Branch Bark of Sour Orange (*Citrus aurantium L.*) Processes, 2019. 7 (363): 1-15.
- [11] Zengan H, Daysal HA, Antibacterial and antioxidant activity of essential oil terpenes against pathogenic and spoilage-forming bacteria and cell structure-activity relationships evaluated by SEM microscopy, *Molecules*, 2015. 19: 17773-17798.
- [12] Vladimir-Knezevic S, Blazevic B, Stefan MB, Babac M, Plant polyphenols as antioxidants influencing the human health, phytochemicals as Nutraceuticals-Global approaches to their role in nutrition and health, 2011. 9: 155-180.
- [13] Campone L, Celano R, Rizzo S, Piccinelli A L, Rastrelli L and Russo M, Development of an Enriched Polyphenol (Natural Antioxidant) Extracts from Orange Juice (*Citrus sinensis*) by Adsorption on Macroporous Resins, 2020. Journal of Food Quality. 2(4):1-9.
- [14] Sales A, Felipe OL, Bicas JL, Production, properties and application of terpineol. Food and bioprocess technology, 2020
- [15] Molina G, Pessôa M G, Bicas JL, Fontanille P, Larroche C, Pastore GM, Optimization of limonene biotransformation for the production of bulk amounts of α -terpineol. Bioresource Technology, 2019
- [16] Khaleel C, Tabanca N, Buchbauer G, α - Terpineol, a natural monoterpene: A review of its biological properties, 2017. Open Chem. 16: 349–361.
- [17] Oke EO, Adeyi O, Okolo BI, Adeyi JA, Ayanyemi J, Osoh KA, Adegoke, T.S. Phenolic compound extraction from Nigerian *Azadirachta Indica* leaves Response surface and neuro-fuzzy modelling performance evaluation with Cuckoo Search multi-objective optimization, 2020. Results in Engineering, 8:100160.
- [18] Soto J, Melin P, Castilo O, A new approach for time series prediction using ensembles of IT2FNN models with optimization of fuzzy integrators. Int. J. Fuzzy Syst. 2018. 20: 701-728.
- [19] Jisieike C F, Betiku E, Rubber seed oil extraction, solvent polarity, extraction time, and solid-solvent ratio on its yield and quality, 2020. Biocatalysis and Agricultural Biotechnology. 24: 1-7
- [20] Onoji S, Iyuke S, Igbafe IA, Daramola OM, *Hevea brasiliensis* (rubber seed) oil: modelling and optimization of extraction process parameters using response surface methodology and artificial neural network techniques, *Biofuels*, 2017.6:1-15
- [21] Almeida JS, Predictive Non-linear Modelling of Complex Data by Artificial Neural Networks, 2002. Curr. Opin. Biotech. 2: 1372–1376.
- [22] Ojediran O J, Okonkwo CE, Adeyi A J, Adeyi O, Olaniran FO, George NE, Olayanju AT, Drying characteristics of yam slices (*Dioscorea rotundata*) in a convective hot air dryer: application of ANFIS in the prediction of drying kinetics., 2020. Heliyon, 6, e03555.
- [23] Roy K, Mukherjee A, Jana K D, Prediction of maximum oil yield from almond seed in the chemical industry: A novel type-2 fuzzy logic approach, S. Afr. J. Chem. Eng. 2019. 29: 1-9
- [24] Khoshnevisan B, Rafiee S, Omid M and Mousazadeh H, Development of an intelligent system based on ANFIS for predicting wheat grain yield on the basis of energy inputs. Information processing in agriculture, 2014. 1: 14-22.
- [25] Agatonovic-Kustrum S, Pustivojevic P, Valdimir G, Litrinova TU and Motron DW, Essential oil quality and purity evaluation via FT-IR spectroscopy and pattern recognition techniques, 2020. Applied science. 10: 1-12.
- [26] Afolabi T J, Onifade K R, Akindipe VO and Odetoye TE, Optimization of benth seed oil (*parinaripolyandra*) using response surface methodology, 2014. British J. Appl. Sci. Tech: 5: 437-445.
- [27] Narayan G, Sondipon C, Shamik G, Samir K.S, Suman B, Estimation of total terpenoids concentration in plants tissues using a monoterpene, linalool as standard reagent, Protocol Exchange, 2012. 5(10):1038-1041.
- [28] Singleton VL, Rossi JA, Colorimetry of total phenolics with phosphomolybdic-phosphotungstic acid reagents, *Am J Enol Vitic*, 1965. 16(3): 144-158.
- [29] Li M, Fan L, Liu H, Guo P and Wu W, A general model for estimating daily global solar radiation using air temperatures and site geographic parameters in Southwest China, Journal of Atmospheric and Solar-Terrestrial Physics, 2013. 92: 145-150.
- [30] Oli CC, Onuegbu TU, Ezeudu EC, Proximate composition, characterization and spectroscopic analysis of luffa aegyptiaca seed. International journal of life sciences biotechnology and pharma research, 2014. 2250-3137.



ISSN: 2067-3809

copyright © University POLITEHNICA Timisoara,
Faculty of Engineering Hunedoara,
5, Revolutiei, 331128, Hunedoara, ROMANIA
<http://acta.fih.upt.ro>

¹Mulualem Bekele NORA, ²Jiratu Wundessa GERBI, ³Basavaraj PARUTI

ANALYSIS OF CONSTRUCTION WASTE IN PUBLIC BUILDINGS USING REGRESSION METHOD: A CASE STUDY OF AMBO TOWN

^{1,3}Department of Hydraulic and Water Resource Engineering, Hachalu Hundessa Institute of Technology Campus , Ambo University, Ambo, ETHIOPIA

²Department of Construction Engineering and Management, Hachalu Hundessa Institute of Technology Campus , Ambo University, Ambo, ETHIOPIA

Abstract: The output of construction and demolition (C&D) waste in Ethiopia has been rapidly increasing in the past decades. The direct landfill of such construction and demolition waste without any treatment accounts for about 98%. Therefore, recycling and utilizing this waste is necessary. The prediction of the output of such waste is the basis for waste disposal and resource utilization. This study takes Ambo town as a case study, the current output of C&D waste is analyzed by regression method. The findings of the study indicated that the level of construction wastages on public buildings construction projects in Ambo town, the weighted average and ranking over-all factors of construction materials wastages for operations factors (0.399), design and documentation factors (0.3798), materials handling and storage factors (0.3797), site management and practices factors (0.334) and site supervision factors (0.316). Therefore, this study recommends improvement in the integration of public buildings construction materials wastages and the importance of evaluating construction materials wastage, serving for the intended purposes sustainably to the construction parties for public buildings construction projects starting from commencement up to its completion.

Keywords: construction and demolition waste; weighted average; public buildings, regression method

INTRODUCTION

Construction and demolition (C&D) waste is produced during the process of building construction, expansion, and demolition. Owing to the gradual progress of urbanization construction, the areas of buildings that have been completed and are still under construction, As a result, the production of C&D waste rapidly increases. The estimated annual production of C&D waste in Ethiopia is approximately 2 billion tons, which accounts for 80–90% of the total municipal waste. Demolition waste mainly consist of concretes, bricks, metals, timbers, plastics, gravels, ceramics, and glasses. Most of the compositions of such waste are reusable materials that are usually disposed in landfills and dumps, thereby causing serious environmental and land occupation issues . The disposal and utilization of C&D waste are common concerns of society. The government also lacks information about the production of C&D waste, which increases the difficulty of implementing comprehensive management for these waste. Quantitative waste prediction is crucial for waste management. Apart from estimation and prediction techniques, no method can be used to accurately and easily estimate the amount of waste produced by C&D projects. Estimation involves calculating the historical quantity of building waste and prediction determines the future production of construction waste on the basis of historical data.

The present study has been focused to conduct a detailed analysis of construction wastes in public buildings in Ambo town in Ethiopia country using regression method. The following are the specific objectives of the study:

- To identify and classify the leading major factors affecting the public building materials wastage in the construction sites.

- To develop a model to analyze the materials wastage using regression method.

- To suggest technique to reduce the impact of public buildings materials wastage

MATERIALS AND METHODS

This study's overall research approach includes the explanation in the choice of methods used to accomplish the objective of the study and review of literature was conducted on the basis of the research aim and a set of identified variables. Additionally, it gives information about the data collection method, research population, sample size, sampling technique and statistical tools (regression technique) used for data processing and results were interpreted.

— Study area description

The study area, Ambo Town, is located the Western Shoa part of Ethiopia, in Oromia National Regional State, at a distance of 110 km from Addis Ababa. Ambois located in the West side of Finfinnee City and located adjacent to the main road from Finfinnee to Wollega. It is situated at an altitude of 2110 meters above mean sea level.

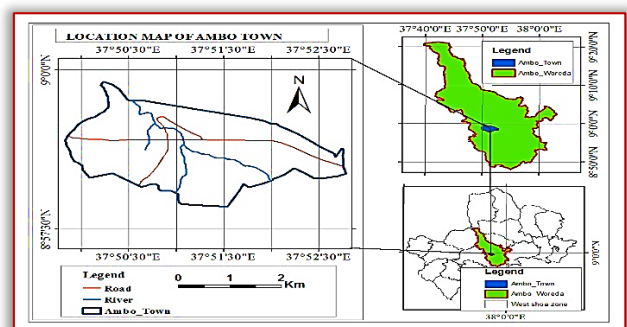
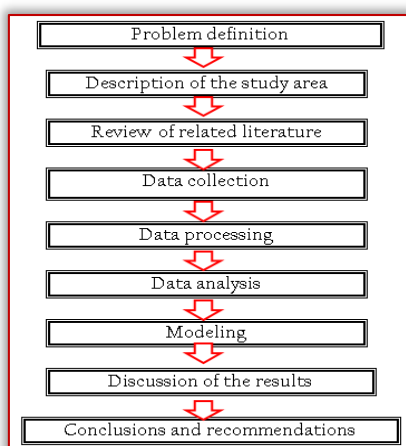


Figure 1: Location map of the study area

Table 1: Details of construction projects of case study area

| S. No | Name of project | Location of the project | Current status |
|-------|---|-------------------------------|--------------------|
| 1 | Ambo University Referral Hospital Public Building Project | Ambo town near to main campus | Under construction |
| 2 | Ambo Town, Bus Station Public Building Project | Ambo Town | Under construction |
| 3 | Ambo University, Awaro Campus Administration Building Project | Ambo town, Awaro campus | Completed |
| 4 | Ambo University, Building Project | Ambo town | Under Construction |
| 5 | Ambo University, Awaro Campus, Stadium Project | Ambo town | Under Construction |

The framework of the study is presented as below.



— Data Collection Method

Various types and sources of data are identified and discussed for this research purpose. The primary task is gathering/collecting relevant information or data of the study area. Multiple evidences approach was used for data collection. These are questionnaire survey, site observations/field visit was made and case study by analyzing different documents. A questionnaire survey was selected as the research instrument owing to its suitability to the level of information required, cost and time limitations and the high number of participants.

— Sample Size and Sampling Technique

Sampling is the process of selecting representative units of a construction parties for the study in this research. The advantage of using a sample is that it is more practical and less costly than collecting data from the construction parties. The risk is that the selected sample might not adequately reflect the behaviors, traits, symptoms, or beliefs of the participate.

The investigation covered five selected public building construction projects. The researcher distributed fifty-six questionnaires for contractors, consultants and employees/engineers which are participated on public building construction projects in Ambo town.

To sample public construction parties (owner, contractor and consultant) in public buildings construction sites in Ambo town, reconnaissance survey was made and five public buildings were identified as project construction parties with project cost more than ten million (10 million) birr

during this study. Therefore, this study paper considers these construction parties as sample representative. Therefore, the following equation is used to determine the sample size [3].

$$Ss = \frac{Z^2 * P * (1-P)}{C^2} \tag{2.1}$$

where Ss = Sample size

Z = Z value (e.g. 1.96 for 95% confidence level)

P = percentage picking a choice, expressed as a decimal (0.50 used for sample size needed)

C = margin of error (9%)

$$Ss = \frac{1.96^2 * (0.05) * (1 - 0.05)}{0.09^2} = 118.57 \approx 119$$

For correction of finite sample:

$$Ss \text{ new} = \frac{Ss}{1 + \frac{Ss-1}{Pop}} \tag{2.2}$$

where total sampled of construction parties = 126 match the proposed contracting companies

$$Ss \text{ new} = \frac{119}{1 + \frac{119-1}{126}} = 55.94 \approx 56$$

Based on the sampling method and criteria cited above, the researcher selected fifty-six (56) construction parties which participated on public buildings projects in Ambo town.

— Data Processing and Analysis

The analysis was done by using Microsoft Excel and the responses which was assigned to each question by the respondents was entered and consequently is subjected to statistical analysis (regression) for further insight. The following statistical techniques which are grouped under various headings were employed to analyze the data which were collected from the survey.

Frequency tables and descriptive statistics were constructed to display results with respect to each of the questions of general information and effect of client material supplying. Whereas the contribution of each of the causes to material wastage generation and optimization strategies for each of the selected materials was examined and the ranking of the attributes in terms of their criticality as perceived by the respondents was done by the use of Relative Importance Index (RII). As a result, the analysis would have combined all groups of respondents (employers, consultants, contractors) in order to obtain significant results. Data were analyzed by calculating frequencies and Relative Importance Index (RII).

Table 2: Levels of responses indication

| The levels of response are: | | |
|-----------------------------|----------------------|-----|
| E.S. | extremely important | [5] |
| V.S. | very important | [4] |
| M.S. | moderately important | [3] |
| S.S. | slightly important | [2] |
| N.S. | not important | [1] |

Recognizing the difference in perceptions of the consultants and contractors, there is also the need to further ascertain if consultants' perception is statistically different from the contractors' perception. This leads to the use of regression methods. There are some regression methods namely linear and multiple regression methods. From this linear regression is selected because of it has an advantage of not requiring the assumption of normality and or homogeneity of variances.

— Model Validation

Model validation is a mandatory step in regression model development. Provided that not much data is commonly available for modelling, on one hand, all the available data should be used to build robust regression model. On the other hand, an external test set may be useful to evaluate the model predictive ability. This test set will be comprised of data that have never been used in model development and then the optimal way to select the test data is the random selection. Linear regression coefficient of determination (R²) value estimated from external test data set is used to measure the predictive ability of the regression model.

The proportion of total variation (SST) that is explained by the regression (SSR) is known as the Coefficient of Determination, and is often referred to as R.

$$R^2 = \frac{SSR}{SST} = \frac{SSR}{SSR+SSE} \quad (2.3)$$

Where: SSR=The Sum of Squares Regression (SSR) is the sum of the squared differences between the prediction for each observation and the population mean.

SST= The Total Sum of Squares (SST) is equal to SSR + SSE Mathematically,

SSR = $\sum (y - \hat{y})^2$ (measure of explained variation)

SSE = $\sum (y - \hat{y})^2$ (measure of unexplained variation)

SST = SSR + SSE = $\sum (y - \hat{y})^2$ (measure of total variation in y)

The value of R² can range between 0 and 1, and the higher its value the more accurate the regression model is. It is often referred to as a percentage.

RESULTS AND DISCUSSIONS

Some techniques are suggested to minimize construction materials wastages on site prevention methods after construction waste analysis were done. Besides, the results that have been obtained from processing of fifty-six (56) respondents used excel and linear regression tool analysis.

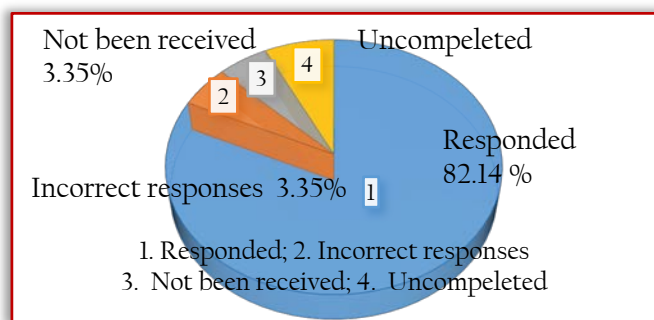


Figure 3: Questionnaires of general response rate

The results are prepared to present the information about the sample size, response rate and contracting company characteristics in Ethiopia especially in Ambo town. It also included the ranking of factors affecting the waste on construction projects based on their relative mean ranks, analysis of construction waste magnitude. In addition to the causes of waste and recommends construction waste minimization strategies after analyzing the present waste and the relative significant of construction waste sources.

Response Rate from 56 questionnaires distributed on the contracting companies, 46 responses were received with 82.14% return rate in this investigation. The other 10 questionnaires as follows: 3 (5.35%) have not been received,

4 (7.14%) are uncompleted and 3 (3.35%) are illogical or incorrect responses, indicated in Figure 3 shown below are the general response rate from questionnaires.

SOURCES AND FACTORS OF CONSTRUCTION MATERIALS WASTAGE ON PUBLIC BUILDING CONSTRUCTION PROJECTS

There are many factors, which contribute to construction materials waste generation on site. Construction materials wastage may occur due to one or combination of many causes. As discussed in literature review parts the sources of waste classified under five categories: Those are design and documentation, site management and practices, materials handling and storage, operation and site supervision.

— Group 1. Design and Documentation Factors

Table 3.1 below displayed that the Relative Importance Index of all the 8 (eight) causes of waste evaluated for the respondents (contractors, employees and consultants). This means that all the thirteen factors are considered as causes of waste arising from design and documentation.

Table 3.1: Ranks of construction materials wastage due to design and documentation factors

| Factors | Contractors | | Consultants | | Clients | | Weighted average (all groups) | |
|--|-------------|---|-------------|---|---------|---|-------------------------------|---|
| | RII | R | RII | R | RII | R | RII | R |
| Design changes and revisions | 0.538 | 1 | 0.318 | 1 | 0.636 | 1 | 0.497 | 1 |
| Designer's inexperience in method and sequence of construction | 0.423 | 3 | 0.250 | 2 | 0.500 | 3 | 0.391 | 3 |
| Lack of attention paid to standard sizes available on the market | 0.404 | 4 | 0.239 | 3 | 0.477 | 4 | 0.373 | 4 |
| Lack of information in the drawings | 0.423 | 3 | 0.250 | 2 | 0.500 | 3 | 0.391 | 3 |
| Ambiguities, mistakes, and changes in specifications | 0.346 | 5 | 0.205 | 5 | 0.409 | 5 | 0.320 | 5 |
| Rework that don't comply with drawings and specifications | 0.327 | 7 | 0.193 | 6 | 0.386 | 6 | 0.302 | 6 |
| Lack of knowledge about construction techniques during design activities | 0.481 | 2 | 0.284 | 4 | 0.568 | 2 | 0.444 | 2 |
| Poor communication leading to mistakes and errors | 0.346 | 5 | 0.205 | 5 | 0.409 | 5 | 0.320 | 5 |

— Group 2. Materials Handling and Storage Factors

Table 3.2 shows that the Relative Importance Index of all the 11 causes of waste evaluated for the respondents (contractors, client and consultants).

Table 3.2: Ranks of construction materials wastage due to materials handling and storage factors

| Factors | Contractors | | Consultants | | Clients | | Weighted average (all groups) | |
|--|-------------|----|-------------|----|---------|----|-------------------------------|----|
| | RII | R | RII | R | RII | R | RII | R |
| Poorly schedule to procurement the materials | 0.404 | 6 | 0.239 | 6 | 0.477 | 6 | 0.373 | 6 |
| Over ordering or under ordering due to mistake in quantity surveys | 0.327 | 8 | 0.193 | 8 | 0.386 | 8 | 0.302 | 8 |
| Purchased materials that don't comply with specification | 0.442 | 5 | 0.261 | 5 | 0.523 | 5 | 0.409 | 5 |
| Damage materials on site/wrong handling of materials | 0.404 | 6 | 0.239 | 6 | 0.477 | 6 | 0.373 | 6 |
| Overproduction/ Production of a quantity greater than required or earlier than necessary | 0.385 | 7 | 0.227 | 7 | 0.455 | 7 | 0.356 | 7 |
| Lack of onsite materials control | 0.269 | 9 | 0.159 | 9 | 0.318 | 9 | 0.249 | 9 |
| Poor storage of materials | 0.212 | 10 | 0.125 | 10 | 0.250 | 10 | 0.196 | 10 |
| Damage during transportation | 0.481 | 4 | 0.284 | 4 | 0.568 | 4 | 0.444 | 4 |
| By bulk | 0.5 | 3 | 0.295 | 3 | 0.591 | 3 | 0.462 | 3 |
| By partial | 0.538 | 2 | 0.318 | 2 | 0.636 | 2 | 0.497 | 2 |
| On time delivery | 0.558 | 1 | 0.330 | 1 | 0.659 | 1 | 0.516 | 1 |

— Group 3. Operation (On site, equipment) factors

The Relative Importance Index each of the sub-factors of the operation/on site group, which causes of construction material waste, is presented in Table 4.3 in a descending order.

Table 3.3: Ranks of construction materials wastage due to operation/ on site factors

| Factors | Contractors | | Consultants | | Clients | | Weighted average (all groups) | |
|---|-------------|---|-------------|---|---------|---|-------------------------------|---|
| | RII | R | RII | R | RII | R | RII | R |
| Rework due to workers' mistakes | 0.385 | 6 | 0.227 | 7 | 0.455 | 6 | 0.356 | 6 |
| Damage to work done caused by subsequent trades | 0.519 | 2 | 0.307 | 2 | 0.614 | 2 | 0.480 | 2 |
| Use of incorrect material, thus requiring replacement | 0.462 | 3 | 0.273 | 6 | 0.545 | 3 | 0.427 | 3 |
| Poor workmanship | 0.308 | 7 | 0.182 | 8 | 0.364 | 7 | 0.285 | 7 |
| Lack of workers or tradesmen or subcontractors' skill | 0.404 | 5 | 0.239 | 5 | 0.477 | 5 | 0.373 | 5 |
| Choice of wrong construction method | 0.558 | 1 | 0.330 | 1 | 0.659 | 1 | 0.516 | 1 |

| | | | | | | | | |
|--|-------|---|-------|---|-------|---|-------|---|
| Lack of coordination among crews | 0.404 | 5 | 0.239 | 5 | 0.477 | 5 | 0.373 | 5 |
| Problems between the contractor and his subcontractors | 0.404 | 5 | 0.239 | 5 | 0.477 | 5 | 0.373 | 5 |
| Equipment frequently breakdown | 0.462 | 3 | 0.273 | 3 | 0.545 | 3 | 0.427 | 3 |
| Poor technology of equipment | 0.404 | 5 | 0.239 | 5 | 0.477 | 5 | 0.373 | 5 |
| Shortage of tools and equipment's required | 0.442 | 4 | 0.261 | 4 | 0.523 | 4 | 0.409 | 4 |

— Group 4. Site Management and Practices Factors

The Relative Importance Index each of the sub-factors of the site management and practices group, which causes construction material waste, is presented in Table 3.4 in a descending order.

Table 3.4: Ranks of construction materials wastage due to site management and practices factors

| Factors | Contractors | | Consultants | | Clients | | Weighted average (all groups) | |
|--|-------------|---|-------------|---|---------|---|-------------------------------|---|
| | RII | R | RII | R | RII | R | RII | R |
| Lack of proper waste management plan and control | 0.212 | 5 | 0.125 | 5 | 0.250 | 7 | 0.196 | 8 |
| Poor project management | 0.250 | 4 | 0.148 | 6 | 0.295 | 6 | 0.231 | 7 |
| Lack of a quality management system aimed at waste optimization | 0.308 | 3 | 0.182 | 5 | 0.364 | 5 | 0.285 | 5 |
| Lack of team work | 0.423 | 2 | 0.250 | 4 | 0.500 | 4 | 0.391 | 4 |
| Poor site layout | 0.442 | 2 | 0.261 | 3 | 0.523 | 3 | 0.409 | 3 |
| Poor qualification of the contractor's technical staff assigned to the project | 0.462 | 2 | 0.273 | 2 | 0.545 | 2 | 0.427 | 2 |
| Poor coordination and communication between parties involved in the project | 0.481 | 1 | 0.284 | 1 | 0.568 | 1 | 0.444 | 1 |
| Poor management and distribution of labors, materials and equipment's | 0.308 | 3 | 0.182 | 5 | 0.364 | 5 | 0.285 | 6 |

— Group 5. Site Supervision Factors

The Relative Importance Index of each of the sub-factors of the site supervisor group, which causes construction material waste, is presented in Table 3.5.

The questionnaires of this study considered 42 factors which cause material waste in construction, and those factors were distributed into five groups as mentioned above. Table 3.6 gives the results based on the collected data from the questionnaire. Causes of construction materials waste, which illustrates the mean and ranking of each group.

Table 3.5: Ranks of construction materials wastage due to site supervisor factors

| Factors | Contractors | | Consultants | | Clients | | Weighted average (all groups) | |
|--|-------------|---|-------------|---|---------|---|-------------------------------|---|
| | RII | R | RII | R | RII | R | RII | R |
| Lack of supervision and delay of Inspections | 0.269 | 4 | 0.159 | 4 | 0.318 | 4 | 0.249 | 4 |
| Poor qualification of contractors' | 0.385 | 1 | 0.227 | 1 | 0.455 | 1 | 0.356 | 1 |
| Poor coordination and communication between the consultant engineer, contractor and client | 0.365 | 2 | 0.216 | 2 | 0.432 | 2 | 0.338 | 2 |
| Change orders by owner | 0.346 | 3 | 0.205 | 3 | 0.409 | 3 | 0.320 | 3 |

Table 3.6: Weighted average and ranking over-all causes of construction wastage

| Group Numbers | Main Groups | All Groups (Weighted Average) | Rank |
|---------------|--|-------------------------------|------|
| Group 3 | Operations factors | 0.399 | 1 |
| Group 1 | Design and documentation factors | 0.37975 | 2 |
| Group 2 | Materials handling and storage factors | 0.37973 | 3 |
| Group 4 | Site management and practices factors | 0.334 | 4 |
| Group 5 | Site supervision factors | 0.316 | 5 |

— Modeling by Linear Regression

≡ Statistical Analysis

Figures below showed the statistical summary of the comparison between design and construction of public building from consultant/contractor/employer for the calibration period. Then, as it was mentioned above, the correlation coefficient (R2) was used to check the results. The construction of materials wastage or construction wastage from design and documentation factors includes:- design changes and revisions, designer's inexperience in method and sequence of construction, lack of attention paid to standard sizes available on the market, lack of information in the drawings, ambiguities, mistakes, and changes in specifications, rework that don't comply with drawings and specifications, lack of knowledge about construction techniques during design activities and poor communication leading to mistakes and errors. The value of correlation coefficient (R2) is calculated from excel sheet as below.

R2=1 (ok) because the value of R2 range is in between of 0 and 1. It is shown on figure 4, above. Cause of Construction materials waste the following factors: procurement poorly schedule to procurement the materials, over ordering or under ordering due to mistake in quantity surveys, purchased materials that don't comply with specification, onsite damage materials on site/wrong handling of materials, overproduction/production of a quantity greater than required or earlier than necessary, lack of onsite materials

control, poor storage of materials, materials transport/shifting damage during transportation, by bulk, by partial and on time delivery.

Table 3.7: Sample excel sheet calculation taken

| Design and Documentation | | Regression Statistics | |
|--------------------------|--------|-----------------------|----------|
| X | Y | Multiple R | 1 |
| 0.1932 | 0.3269 | R Square (R2) | 1 |
| 0.2045 | 0.3462 | Adjusted R Square | 1 |
| 0.2045 | 0.3462 | Standard Error | 3.02E-17 |
| 0.2386 | 0.4038 | Observations | 10 |
| 0.2500 | 0.4231 | | |
| 0.2500 | 0.4231 | | |
| 0.2841 | 0.4808 | | |
| 0.3182 | 0.5385 | | |

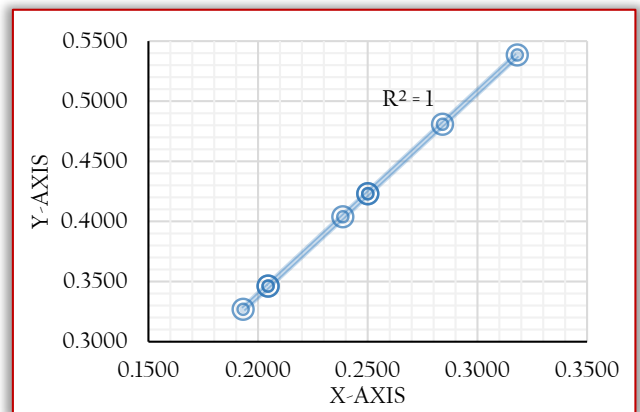


Figure 4: Construction materials wastage due to design and documentation factors comparison

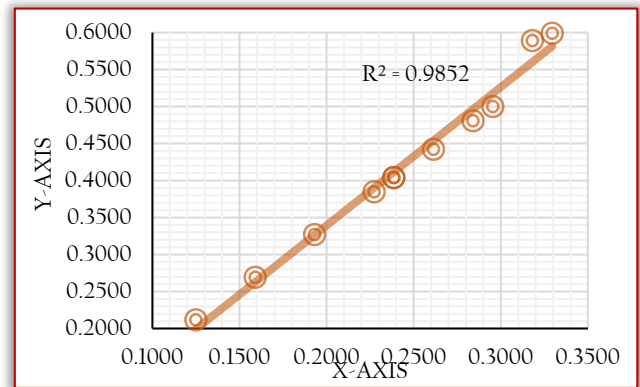


Figure 5: Construction materials wastage due to procurement and handling factors

R2=0.9852 (ok) because the value of R2 range is in between of 0 and 1. It is shown on figure 5 above.

The followings are Causes of construction materials wastage due to operation:- rework due to workers' mistakes, damage to work done caused by subsequent trades, use of incorrect material, thus requiring replacement, poor workmanship, lack of workers or tradesmen or subcontractors' skill, choice of wrong construction method, lack of coordination among crews, problems between the contractor and his subcontractors, equipment frequently breakdown, poor technology of equipment and shortage of tools and equipment's required.

R2=0.999 (ok) because the value of R2range is in between of 0 and 1. It is shown on figure 6 above. The followings are causes of construction materials wastage due to site

management and practices: lack of proper waste management plan and control, lack of a quality management system aimed at waste optimization, lack of team work, poor site layout, poor qualification of the contractor's, technical staff assigned to the project, poor coordination and communication between parties involved in the project, poor management and distribution of labors, materials and equipment's.

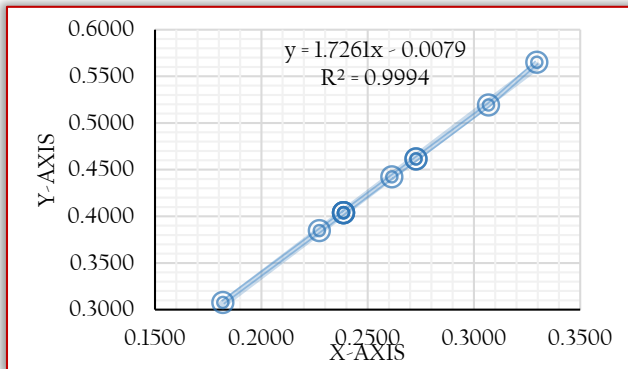


Figure 6: Construction materials wastage due to operation comparison

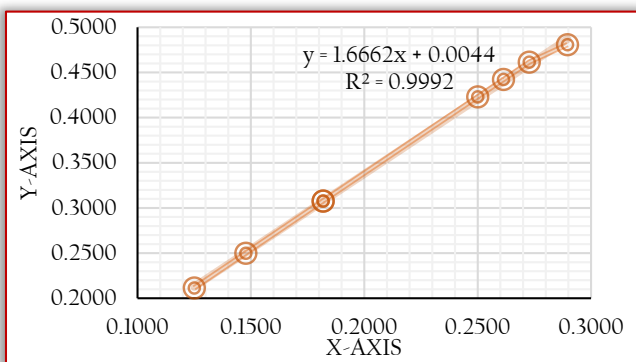


Figure 7: Construction materials wastage due to site management and practices factors

R2 = 0.999 (ok) because the value of R2 range is in between of 0 and 1. It is shown on figure 7 above.

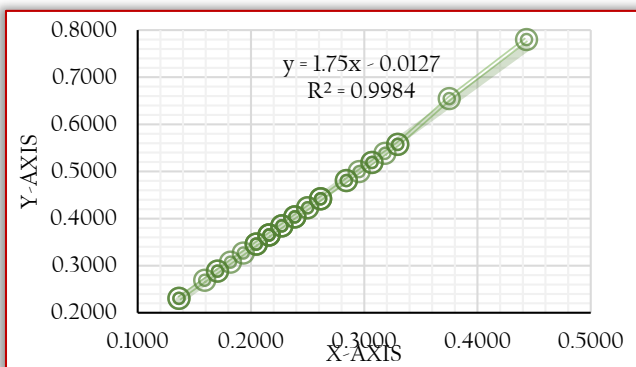


Figure 8: Construction materials wastage due to lack of proper site supervision factors

R2=0.998 (ok) because the value of R2range is in between of 0 and 1. It is shown on figure 8 above.

CONCLUSION

Construction waste corresponds to a significant portion of the total waste produced by the society. Solutions that reduce construction waste generation are a challenge in the construction

industry. This study contributes to the understanding of waste generation at construction sites through statistical modelling. A method for waste measurement was developed, and data were obtained from selected building sites. The proposed regression models had a satisfactory statistical performance and thus may be acceptable for estimating generated wastes to guide management plans. The models propose a comprehensive relationship between waste and building characteristics. The model to estimate total Waste had a simple yet effective linear format and was based on building characteristics, data for which may be collected directly from the project sites. The second model considered Time, and it indicated a link between waste generation and building schedules. This model suggested a small nonlinear influence of the Time attributes on Waste, through an S-shaped curve.

In summary, the models based on regression analysis could contribute to waste generation understanding by showing the most relevant attributes and their weights. Under these circumstances, they can be used to predict waste generation in projects with similar characteristics. The models can preview waste before construction commences and help builders improve onsite waste management. Therefore, this approach could be used to reduce cost and waste in new projects

Acknowledgment

The authors are great full to the authorities of construction projects, contractors and consultants for their kind co-operation and giving permission to carry out this study. The author wishes to acknowledge staff members for their valuable critics that have contributed much to improving this paper.

References

- [1] Andrew R.J. Dainty and Richard J. Brooke (2204) "Towards improved construction waste minimization" Structural Survey 22(1) 20–29
- [2] Ayarkwa, J, K. Agyekum and E. Adinyira, (n.d), "Exploring Waste Minimization Measures in the Ghanaian Construction Industry" College of Architecture and Planning, Kwame Nkrumah University of Science and Technology Kumasi, Ghana
- [3] Baniyas, G.; Achillas, C.; Vlachokostas, C.; Moussiopoulos, N.; Tarsenis, S. Assessing multiple criteria for the optimal location of a construction and demolition waste management facility. *Build. Environ.* 2010, 45, 2317–2326
- [4] Begum, R. A., & Siwar, C. (2006). A Benefit-Cost Analysis on the economic feasibility of construction waste minimization: The Case of Malaysia. *Resource Conservation & Recycling*, 86–98.
- [5] Bossink BAG, Brouwers HJH (1996). Construction waste: quantification and source evaluation; *J. Construction Eng. Manage.*, 122(1): 55-60.
- [6] Carlos Torres Formoso, L. S. (2002). Material Waste in Building Industry: Main Causes and Prevention. *Journal of construction Engineering and Management*, Vol. 128, No. 4, pp, 316- 317
- [7] Central Statistical, a. (2008/09).The Federal Democratic Republic of Ethiopia. Report on Contract construction survey.
- [8] Chris Reardon, Emily Fewster "Waste minimization" Australian Guide to Environmentally Sustainable homes, 2013

- [9] Conway, H. C. (2005). Construction. A Report on the Industry submitted to Industrial College of the Armed Forces National Defense University.
- [10] C.W.F. Che Wan Putra, A. Ahmad, M.Z. Abd Majid, and N. Kasim, (1999) "Improving material scheduling for construction industry in Malaysia," In Malaysian Science & Technology Congress 99, 6-8, Johor Bahru, Malaysia
- [11] Dennis S. Macozoma (2002) "Construction site waste management and minimization", International council for research and innovation in building and construction.
- [12] Ekanayake, L.L. & Ofori, G. (2000). Construction material waste source evaluation, Proceedings of the 2nd South African Conference on Sustainable Development in the Built Environment, Pretoria, South Africa.
- [13] Enshassi, A. (1996), "Material Control and Waste on Building Sites", Building Research Information. 24(1), 31-34.
- [14] Environmental Protection Agency of USA, (2000). Solid Waste and Emergency Response. EPA-530-F-00-001. United States.
- [15] Ethiopian, E. A. (2006/07). The current state of the construction industry. Report on the Ethiopian economy, Volume VI.
- [16] Faniran, O.O and Caban, G. (1998) Minimizing Waste on Construction Project Sites. Engineering, Construction and Architectural Management, Vol. 5, No. 2, pp. 182-188.
- [17] Formoso, C.T., Isatto, E.L. & Hirota, E.H. 1999. Method for waste control in the building industry. Journal of the University of California, Berkeley, USA.
- [18] Formoso, C.T., Lucio Soibelman, M., De Cesare, C. and Isatto, E.L. (2002). Materials Waste in Building Industry: Main causes and prevention. Journal of Construction Engineering and Management, 128(4), 316-325.
- [19] Getachew Araya Kassa, November, 2009 AAU School of Graduate Studies; Master of Science of Civil Engineering, Construction Technology and Management Major Thesis.
- [20] Horsley A. et.al, (2003), 'Delivering Energy Efficient Buildings: A Design Procedure to Demonstrate Environmental and Economic Benefits', Journal of Construction Management and Economics, Vol. 21, Pg 345
- [21] International Investment and Services Directorate Industry. (1999). the Canadian Construction Industry; A Consultation Paper in Preparation for World Trade Organization (WTO) General Agreement on Trade in Services (GATS) Negotiations. pp 10- 12.
- [22] Koskela, L. (1992). Application of the New Production Philosophy to Construction. CIFE, Technical Report No. 72, Stanford, USA
- [23] Lauritzen, E. (1998, October). Emergency construction waste management. Safety Science
- [24] Lee, S., Diekman, J.E., Songer, A.D., & Brown, H., (1999). Identifying waste: applications of construction process analysis. Proceedings of IGLC-7.
- [25] Milke, M., Brown, C., & Seville, E. (2011). Disaster waste management. Waste Management, 31(6), 1085, 1098-1085, 1098
- [26] Sepa. Guidance on Using the European Waste Catalogue (EWC) to Code Waste. Available online: www.sepa.org.uk/media/162682/sepa-waste-thesaurus.pdf (accessed on 19 July 2017).
- [27] Shen, L. Y., Tam, W. Y. Vivian, Tam, C. M. and Drew, D., (2004). Mapping Approach for Examining Waste Management on Construction Sites. Journal of Construction Engineering and Management, 130(4), 472-481.
- [28] Tam, C., & Tam, V. (2006). A review on the viable technology for construction waste recycling. Resources, Conservation and Recycling, 47(3), 1049, 1059-1049, 1059



ISSN: 2067-3809

copyright © University POLITEHNICA Timisoara,
Faculty of Engineering Hunedoara,
5, Revolutiei, 331128, Hunedoara, ROMANIA
<http://acta.fih.upt.ro>

Fascicule 4

[October – December]

t o m e

XIV

[2021]

ACTA Technica CORVINIENSIS
BULLETIN OF ENGINEERING



ISSN: 2067-3809

copyright © University POLITEHNICA Timisoara,
Faculty of Engineering Hunedoara,
5, Revolutiei, 331128, Hunedoara, ROMANIA
<http://acta.fih.upt.ro>

¹Tajudeen Kolawole AJIBOYE, ²Sulyman Age ABDULKAREEM,
³Olusegun Samuel BALOGUN

ANALYSIS OF SLIDING PARAMETERS ON WEAR BEHAVIOUR OF BRAKE LINING MATERIALS

¹ Department of Engineering, University of Ilorin, Ilorin, NIGERIA

Abstract: In this study, the effect of sliding parameters on the wear behaviour of brake pad lining materials was analyzed. The test samples were procured and coded as TY, HN and MZ respectively. The sliding parameters considered for this research were application load, sliding speed and application time. The application load considered are those of vehicles gross weights ranging between 1500 – 3500 Kg, the sliding speed was varied between 100 – 200 rpm while the application time was from 20 – 100 seconds at an interval of 20 seconds. Using standard equipment and test methods, the test samples were subjected to elemental composition analysis, wear characteristics and microstructural examination. The elemental composition test carried out revealed that the reinforcing fibre which gives an optimum performance in the formulation of these brake pads was carbon. The wear characteristics was conducted using the pin on disc test method and the results showed that wear rate of brake pads lining materials increased with increase in applied load and sliding speed but decreased with an increase in the application time.

Keywords: brake pads; elemental composition; lining materials; sliding parameter, wear behaviour

INTRODUCTION

Brake pad is a component part of automobiles that is essential for the purpose of safety and controlled performance. The presence of this component in automobiles provides a lot of assistance for safe reduction in the speed of automobile vehicles and apparently bringing it to a halt as the case may be [1]

The principle of operation of brake pad is based on the transformation of energy in which the kinetic energy of a moving vehicle is been transformed into thermal energy which results in either retardation of the vehicle or bringing the vehicle to a halt [2].

The materials used in the formulation of brake pads play significant role in deciding the suitability and their respective individual properties combine to determine the properties possessed by the brake pads [3]. Since brake pads lining material is a crucial component from the safety point of view, materials used for the brake systems should possess stable frictional and wear properties under varying conditions of load, speed and environment [4, 5].

Wear behaviour refers to how materials react under a specific service condition. The most useful method of characterization of wear behaviour is to classify the service condition of the material under investigation in terms of the broad types of wear and then examine the behaviour in terms of specific operational features. The characterization enables the sorting and identification of appropriate information on wear behavior, model development, and selection of wear data [6].

Due to the service condition brake pads are regularly exposed to in which they are opened to the activities of different sliding parameters that contribute to wear and consequently may serve as a contributory factor to vehicle brake failure, this research work was embarked on to provide useful information on the cause of wear of vehicle brake pads lining materials through analysis of the wear effect contributed by application pressure and other

associated sliding parameters on the brake pad lining materials as well as the effect of the application environment (dry). So the focus of this study is to analyse the effect of sliding parameters such as load, speed and environmental conditions on the wear behaviour of brake pad lining materials.

MATERIALS AND METHODS

The brake pads employed for this research are those used in light weight vehicles with gross weight ratings between 1500 – 3500 Kg [7, 8] and the specification is as stated [9].

The materials used for this experiment were procured from the local market in Nigeria and were subjected to composition analysis using ARL 4460 Optical Emission Spectrometry equipment and the result is presented in Table 1

Table 1: Elemental composition of brake pads lining materials used for the experiment

| S/N | Test Specimen | % Composition | | | | | |
|-----|---------------|---------------|---------|-------|------|------|------|
| | | Fe | C | Si | V | W | Sn |
| 1 | SA | 26.45 | >59.39 | 0.39 | 0.48 | 9.83 | 9.83 |
| 2 | SB | 0.41 | >94.054 | >4.65 | 0.00 | 0.12 | 0.01 |
| 3 | SC | 0.87 | >89.20 | >9.25 | 0.00 | 0.11 | 0.04 |

SAMPLE PREPARATION

The brake pad was carefully mounted on a bench vice and the metallic back plate was removed using hacksaw. Afterwards, the brake pad lining material was prepared for the property tests according to the standard dimensions required.

— Brinell Hardness

Brinell hardness testing equipment with model number EEDB00006/13 was used to test for the resistance of the specimen to indentation. A hardened steel ball of 10mm indentation diameter was pressed into the test specimen under a constant load of 3000 Kgf for a dwell time of 15 secs. The indentation created was measured using a micrometer screw gauge across two different directions with the mean

value substituted for in the formula for Brinell hardness number (BHN) [1].

$$BHN = \frac{2P}{\pi D(D - \sqrt{D^2 - d^2})} \quad (1)$$

where: P= Applied load (Kgf)

D= Diameter of hardened steel ball (mm)

d= Diameter of indentation created (mm)



Figure 1: Brinell hardness test of test material

— Izod impact test

Avery Denilson Impact testing equipment with a capacity of 150 J and an impact velocity of 3.65 m/s was employed for the test. According to ASTM E23-2013 test standard, the test samples were prepared into 64 x 12 x 3.2 mm dimension with a 2 mm deep notch at the centre. Each of the test specimens was firmly fixed with the notched area positioned in the opposite direction of the falling hammer. The hammer was released at maximum load of 150 J to create an impact on the test specimen and the result of the impact was read on the equipment scale.



Figure 2: Izod impact test on test specimen

— Tensile strength

A Testometric Universal Testing Machine (UTM) FS was used for this test. The test specimen was prepared into a dimension of 120 x 10 x 5 mm according to ASTM E8-2013 standard. The test piece was fixed into the jaw of the equipment and an initial load of 5,000 N which was gradually varied was applied until samples SA, SB and SC fractured at 520.87 N, 426.51 N and 815.03 N respectively.

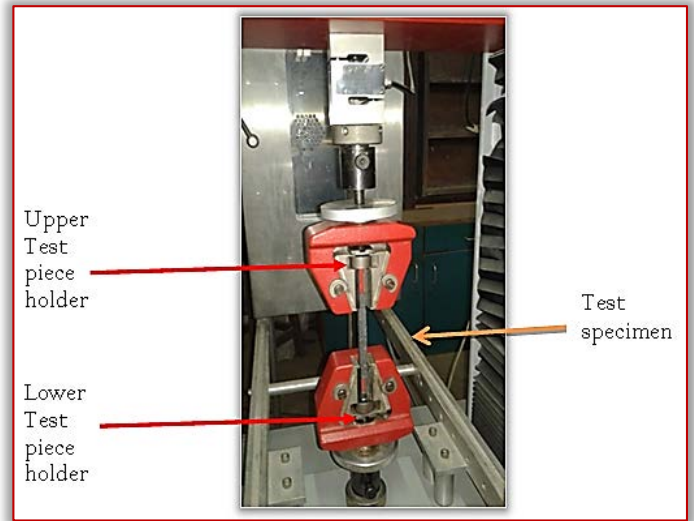


Figure 3: Tensile test of test specimen

— Compressive strength

The test specimens were prepared into a determined shape of 10 mm x 10 mm x 30 mm according to ASTM E9-2013 test standard after which it was placed between the jaws of the testometric Universal Testing Machine with a capacity of 50 kN. An initial force of 5 kN was applied on the specimen and was gradually increased until the material finally yielded under load. Samples SA, SB and SB yielded at 17.68 kN, 32.46 kN and 14.59 kN load respectively.



Figure 4: Compression test of test specimen

— Coefficient of friction

The co-efficient of friction (COF) of the test specimens were carried out using simple inclined plane method in which the specimen was allowed to freely slide down over the cast iron plane.

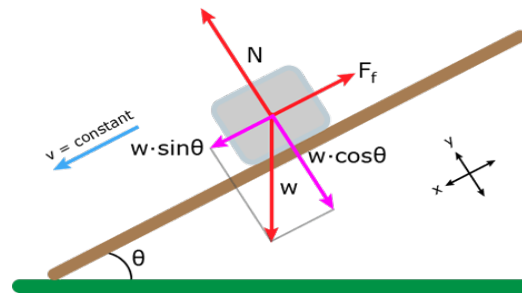


Figure 5: Free Body Diagram of a Simple Inclined Plane
At the point of sliding, the plane was clamped and the angle of inclination (θ) was measured after which the coefficient of friction (μ) was calculated using equation 2 [10, 11].

$$COF(\mu) = \tan \theta \quad (2)$$

— Wear Characteristics

The test sample was firmly held in the specimen holder which has a combined weight of 1174.28 Kg with the handle. The weight of the samples were measured before and after each test time with a measuring electronic scale with 0.001 mg precision as the test time were varied between 20 to 100 seconds at an interval of 20 seconds. Prior to weighing, the worn out samples were cleaned with wool soaked in acetone and wear particles debris on the emery paper were intermittently removed by compressed dry air blower.

— Microstructural Examination

The microstructural examination of the test specimens were carried out by polishing the surface of the samples with an emery cloth of 600grit on a polishing machine after which it was viewed under the computerized metallurgical microscope.



Figure 6: Test specimen under wear test



Figure 7: Metallurgical microscope for examination

RESULTS

The results obtained for each of the test were detailed in Tables 2 to 6 and Figures 8 to 13 which clearly shows the behavior of the material under the application of the designed load

Table 2: Brinell Hardness Test Results

| S/N | Test Specimen | Test No | Load (Kgf) | Steel ball diameter, D (mm) |
|-----|---------------|-----------------|------------|-----------------------------|
| 1 | SA | SA ₁ | 3000 | 10 |
| | | SA ₂ | 3000 | 10 |
| | | SA ₃ | 3000 | 10 |
| 2 | SB | SB ₁ | 3000 | 10 |
| | | SB ₂ | 3000 | 10 |
| | | SB ₃ | 3000 | 10 |
| 3 | SC | SC ₁ | 3000 | 10 |
| | | SC ₂ | 3000 | 10 |
| | | SC ₃ | 3000 | 10 |

| S/N | Test Specimen | Indentation diameter, d (mm) | Mean Value, d (mm) | BHN |
|-----|---------------|------------------------------|--------------------|--------|
| 1 | SA | 5.46 | 5.46 | 117.15 |
| | | 5.44 | | |
| | | 5.47 | | |
| 2 | SB | 5.70 | 5.71 | 106.68 |
| | | 5.71 | | |
| | | 5.71 | | |
| 3 | SC | 5.79 | 5.78 | 103.22 |
| | | 5.78 | | |
| | | 5.78 | | |

Table 3: Result of Izod Impact Test

| S/n | Test Specimen | Test No | Impact Strength(J) | Avg. Impact Strength(J) |
|-----|---------------|-----------------|--------------------|-------------------------|
| 1 | SA | SA ₁ | 69.50 | 69.08 |
| | | SA ₂ | 68.75 | |
| | | SA ₃ | 69.00 | |
| 2 | SB | SB ₁ | 69.00 | 69.17 |
| | | SB ₂ | 69.50 | |
| | | SB ₃ | 69.50 | |
| 3 | SC | SC ₁ | 69.50 | 69.00 |
| | | SC ₂ | 68.50 | |
| | | SC ₃ | 69.00 | |

Table 4: Results of Tensile Test

| S/N | Test Specimen | Test No | Yield Force(N) | Avg. Yield force (N) |
|-----|---------------|-----------------|----------------|----------------------|
| 1 | SA | SA ₁ | 520.10 | 520.87 |
| | | SA ₂ | 520.90 | |
| | | SA ₃ | 521.60 | |
| 2 | SB | SB ₁ | 426.05 | 426.51 |
| | | SB ₂ | 429.90 | |
| | | SB ₃ | 423.58 | |
| 3 | SC | SC ₁ | 816.10 | 815.03 |
| | | SC ₂ | 813.22 | |
| | | SC ₃ | 815.76 | |

| S/N | Time to failure (Secs) | Avg. time to failure (Secs) | Elong. at Yield(mm) | Average Elong. at yield (mm) |
|-----|------------------------|-----------------------------|---------------------|------------------------------|
| 1 | 9.43 | 9.44 | 0.61 | 0.61 |
| | 9.42 | | 0.62 | |
| | 9.48 | | 0.61 | |
| 2 | 6.80 | 6.76 | 0.42 | 0.42 |
| | 6.82 | | 0.42 | |
| | 6.67 | | 0.41 | |
| 3 | 10.82 | 10.79 | 0.71 | 0.72 |
| | 10.72 | | 0.72 | |
| | 10.83 | | 0.73 | |

Table 5. Result of Compressive Test

| S/N | Test Specimen | Test No | Yield force (kN) | Avg. Yield force (kN) |
|-----|---------------|-----------------|------------------|-----------------------|
| 1 | SA | SA ₁ | 17.57 | 17.68 |
| | | SA ₂ | 17.65 | |
| | | SA ₃ | 17.83 | |
| 2 | SB | SB ₁ | 32.44 | 32.46 |
| | | SB ₂ | 32.45 | |
| | | SB ₃ | 32.49 | |
| 3 | SC | SC ₁ | 14.57 | 14.59 |
| | | SC ₂ | 14.56 | |
| | | SC ₃ | 14.63 | |

| S/N | Time to failure (Secs) | Avg. time to failure (Secs) | Def. At Yield (mm) | Avg. def. At yield (mm) |
|-----|------------------------|-----------------------------|--------------------|-------------------------|
| 1 | 15.99 | 16.09 | 2.57 | 2.62 |
| | 16.21 | | 2.61 | |
| | 16.06 | | 2.68 | |
| 2 | 13.37 | 13.41 | 2.30 | 2.24 |
| | 13.52 | | 2.18 | |
| | 13.33 | | 2.24 | |
| 3 | 7.77 | 7.73 | 1.30 | 1.29 |
| | 7.66 | | 1.29 | |
| | 7.75 | | 1.29 | |

Table 6. Co-efficient of Friction of the Brake Pads

| S/N | Test specimen | Test No | Inclination Angle, $\theta(^{\circ})$ | Calc. | Average COF (μ) |
|-----|---------------|-----------------|---------------------------------------|-----------------------------------|-----------------------|
| | | | | Coefficient of Friction (μ) | |
| 1 | SA | SA ₁ | 18.78 | 0.34 | 0.34 |
| 2 | | SA ₂ | 18.78 | 0.34 | |
| 3 | | SA ₃ | 18.26 | 0.33 | |
| 1 | SB | SB ₁ | 18.51 | 0.33 | 0.32 |
| 2 | | SB ₂ | 17.99 | 0.32 | |
| 3 | | SB ₃ | 17.86 | 0.32 | |
| 1 | SC | SC ₁ | 18.95 | 0.34 | 0.33 |
| 2 | | SC ₂ | 17.55 | 0.32 | |
| 3 | | SC ₃ | 18.40 | 0.33 | |

Table 2 shows the results obtained for the Brinell Hardness Test for each of the sample specimens under the same loading and experimental conditions. Tables 3, 4, 5 and 6 indicate the results obtained for Impact, Tensile, Compressive, and Coefficient of friction tests in that order.

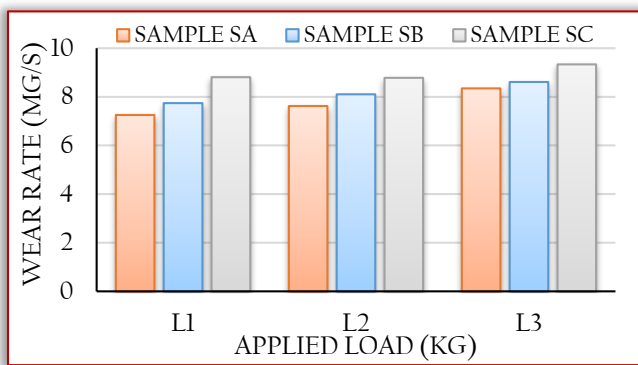


Figure 8: Variation of wear rate with the variation of applied load at 100 rpm; (L1 = 1569.05g, L2=1583.72g and L3 = 1603.83g)

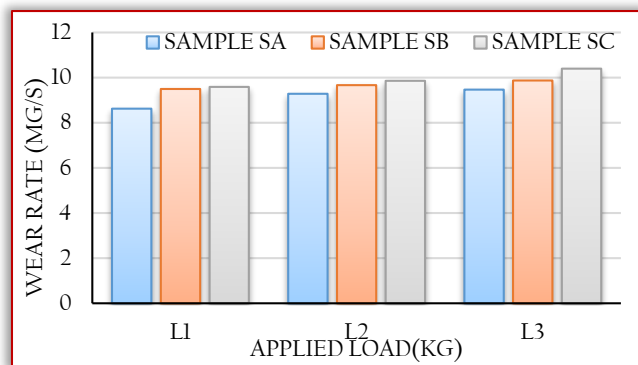


Figure 9: Variation of wear rate with the variation of applied load at 150 rpm(L1 = 1569.05g, L2=1583.72g and L3 = 1603.83g)

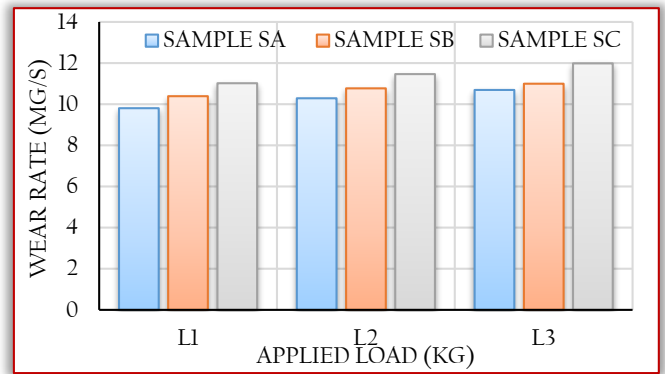


Figure 10: Variation of wear rate with the variation of applied load at 200 rpm (L1 = 1569.05g, L2=1583.72g and L3 = 1603.83g)
Figures 8, 9 and 10 shows the variation of the wear rate with load at 100 rpm, 150 rpm and 200 rpm respectively for the three samples under consideration.

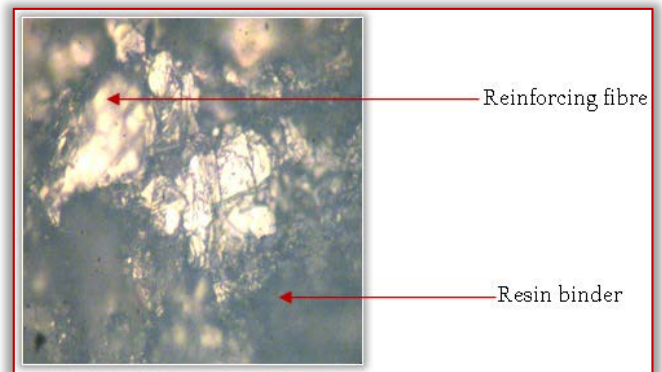


Figure 11: Microstructure of Sample SA at x400

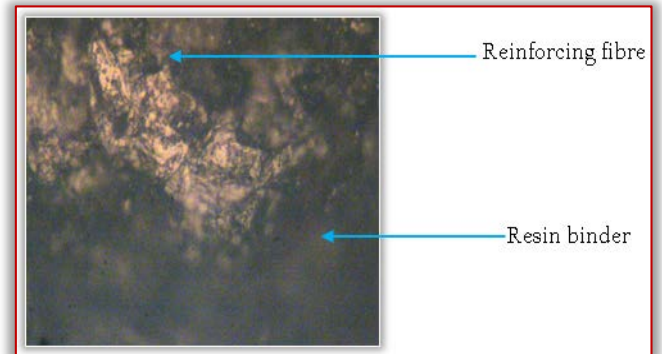


Figure 12: Microstructure of Sample SB at X400

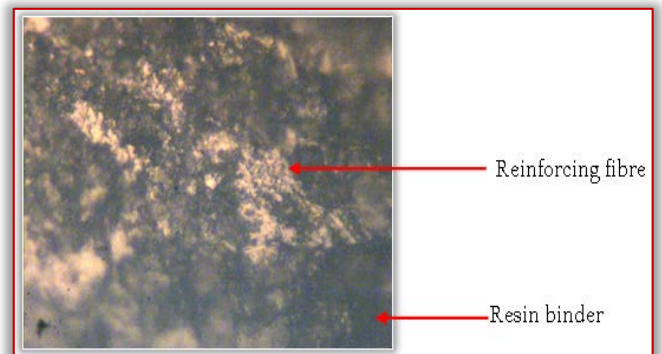


Figure 13: Microstructure of Sample SC at X400

Figures 11, 12 and 13 show the microstructure of each of the test sample. These depict the structural arrangement of the

constituents which is an indication of the behaviour of the samples under the application of loads.

DISCUSSIONS

— Brinell hardness

From the result table, it can be inferred that SA possesses the best hardness property when compared with SB and SC respectively under the same load condition of 3000 Kgf while that of SB is slightly higher than that of SC. The high brinell hardness number indicated by SA is as result of its high tungsten content which stands at an average of 9.83% when compared with the respective average values of tungsten contents in SB (0.12%) and SC (0.11%) as indicated by the elemental composition results for each of the test specimen.

— Izod impact strength

The three test specimens tend to have an approximately same value of impact strength when subjected to the same hammer drop at a maximum load of 150 J with the average izod impact strength of SA, SB and SC at 69.08 J, 69.17 J and 69.0 J respectively. This could be as a result of their respective high carbon content with that of SA supplemented with the high iron content.

— Tensile strength

Generally, the test results indicated that the brake pad lining materials are highly brittle in nature, a condition that could be associated to the high carbon contents. Due to the very high carbon content of SB, it has the earliest average yield time to failure and the lowest average yield force respectively when compared with the corresponding parameters for both SA and SC respectively. Also, the average elongation at yield point for SB is the lowest of the three samples which is also as a result of the high carbon content while that of SC is slightly higher than the corresponding obtained values for SA.

The test result showed that SC possesses the highest average yield force which stands at 815.03 N with SA and SB having a value of 520.87 N and 426.51 N, respectively. The average time to failure for SA is 9.44 seconds, SB is 6.76 secs and SC is 10.79 secs while the average elongation at yield for Samples SA, SB and SC are 0.61 mm, 0.42 mm and 0.72 mm respectively.

— Compressive strength

From the above test results obtained for each of the test specimen, SA shows an average compressive strength value of 17.68 kN which is slightly higher than that of SC at 14.59 kN despite the higher carbon content of SC though it is lower than that of SB. One of the factors that could be responsible for this variation is the higher tungsten percentage in SA (9.83%) when compared with that of SC (0.11%).

The high average yield force indicated by SB is as a result of its extremely high carbon content though its tungsten percentage is at 0.12%. Comparatively, SA has the longest average time to failure due to its higher tungsten and iron contents though with a higher deflection while SC has the lowest average time to failure and deflection respectively.

— Coefficient of friction

The calculated coefficient of friction for the three test specimens were virtually the same and they all fall within the range of coefficient of friction for brake pad lining materials as stipulated by NIS 323(1997) which is between 0.3 and 0.4 as obtained by other researcher in a similar research [8].

— Wear Characteristics

In general, from the various results obtained at varying application time, applied loads and sliding speed conditions, it was observed under each load applications that the wear rates of samples SA, SB and SC respectively were decreasing as the application time was increasing and the average wear rates increased with each sliding speed and applied loads. That is, the wear rate of brake pads lining materials increase as the sliding speed and applied loads increase but it decreases as the application time increases.

Under each test condition, it was observed that the average wear rate values of both sample B and sample C were consistently higher than that of sample A with that of sample C slightly higher than that of sample B, a condition that could be related to the amount of resin binder inclusion in the brake pads. The results clearly showed that wear rate is at maximum at the shortest time of application.

— Microstructural Examination

In general, the graphite which is the reinforcing fibre, is martensitic in nature, a condition that is responsible for the brittle nature of the brake pads used for the purpose of this research and the distribution of particles in the friction materials are different for each test samples.

CONCLUSIONS

- ≡ The brake pads have carbon as the reinforcing fibres and it is in larger percentage than other constituent elements used in the brake pads formulation
- ≡ The high carbon element present in these brake pads makes it highly brittle in nature consequently resulting in their respective low tensile strength capacity.
- ≡ The brake pads displayed a good co-efficient of friction that it falls within the range of results obtained by Dagwa and Fono-tamo on similar vehicle size.
- ≡ The wear rates of the brake pads decreased with increased application time but it increased with increased applied load and sliding speed.
- ≡ The amount and distribution of binder in the brake pads affects the wear characteristics as it determines the structural stability of material under mechanical stress and thermal stresses and also prevents it from crumbling

Acknowledgement

The authors which to acknowledge the Technical team of the Mechanical Engineering Workshop, University of Ilorin for their contributions towards the successful completion of the research work.

References

- [1] Elakhame Z. U., Alhassan O.A., Samuel A.E., (2014) "Development and Production of Brake Pads from Palm Kernel Shell Composites" International Journal of Scientific and Engineering Research, 5(10), pp. 726-742.
- [2] Surojo E., Jamasri, Malau V., Ilman N., (2014) "Effects of phenolic Resin and Fly Ash on Coefficient of Friction of Brake

- Shoe Composite” ARPJ Journal of Engineering and Applied Sciences, 9(11),pp. 2234-2238.
- [3] Darius G., Solomon, Mohamad N.B., (2007) “Characterization of Friction Material Formulations for Brake Pads” Proceedings of the World Congress on Engineering, London Uk.,2, pp. 234.
- [4] Maleque M.A., Dyuti S.,Rahman M.M.,(2010) “Material Selection Method in Design of Automotive Brake Disc” Proceedings of the World Congress on Engineering.
- [5] Riyadh A.,Al-Samarai, Haftirman, Khairel R. A.,Al-Douri Y.,(2012) “Effect of Load and Sliding Speed on Wear and Friction of aluminium-Silicon Casting Alloy” International Journal of Scientific and Research Publications, 2(3), pp. 1-4.
- [6] Bayer R.G, (2002) “Wear Analysis for Engineers” HNB Publishing, New York, USA.
- [7] Blau J.P., (2001) “Compositions, Functions and Testing of Friction Brake Materials and their Additives”, Oak Ridge National Laboratory, USA Department of Energy, pp. 1-29.
- [8] Miller-Wilson K. (2016) “List of Car Weights” Available at “http://cars.lovetoknow.com/List_of_Car_Weights” accessed 08/09/2017 10:40am
- [9] Nigeria Industrial Standard (1997), Specification for Friction Materials for Road Vehicles Brake Lining and Pads, NIS 323: 1997, Standard Organization of Nigeria.
- [10] Fono-Tamo .R.S, Olufemi A.K, (2015) “Weibull Approach to Brake Pad Wear Analysis in the Nigerian Market”, 3(10), Tsinghua University Press, pp 228-233.
- [11] Nagesh S.N., Siddarju C., Prakash S. V., Ramesh M.R., (2014) “Characterization of Brake Pads by Variation in Composition of Friction Materials” International Conference on Advances in Manufacturing and Materials Engineering, Procedia Materials Science 5, pp. 295-302.



ISSN: 2067-3809

copyright © University POLITEHNICA Timisoara,
Faculty of Engineering Hunedoara,
5, Revolutiei, 331128, Hunedoara, ROMANIA
<http://acta.fih.upt.ro>

¹Sakina TOUZARA, ¹Abdelilah CHTAINI, ¹Amina AMLIL, ¹Olivier F.A.B. KOFFI

ELECTROANALYSIS OF COPPER IONS BY SENSOR BASED ON CARBON PASTE AND EDTA

¹ Molecular Electrochemistry and Inorganic Materials Team, Faculty of Science and Technology of Beni Mellal, Sultan Moulay Slimane University, MOROCCO

Abstract: In this article we have set ourselves the objective of developing new functional materials applied in electroanalysis. The aim is to develop new modified electrodes having analytical performance by immobilizing an organic film based on Disodium ethylenediaminetetraacetate dihydrate (EDTA) on the surface of carbon paste electrode (CPE). We performed electrochemical analysis traces of copper ions by the technique of square wave voltammetry (SWV) and cyclic voltammetry (CV). The objective of studying the electrochemical reactivity of the electrodes produced is to consider their use as voltammetric sensors dedicated to the detection of copper ions. The EDTA cation chelator power to improve the analytical characteristics of our electrodes, gives a high sensibility and stability, for determination of Cu(II) in a solution.

Keywords: EDTA; cyclic voltammetry; sensor; square wave voltammetry

INTRODUCTION

Sensitive and selective detection of heavy metal ions is particularly critical and challenging research area. Including several metal ions Cu(II) exposes essentiality as micronutrient element, it similarly has considerable value in biochemistry and metabolic processes of various living organisms [1,2]. Absence of Cu(II) may be to blame for the anemia, ischemic heart diseases, bone demineralization, cardiovascular effects, skin diseases etc. [3]. But recently, due to contamination instead of being an essential element, excessive doses of Cu(II) ion become threatening life issue for the living organisms [4]. Therefore, a number of methods and technologies have been produced for the sensitive and selective detection of metal ions. Highly identified techniques are liquid chromatography, atomic emission spectroscopy, spectrophotometry, and inductively coupled plasma mass spectrometry [5–10] etc.

several researchers based on the utilization of electrochemical sensors due to many advantages such as high sensitivity, rapidity of response, simplicity, low cost, miniaturized and automated devices [11,12]. In recent years, the development of innovative materials and new manufacturing processes has seen an increase due to improvement in research activities in the formulation of electrochemical sensors for the detection of heavy metals have considerably [13,14].

Carbon paste electrodes (CPE) have become a subject of development and research. CPE's are considerably more convenient, the electrode material cheaper and easy to handle and prepare with the desired composition and predetermined properties [15,16]. The electrochemical response of CPE varies mostly on the properties of the modifier species. The modification of the CPE can be done in several methods [17–20] and the immobilization method [21].

EXPERIMENTAL

— Apparatus

Voltammograms were recorded using a voltalab potentiostat model PGSTAT 100, controlled by voltalab master 4. The three-electrode electrolytic cell was utilized. As a working

electrode modified paste electrode, with a geometric area 0.1256 cm². A reference electrode was a saturated calomel electrode (SCE) while the counter electrode was a Pt wire.

— Reagents

Graphite powder (Carbone, Lorraine, ref 9900, French), CuSO₄ and all other reagents utilized were of analytical grade. All chemicals were employed without further purification. The supporting electrolyte was trisHCl buffer (pH = 5.06). Distilled water was utilized for all preparation of the solution. All chemicals employed for handling were of analytical grade.

— Preparation of the CPE

The carbon paste electrode (CPE) was made by hand mixing graphite powder and paraffin oil. The resulting paste was grounded into a PTFE cylindrical tube electrode. The electrode obtained was dried at room temperature. Electrical contact was made with a carbon bar. Modified CPE electrodes (EDTA-CPE) were prepared by immobilizing EDTA by soaking the prepared CPE electrode in a solution containing the EDTA solution.

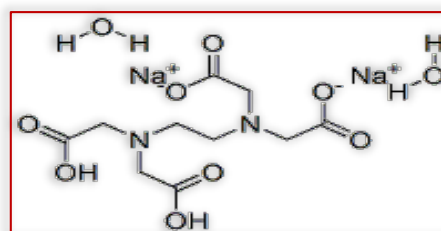


Figure 1. Molecule of disodium ethylenediaminetetraacetate dihydrate

RESULTS AND DISCUSSION

The influence of pH on EDTA immobilized on the CPE surface was studied in the pH range between 4 and 8 (Figure 2). By comparing the results obtained for the four pHs studied, we find that the highest activity and current densities are recorded at slightly acidic pH at pH 5. The pH 5 is therefore retained for the rest of the manipulations.

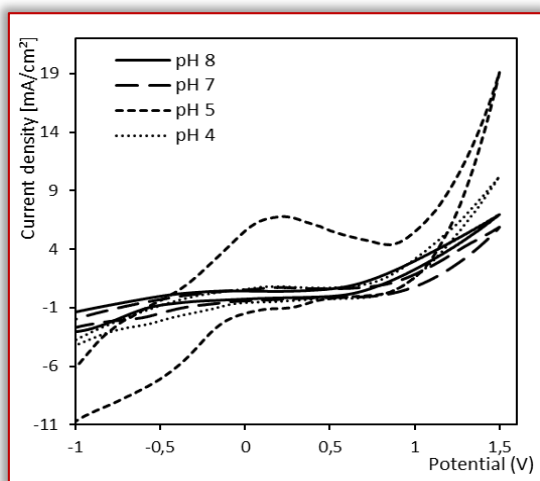


Figure 2. Cyclic voltammograms recorded in a Tris HCl solution at different pH, scan rate 100 mV/s.

Figure 3 illustrates the cyclic voltammograms recorded for the carbon paste electrode and the carbon paste electrode modified by the organic molecule, in a trisHCl electrolytic medium. The appearance of the voltammogram has completely changed in the existence of the EDTA molecule on the carbon surface, which proves the modification of the base electrode corresponding to the reaction proposed below:

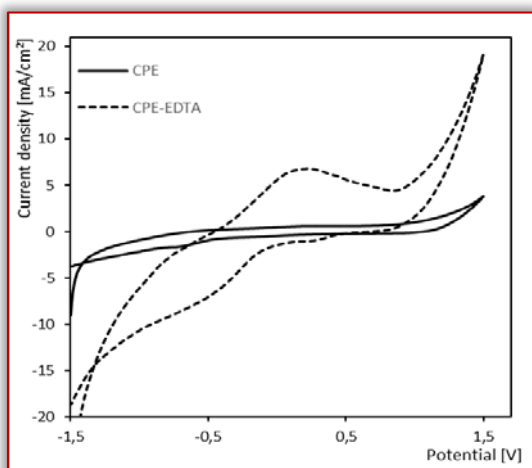
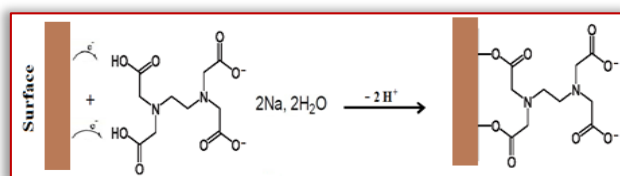


Figure 3. Cyclic voltammograms recorded in buffer solution (pH 5.06), CPE (a) and EDTA-CPE (b), Scan rate 100 mV/s.



Scheme 1. The proposed mechanism for the immobilization of the EDTA molecule on the surface of CPE.

In order to study the ability of EDTA on detection, the comparative study of the capacity for determining Cu (II) ion concentration by the CPE / EDTA electrode before and after preconcentration in a solution contains Cu²⁺ ions have been studied. The modified EDTA was preconcentrated in the analysed solution containing 70 mg/l copper ions in TrisHCl buffer solution. The CPE/EDTA electrode has two overlaid redox peaks of SWV significant for Cu (II) ions,

however, the CPE / EDTA electrode after preconcentration in Cu (II) ions has a superior current density than the modified electrode after preconcentration (Figure 4), result to the selective chelation capacity of EDTA molecules towards Pb (II) ions. VC method confirmed this result figure 5.

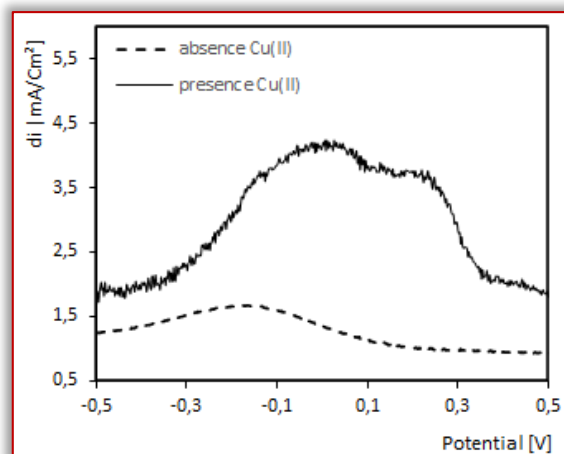


Figure 4. SQW voltammograms recorded for EDTA-CPE in buffer solution (pH 5.06), before and after preconcentration in copper solution, scan rate 100 mV/s.

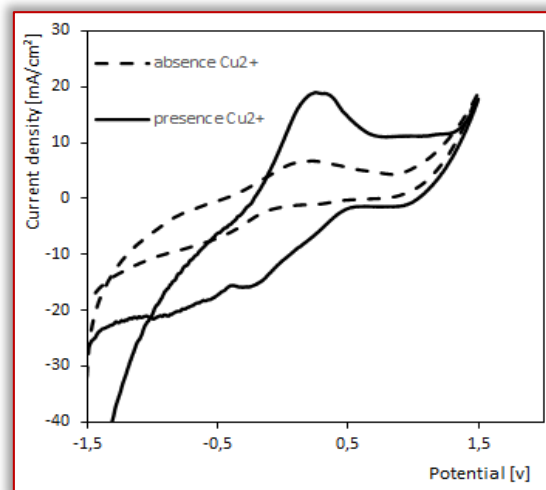


Figure 5. Cyclic voltammograms recorded for EDTA-CPE in buffer solution (pH 5.06), before and after preconcentration in copper solution, scan rate 100 mV/s.

The Figure shows typical curves, respectively, of CV and SWV recorded for the EDTA-CPE electrode, on solutions containing Cu(II) concentrations between $3,01 \times 10^{-4}$ mol/l à $4,816 \times 10^{-3}$ mol/l. The densities of the oxidation and reduction peaks increase linearly with the concentration of copper ions (Figure 6).

The linear calibration equation is as follows:

$$i_{P_{\text{anodique}}} \text{ (mA)} = 187,6 [\text{Cu}^{2+}] \text{ (mol l}^{-1}\text{)} + 2,7803, \\ R^2 = 0,9033$$

$$i_{P_{\text{cathodique}}} \text{ (mA)} = -201,6 [\text{Cu}^{2+}] \text{ (mol l}^{-1}\text{)} - 3,2372, \\ R^2 = 0,9143$$

According to Miller and Miller, the basic deviation of the mean current (SD) determined at the oxidation potential of copper for seven voltammograms of the solution contains Cu (II) concentrations in the pure electrolyte be able to be formed by l'equation:

$$SD = \frac{1}{(n-2)} \sum_{j=0}^n (i_j - I_j)^2 \quad (10)$$

where i_j is the experimental value of the current calculated at manipulation j and I_j is the corresponding value recalculated at the same concentration using the calibration equation. The calculated S.D. value was utilized for the determination of limit detection (DL, $3 \times \text{S.D.} / \text{slope}$) and limit quantization (QL, $10 \times \text{S.D.} / \text{slope}$). From this equation we deduce the following values:

≡ Detection limit (DL): $2.4 \times 10^{-4} \text{ mol/l}$

≡ Limit quantification (QL) : $8,3 \times 10^{-4} \text{ mol/l}$

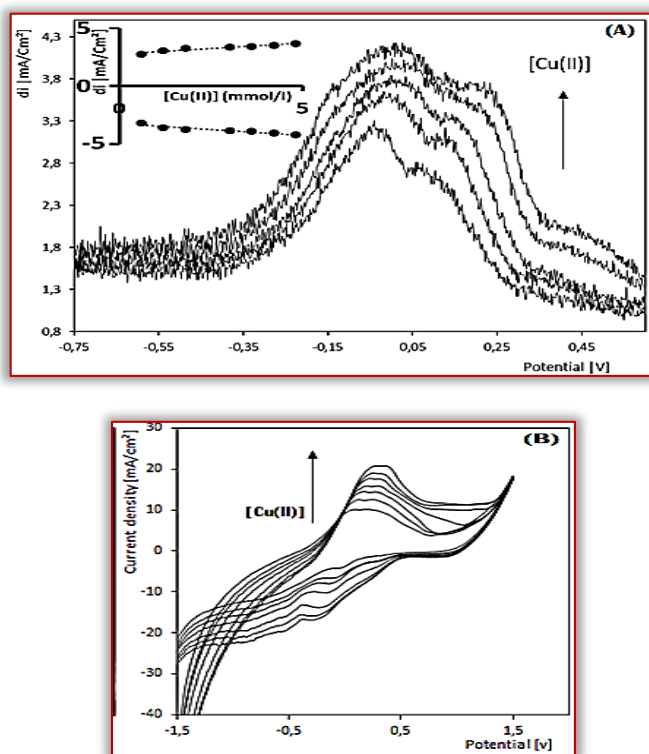
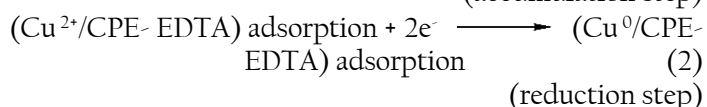
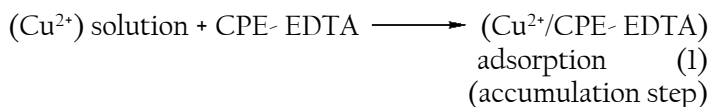
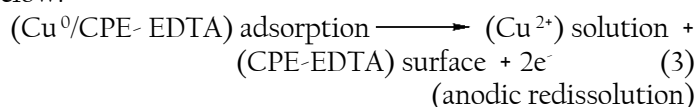


Figure 6. SQW (A) and CV (B) voltammograms obtained in EDTA-CPE, in buffer solution containing different concentrations of copper. Inset: Calibration curve obtained by analyzing copper ions in the range comprised between 3,01 and 4,16 mol/l.

After determining the calibration curves for the electroanalysis of Cu(II) ions, we propose the following mechanism:



The peak P2 corresponds to the phenomenon of oxidation of Cu and of salting out of Cu^{2+} , by following the mechanism below:



CONCLUSION

In this work we have studied the possibility of determining the Cu(II) ions by the carbon paste electrode modified by EDTA. The EDTA-CPE electrode prepares by self-assembly

method. The latter showed a great activity vis-à-vis the chelation of Cu^{2+} ions. Copper (II) analysis is possible by monitoring the oxidation peak of Pb^{2+} ions in the electrolytic solution. We work on the validation of the recommended method and the study of the interference of different metals for example Cd^{2+} , Hg^{2+} , etc.

References

- [1] Feier B., B'ajan I., Fizes I., an, Floner D., Cristea C., Geneste F., S'andulescu R. (2015) Highly selective electrochemical detection of Copper(II) using N, N'bis(acetylaceton) ethylenediimine as a receptor, *Int. J. Electrochem. Sci.* 10:121–139.
- [2] Niu L.M., Luo H.Q., Li N.B., Song L. (2007). Electrochemical detection of copper(II) at gold electrode modified with a self-assembled monolayer of penicillamine, *J. Anal. Chem.* 62:470–474.
- [3] Romana D.L., Olivares M., Uauy R., Araya M. (2011). Risks and benefits of copper in light of new insights of copper homeostasis, *J. Trace Elem. Med. Biol.* 253–13.
- [4] L.M. Gaetke, C.K. Chow. (2003). Copper toxicity, oxidative stress, and antioxidant nutrients, *Toxicology* 189:147–163.
- [5] Gillicuddy N. Mc, Nesterenko E.P., Nesterenko P.N., Jones P., Paull B. (2013). Chelation ion chromatography of alkaline earth and transition metals using monolithic silica column with bonded N-hydroxyethyliminodiacetic acid functional groups, *J. Chromatogr. A* 1276:102–111.
- [6] Lopes F.S., Junior O.A., Gutz I.G.R. (2010). Fully electrochemical hyphenated flow system for preconcentration cleanup, stripping, capillary electrophoresis with stacking and contactless conductivity detection of trace heavy metals, *Electrochem. Commun.* 12:1387–1390.
- [7] Xiaodong W., Qiuling Y., Zhidong Y. (2011). Qingwen, Determination of cadmium and copper in water and food samples by dispersive liquid-liquid microextraction combined with UV-vis spectrophotometry, *Microchem. J.* 97:249–254.
- [8] Kamal G., Yadollah N., Omid O., Ammar M. (2011). Sulfur-nanoparticle-based method for separation and preconcentration of some heavy metals in marine samples prior to flame atomic absorption spectrometry determination, *Talanta* 85:763–769.
- [9] Li W., Simmons P., Shrader D., Herrman T.J., Dai S.Y. (2013). Microwave plasma-atomic emission spectroscopy as a tool for the determination of copper iron, manganese and zinc in animal feed and fertilizer, *Talanta* 11:243–48.
- [10] Dai B., Cao M., Fang G., Liu B., Dong Xv., Pan M., Wang S. (2012). Schiff base-chitosan grafted multiwalled carbon nanotubes as a novel solid-phase extraction adsorbent for determination of heavy metal by ICP-MS, *J. Hazard. Mater.* 219–220:103–110.
- [11] Beilsteins Handbuch der organischen Chemie (1971) Bd IX, U5, Springer Verlag, Berlin 4234.
- [12] Nikolski B.P., Krylow L.I., Zakhvataev B.B. (1973) *Radiokhimija* 15: 810-813.
- [13] Gao H, Qi X, Chen Y, Sun W (2011) Electrochemical deoxyribonucleic acid biosensor based on the self-assembly film with nanogold decorated on ionic liquid

- modified carbon paste electrode. *Anal Chim Acta* 704: 133-138.
- [14] Wang J. (2003) Nanoparticle-based electrochemical DNA detection. *Anal Chim Acta* 500: 247-257.
- [15] Svancara I., Vytras K., Barek J., Zima J. (2001) Carbon paste electrodes in modern electroanalysis. *Critical Reviews in Analytical Chemistry* 31: 311-345.
- [16] Rice M.E., Galus Z., Adams R.N. (1983) Graphite paste electrodes: Effects of paste composition and surface states on electron-transfer rates. *J Electroanal Chem Interfacial Electrochem* 143: 89-102.
- [17] Reddy S., Swamy B.K., Chandra U., Sherigara B.S., Jayadevappa H. (2010) Synthesis of CdO nanoparticles and their modified carbon paste electrode for determination of dopamine and ascorbic acid by using cyclic voltammetry technique. *Int J Electrochem Sci* 5: 10-17.
- [18] Tanuja S.B., Swamy B.E.K., Vasantakumar K.P. (2016) Electrochemical Response of Dopamine in Presence of Uric Acid at Pregabalin Modified Carbon Paste Electrode: A Cyclic Voltammetric Study. *J Anal Bioanal Tech* 7: 1.
- [19] Gilbert O., Chandra U., Swamy B.K., Char M.P., Nagaraj C., et al. (2008). Poly (alanine) modified carbon paste electrode for simultaneous detection of dopamine and ascorbic acid. *Int J Electrochem Sci* 3: 1186-1195.
- [20] Gilbert O., Swamy B.K., Chandra U., Sherigara B.S. (2009) Electrocatalytic oxidation of dopamine and ascorbic acid at poly (Eriochrome Black-T) modified carbon paste electrode. *Int J Electrochem Sci* 4: 582-591.
- [21] Shankar S.S., Swamy B.K., Ch U., Manjunatha J.G., Sherigara B.S. (2009) Simultaneous determination of dopamine, uric acid and ascorbic acid with CTAB modified carbon paste electrode. *Int J Electrochem Sci* 4: 592-601.



ISSN: 2067-3809

copyright © University POLITEHNICA Timisoara,
Faculty of Engineering Hunedoara,
5, Revolutiei, 331128, Hunedoara, ROMANIA
<http://acta.fih.upt.ro>

¹Precious EHIOMOGUE, ²Israel I. AHUCHAOGU, ¹Isiguzo Edwin AHANEKU

REVIEW OF ADSORPTION ISOTHERMS MODELS

¹Department of Agricultural and Bioresources Engineering, Michael Okpara University of Agriculture, Umudike, NIGERIA

²Department of Agricultural and Food Engineering, Faculty of Engineering, University of Uyo, NIGERIA

Abstract: Adsorption phenomenon is a popular separation process in environmental remediation and wastewater treatment due to its simplicity, low cost, efficiency, and environmentally friendliness. The amount of material absorbed by a substrate is often expressed as a function of the equilibrium concentration at a constant temperature in a process known as Adsorption Isotherm. The study of adsorption isotherms is essential to gain insight into the design and operation of adsorption systems. In this review paper, the general knowledge and application of the isotherm model to date have been highlighted for an insight into the concept and application of adsorption isotherm models. The classification of the isotherm model has also been highlighted. In addition, various types of isotherm models in terms of the number of parameters have been extensively discussed. The criteria for selecting the appropriate model as well as the modern trend in the modelling approach have also been discussed. This review will enable researcher make informed choices in selecting adsorption isotherm models.

Keywords: Adsorption, Isotherms, sorption, Chemisorption, Physiosorption

INTRODUCTION

Increase in human activities leading to agricultural and industrial waste has a severe impact on soil contamination (Garbuio, Howard and dos Santos, 2012). An increase in population implies a proportionate increase in environmentally unfriendly activities. Roser, Ritchie, and Ortiz-Ospina (2013) reported an exponential population growth in recent times. Industrial activities have also increased in China, India, and other developing countries like Nigeria. This increase in population and industrial activities leads to an increase in the deterioration of the ecosystem with more threat to the human physical environment. Continuous release of pollutants into the environment by human activities calls for the integration of various methodologies in place to minimize or eliminate toxic material materials from the environment. Wide range of researches on the treatment process have been carried out and are still ongoing in areas such as sedimentation, precipitation, coagulation, flocculation, flotation, filtration, membrane processes, electrochemical techniques, biological process, chemical reactions, ion exchange and adsorption (Food and Hameed, 2010). Of the technologies applied to environmental remediation, adsorption is of major interest due to its high efficiency and wider use. It is one of the most popular separation and purification/remediation processes (Al-Ghouti and Da'ana, 2020).

The study of adsorption isotherms is essential to gain insight into the design and operation of adsorption systems and process, especially for the sake of environmental remediation and wastewater treatment plants. The study of adsorption chemical kinematics is an important subject matter in environmental analysis (Gautam and Chattopadhyaya, 2016). A proper understanding of adsorption isotherm models is useful to gain an understanding of the adsorption process of pollutants on adsorbents (El-Khaiary, 2008). In addition, adsorption isotherms show the equilibrium of the sorption of adsorbate on the surface of adsorbents and are

useful knowledge in the optimization of adsorbent for the removal of pollutants from the environment.

The use of linear regression techniques to model adsorption isotherms has been popularly used in recent times to analyse adsorption systems due to their simplicity (Fost and Aly, 1981). Linear regression is capable of verifying the consistency of the models based on the assumptions made while quantifying the distribution of the adsorbate. The evolution and increase in computer technology have increased the use of nonlinear regression techniques in the analysis of adsorption isotherm as well (Ayawei, Ebelegi and Wankasi, 2017). The nonlinear regression approach has the advantage of minimizing errors due to linearization.

ADSORPTION AND ADSORPTION ISOTHERM MODEL

In environmental and bioremediation, molecules are absorbed from the bioavailable water-dissolved state through sorption to soil constituent (Harms, 2011). Sorption, in general, involves gas or liquid accumulation in another phase and includes absorption and adsorption. In other words, chemical and physical processes, which enable a gas or a liquid accumulate within another phase or phase boundary of two phases are popularly known as sorption. Sorption to natural solids is an underlying activity that affects the degradation, transport, and biological activities of organic compounds in the surroundings (Pignatello and Xing, 1995). When the liquid or gas accumulates on the boundary of two other phases, it is known as adsorption. Absorption, on the other hand, is the accumulation of two phases within another phase. While the molecules penetrate a three-dimensional matrix in absorption, the molecules attach to a two-dimensional matrix usually between phase boundaries in adsorption (Prasad and Srivastava, 2009; Qi et al., 2017). The adsorption phenomenon is a widely used separation process in environmental remediation and wastewater treatment due to its simplicity, low cost, efficiency, and environmentally friendliness (Wang and Guo, 2020). The amount of material absorbed by a substrate

is often expressed as a function of the equilibrium concentration after adsorption at a constant temperature. The process of representing this function is known as Adsorption Isotherms (Tadros, 2013). In other words, adsorption isotherm models are curves describing the variation of gas absorbed with pressure. Adsorption isotherms profile equilibrium behaviour of adsorbents at constant temperature (Al-Ghouti and Da'ana, 2020a).

Depending on the interaction between the adsorbate and the adsorbent, the adsorption processes can be physisorption or chemisorption (Sims, Harmer and Quinton, 2019). Physisorption is a phenomenon, which occurs whenever an adsorptive (the substance in the fluid phase which is capable of being absorbed) is brought into contact with the surface of the adsorbent by intermolecular forces involving the same kind as those responsible for the imperfection of real gases and the condensation of vapours (Sing, 1982). However, when the processes involve forming transient chemical bonds to the surface, it is known as chemisorption (Jiang et al., 2019). An effective design of adsorption systems through the general improvement of adsorption pathways requires good knowledge and understanding of adsorption isotherms (El-Khaiary, 2008).

Three things are considered in the design of the adsorption mechanism, the physical adsorption that has to do with van der Waals force, the chemical adsorption that is made by the chemical bond and ion exchange. Modelling of adsorption equilibrium data by isotherm models is the most widely used method of investigating adsorption mechanisms (Wang and Guo, 2020). Adsorption isotherms are determined by the adsorbate adsorbent, adsorbed species, and physical properties such as ionic strength, temperature and pH (Yan et al., 2017). In the physical environment, the presence of the mixture of solids leads to the sorbate-sorbent associations which are governed by several interactions with varieties of behaviours described by different types of adsorption isotherms. According to IUPAC (International Union of Pure and Applied Chemistry), there are six types of adsorption isotherm models (types I, II, III, IV, V, and VI) based on the shape of the isotherm models as shown in figure 1 (Sing, 1982). The type I model is reversible and is concave on the relative pressure axis. A typical example of this model can be found in molecular zeolites and activated carbon (Hauchhum and Mahanta, 2014). The reversible type II isotherm model is the regular type, which can be derived from a non-porous adsorbent. An example is the adsorption of Nitrogen on silica gel (Zhou et al., 2002; Sultan, Miyazaki and Koyama, 2018). The reversible type III isotherm model is convex on the pressure axis and a typical example is water vapour adsorption of nonporous carbon (Carrott, 1992). The type IV isotherms are characterized by their hysteresis loops due to capillary condensation occurring in the mesopores and limiting uptake over the range of high pressure. An example of the type IV isotherm model is the adsorption of humid air or water on a specific type of activated carbon (Buttersack, 2019; Wang et al., 2020).

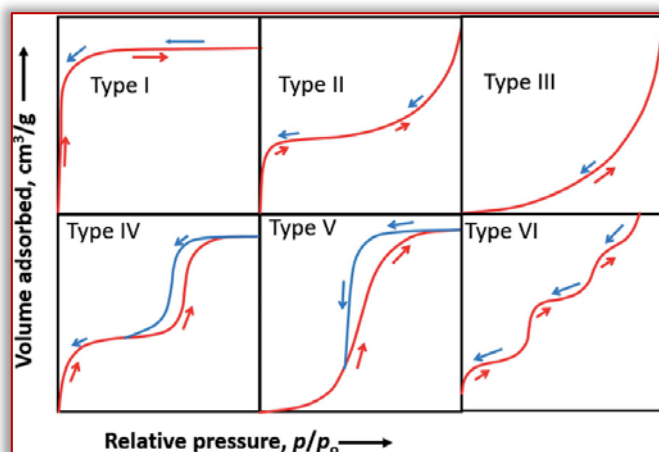


Figure 1: The IUPAC Classification of Adsorption Isotherms (Sing, 1982)

The type V isotherm model is related to the type III model by its weak adsorbent-adsorbate interaction. The model is uncommon but can be found in the certain porous adsorbent. A typical example is the adsorption of water on a carbon molecular sieve or activated carbon fibre (Inglezakis, Pouloupoulos and Kazemian, 2018; Buttersack, 2019). The type VI isotherm model is a multilayer and stepwise adsorptions which occurs on a uniform nonporous surface. This type of model can be found in the adsorption of inert gases on the surface of planer graphite (Sultan, Miyazaki and Koyama, 2018; Al-Ghouti and Da'ana, 2020a).

CLASSIFICATION OF ISOTHERM MODELS BASED ON THE NUMBER OF PARAMETERS

— One-Parameter Isotherm Models

≡ Henry's Isotherm Model

In Henry's isotherm model, the partial pressure of the adsorptive fluid is directly proportional to the amount of adsorbate (Fost and Aly, 1981; Erbil, 2006; Al-Ghouti and Da'ana, 2020b). It is considered one of the simplest adsorption isotherms (Ayawei, Ebelegi and Wankasi, 2017). Henry's adsorption isotherm derived its name from Henry's adsorption constant, i.e., the constant appearing in the linear adsorption isotherms, which is similar to Henry's gas law (Wikipedia, 2021). It is derived from Gibbs adsorption (Deocariz and Osio, 2020) and is used in the determination of the equilibrium state of adsorption for adsorbates that are secluded at a low and constant temperature. Thus, in Henry's adsorption isotherm, the equilibrium amount of adsorbate in the fluid is related to the partial pressure of the adsorptive fluid by Equation 1.

$$Q_e = K_H C_e \quad (1)$$

where Q_e is the amount of adsorbate at equilibrium condition (mg/g), K_H is Henry's adsorption constant, and C_e is the equilibrium concentration of the adsorbate on the adsorbent.

It is important to note that Henry's isotherm is not advisable for high temperature and pressure experimentation due to violent molecular motion caused by large interaction force and potential energy (Wang et al., 2016).

— Two-Parameter Isotherm

≡ Freundlich Isotherm Model

Freundlich adsorption isotherm model is a type of isotherm model in which the adsorbates form a monomolecular layer on the surface of the adsorbent (Singh, 2016), but unlike the Langmuir model, application to multilayer adsorption is also possible (Al-Ghouti and Da'ana, 2020b). The Freundlich model expression shows the heterogeneity of the surface of the molecules (Gast and Adamson, 1997) as well as the exponential distribution of active sites and their energies. The non-linearized form of Freundlich isotherm model expression is shown in Equation 2, while the linearized form is shown in Equation 3.

$$Q_e = K_F C_e^{1/n} \quad (2)$$

$$\ln Q_e = \ln K_F + \frac{1}{n} \ln C_e \quad (3)$$

where K_F is the Freundlich constant or maximum absorption capacity (L/mg), n is the adsorption intensity or surface heterogeneity, which indicates the energy distribution and the adsorbate site's heterogeneity.

Freundlich isotherm is a power function and isotherms of this form have been observed for wide varieties of heterogeneous surfaces such as silica, clays, metals, activated carbon, and polymers (Fabrizius-Homan and Cooper, 1992; Keyes and Silcox, 1994; Murai et al., 1998). Umpleby et al. (2001) tested the generality of the Freundlich isotherm concerning molecularly imprinted polymers (MIPs) using a survey of systems from the literature. The results show that the Freundlich isotherm model gives a good mathematical approximation of the binding characteristics for non-covalently imprinted polymers. It has also been used in the fitting of the isotherm model for the removal of methyl orange by periphytic biofilms (Wu, 2017).

≡ Hill Deboer Model

Hill Deboer Model (Deboer, 1953) applies to cases of lateral interaction between adsorbed molecules and mobile adsorption (Hill, 1946). When water adsorbed on pure and methylated quartz, there is an adsorption isotherm in which the amount adsorbed increases with increasing temperature when plotted in terms of relative pressure and is completely described by the Hill-de Boer equation (Tornquist et al., 1978). The linear form of the Hill Deboer Model is as shown in equation 4 (Kumara et al., 2010).

$$\ln \left[\frac{C_e(1-\theta)}{\theta} \right] - \frac{\theta}{1-\theta} = \ln K_1 - \frac{K_2\theta}{RT} \quad (4)$$

where K_1, K_2 are the Hill-Deboer constant (Lmg^{-1}) and the energetic constant of the interaction between adsorbed molecules, respectively. A positive K_2 mean attraction while a negative K_2 means repulsion between the adsorbed species while zero value of K_2 means lack of attraction between the adsorbed species. θ is the fractional coverage, R is the universal gas constant ($KJmol^{-1}K^{-1}$) and T is the temperature (K). To analyse the equilibrium data from adsorption experiments, a graph of $\ln(C_e(1-\theta)/\theta) - (\theta/1-\theta)$ against θ is usually plotted (Redlich and Peterson, 1959).

Hill Deboer isotherm model proved to be effective in the modelling of adsorption equilibrium isotherms of phenolic

compounds from aqueous solutions onto granular activated carbon (Hamdaoui and Naffrechoux, 2007).

≡ Langmuir Isotherm

The Langmuir isotherm model assumes that the distribution of the reactive groups over the surface of the particles are homogeneous and there is no lateral interaction between the particles (Miedaner, Weerasooriya and Tobschall, 2006). The Langmuir equation, which was developed based on the theory of gases, is used extensively to describe gas adsorption on solids (Olsen and Watanabe, 1957). The Langmuir sorption isotherm is valid when the adsorption of a solute from the solution is monolayer, the adsorption on a surface contains a definite number of identical sites with uniform strategy of adsorption, and there is no transmigration of adsorbate in the plane of surface (Gautam et al., 2014). The non-linearized form of the Langmuir isotherm model Langmuir (1918) is shown in equation 5

$$Q_e = \frac{Q_0 K_L C_e \theta}{(1 + K_L C_e)} \quad (5)$$

The linearized form of the Langmuir model is given by Equation 6

$$\frac{C_e}{Q_e} = \frac{1}{(K_L Q_0)} + \frac{C_e}{K_L} \quad (6)$$

where Q_e is the maximum adsorption capacity on a monolayer (mg/g) and K_L is the Langmuir adsorption constant (L/mg) that is related to the apparent energy of sorption. When a graph of C_e/Q_e against C_e will give a straight line of slope $1/(K_L Q_0)$.

The separation factor (R_1) is another key parameter that is often used to determine the nature of the adsorption process described in the Langmuir model. The separation factor is defined by equation 7 (Karagöz et al., 2008).

$$R_1 = \frac{1}{(1 + K_L C_0)} \quad (6)$$

where C_0 is the starting concentration of the adsorbate (mg/L).

Langmuir model was used by Kausar, Bhatti and MacKinnon (2013) in the equilibrium kinetic studies on the removal of uranium from low-cost agricultural waste such as rice husk. The results showed that the model correlated best with the uranium biosorption equilibrium data at 10-100mgL⁻¹ concentration range.

≡ Temkin Isotherm Model

Temkin isotherm ignores the extremely low and high values of the concentrations and assumes that the heat of adsorption of all molecules in the layer would not decrease logarithmically but linearly (Aharoni and Tompkins, 1970; Piccin). The Temkin isotherm (Piccin, Dotto and Pinto, 2011) can be described by the following equation (equation 7).

$$Q_e = \frac{RT}{b} \ln K_T + \left(\frac{RT}{b} \right) \ln C_e \quad (7)$$

where K_T is the maximum binding energy or the Temkin isotherm equilibrium-binding constant ($Lmol^{-1}$), b is the Temkin isotherm constant related to the adsorption heat.

≡ Kiselev Isotherm

The Kiselev adsorption isotherm is a localized single-molecular layer model (Song et al., 2014). Like other isotherm models, it is only valid for surface coverage

(Ayawei, Ebelegi and Wankasi, 2017). The linearized Kiselev isotherm model is shown below (Ojediran et al., 2019)

$$\ln \left[\frac{1}{C_e(1-\theta)} \right] = \frac{K_1}{\theta} + K_1 K_n \quad (8)$$

where K_1 is the Kiselev equilibrium constant (Lmg^{-1}), K_n is the equilibrium constant of the formation of complexes between adsorbed molecules.

≡ Flory-Huggins Isotherm

Flory-Huggins isotherm model considers the characteristics of surface coverage of the fluid on the adsorbent (Nechifor et al., 2015). The equation deals with similar chemical molecules, which differs in physical properties such as length. The linearized form of the equation is expressed as:

$$\ln \left(\frac{\theta}{C_0} \right) = \ln K_{FH} + n \ln(1 - \theta) \quad (9)$$

where n is the ion number occupying adsorption sites on two membranes, K_{FH} is the Flory-Huggins equilibrium constant, C_0 is the initial concentration of the adsorbate ions (mEq/L). $C_0 = (1 - C_e/C_0)$ is the degree of membrane surface coverage, C_e is the equilibrium concentration of the adsorbate.

Flory-Huggins isotherm model has been applied in the study of the adsorption of phosphate in drinking water (Nechifor et al., 2015). Flory-Huggins isotherm model can express the spontaneity of an adsorption process. The relationship between the Flory-Huggins equilibrium constant and Gibbs free energy is shown in the following expression (Ayawei, Ebelegi and Wankasi, 2017):

$$\Delta G^\circ = RT \ln K_{FH} \quad (10)$$

where ΔG° is standard free energy change, R is the universal gas constant, and T is the absolute temperature.

≡ Dubinin-Kaganer-Radushkevich Isotherm Model

Dubinin-Kaganer-Radushkevich isotherm is mostly used for cases where the Gaussian energy spread onto a heterogeneous surface (Celebi et al., 2007). The model is a semiempirical equation and follows a pore-filling mechanism with unrealistic asymptotic behaviour which is unable to predict Henry's law at low pressure (Vijayaraghavan et al., 2006; Theivarasu and Mysamy, 2011). The model is used to distinguish between physisorption and chemisorption of metal iron, Vijayaraghavan et al., 2006). The Dubinin-Kaganer-Radushkevich isotherm model is shown below (Kadhim, 2016):

$$\ln Q_e = \ln Q_m - K\varepsilon^2 \quad (11)$$

where C_a is the number of metal ions adsorbed per unit weight of adsorbent (mol/g), X_z is the maximum sorption capacity (mol/g), K_a is the activity coefficient related to mean sorption energy (mol^2/J^2) and ε is Dubinin-Kaganer-Radushkevich isotherm constant which can be determined using the equation below:

$$\varepsilon = RT \ln \left(1 - \frac{1}{C_0} \right) \quad (12)$$

R and T are gas constant and absolute temperature (K), respectively, while C_0 is the initial concentration. The sorption energy is determined using equation 11 below:

$$E = \left(\frac{1}{\sqrt{2K_a}} \right) \quad (13)$$

≡ Fowler-Guggenheim Model

The Fowler-Guggenheim isotherm model (Febrianto et al., 2009; Foo and Hameed, 2010) includes the study of the lateral interaction of the adsorbate in the adsorbent (Sampranpiboon, Charnkeitkong and Feng, 2014; Ojediran et al., 2019). The heat of adsorption varies linearly as the loading in the Fowler-Guggenheim isotherm model and is applicable only when the surface coverage is less than 0.6 (Ayawei, Ebelegi and Wankasi, 2017). The linearized form of the Fowler-Guggenheim isotherm model is stated as follows (Ojediran et al., 2019).

$$\ln \left[\frac{C_e(1-\theta)}{\theta} \right] = \ln K_{FG} + \frac{2\omega\theta}{RT} \quad (14)$$

where K_{FG} is the Fowler-Guggenheim equilibrium constant (Lmg^{-1}), and θ is the fractional

≡ Jovanovic Isotherm

The Jovanovic isotherm model shares a similar assumption as the Langmuir. In addition to the Langmuir model, however, it considers the possibility of mechanical contacts between the adsorbing molecules (Panahi, Vasheghani-Farahani and ShojoSadati, 2008). Furthermore, unlike the Langmuir model which is valid for mobile adsorption, the Jovanovic model is valid for localized adsorption (Rudzinski and Wojciechowski, 1977). The general Jovanovic equation for the homogeneous surface is given by the expression (Jovanovic, 1969; Hines, Kuo and Dural, 1990):

$$Q_e(P, T, e) = A[1 - \exp(-bP)] \quad (15)$$

where A is the adsorption capacity at equilibrium and b is the Jovanovic parameter defined by:

$$b = b_0 \exp(q/RT) \quad (16)$$

b_0 is the corresponding limiting value of b as the temperature approaches infinity, q is the isosteric heat of adsorption. The linearized form of the Jovanovic isotherm model is shown below (Ayawei, Ebelegi and Wankasi, 2017):

$$\ln Q_e = \ln Q_{\max} - K_J C_e \quad (17)$$

where Q_e is the amount of adsorbate in the adsorbent at equilibrium (mg g^{-1}), Q_{\max} is the maximum uptake of adsorbate obtainable when $\ln Q_e$ is plotted against C_e , K_J is the Jovanovic constant.

A modified form of the Jovanovic isotherm model known as the Jovanovic-Freundlich isotherm model has proven to better fit the optimization model for L-Lysine imprinted Polymer (Panahi, Vasheghani-Farahani and ShojoSadati, 2008).

≡ Halsey Isotherm

Halsey Isotherm (Halsey, 1948) is applied to a multilayer adsorption system with distance from the surface especially for metal ions (Kausar, Bhatti and MacKinnon, 2013; Liu and Wang, 2013; Singha and Das, 2013). This model is expressed as follows (Liu and Wang, 2013):

$$\ln Q_e = \frac{1}{n_H} \ln K_H - \frac{1}{n_H} \ln C_{qe} \quad (18)$$

where K_H and n_H are the Halsey constants.

The Halsey Isotherm model fitted well for the analysis of Novel Silica-Based Hybrid adsorbents using lead (II) as presented by Liu and Wang (2013).

The model has also been applied in fitting the adsorption removal of copper from aqueous solution and industrial effluent using agricultural wastes (Singha and Das, 2013)

≡ **Harkin-Jura Isotherm**

Harkin-Jura isotherm model applies to solid-gas systems (Iyer and Kunju, 1992) and it is based on the assumption that there is a possibility of multilayer adsorption occurring on the surface of adsorbents with heterogeneous pore distribution (Foo and Hameed, 2010; Ayawei, Ebelegi and Wankasi, 2017). This Harkin-Jura isotherm model is expressed as follows (Nworie et al., 2019):

$$\frac{1}{Q_e^2} = \frac{B}{A} - \left(\frac{1}{A}\right) \log C_e \quad (19)$$

where A and B are Harkin-Jura constants.

The Harkin-Jura isotherm model has been used in the study of adsorption isotherms, kinetics and error analysis of the removal of methylene blue from aqueous solution using activated rice husk biochar (Nworie et al., 2019).

— **Three-Parameter Isotherms**

≡ **Toth Isotherm**

Another useful modification of the Langmuir isotherm model is the Toth isotherm model (Tóth, Berger and Dékány, 1999). The Langmuir model was modified to minimize the error between the predicted value and the experimental data (Behbahani and Behbahani, 2014). The model is applied in the description of the high and low-end boundary of adsorbate concentration that is heterogeneous in Nature (Ayawei, Ebelegi and Wankasi, 2017). The Toth isotherm model is expressed as shown below (Ayawei, Ebelegi and Wankasi, 2017).

$$\frac{Q_e}{Q_m} = \frac{K_L C_e}{[1+(K_L C_e)^n]^{1/n}} \quad (20)$$

where K_L , Q_m , and n are Toth isotherm constants (mg g^{-1}). The Toth isotherm may be rearranged to a linearized form as follows.

$$\ln \frac{Q_e^n}{Q_m^n - Q_e^n} = n \ln K_L + n \ln C_e \quad (21)$$

≡ **Redlich-Peterson Isotherm**

The Redlich-Peterson isotherm model (Redlich and Peterson, 1959) is shown in equation 8 below (Ayawei, Ebelegi and Wankasi, 2017). While the linearized form is shown in equation 9 (Piccin, Dotto and Pinto, 2011). The model is used in a situation where there is a wide range of adsorbent concentrations in equilibrium. It can also be used in either homogeneous or heterogeneous systems (Piccin, Dotto and Pinto, 2011). The model combines the Langmuir and Freundlich isotherms with the numerator of Langmuir and is capable of approaching Henry's region when the dilution is infinite (Davoudinejad and Ghorbanian, 2013; Ayawei, Ebelegi and Wankasi, 2017)

$$Q_e = \frac{K_R C_e}{1 + B C_e^\beta} \quad (22)$$

$$\ln \left(K_R \frac{C_e}{Q_e} - 1 \right) = \ln(B) + \beta \ln(C_e) \quad (23)$$

where K_R is the Redlich-Peterson isotherms constant (Lg^{-1}), B is the Redlich-Peterson constant (L mg^{-1}), β is an exponent which lies between 1 and 0 (Mane, Mall and Srivastava, 2007).

Due to the presence of three additional unknown, K_R , B, and β , plotting the left-hand side of Equation 9 against $\ln C_e$ for obtaining the isotherm constants is not applicable. Therefore, a maximization procedure of the coefficient of correlation is usually adopted for solving the equation (Piccin, Dotto and Pinto, 2011).

≡ **Koble-Carrigan Isotherm**

Koble-Carrigan isotherm model combines the Langmuir and Freundlich isotherms with other modifications for representing equilibrium adsorption data (Han et al., 2005). The linear form of this module is represented by the following equation [56]:

$$Q_e = \frac{A_k P}{1 + B_k C_e^p} \quad (24)$$

where A_k , B_k , and p are Koble-Carrigan's parameters. The three Koble-Carrigan isotherm parameters are usually evaluated using Microsoft Excel or manually using trial and error on equation 25 (Han et al., 2005; Ayawei, Ebelegi and Wankasi, 2017).

$$\frac{1}{Q_e} = \frac{1}{A_k} * \frac{1}{C_e^p} + \frac{B_k}{A_k} \quad (25)$$

Koble-Carrigan isotherm has proven to best fit the data for the use of cereal chaff in the removal of lead ions from aqueous solutions as described by (Han et al., 2005)

≡ **Radke-Prausnitz Isotherm**

The Radke-Prausnitz isotherm model is used mostly in adsorption systems at low adsorbate concentration. The Radke-Prausnitz isotherm model is mathematically represented by the following expression (Khalid et al., 2015; Ayawei, Ebelegi and Wankasi, 2017):

$$Q_e = \frac{Q_M K_R C_e}{1 + K_R C_e^p} \quad (26)$$

Where Q_M and K_R are the Radke-Prausnitz equilibrium constant, and p is Radke-Prausnitz model exponent.

The Radke-Prausnitz isotherm model fitted well for the modelling of surface diffusion in the adsorption of aromatic compounds on activated carbon (Ocampo et al., 2013). Khalid et al. (2015) also used it in the modelling of copper biosorption with good performance and representation.

≡ **Langmuir-Freundlich Isotherm**

Langmuir-Freundlich isotherm is a versatile model that is capable of simulating both the Freundlich and Langmuir behaviour of adsorbates and adsorbents (Jeppu and Clement, 2012). The Langmuir-Freundlich isotherm has shown to best fit arsenate adsorption on metal oxides using different types of adsorption isotherms (Rau et al., 2003). At low and high adsorbate concentration, the Langmuir-Freundlich isotherm model becomes the Freundlich isotherm model and Langmuir isotherms model respectively (Ayawei, Ebelegi and Wankasi, 2017). Langmuir-Freundlich isotherm model can be mathematically represented by the expressed (Jeppu and Clement, 2012):

$$Q_e = \frac{Q_M (K_{LF} C_e)^n}{(K_{LF} C_e)^n + 1} \quad (27)$$

where Q_M is the adsorption capacity of the system ($\text{mg of sorbate/g sorbent}$), K_{LF} is the affinity constant for adsorption (L/mg), and n is the index of heterogeneity

≡ **Jossens Isotherm**

The Jossens isotherm model (Jossens et al., 1978; El Nemr, El-Sikaily and Khaled, 2010) takes into account the distribution of interaction energy between the adsorbate-adsorbent on the site of adsorption (El Nemr, El-Sikaily and Khaled, 2010; Ayawei, Ebelegi and Wankasi, 2017). This Jossen model accounts for the heterogeneous nature of the adsorbent surface due to the interaction within the adsorbate molecules. Equation 28 below shows the mathematical representation of the model:

$$C_e = \frac{Q_e}{H} \exp(FQ_e^p) \quad (28)$$

$$\ln\left(\frac{C_e}{Q_e}\right) = -\ln(H) + FQ_e^p \quad (29)$$

The linearized form of the Jossen equation is shown in equation 29, where H, F and p are the Jossens isotherms constant.

≡ **Sips Isotherm**

The sips isotherm model was developed to recognize and solve the problem of continuous increase in the adsorbed amount when the concentration increases which is usually experienced in the Freundlich isotherms model (Sips, 1948). Sips Isotherm model is mathematically represented by the following equation (El Nemr, El-Sikaily and Khaled, 2010):

$$Q_e = \frac{Q_{ms}K_s C_e^{ms}}{1 + K_s C_e^{ms}} \quad (30)$$

where Q_{ms} is the Sips maximum adsorption capacity (mg/g), K_s is the Sips constant (L/mg)^{ms}, and ms is the Sips model exponent. The sip model is also sometimes called the Langmuir

— **Four-Parameter Isotherms**

≡ **Baudu Isotherm Model**

Baudu isotherm model was developed to minimize the discrepancies in solving the Langmuir constant and coefficient from the gradient and tangent of the isotherm over a wider range of concentration (El Nemr, El-Sikaily and Khaled, 2010; Ramadoss and Subramaniam, 2018). The model is a modification of the Langmuir model and it is given by the expression below (El Nemr, El-Sikaily and Khaled, 2010).

$$Q_e = \frac{Q_{m0}b_0 C_e^{(1+x+y)}}{1 + b_0 C_e^{(1+x)}} \quad (31)$$

where Q_{m0} is the Baudu maximum adsorption capacity (mg/g), b_0 is the equilibrium constant, x and y are the Baudu parameters.

≡ **Fritz-Schlunder model**

The Fritz-Schlunder model empirically developed another four-parameter equation that follows the Langmuir-Freundlich to cater for the case of low liquid phase concentration of the adsorbate (Fritz and Schlunder, 1974). The mathematical expression of the model is shown below (Yaneva, Koumanova and Georgieva, 2013).

$$Q_e = \frac{A \cdot C_e^\alpha}{1 + B \cdot C_e^\beta} \quad (32)$$

A and B are the Fritz-Schlunder maximum equilibrium constants, α and β are the Fritz-Schlunder equilibrium exponents.

≡ **Weber-Van Vliet Isotherms Model**

The Weber-Van Vliet Isotherms Model (Weber Jr and Morris, 1963) has been used along with other isotherm models in fitting experimental data for the modelling of adsorption isotherms of phenol and chlorophenols onto granular activated carbon (Hamdaoui and Naffrechoux, 2007).

The model is an empirical relation with four parameters to which is proposed for describing equilibrium data and it is shown in the expression below (Hamdaoui and Naffrechoux, 2007).

$$C_e = P_1 Q_e^{(P_2 (Q_e)^{P_3 + P_4})} \quad (33)$$

P_1 , P_2 , P_3 and P_4 are the Weber-Van Vliet isotherms parameters.

— **Five-Parameter Isotherms**

≡ **Fritz-Schlunder isotherm model**

Fritz and Schlunder (1974) proposed an additional five parameter empirical model known as the Fritz-Schlunder isotherm model, which can be used for a broad field of equilibrium data. The expression of the model is shown below (Hamdaoui and Naffrechoux, 2007).

$$Q_e = \frac{Q_{mFS} K_1 C_e^{m_1}}{1 + K_2 C_e^{m_2}} \quad (34)$$

$(m_1 \text{ and } m_2 \leq 1)$

where Q_{mFS} is the Fritz-Schlunder maximum adsorption capacity (mg/g), K_1 , K_2 , m_1 , and m_2 are the Fritz-Schlunder parameters.

CRITERIA FOR CHOOSING THE OPTIMUM ISOTHERM MODEL

The first and one of the most important conditions for selecting any isotherm model is that there should be a good fit between the experimental data and the isotherm function. Conventionally, the isotherm models are linearized and the parameters obtained from linear regression and the model with the coefficient of determination close to unity is the best fit (Marković et al., 2014). Another common procedure for determining the best-fit model is by using the reduced chi-square statistics technique. The reduced chi-square statistics (< 1) is estimated by dividing the variance of the fit by the average variance of the experimental data. A larger value of the reduced chi-square implies a poor-fitting (Parker, 1995; Al-Ghouti and Da'ana, 2020b). The general procedures are to fit as many relevant models as possible to the experimental data and then selecting the one with the best fit using the methods highlighted above. Secondly, the selected isotherm model should be feasible thermodynamically and for this, Al-Ghouti and Da'ana, (2020b) gave three conditions for an isotherm model to be thermodynamically feasible.

≡ The isotherm model should be linear when the concentration is zero

≡ There should be a finite capacity at maximum concentration and

≡ The gradient of the function should be positive for all concentrations.

RECENT ADVANCES IN THE SELECTION OF OPTIMUM ISOTHERM MODELS

The conventional method of determining the best fit isotherm model involves linearizing the model and then checking for fit using linear regression. The least-squares method has been frequently used for finding the parameters of the models.

However, linearization of the isotherm model violates the least square assumptions and also capable of altering their error structure (Ratkowsky and Giles, 1990). Given the advancement in computer abilities, the nonlinear regression approach has gained popularity in recent time. In this approach, the parameters of the model are obtained through minimization of the quadratic error between experimental data and model outputs of the model (Marković et al., 2014). Coefficient of determination, some of the errors squared, sum of absolute errors, Marquardt's per cent standard deviation, the average relative error and hybrid error function are some of the techniques used in recent times to determine the goodness of fit (Ho, Porter and McKay, 2002; Allen et al., 2003; Ho, 2004; Marković et al., 2014).

CONCLUSION

In this paper, the general concept of sorption, adsorption isotherms has been reviewed and presented. The various types, application and expression of most isotherm models have also be outlined. From the studies, it is clear that several studies have been carried out by researchers, giving rise to several isotherms models applicable in different specific areas. In selecting an appropriate isotherm model for a specific application, it is necessary to ensure that the model fits well and also thermodynamically feasible.

Conventional method modelling isotherm systems involves using a linearized form of an isotherm model of interest to fit experimental data using linear regression techniques. To minimize error in fitting the regression models, nonlinear regression has been employed in recent times.

Performance parameters used in most cases include coefficient of determination, sum of errors squared, and sum of absolute errors, Marquardt's per cent standard deviation, the average relative error and hybrid error function.

References

- [1] Aharoni, C. and Tompkins, F. C. (1970) 'Kinetics of adsorption and desorption and the Elovich equation, in *Advances in catalysis*. Elsevier, pp. 1–49.
- [2] Al-Ghouti, M. A. and Da'ana, D. A. (2020a) 'Guidelines for the use and interpretation of adsorption isotherm models: A review', *Journal of Hazardous Materials*, 393, p. 122383
- [3] Al-Ghouti, M. A. and Da'ana, D. A. (2020b) 'Guidelines for the use and interpretation of adsorption isotherm models: A review', *Journal of hazardous materials*, 393, p. 122383.
- [4] Allen, S. J. et al. (2003) 'Comparison of optimised isotherm models for basic dye adsorption by kudzu', *Bioresource technology*, 88(2), pp. 143–152.
- [5] Ayawei, N., Ebelegi, A. N. and Wankasi, D. (2017) 'Modelling and Interpretation of Adsorption Isotherms', *Journal of Chemistry*, 2017, p. e3039817
- [6] Behbahani, T. J. and Behbahani, Z. J. (2014) 'A New study on Asphaltene Adsorption in Porous Media.', *Petroleum & Coal*, 56(5).
- [7] Buttersack, C. (2019) 'Modeling of type IV and V sigmoidal adsorption isotherms', *Physical Chemistry Chemical Physics*, 21.
- [8] Carrott, P. J. M. (1992) 'Adsorption of water vapour by non-porous carbons', *Carbon*, 30(2), pp. 201–205
- [9] Celebi, O. et al. (2007) 'A radiotracer study of the adsorption behaviour of aqueous Ba²⁺ ions on nanoparticles of zero-valent iron', *Journal of Hazardous Materials*, 148(3), pp. 761–767.
- [10] Davoudinejad, M. and Ghorbanian, S. A. (2013) 'Modeling of adsorption isotherm of benzoic compounds onto GAC and introducing three new isotherm models using the new concept of Adsorption Effective Surface (AES)', *Scientific Research and Essays*, 8(46), pp. 2263–2275.
- [11] Deboer, J. H. (1953) *The dynamical character of adsorption*. LWW.
- [12] Deocaris, C. and Osio, L. (2020) 'Fitting Henry's Adsorption Isotherm model in R using PUPAIM package'.
- [13] El Nemr, A., El-Sikaily, A. and Khaled, A. (2010) 'Modeling of adsorption isotherms of Methylene Blue onto rice husk activated carbon', *Egyptian Journal of Aquatic Research*, 36, pp. 403–425.
- [14] El-Khaiary, M. I. (2008) 'Least-squares regression of adsorption equilibrium data: comparing the options', *Journal of Hazardous Materials*, 158(1), pp. 73–87.
- [15] Erbil, H. Y. (2006) *Surface Chemistry of Solid and Liquid Interfaces*. Wiley
- [16] Fabrizio-Homan, D. J. and Cooper, S. L. (1992) 'A comparison of the adsorption of three adhesive proteins to biomaterial surfaces', *Journal of Biomaterials Science, Polymer Edition*, 3(1), pp. 27–47.
- [17] Febrianto, J. et al. (2009) 'Equilibrium and kinetic studies in adsorption of heavy metals using biosorbent: a summary of recent studies', *Journal of hazardous materials*, 162(2–3), pp. 616–645.
- [18] Foo, K. Y. and Hameed, B. H. (2010) 'Insights into the modelling of adsorption isotherm systems', *Chemical Engineering Journal*, 156(1), pp. 2–10
- [19] Fost, S. D. and Aly, M. O. (1981) *Adsorption Processes for Water Treatment*. Betterworth Publications, Stoneham, Massachusetts, Mass, USA.
- [20] Fritz, W. and Schluender, E.-U. (1974) 'Simultaneous adsorption equilibria of organic solutes in dilute aqueous solutions on activated carbon', *Chemical Engineering Science*, 29(5), pp. 1279–1282.
- [21] Garbuio, F. J., Howard, J. L. and dos Santos, L. M. (2012) 'Impact of Human Activities on Soil Contamination', *Applied and Environmental Soil Science*, 2012, p. e619548
- [22] Gast, A. P. and Adamson, A. W. (1997) *Physical Chemistry of Surfaces*, 6th Edition | Wiley, Wiley.com. Available at: <https://www.wiley.com/en-us/Physical+Chemistry+of+Surfaces%2C+6th+Edition-p-9780471148739> (Accessed: 28 May 2021).
- [23] Gautam, R. K. et al. (2014) 'Biomass-derived biosorbents for metal ions sequestration: Adsorbent modification and activation methods and adsorbent regeneration', *Journal of environmental chemical engineering*, 2(1), pp. 239–259.

- [24] Gautam, R. K. and Chattopadhyaya, M. C. (2016) 'Chapter 5 - Kinetics and Equilibrium Isotherm Modeling: Graphene-Based Nanomaterials for the Removal of Heavy Metals From Water', in Gautam, R. K. and Chattopadhyaya, M. C. (eds) *Nanomaterials for Wastewater Remediation*. Boston: Butterworth-Heinemann, pp. 79–109
- [25] Halsey, G. (1948) 'Physical Adsorption on Non-Uniform Surfaces', *The Journal of Chemical Physics*, 16(10), pp. 931–937
- [26] Hamdaoui, O. and Naffrechoux, E. (2007) 'Modeling of adsorption isotherms of phenol and chlorophenols onto granular activated carbon: Part I. Two-parameter models and equations allowing determination of thermodynamic parameters', *Journal of hazardous materials*, 147(1–2), pp. 381–394.
- [27] Han, R. et al. (2005) 'Equilibrium biosorption isotherm for lead ion on chaff', *Journal of Hazardous Materials*, 125(1–3), pp. 266–271. DOI: 10.1016/j.jhazmat.2005.05.031.
- [28] Harms, H. (2011) '6.09 - Bioavailability and Bioaccessibility as Key Factors in Bioremediation', in Moo-Young, M. (ed.) *Comprehensive Biotechnology (Second Edition)*. Burlington: Academic Press, pp. 83–94
- [29] Hauchhum, S. and Mahanta, P. (2014) 'Carbon dioxide adsorption on zeolites and activated carbon by pressure swing adsorption in a fixed bed', *International Journal of Energy and Environmental Engineering*, 5, pp. 349–356
- [30] Hill, T. L. (1946) 'Statistical mechanics of multimolecular adsorption II. Localized and mobile adsorption and absorption', *The Journal of Chemical Physics*, 14(7), pp. 441–453.
- [31] Hines, A. L., Kuo, S.-L. and Dural, N. H. (1990) 'A New Analytical Isotherm Equation for Adsorption on Heterogeneous Adsorbents', *Separation Science and Technology*, 25(7–8), pp. 869–888
- [32] Ho, Y. S., Porter, J. F. and McKay, G. (2002) 'Equilibrium isotherm studies for the sorption of divalent metal ions onto peat: copper, nickel and lead single component systems', *Water, air, and soil pollution*, 141(1), pp. 1–33.
- [33] Ho, Y.-S. (2004) 'Selection of optimum sorption isotherm', *Carbon*, 42(10), pp. 2115–2116
- [34] Inglezakis, V. J., Pouloupoulos, S. G. and Kazemian, H. (2018) 'Insights into the S-shaped sorption isotherms and their dimensionless forms', *Microporous and Mesoporous Materials*, 272, pp. 166–176.
- [35] Iyer, K. P. D. and Kunju, A. S. (1992) 'Extension of Harkins—Jura adsorption isotherm to solute adsorption', *Colloids and Surfaces*, 63(3), pp. 235–240
- [36] Jeppu, G. and Clement, P. (2012) 'A modified Langmuir-Freundlich isotherm model for simulating pH-dependent adsorption effects', *Journal of contaminant hydrology*, 129–130, pp. 46–53
- [37] Jiang, H. et al. (2019) 'Imaging covalent bond formation by H atom scattering from graphene', *Science*, 364(6438), pp. 379–382.
- [38] Jossens, L. et al. (1978) 'Thermodynamics of multi-solute adsorption from dilute aqueous solutions', *Chemical Engineering Science*, 33(8), pp. 1097–1106.
- [39] Jovanovic, D. S. (1969) 'Physical adsorption of gases. I. Isotherms for monolayer and multilayer adsorption', *Kolloid-Zeitschrift and Zeitschrift Fur Polymere*, 235(1), pp. 1203–+.
- [40] Kadhim, Z. N. (2016) 'Using of Isolated Hydroxyapatite from Sheep Bones to Remove Lead (II) from Aqueous Solution and Studying the Thermodynamics and Adsorption Isotherm', 4, pp. 149–160.
- [41] Karagöz, S. et al. (2008) 'Activated carbons from waste biomass by sulfuric acid activation and their use on methylene blue adsorption', *Bioresource technology*, 99(14), pp. 6214–6222.
- [42] Kausar, A., Bhatti, H. N. and MacKinnon, G. (2013) 'Equilibrium, kinetic and thermodynamic studies on the removal of U (VI) by low-cost agricultural waste', *Colloids and Surfaces B: Biointerfaces*, 111, pp. 124–133.
- [43] Keyes, B. R. and Silcox, G. D. (1994) 'Fundamental study of the thermal desorption of toluene from montmorillonite clay particles', *Environmental science & technology*, 28(5), pp. 840–849.
- [44] Khalid, A. et al. (2015) 'Kinetic & Equilibrium Modelling of Copper Biosorption', *Journal of Faculty of Engineering and Technology*, 22(1), pp. 131–145.
- [45] Kumara, P. S. et al. (2010) 'Adsorption behaviour of Nickel (II) onto cashew nut shell', *Equilibrium, Thermodynamics, Kinetics, Mechanism and Process design. Chemical Engineering Journal*, 1169, pp. 122–131.
- [46] Langmuir, I. (1918) 'The adsorption of gases on plane surfaces of glass, mica and platinum.', *Journal of the American Chemical Society*, 40(9), pp. 1361–1403.
- [47] Liu, J. and Wang, X. (2013) 'Novel Silica-Based Hybrid Adsorbents: Lead(II) Adsorption Isotherms', *TheScientificWorldJournal*, 2013, p. 897159
- [48] Mane, V. S., Mall, I. D. and Srivastava, V. C. (2007) 'Kinetic and equilibrium isotherm studies for the adsorptive removal of Brilliant Green dye from aqueous solution by rice husk ash', *Journal of environmental management*, 84(4), pp. 390–400.
- [49] Marković, D. D. et al. (2014) 'A New Approach in Regression Analysis for Modeling Adsorption Isotherms', *The Scientific World Journal*, 2014, p. e930879
- [50] Miedaner, M. M., Weerasooriya, R. and Tobschall, H. J. (2006) 'Chapter 17 - 1-pK modeling strategies for the adsorption of some trace elements onto gibbsite', in Lützenkirchen, J. (ed.) *Interface Science and Technology*. Elsevier (Surface Complexation Modelling), pp. 469–490
- [51] Murai, S. et al. (1998) 'Removal of phthalic acid esters from aqueous solution by inclusion and adsorption on β -cyclodextrin', *Environmental science & technology*, 32(6), pp. 782–787.
- [52] Nechifor, G. et al. (2015) 'Comparative study of Temkin and Flory-huggins isotherms for adsorption of phosphate anion on membranes', *Sci Bull B [Internet]*, 77(2), pp. 63–72.
- [53] Nworie, F. S. et al. (2019) 'Removal of Methylene Blue From Aqueous Solution Using Activated Rice Husk Biochar: Adsorption Isotherms, Kinetics and Error Analysis', *Journal of the Chilean Chemical Society*, 64(1), pp. 4365–4376
- [54] Ocampo, R. et al. (2013) 'Role of pore volume and surface diffusion in the adsorption of aromatic compounds on activated carbon', *Adsorption*, 19.

- [55] Ojediran, J. et al. (2019) 'Modeling of Biosorption of Pb(II) and Zn(II) Ions Onto Pamrh: Langmuir, Freundlich, Temkin, Dubinin-Raduskevich, Jovanovic, Flory-Huggins, Fowler-Guggenheim And Kiselev Comparative Isotherm Studies'.
- [56] Olsen, S. R. and Watanabe, F. S. (1957) 'A method to determine a phosphorus adsorption maximum of soils as measured by the Langmuir isotherm', *Soil Science Society of America Journal*, 21(2), pp. 144–149.
- [57] Panahi, R., Vasheghani-Farahani, E. and Shojosadati, S. A. (2008) 'Determination of adsorption isotherm for l-lysine imprinted polymer', *Iranian Journal of Chemical Engineering*, 5(4), pp. 49–55.
- [58] Parker, G. R. (1995) 'Optimum isotherm equation and thermodynamic interpretation for aqueous 1, 1, 2-trichloroethene adsorption isotherms on three adsorbents', *Adsorption*, 1(2), pp. 113–132.
- [59] Petrovic, M., Radjenovic, J. and Barcelo, D. (2011) 'Advanced oxidation processes (AOPs) applied for wastewater and drinking water treatment. Elimination of pharmaceuticals', *The holistic approach to Environment*, 1(2), pp. 63–74.
- [60] Piccin, J. S., Dotto, G. L. and Pinto, L. A. A. (2011) 'Adsorption isotherms and thermochemical data of FD&C Red n° 40 bindings by Chitosan', *Brazilian Journal of Chemical Engineering*, 28(2), pp. 295–304
- [61] Pignatello, J. J. and Xing, B. (1995) 'Mechanisms of slow sorption of organic chemicals to natural particles', *Environmental science & technology*, 30(1), pp. 1–11.
- [62] Prasad, R. K. and Srivastava, S. N. (2009) 'Sorption of distillery spent wash onto fly ash: kinetics and mass transfer studies', *Chemical Engineering Journal*, 146(1), pp. 90–97.
- [63] Qi, Y. et al. (2017) 'Sorption of Cu by humic acid from the decomposition of rice straw in the absence and presence of clay minerals', *Journal of Environmental Management*, 200, pp. 304–311
- [64] Ramadoss, R. and Subramaniam, D. (2018) 'Adsorption of chromium using blue-green algae-Modeling and application of various isotherms', *International Journal of Chemical Technology*, 10, pp. 1–22.
- [65] Ratkowsky, D. A. and Giles, D. E. (1990) *Handbook of nonlinear regression models*. M. Dekker New York.
- [66] Rau, I. et al. (2003) 'Modelling the arsenic (V) and (III) adsorption', *Czechoslovak Journal of Physics*, 53(1), pp. A549–A556.
- [67] Redlich, O. and Peterson, D. L. (1959) 'A useful adsorption isotherm', *Journal of physical chemistry*, 63(6), pp. 1024–1024.
- [68] Rudzinski, W. and Wojciechowski, B. W. (1977) 'On the Jovanovic model of adsorption', *Colloid and Polymer Science*, 255(11), pp. 1086–1097
- [69] Sampranpiboon, P., Charnkeitkong, P. and Feng, X. (2014) 'Equilibrium isotherm models for the adsorption of zinc (II) ion from aqueous solution on pulp waste', *WSEAS Transactions on Environment and Development*, 10, pp. 35–47.
- [70] Sims, R. A., Harmer, S. L. and Quinton, J. S. (2019) 'The Role of Physisorption and Chemisorption in the Oscillatory Adsorption of Organosilanes on Aluminium Oxide', *Polymers*, 11(3), p. 410
- [71] Sing, K. S. W. (1982) 'Reporting physisorption data for gas/solid systems with special reference to the determination of surface area and porosity (Provisional)', *Pure and applied chemistry*, 54(11), pp. 2201–2218.
- [72] Singh, A. K. (2016) 'Chapter 8 - Nanoparticle Ecotoxicology', in Singh, A. K. (ed.) *Engineered Nanoparticles*. Boston: Academic Press, pp. 343–450
- [73] Singha, B. and Das, S. K. (2013) 'Adsorptive removal of Cu (II) from aqueous solution and industrial effluent using natural/agricultural wastes', *Colloids and Surfaces B: Biointerfaces*, 107, pp. 97–106.
- [74] Sips, R. (1948) 'On the structure of a catalyst surface', *The journal of chemical physics*, 16(5), pp. 490–495.
- [75] Song, C. et al. (2014) 'Adsorption studies of coconut shell carbons prepared by KOH activation for removal of lead (II) from aqueous solutions', *Sustainability*, 6(1), pp. 86–98.
- [76] Sultan, M., Miyazaki, T. and Koyama, S. (2018) 'Optimization of adsorption isotherm types for desiccant air-conditioning applications', *Renewable Energy*, 121, pp. 441–450
- [77] Tadros, T. (2013) 'Adsorption Isotherm', *Encyclopedia of Colloid and Interface Science*. Edited by T. Tadros. Berlin, Heidelberg: Springer Berlin Heidelberg
- [78] Theivarasu, C. and Mysamy, S. (2011) 'Removal of malachite green from aqueous solution by activated carbon developed from cocoa (Theobroma Cacao) shell-A kinetic and equilibrium studies', *E-Journal of Chemistry*, 8(S1), pp. S363–S371.
- [79] Tornquist, A. et al. (1978) 'The Hill-de Boer equation in the adsorption of water on quartz', *Journal of Colloid and Interface Science*, 66(3), pp. 415–420
- [80] Tóth, J., Berger, F. and Dékány, I. (1999) 'Separation of the first adsorbed layer from others and calculation of the BET compatible surface area from Type II isotherms', *Journal of colloid and interface science*, 212(2), pp. 411–418.
- [81] Umpleby, R. et al. (2001) 'Application of the Freundlich adsorption isotherm in the characterization of molecularly imprinted polymers', *Analytica Chimica Acta*, 435, pp. 35–42
- [82] Vijayaraghavan, K. et al. (2006) 'Biosorption of nickel (II) ions onto Sargassum wightii: application of two-parameter and three-parameter isotherm models', *Journal of hazardous materials*, 133(1–3), pp. 304–308.
- [83] Wang, G. et al. (2020) 'Gaseous adsorption of hexamethyldisiloxane on carbons: Isotherms, isosteric heats and kinetics', *Chemosphere*, 247, p. 125862.
- [84] Wang, J. and Guo, X. (2020) 'Adsorption isotherm models: Classification, physical meaning, application and solving method', *Chemosphere*, 258, p. 127279
- [85] Wang, Z. et al. (2016) 'Analyzing the adaption of different adsorption models for describing the shale gas adsorption law', *Chemical Engineering & Technology*, 39(10), pp. 1921–1932.
- [86] Weber Jr, W. J. and Morris, J. C. (1963) 'Kinetics of adsorption on carbon from solution', *Journal of the sanitary engineering division*, 89(2), pp. 31–59.
- [87] Wikipedia (2021) 'Henry adsorption constant', Wikipedia. Available at: https://en.wikipedia.org/w/index.php?title=Henry_adsorp

- tion_constant&oldid=998548677 (Accessed: 28 May 2021).
- [88] Wu, Y. (2017) 'Chapter 16 - The Removal of Methyl Orange by Periphytic Biofilms: Equilibrium and Kinetic Modeling', in Wu, Y. (ed.) Periphyton. Boston: Elsevier, pp. 367–387
- [89] Yan, X.-F. et al. (2017) 'An adsorption isotherm model for adsorption performance of silver-loaded activated carbon', Thermal Science, 21(4), pp. 1645–1649.
- [90] Yaneva, Z., Koumanova, B. and Georgieva, N. (2013) 'Linear and Nonlinear Regression Methods for Equilibrium Modelling of p-Nitrophenol Biosorption by Rhizopus Oryzae - Comparison of Error Analysis Criteria', E-Journal of Chemistry, 2013
- [91] Zhou, L. et al. (2002) 'Adsorption of Nitrogen on Silica Gel Over a Large Range of Temperatures', Adsorption, 8, pp. 79–87.



ISSN: 2067-3809

copyright © University POLITEHNICA Timisoara,
Faculty of Engineering Hunedoara,
5, Revolutiei, 331128, Hunedoara, ROMANIA
<http://acta.fih.upt.ro>

COMPUTER SOFTWARE FOR INTERACTIVE DESIGN OF CNC MACHINE TOOLS MAIN SPINDLE DRIVES

¹ Ss. Cyril and Methodius University in Skopje, Faculty of Mechanical Engineering, Skopje, NORTH MACEDONIA

Abstract: The object of this paper is to present the investigation of principles for analysis and design of CNC machine tool main spindle drives. Main spindle drives analysis and design are very seldom presented in the literature. Characteristics of CNC machine tools main spindle drives highly depends upon skillfulness of composing motors and mechanical transmission elements. This paper gives short description of an originally developed computer software which enables interactive design of main spindle drives for CNC machine tools and analysis of different design variants.

Keywords: interactive design, CNC machine tools, main spindle drives

INTRODUCTION

The object of this paper is to present the investigation of principles for analysis and design of CNC machine tool main spindle drives. Main spindle drives analysis and design are very seldom presented in the literature.

Contemporary development in machine tools is connected with improvements in drive systems [1,2,3,4]. A special characteristic of CNC machine tool drives is application of variable speed (AC or DC) motors which provide continuous changing of cutting speeds [4,5,6].

Application of variable speed motors created a question of their appropriate composing with mechanical transmission elements in order to get better output characteristics of the main spindle [2,4,7,8].

CHARACTERISTICS OF THE MAIN SPINDLE DRIVES FOR CNC MACHINE TOOLS

Main spindle drives for CNC machine tools must provide constant power at wide range of speeds on the output of the main spindle. They consist of three parts: 1. variable speed motor, 2. mechanical transmission elements which provide appropriate output characteristics of the main spindle and 3 main spindle [2,4,7,8].

Usually mechanical transmission elements consist of: belt transmission or combination of belt transmission with gearbox (with two, three or four speeds) [2,4,7,8,9].

Intensive development of quality tool materials enable using of very high cutting speeds and power.

Necessary output power on the main spindle can be calculated as:

$$P = \frac{F_t \cdot v}{60 \cdot 10^3} \quad [\text{kW}] \quad (1)$$

where:

F_t -tangential cutting force component [N];

v -cutting speed [m/min].

CNC machine tools are used for production of workpieces with different shapes, dimensions and materials, with wide range of cutting data [2,6,7,9,10].

For ensuring these requirements the speeds on the main spindle must be regulated in very wide range [2,4,6,7,8],

$$R_{ms} = \frac{n_{max}}{n_{min}} = \frac{v_{max}}{v_{min}} \cdot \frac{D_{max}}{D_{min}} = R_v \cdot R_d \quad (2)$$

where:

R_{ms} -range of regulation of output main spindle speeds;

R_v -range of regulation of cutting speeds;

R_d -range of diameters of the parts, or of the cutting tools;

n_{max} , n_{min} -maximal and minimal main spindle speed;

v_{max} , v_{min} -maximal and minimal cutting speed;

D_{max} , D_{min} -maximal and minimal diameters of the parts or the cutting tools.

According to our empirical investigation the range of regulation of main spindle speeds for CNC machine tools usually is within $R_{ms}=20-350$ (exclusively rare to 600). Such kind of wide regulation of main spindle speeds needs particular attention in selection of variable speed motors and mechanical transmission elements.

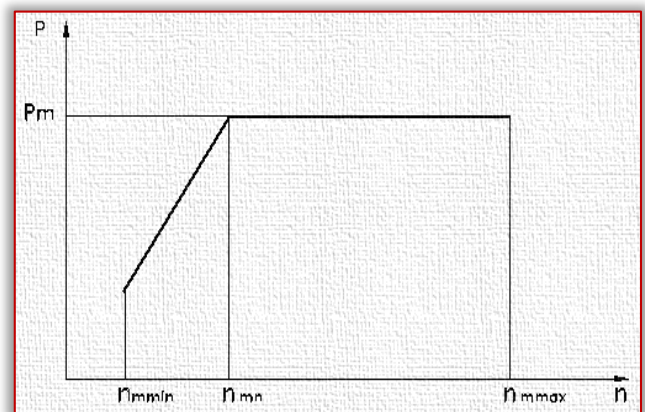


Figure 1. Power-speed diagram of variable speed AC motor

Figure 1 presents power-speed diagram of variable speed motor, where n_{min} , n_{mn} and n_{mmax} are minimal, nominal and maximal speed of the motor, and P_m is nominal power of the variable speed motor.

Usually range of regulation of speed at constant power of variable speed motors is (2-8) (sometimes reaches values 12-16), which is far below required range $R_{ms} = 20-350$.

The overall range of regulation of output main spindle speeds can be calculated as:

$$R_{ms} = R_{msm} \cdot R_{msp}, \quad (3)$$

where:

$R_{msm}=2-50$ -range of regulation of main spindle speeds at constant torque;

$R_{msp}=2-45$ (exclusively rare 70)-range of regulation of main spindle speeds at constant power.

There are two alternative methods of obtaining wide range of main spindle speeds at constant power: overrating of the AC or DC motor or combining the motor with gearbox with two, three or four speeds [4,7,8,11].

The second solution with two, three or four speed gearbox is widely used at the CNC machine tools.

Selecting the number of steps Z of the gearbox is in the range of regulation of the variable speed motor with constant power R_{mp} , while with using the range of variable speed motor with constant torque $R_{mm} = R_{msm}$, the whole range of regulation of output speeds of the main spindle is obtained [7,8,11].

Because of that, we can write:

$$R_{msp} = R_{mp} \cdot R_z \quad (4)$$

where:

R_{mp} -range of regulation of variable speed motor with constant power;

R_z -range of regulation of the gearbox.

Variable speed motor can be treated as a particular group of gearbox with continuous changing speeds, which is first in the kinematic chain, with infinitely large number of transmissions, with transmission ratios which obtain geometrical progression with progression ratio $\phi \rightarrow 1$ and range R_{mp} .

Gearbox can be treated as a transmission group which extends the speed range of the motor at constant power. Because of that characteristic of a transmission group ϕ_z is:

$$\phi_z = R_{mp} \cdot \phi \quad (5)$$

Because $\phi \rightarrow 1$, we obtain

$$\phi_z = R_{mp} \quad (6)$$

As,

$$R_z = \phi_z^{(z-1)} \quad (7)$$

we can write

$$R_z = R_{mp}^{(z-1)} \quad (8)$$

With the substitution equation (8) in (4), we get

$$R_{msp} = mp \cdot R_{mp}^{(z-1)} = R_{mp}^z \quad (9)$$

where: Z -number of speeds of the gearbox.

With known R_{msp} and R_{mp} , using the equation (9), we can calculate the necessary number of speeds of the gearbox ZE :

$$ZE = \frac{\log R_{msp}}{\log R_{mp}} \quad (10)$$

The equation (10) is recommended also in the literature [7,8,11].

Because ZE is usually a decimal number, it is round to the nearest full number.

If $Z > ZE$ we get characteristic with overlapping speeds (Figure 2a). In case $Z < ZE$ we get characteristic with step decrease of the power ΔP (Figure 2b).

For example, if from equation (10) we get $ZE=2.5$, than Z can be 2 or 3. In case of $Z=3$ we get $P-n$ characteristic as in the

Figure 2a, and if is accepted $Z=2$ we obtain characteristic as in the Figure 2b.

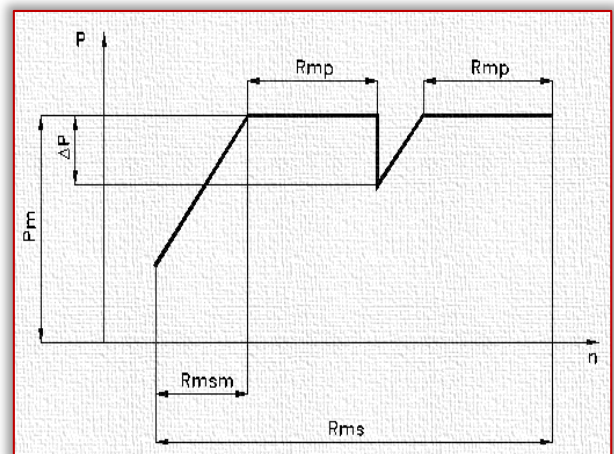
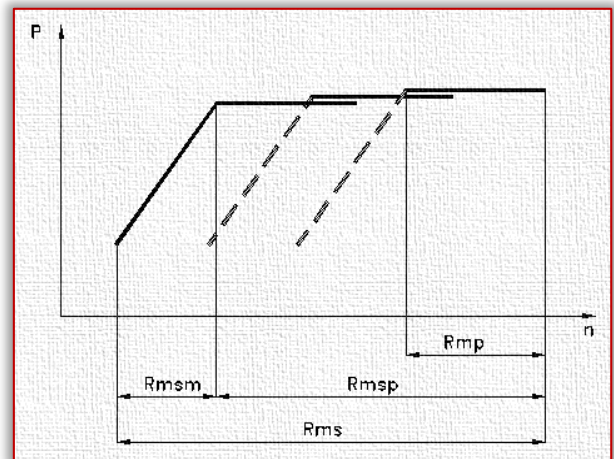


Figure 2. Diagram $P-n$ of the main spindle
a) with $Z=3$ and b) with $Z=2$

Percentual decrease of the power ΔP in relation with the nominal power P_m of the motor, when $Z < ZE$ can be calculated with the equation (11),

$$\frac{\Delta P}{P_m} = \left(1 - R_{mp} \cdot z^{-1} \sqrt{R_{mp} / R_{msp}}\right) 100 [\%] \quad (11)$$

Usually $\Delta P/P_m$ should not be greater than 30% [7,8,11].

DESCRIPTION OF COMPUTER SOFTWARE FOR DESIGNING MAIN SPINDLE DRIVES

Theoretical considerations mentioned in previous chapter are implemented in the computer software. An original computer software for interactive design of main spindle drives and analysis of different design variants was created for PC in C++ language [12].

Flow chart of the computer software is given on Figure 3.

The software begins with input of tangential cutting force component F_t and cutting speed v . They are necessary for calculation of required power. There is a possibility to enter directly required power for particular size of CNC machine tool based on recommendations implemented in the computer software. Recommendations are result of the empirical investigations of main spindle drives of CNC machine tools. More than 3000 different CNC machine tools were investigated and appropriate recommendations were derived.

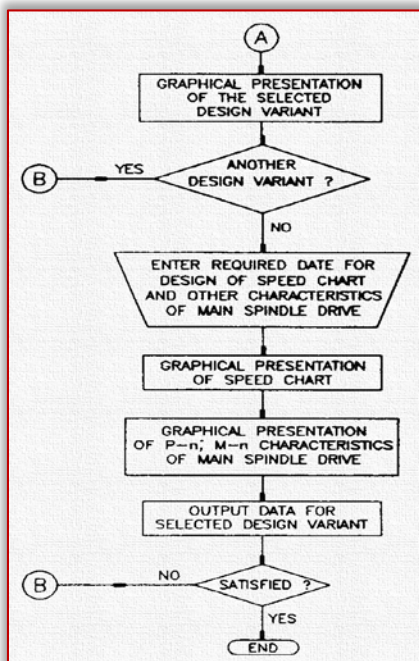
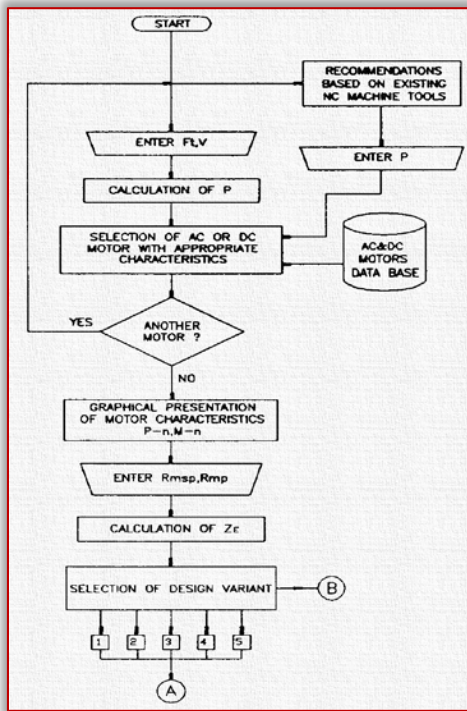


Figure 3. Flow-chart of the computer software

In the next step, the computer software selects variable speed motor from the AC and DC motor database. For the selected motor the program draw power-speed (P-n) diagram and torque-speed (M-n) diagram. The P-n and M-n diagram are shown on Figure 4.

The next step requires input of Rmsp-range of regulation of main spindle speeds at constant power and Rmp-range of regulation of the variable speed motor with constant power. This is necessary for calculation of number of speeds of the gearbox ZE.

Then the computer software gives opportunity of selection one of the most usually used design variants of main spindle drives for CNC machine tools: 1. motor-belt-main spindle, 2.

motor-planetary gearbox-belt-main spindle, 3. motor-belt-gearbox-main spindle, 4. motor-belt-gearbox-belt-main spindle, 5. motor-belt-reducer-main spindle. After selection of particular design variant its graphical presentation is shown (Figure 5).

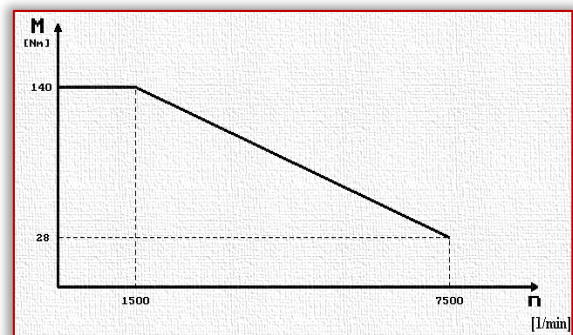
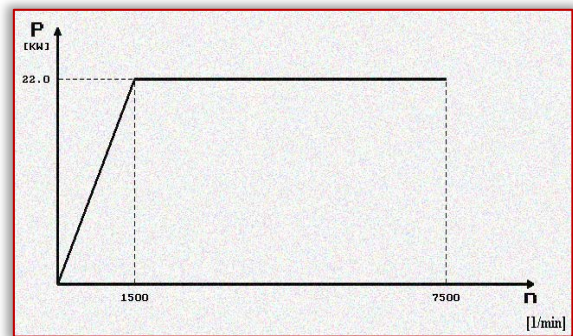


Figure 4. P-n and M-n diagram for the selected variable speed motor

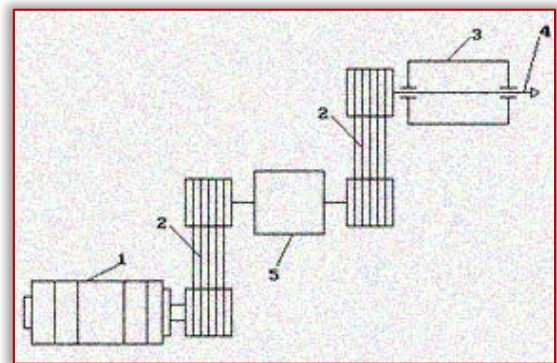


Figure 5. Graphical presentation of design variant motor-belt-gearbox-belt-main spindle:
1.variable speed motor, 2.belt transmission, 3.spindle unit, 4.main spindle, 5.gearbox (z=2,3 or 4)

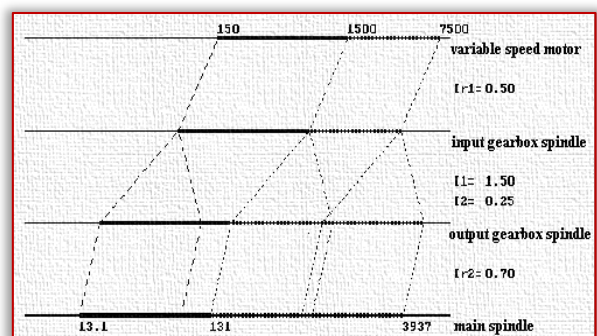


Figure 6. Speed chart for the selected design variant motor-belt-gearbox (Z=2)-belt-main spindle

In the next step elements for drawing speed chart (transmission ratios in the gearbox, transmission ratio(s) of the belt transmission(s) etc.) are required.

Follows graphical presentation of speed chart (Figure 6), power-speed (P-n) and torque-speed (M-n) diagrams (Figure 7) and textual presentation of the output data for selected design variant (Figure 8).

If we are not satisfied with output data, we can select another design variant.

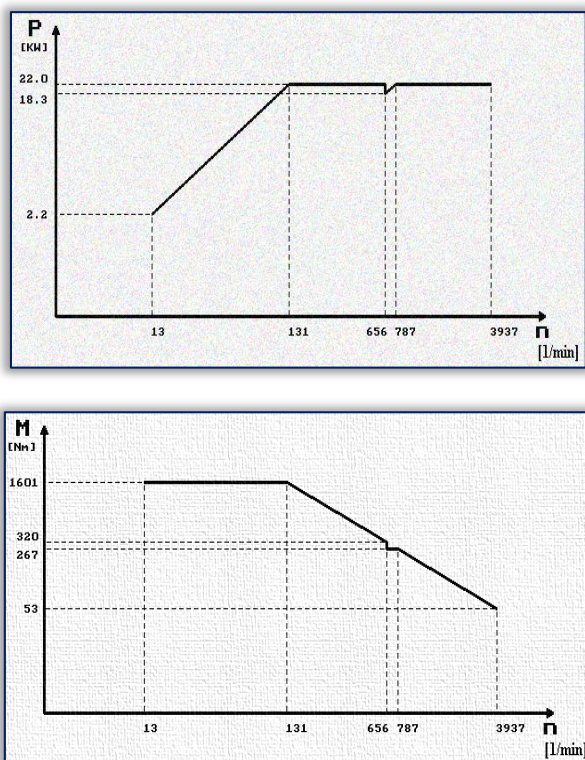


Figure 7. P-n and M-n diagram of the main spindle

| |
|---|
| motor-belt-gearbox (Z=2)-belt-main spindle |
| Nmin-minimal main spindle speed, Nmin=13.1 [1/min] |
| Nmax-maximal main spindle speed, Nmax=3937 [1/min] |
| P-maximal main spindle power, P=22 [KW] |
| Pmin-minimal main spindle power, Pmin=2 [KW] |
| Mmax-maximal main spindle torque, Mmax=1601 [Nm] |
| Mmin-minimal main spindle torque, Mmin=53 [Nm] |
| Rms-range of regulation of the main spindle, Rms =300.00 |
| Rmsp-range of regulation of the main spindle at constant power, Rmsp=30.00 |
| Rmsm-range of regulation of the main spindle at constant torque, Rmsm=10.00 |

Figure 8. Output data for the main spindle design variant

CONCLUSION

Characteristics of main spindle drives for CNC machine tools directly depend upon skillfulness of composing variable speed motors and mechanical transmission elements. The presented computer software enables interactive design and analysis of different variants, reduces

the design time and modernizes design process of main spindle drives.

References

- [1] H. Cao, X. Zhang, X. Chen: The concept and progress of intelligent spindles: A review, International Journal of Machine Tools & Manufacture, Vol. 112, 2017, pp. 21–52
- [2] L.N. López de Lacalle, A. Lamikiz, (Editors): Machine Tools for High Performance Machining, Springer-Verlag London Limited, 2009
- [3] C. Brecher, M. Weck: Werkzeugmaschinen Fertigungssysteme 2: Konstruktion, Berechnung und messtechnische Beurteilung, Springer, 2017,
- [4] M. Osamu: Expert spindle design system, MSc Thesis, University of British Columbia, 2003
- [5] E. Abele, Y. Altintas C. Brecher: Machine tool spindle units, CIRP Annals - Manufacturing Technology, Vol. 59, 2010, pp. 781–802
- [6] P.H. Joshi: Machine Tools Handbook: Design And Operation, McGraw-Hill Education, 2015
- [7] N. K. Mehta: Machine Tool Design and Numerical Control, Third Edition, Tata McGraw Hill Education Private Limited, New Delhi, 2012
- [8] V. Dukovski, Lj. Dudeski: Design of machine tools, Second Edition, Publisher-Ss. Cyril and Methodius University in Skopje, 2003 (in Macedonian)
- [9] S. Y. Liang, A. J. Shih, Analysis of Machining and Machine Tools, Springer, 2016
- [10] H. A. Youssef, H. El-Hofy: Machining Technology: Machine Tools and Operations, CRC Press Taylor & Francis Group, 2008
- [11] V. E. Push: Machine tools, Machinostroenie, Moscow, 1986 (In Russian)
- [12] B. Stroustrup: The C++ Programming Language, 4th Edition, Addison-Wesley Professional, 2013



ISSN: 2067-3809

copyright © University POLITEHNICA Timisoara,
Faculty of Engineering Hunedoara,
5, Revolutiei, 331128, Hunedoara, ROMANIA
<http://acta.fih.upt.ro>

¹Abhishek Kumar MEENA, ²Abhishek VAISHNAV, ³Akshat GOVIL,
⁴Ekta SHARMA, ⁵Mohd. IMRAN

VEHICLE NUMBER PLATE RECOGNITION SYSTEM USING MATLAB: A HISTOGRAM BASED APPROACH

¹⁻⁵Swami Keshvanand Institute of Technology, Management and Gramothan - [SKIT], Jaipur, INDIA

Abstract: Vehicle number plate recognition technique is used for extracting an area of number plate from captured vehicle image. We use this technique because as we know there is highly increase in number of vehicles all over the world and it keeps increasing. So for the purpose of law enforcement and traffic management it become difficult to track each and every single vehicle so to overcome this, we need this type of technique. This system is very helpful for traffic police in order to find the details of a vehicle violating the traffic rules. This technique is used for various applications such as automatic toll collection, Border crossings, parking system, Traffic control, stolen cars tracking etc. The technique used in this paper is a histogram based approach which has advantage of simple and fast response as compare to other techniques. In this paper we use various algorithms from distinct edge detection to region of interest extraction.

Keywords: vehicle number plate, region of interest, Red Green Blue

INTRODUCTION

With rising number of vehicles on roads, it is getting very difficult to manually handle laws, traffic rules and regulations for smooth traffic moment. Identify VNP quickly is beneficial for many businesses and organizations for a variety of applications such as traffic management, automatic payment systems for car parking, stolen cars, security and crime detection.

A VNP recognition System is a mass surveillance method that uses character recognition on images in order to read vehicle registration plates in the form of segmented characters. This technique also helps to get the correct result compared to manually one. The main focus of this method is the detection of the region of interest and the identification of the number plate. This whole algorithm work step wise. First VNP image is captured by camera after that image is converted into grey scale for preprocessing.

Once grey scaling is done than dilation process start. Dilation help in reducing the noise and add pixels at the boundary of image. After dilation, horizontal and vertical edge processing has been done and passed these histograms through low pass filters. Low pass filter help in reducing the unwanted region or unwanted noise from the image. After this filtering in fifth stage, image will segment, and ROI has extracted. The advantage of this approach is success full recognition of a moving vehicle.

METHODOLOGY

Methodology is shown in flowchart for detection and extraction of plate.

— Input raw image/ Image Acquisition

In this first step, an image is captured by camera at some fixed angle and taken as an input in RGB form. The quality of image depend on various factors like lighting condition, quality of camera, distance and also size of the vehicle. For a better result, quality of image should be sharp or at high resolution.

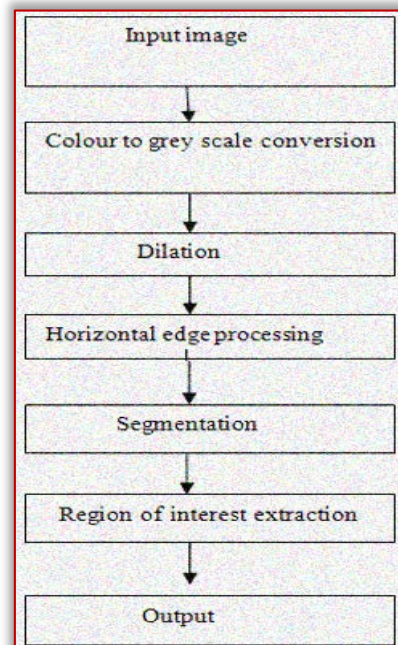


Figure 1: Recognition algorithm of VNP

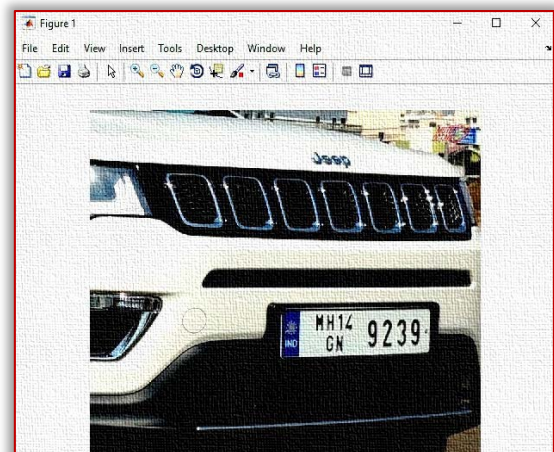


Figure 2: Input image

— Gray scaling of image

This algorithm is independent of the type of colours. In this step coloured RGB image is converted into the Gray scale image in order to reduce colours. Also it help to reduce noise to some extent. So, if the input image is a colored image represented by 3-dimensional array in MATLAB, it is converted to a 2-dimensional gray image before further processing.

— Dilation

Dilation is a process of improving the quality of an image by filling holes, adding pixels and joining the broken lines for sharpening the boundary of an image and it also help for increasing brightness. By the help of dilation, unwanted noise is reduced at large extent. By making the edges sharper, the difference of gray Dilation is a process of improving the quality of an image by filling holes, adding pixels and joining the broken lines for sharpening the boundary of an image and it also help for increasing brightness. By the help of dilation, unwanted noise is reduced at large extent. By making the edges sharper, the difference of gray value between neighbouring pixels at the edge of an object can be increased. This enhances the edge detection. Also the process of dilation help to nullify losses which occur during grey scaling.

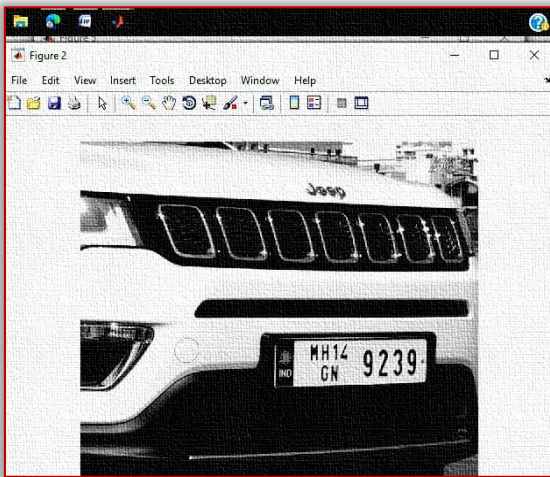


Figure 3: Gray scale image

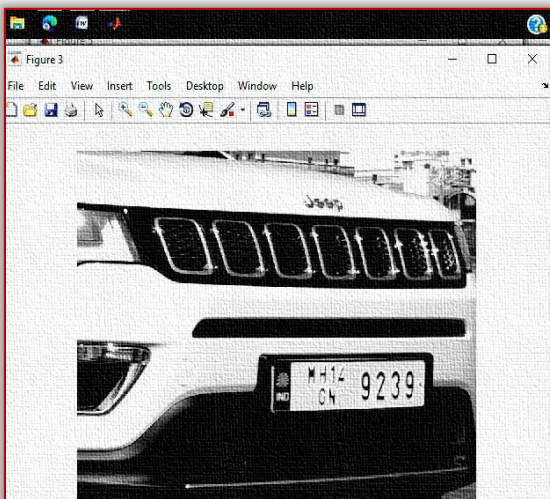


Figure 4: Dilated image

— Horizontal and Vertical Edge Processing

In this step, the dilated image from the previous step passes through successive edge processing techniques which are horizontal and vertical edge processing. These histograms represent the sum of differences of gray values between neighbouring pixels of an image, column-wise and row-wise. First we perform horizontal edge processing to get horizontal histogram. In this algorithm, it moves from each column of the image and work from second pixel from the top of image to get difference between first and second pixel. Similarly, this algorithm moves downward and calculate the difference between second and third pixel and so on. At the end, an array containing column wise is created. The similar process is carried out to find the vertical histogram. In this case, rows are processed instead of columns.

≡ Passing histograms through low pass filter

In the figures number 5 and figure number 6 shown below, we can clearly understood that the histogram values varies drastically between consecutive columns and rows. So, In order to prevent loss of important information in further steps, it is suitable to smooth out such drastic changes in values of histogram. For the smoothing, the histogram is passed through a low-pass digital filter. This step is performed by considering the right and left hand side values. This step is performed on both the horizontal histogram as well as the vertical histogram. Below figures number 5 and 6 shows the histogram before passing through a low-pass digital filter and after passing through a low-pass digital filter.

≡ Filtering out Unwanted Areas in Image

After passing the histograms through low pass filter, the unwanted region is removed from the image using another filter. The rows and columns with low histogram values are considered as unwanted regions. Because lower histogram values show very less variation with their neighbouring pixels. Since the region of VNP contain high variation of pixels therefore histogram with lower values not required. So, in this process it contain high probability of region containing number plate.

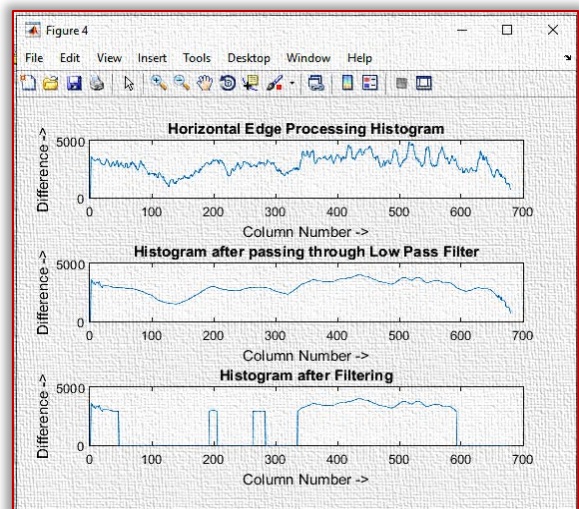


Figure 5: Horizontal Edge Processing Histogram

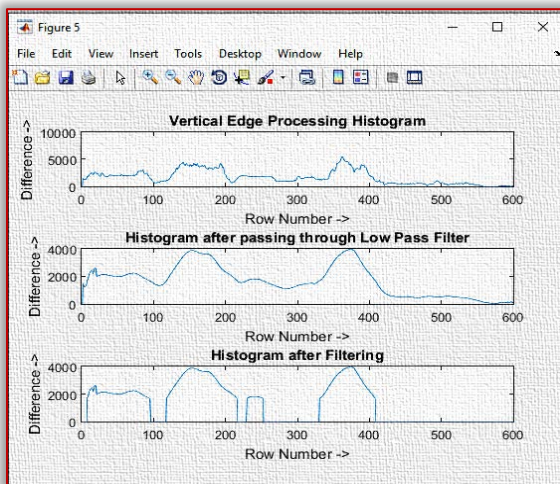


Figure 6: Vertical Edge Processing Histogram

— Segmentation of Region of Interest

In this step we find all the regions in an image that has high probability of containing a license plate. The below figure 7 shows the regions having most possibility of license plate.

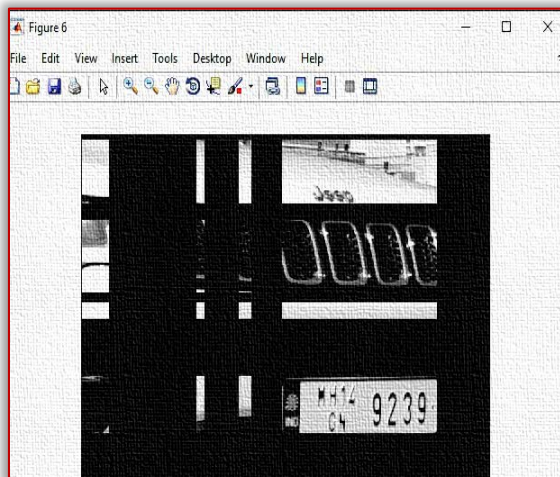


Figure 7: Segmented image

A. Extraction of region of interest

After the segmentation process, the region with maximum histogram value is taken as the most probable region for number plate. All areas are processed in rows and columns to find a common area with maximum values of the horizontal and vertical histogram. Below figure number 8 shows the output of ROI.

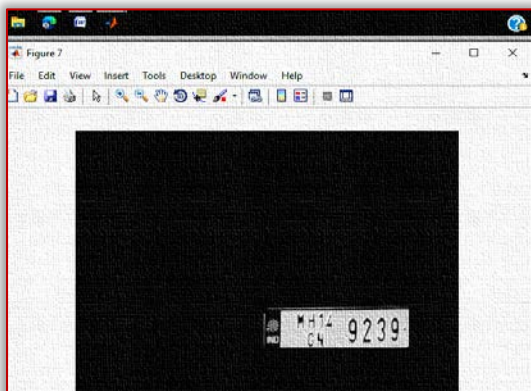


Figure 8: Final output showing VNP

CONCLUSION

In our work, we have successfully implemented vehicle number plate recognition technique. And our algorithm is successfully detect the number plate region from the image which consists vehicle number. We have applied this algorithm on many images and found that it successfully recognise the plate. The designed system can help to overcome the drawbacks of the manual system of vehicle plate identification. By optimizing various parameters further improvement can be achieved in the accuracy of the designed system.

References

- [1] Manisha Rathore and Saroj Kumari, "Tracking number plate from vehicle using matlab", International Journal in Foundations of Computer Science & Technology (IJFCST), Vol.4, No.3, May 2014.
- [2] Hana Demma and Dr. Mandeep Kaur, "Automatic Ethiopian Vehicle Number Plate Detection System using MATLAB", International Journal of Engineering Research & Technology (IJERT), ISSN: 2278-0181, Vol. 8 Issue 06, June-2019.
- [3] M. K. B. Ashan and N. G. J. Dias, "Recognition of vehicle license plates using Matlab", European International Journal of Science and Technology, Vol. 5, No. 6, August, 2016.
- [4] Dipayan Mitra and Soumit Banerjee, "Automatic Number Plate Recognition System: A Histogram Based Approach", IOSR Journal of Electrical and Electronics Engineering (IOSR-JEEE) Volume 11, Issue 1 Ver. IV (Jan. – Feb. 2016), PP 26-32.
- [5] Divyang Goswami and Mrs. Rama Gaur, "Automatic License Plate Recognition System using Histogram Graph Algorithm", International Journal on Recent and Innovation Trends in Computing and Communication ISSN: 2321-8169, Volume: 2 Issue: 11, 3521 – 3527.



ISSN: 2067-3809

copyright © University POLITEHNICA Timisoara,
Faculty of Engineering Hunedoara,
5, Revolutiei, 331128, Hunedoara, ROMANIA
<http://acta.fih.upt.ro>

Fascicule 4

[October – December]

t o m e

XIV

[2021]

ACTA Technica CORVINIENSIS
BULLETIN OF ENGINEERING



ISSN: 2067-3809

copyright © University POLITEHNICA Timisoara,
Faculty of Engineering Hunedoara,
5, Revolutiei, 331128, Hunedoara, ROMANIA
<http://acta.fih.upt.ro>

¹ Suleiman I. SALAWU, ² A.M. SALIU

CHARACTERIZATION AND BENEFICIATION OF OBAJANA IRON ORE, KOGI STATE, NIGERIA

¹Department of Mechanical Engineering, Kogi State Polytechnic, Itakpe, NIGERIA

²Department of Metallurgical and Materials Engineering, Kogi State Polytechnic Itakpe, NIGERIA

Abstract: The ore sample was sourced from Obajana (oyo) village, Lokoja Local Government Area of Kogi State. Characterization of Obajana iron ore deposit, Kogi State, Nigeria was carried out using XRF, XRD, SEM and petrological microscope. The XRF result revealed that the ore contained 0.38%P, 15.91K, 2.48%Ca, 39.24%Fe, 1.02%Mg, 3.54%Al and 25.56%Si. The XRD result revealed that the mineral phases of the ore as Quartz (SiO_2), Hematite (Fe_2O_3) and Biotite $\text{K}(\text{Mg},\text{Fe})_3\text{AlSi}_3\text{O}_{10}(\text{OH})_2$ which are also the major minerals phases. The SEM and petrographic examination revealed that the ore matrix is an assemblage of inter-layered different minerals crystals with different shapes, sizes and angles of orientations and separated by grain boundaries. Low intensity magnetic separator was used to separate the ore into concentrate and tailing. Both the concentrate and tailing were weighed and analyzed using XRF machine

Keywords: Chemical, Mineralogical, Characterization, Beneficiation, Obajana iron ore

INTRODUCTION

Nigeria has the potentials of becoming a regional economy hub in the West African sub-region, but the economy of the country cannot be strong and vibrant without growth in its iron and steel sector or without the use of iron and steel in the manufacturing sector among others (Agbu, 2007).

Iron is the major component in steel production; usually over 90 percent, at present there is no satisfactory substitute for steel even in modern industrialized societies, the supply of iron will therefore remain an important fundament to industrial development in the twenty-first century (Jens and Nicolas, 2003). The most commonly used iron minerals include; hematite, Fe_2O_3 (70% Fe); magnetite, Fe_3O_4 (72% Fe) and of much less importance: limonite, $\text{Fe}_2\text{O}_3 \cdot 3\text{H}_2\text{O}$ (60% Fe); siderite, FeCO_3 (48.3% Fe); and pyrite, FeS_2 (46.6% Fe) (Biswas, 2005).

Characterization of iron ore is a very important step required before beneficiation and iron production takes place. In this procedure, the quantity, grade or quality, densities, shape, and physical characteristics are determined to allow for appropriate application of technical and economic parameters to support production planning and evaluation of the economic viability of deposits (John *et al.*, 2015). Iron ore deposits have not been fully explored and exploited in Nigeria and if fully exploited can serve as foreign exchange for the country (Danmola and Abba, 2013).

Agbado Okudu iron ore deposit has been worked on by Agava (2006). Who reported that the iron ore contained, on the average, total iron content of 38.82% and mineralogical analysis revealed that the iron bearing minerals are predominantly magnetite and haematite.

Agava *et al.* (2016) determined the chemical, mineralogical and liberation size of Ochokochoko iron ore. They reported that the ore is predominantly magnetite, hematite, calcite, alumina, and silica, they also reported that the ore can be classified as medium grade and liberated at $-180+125 \mu\text{m}$ sieve size. Salawu (2015) investigated the chemical and

mineralogical characterization of Gujeni iron ore deposit Kaduna State, Nigeria and the findings showed that the ore contained majorly hematite, goethite, rutile while, manganese oxide, zincite, zirconium and silicate minerals were present in minor quantities. Table 1 shows the iron ore deposits in Nigeria

EXPERIMENTAL PROCEDURE

— Materials collection, equipment and preparation

The outcropped iron ore samples that were characterised in this study were collected from Obajana (oyo) village about 5km from Obajana cement company ($7^\circ 45' \text{N}$ and $6^\circ 67' \text{N}$) shown in figure 1 and equipment used in this research were Laboratory sledge hammer, Jaw crusher, Ball mill, Xray florescence (XRF) Machine, X-ray diffractometer (XRD) Machine, Petrological microscope and Scanning electron microscope (SEM). Samples of the iron ore were collected from 3 points on the deposit located at Obajana (oyo) village located, in Lokoja Local Government Area of Kogi State. Grab method of sampling was used in assembling the samples. 35kg of the samples were collected at interval of 180m apart and 4m depth, the lump sizes of the ore samples were crushed and ball milled.

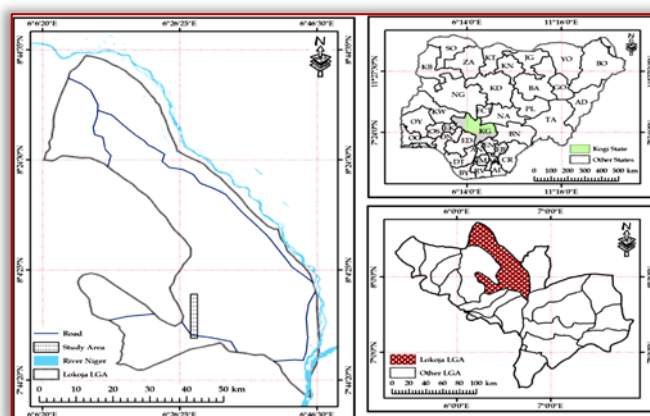


Figure 1: Location map of the study area inset on Lokoja map, north central Nigeria (Olasunkanmi N.K. *et al.*, 2017)

— Characterization and beneficiation techniques

The representative sample was taken and analysed using X ray Florescence (XRF) machine to determine the elemental composition of the ore. The mineralogy of the ore was determined using X-ray diffraction (XRD) machine, the thin section of minerals and rocks were examined with the mineral fragment using petrological microscope and the microscopic features of the ore using scanning electron microscope. 200g of the iron ore was reduced to the liberation size of the ore (-355+250µm) using ball milling machine before separation. Low intensity magnetic separator was used to separate the ore into concentrate and tailing. Both the concentrate and tailing were weighed and analyzed using XRF machine.

as minor constituents. Figure 2 shows the XRF pattern of the ore.

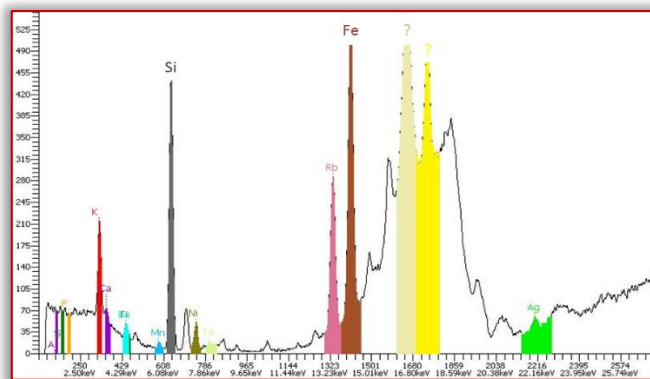


Figure 2: XRF pattern of the obajana iron ore

Table 2: Chemical analysis of the elemental composition Obajana iron ore

| Element number | Element symbol | Element name | Atomic conc. | Weight conc. |
|----------------|----------------|--------------|--------------|--------------|
| 14 | Si | Silicon | 25.56 | 20.84 |
| 13 | Al | Aluminium | 3.54 | 5.97 |
| 19 | K | Potassium | 15.91 | 18.80 |
| 26 | Fe | Iron | 39.24 | 33.30 |
| 39 | Y | Yttrium | 1.35 | 3.64 |
| 41 | Nb | Niobium | 1.29 | 3.61 |
| 47 | Ag | Silver | 1.09 | 3.56 |
| 20 | Ca | Calcium | 2.48 | 3.00 |
| 17 | Cl | Chlorine | 1.36 | 1.46 |
| 22 | Ti | Titanium | 1.00 | 1.44 |
| 6 | C | Carbon | 3.19 | 1.16 |
| 16 | S | Sulphur | 1.11 | 1.07 |
| 11 | Na | Sodium | 1.48 | 1.03 |
| 12 | Mg | Magnesium | 1.02 | 0.75 |
| 15 | P | Phosphorus | 0.38 | 0.36 |

Table 3: Chemical analysis of the oxide composition Obajana iron ore

| Chemical Compound | Assay (%) |
|--------------------------------|-----------|
| SiO ₂ | 24.1 |
| Al ₂ O ₃ | 1.45 |
| K ₂ O | 11.43 |
| CaO | 7.2 |
| TiO ₂ | 4.61 |
| V ₂ O ₅ | 0.08 |
| MgO | 0.24 |
| Fe ₂ O ₃ | 47.82 |
| CuO | 0.067 |
| PbO | 0.23 |
| BaO | 0.10 |
| P ₂ O ₅ | 2.744 |
| Na ₂ O | 0.049 |

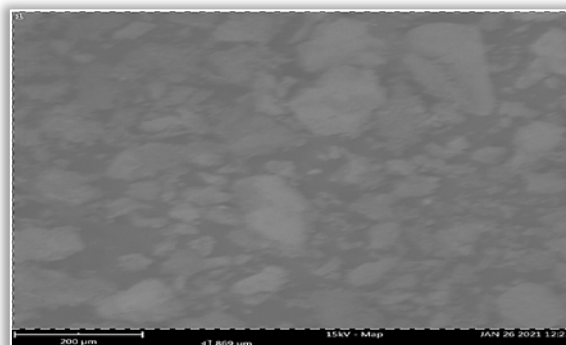


Figure 3: SEM micrograph of Head Sample

Table 1: The Nigerian iron ore deposits and their proven reserves (in million tonnes)

| S/NO | State | Location | Iron content | Proven reserves |
|------|----------|------------------|---------------------|---------------------|
| 1 | Kogi | Bassa-Nge | 43-49% | 400 million tonnes |
| 2 | | Agbado Okadu | 38-48% | 60 million tonnes |
| 3 | | Ajabanoko | 40% | 60 million tonnes |
| 4 | | Jatti | 40% | - |
| 5 | | Koton Karfe | 43-53% | 428 million tonnes |
| 6 | | Itakpe | 36-38% | 200 million tonnes |
| 7 | | Chokochoko | 30-40% | 14 million tonnes |
| 8 | | Akoina | 41-47% | - |
| 9 | | Tajimi | 39-58% | 200 million tonnes |
| 10 | | Ero | Under investigation | - |
| 11 | | Ebiya | Under investigation | - |
| 12 | | Obanaja | Under investigation | - |
| 13 | | Agbaja | 43-49% | 2 billion tonnes |
| 14 | | Kakun (Kabba) | 38-42% | - |
| 15 | | Ubo-Toso | Under investigation | - |
| 16 | Kaduna | Kagara (Kubacha) | 58-63% | - |
| 17 | | Birni Gwari | 30-35% | - |
| 18 | Ondo | Akunu (Ikare) | Under investigation | - |
| 19 | Bauchi | Reshi | 10-19% | - |
| 20 | | Ayiwawa | 6-23% | - |
| 21 | | Gamawa | 40-45% | - |
| 22 | Plateau | Veketuwo | 40-50% | - |
| 23 | Nasarawa | Toto Muro | 25-38% | 3.8 million tonnes |
| 24 | Kebbi | Dakingari | 37% | - |
| 25 | Anambra | Nsude Hill | 43-50% | 40.6 million tonnes |

Source: (Uwadiale, 1989; Thomas, 2002)

RESULTS AND DISCUSSION

Table 2 present the result of the chemical analysis of Obajana iron ore using XRF in weight percentages. The ore contains 39.24 % Fe and 25.56 % Si as major constituents; with 15.91 % K, 3.5 % Al, and P is the least with 0.38% while Table 3 shows the chemical analysis of the oxide composition Obajana iron ore.

The result shows that the ore contains 47.82% Fe₂O₃ and 24.1% SiO₂ as major constituents, with 11.43%K₂O, 0.24%MgO, 4.61TiO₂, 2.744P₂O₅, 0.23%PbO and 1.45%Al₂O₃

Table 4 presents the mineralogical composition of the ore sample, it could be observed from table 4 that the ore contained quartz (SiO₂), hematite (Fe₂O₃), and biotite (K(Mg,Fe)₃AlSi₃O₁₀(OH)₂) as the major mineral phases. From the SEM examination (figures 3), it is observed that the minerals are separated by grain boundaries, no interlocking of minerals and the mineral particles vary in sizes.

Table 4: XRD Analysis Result of the Composite Sample

| Mineral Name | Chemical Name | Chemical Formula |
|--------------|--|---|
| Quartz | Silicate | SiO ₂ |
| Hematite | Iron Oxide | Fe ₂ O ₃ |
| Biotite | Potassium Iron Magnesium Aluminum Silicate Hydroxide | K(Mg,Fe) ₃ AlSi ₃ O ₁₀ (OH) ₂ |

The iron minerals have relatively smaller grains and smooth boundaries that created segregations between the iron and other minerals. Petrographic Microscopy of Obajana Iron Ore in

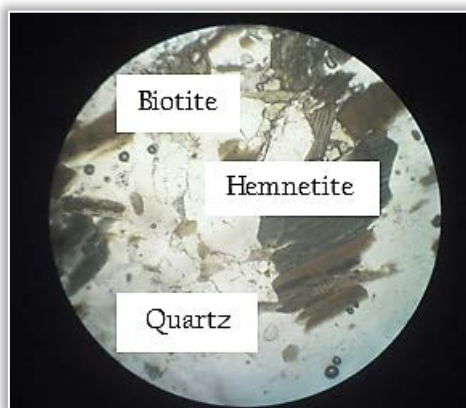


Figure 4: Petrographic Microscopy of Obajana Iron Ore

Table 5: Composition of the concentrate and the tailing after magnetic concentration

| Compounds | Concentrates | Tailings |
|--------------------------------|--------------|----------|
| SiO ₂ | 15.90 | 32.83 |
| Al ₂ O ₃ | 0.43 | 7.27 |
| CaO | 5.11 | 5.42 |
| TiO ₂ | 3.31 | 15.27 |
| V ₂ O ₅ | 0.17 | 0.14 |
| K ₂ O | 7.21 | 0.061 |
| MgO | 0.39 | 0.11 |
| Fe ₂ O ₃ | 56.32 | 43.09 |
| BaO | 0.23 | < LOD |
| P ₂ O ₅ | 1.15 | 0.13 |
| MgO | < LOD | 3.0 |

Figure 4 shows A whitish portion the quartz minerals, brown portion which is the area partially replaced by hematite and the dark portion is the biotite. This phenomenon enhances easy liberation of valuable minerals from the gangues. 200g of the iron ore vs. reduced to the liberation size of the ore (-355+250µm) using ball milling machine before separation. Low intensity magnetic separator was used to separate the ore into concentrate and tailing. Both the concentrate and tailing were weighed and

analyzed using XRF machine. Table 5 shows Composition of the concentrate and the tailing after magnetic concentration. The chemical analysis shows that the concentrate produced contained 56.32%Fe and 15.9% SiO₂, while the tailing gave 43.09% Fe₂O₃ and 32.83% SiO₂.

CONCLUSIONS

The following conclusions were drawn:

- ≡ The result shows that the ore contains 47.82% Fe₂O₃ and 24.1% SiO₂ as major constituents, with 11.43%K₂O, 0.24%MgO, 4.61TiO₂, 2.744P₂O₅, 0.23%PbO and 1.45%Al₂O₃ as minor constituents and thus can be regarded as medium grade iron ore.
- ≡ The mineralogical analysis of the ore revealed that the iron bearing minerals are mainly Biotite, Hematite and Magnetite.
- ≡ The SEM analysis results revealed that the iron bearing minerals are separated from other minerals contained in the ore by smooth grain boundaries.
- ≡ From the results gotten, Obajana iron ore is a deposit that can be explored and exploited for usage in iron and steel production.

Acknowledgment

The authors are grateful for the financial support provided by Tertiary Education Trust Fund (TETFund) Nigeria through Institution Based Research sponsorship to carry out this research. We would like to express our appreciation to the management of Kogi State Polytechnic Lokoja for this opportunity.

References

- [1] Agava, A.A., (2006): Beneficiation of Agbado-Okudu iron ore deposit, Department of Metallurgical Engineering, A.B.U. Zaria, unpublished.
- [2] Agava, A. A., Murina, R. A., Abdurrahman A. S., Egbe, E. A. P. and Thomas D. G. (2016)
- [3] Determination of Chemical, Mineralogical Composition and Liberation Size of Ochokochoko Iron Ore, Kogi State, Nigeria. Nigerian Journal of Engineering, 23, pp 77-86
- [4] Agbu, O. (2007). The iron and steel industry and industrialization. Exploring Nigeria's cooperation with Japan. Report Institute of developing economics, Japan External Trade Organization
- [5] Biswas A.K.,(2005). Principles of Blast Furnace Iron Making, SBA Publications, Calcutta, India, pp200.
- [6] Danmola, R. and Abba, M.W (2013). Solid Mineral Resources: Alternative Source of Revenue for the Nigerian Economy. Journal of Emerging Trends in Economics and Management Sciences (JETEMS), 4, PP.487-492
- [7] Jens Gutzmer and Nicolas J. Beukes. "Iron and Manganese Ore Deposit: Mineralogy, Geochemistry and Economic Geology." Geology-Vol. IV www.eolss.net/sample-chapters/c01/e6-15-06-03.pdf
- [8] Olankanmi, N.K., Olufemi S.B., Adebayo.A. (2017). Exploration for Iron Ore in Agbado-Okudu, Kogi State, Nigeria. Arabian Journal of Geosciences,10, pp.54
- [9] Oloche, B. Yaro, S. A. and Thomas, D. G. (2001): The chemical and mineralogical characteristics of Muro iron ore deposit. Journal of Engineering Technology and Industrial Application, 1, pp. 71-72

- [10] Oyeyinka, A., (1997). Chemical Compositions of some major Nigerian Iron Ore Deposits, Journal of the Raw Material Research Development Council, 2, pp. 23-28.
- [11] Salawu, A. O. Characterization of Gujeni iron ore deposit, Kaduna state, Nigeria. Department of Metallurgical and Materials Engineering, Ahmadu Bello University, Zaria. M.Sc. Thesis. Unpublished. 2015.
- [12] Thomas, D. G. and Yaro, S. A. (2009). Chemical and Mineralogical Characteristics of Koton-Karfe Iron Ore, Journal of Engineering and Technology Bayero University, Kano, 4, pp 65-71.
- [13] Uwadiae, G.O. (1989). Up-grading of Nigerian Iron Ore, Journal of Mineral and Metallurgical Processing, 2, pp34-37.



ISSN: 2067-3809

copyright © University POLITEHNICA Timisoara,
Faculty of Engineering Hunedoara,
5, Revolutiei, 331128, Hunedoara, ROMANIA
<http://acta.fih.upt.ro>

¹Mustefa JIBRIL, ¹Messayy TADESE, ¹Reta DEGEFA

DESIGN & CONTROL OF A GANTRY CRANE SYSTEM WITH LIMITED PAYLOAD ANGLE USING ROBUST & STATE FEEDBACK CONTROLLERS

¹ School of Electrical & Computer Engineering, Dire Dawa Institute of Technology, Dire Dawa, ETHIOPIA

Abstract: In this paper, the performance improvement of a payload angle deflection of a gantry crane has been studied and simulated using Matlab/Simulink toolbox successfully. H 2 optimal and observer based controllers has been used to minimize the payload angular deflection by controlling the trolley position. The gantry crane has been compared with the proposed controllers to track the reference trolley position using step and sine wave signals and a promising results have been achieved.

Keywords: Gantry crane, Trolley, Payload, H 2 optimal, Observer based controller

INTRODUCTION

A gantry crane is one of the many types of crane which is built at the top of a gantry, which is a structure used to support an object to be lifted. They are huge machines that capable of lifting heavy loads like lifting automobile engines out of vehicles. The terms gantry crane and overhead crane (or bridge crane) are often used interchangeably, as both types of crane straddle their workload. The distinction mass often drawn between the two is that with gantry cranes, the entire composition (including gantry) is usually wheeled (often on rails). By contrast, the promoting makeups of an overhead crane is fixed in location, often in the example of the walls or ceiling of a building, to which is attached a movable hoist running overhead along a bannister or ray (which may itself move). Further confusing the issue is that gantry cranes may also incorporate a movable beam-mounted hoist in addition to the entire structure entity wheeled, and some overhead cranes are suspended from a freestanding gantry. Full gantry cranes (where the load remnants beneath the gantry structure, supported from a beam) are well suited to lifting massive thing such as ships' engines, as the entire disposition can resist the torque created by the load, and counterweights are generally not required. These are often found in shipyards where they are used to move large boat part together for construction.

MATHEMATICAL MODELING OF GANTRY CRANE

The gantry crane system design is shown in Figure 1 below.

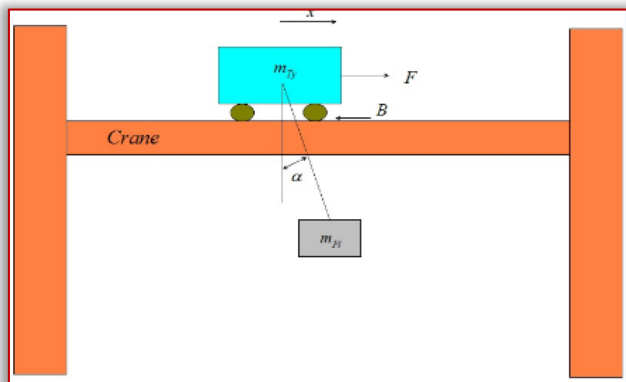


Figure 1. Gantry crane system

To solve the mathematical model of the system, Lagrange's equations are used which is given as

$$\frac{d}{dt} \left(\frac{\partial L}{\partial \dot{\theta}} - \frac{\partial L}{\partial \theta} \right) = Q \quad (1)$$

$$L = T - V \quad (2)$$

where: θ System variable, L Lagrange equation, Q Sum of forces or moments, T Kinetic energies, V Potential energies
The kinetic energy of the trolley given as:

$$T_1 = \frac{1}{2} m_T \dot{x}^2 \quad (3)$$

The kinetic energy of the payload is given as

$$T_2 = \frac{1}{2} m_P v^2 \quad (4)$$

And the velocity is found by taking the first derivative of the position:

$$v^2 = \dot{x}^2 + 2l\dot{\alpha}\dot{x}\sin\alpha + l^2\dot{\alpha}^2 \quad (5)$$

$$T_2 = \frac{1}{2} m_P (\dot{x}^2 + 2l\dot{\alpha}\dot{x}\sin\alpha + l^2\dot{\alpha}^2)$$

The Lagrangian for this system can be written as:

$$L = \frac{1}{2} m_P (\dot{x}^2 + 2l\dot{\alpha}\dot{x}\sin\alpha + l^2\dot{\alpha}^2) + \frac{1}{2} m_T \dot{x}^2 + m_P g l \cos\alpha \quad (6)$$

And the equation of motion follows from:

$$\frac{d}{dt} \left(\frac{\partial L}{\partial \dot{x}} - \frac{\partial L}{\partial x} \right) = F - B\dot{x}$$

Where B is the damping friction coefficient

$$\frac{d}{dt} \left(\frac{\partial L}{\partial \dot{\alpha}} - \frac{\partial L}{\partial \alpha} \right) = 0$$

Resulting in:

$$(m_T + m_P) \ddot{x} + B\dot{x} + m_P l \ddot{\alpha} \cos\alpha - m_P l \dot{\alpha}^2 \sin\alpha = F \quad (7)$$

$$m_P l^2 \ddot{\alpha} + m_P l \ddot{x} \cos\alpha + m_P l g \sin\alpha = 0 \quad (8)$$

For small angle approximation: $\alpha < 1^\circ$ the sine and cosine can be linearized as

$$\alpha \approx 0$$

$$\sin\alpha \approx \alpha$$

$$\cos\alpha \approx 1$$

$$\dot{\alpha}^2 \approx 0$$

Hence, the derived Equation (7) and (8) of the non-linear model can be approximately linearized as:

$$(m_{Ty} + m_{pl})\ddot{x} + B\dot{x} + m_{pl}l\ddot{\alpha} = F \quad (9)$$

$$m_{pl}l^2\ddot{\alpha} + m_{pl}l\ddot{x} + m_{pl}lg\alpha = 0 \quad (10)$$

Rearranging Equation (9) and (10)

$$\ddot{x} = -\frac{B}{m_{pl}}\dot{x} + \frac{m_{Ty}g}{m_{pl}}\alpha + \frac{F}{m_{pl}} \quad (11)$$

$$\ddot{\alpha} = \frac{B}{m_{pl}l}\dot{x} - \frac{(m_{pl} + m_{Ty})}{m_{pl}l}g\alpha + \frac{F}{m_{pl}l} \quad (12)$$

Let

$$x_1 = x, x_2 = \dot{x}, x_3 = \alpha \text{ and } x_4 = \dot{\alpha}$$

The state space equation becomes

$$\begin{bmatrix} \dot{x}_1 \\ \dot{x}_2 \\ \dot{x}_3 \\ \dot{x}_4 \end{bmatrix} = \begin{bmatrix} 0 & 1 & 0 & 0 \\ 0 & -\frac{B}{m_{pl}} & \frac{m_{Ty}g}{m_{pl}} & 0 \\ 0 & 0 & 0 & 1 \\ 0 & \frac{B}{m_{pl}l} & -\frac{(m_{pl} + m_{Ty})}{m_{pl}l}g & 0 \end{bmatrix} \begin{bmatrix} x_1 \\ x_2 \\ x_3 \\ x_4 \end{bmatrix} + \begin{bmatrix} 0 \\ \frac{1}{m_{pl}} \\ 0 \\ -\frac{1}{m_{pl}l} \end{bmatrix} F$$

$$y = \begin{bmatrix} 1 & 0 & 0 & 0 \\ 0 & 0 & 1 & 0 \end{bmatrix} \begin{bmatrix} x_1 \\ x_2 \\ x_3 \\ x_4 \end{bmatrix}$$

The system parameters are shown in Table 1 below.

Table 1. System parameters

| No | Parameters | Symbols | Values |
|----|-----------------------------|----------|---------------------|
| 1 | Trolley mass | m_{Ty} | 80 Kg |
| 2 | Payload mass | m_{pl} | 32 Kg |
| 3 | Surface friction | B | 25 N-m/s |
| | Cable length | l | 3.5 m |
| | Acceleration due to gravity | g | 10 m/s ² |

Then the state space equation numerically becomes

$$\begin{bmatrix} \dot{x}_1 \\ \dot{x}_2 \\ \dot{x}_3 \\ \dot{x}_4 \end{bmatrix} = \begin{bmatrix} 0 & 1 & 0 & 0 \\ 0 & -0.22 & 25 & 0 \\ 0 & 0 & 0 & 1 \\ 0 & 0.22 & -10 & 0 \end{bmatrix} \begin{bmatrix} x_1 \\ x_2 \\ x_3 \\ x_4 \end{bmatrix} + \begin{bmatrix} 0 \\ 0.03 \\ 0 \\ -0.009 \end{bmatrix} F$$

$$y = \begin{bmatrix} 1 & 0 & 0 & 0 \\ 0 & 0 & 1 & 0 \end{bmatrix} \begin{bmatrix} x_1 \\ x_2 \\ x_3 \\ x_4 \end{bmatrix}$$

THE PROPOSED CONTROLLERS DESIGN

— Observer-Based Controller Design

The deal with the general argument where only a subset of the states, or linear combinations of them, are obtained from measurements and are available to our controller. Such a handbooks lines is referred to as the output feedback problem.

The output is of the form

$$y = Cx + Du \quad (13)$$

The block diagram of the gantry crane system with the observer-based controller is shown in Figure 2 bellow.

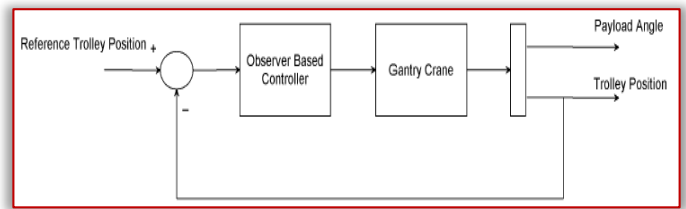


Figure 2. Block diagram of the gantry crane system with the observer-based controller

The observer based controller $G_c(s)$ can be further derived in the following form:

$$G_c(s) = I - K(sI - A + BK + HC)^{-1}B \quad (14)$$

With its state space realization

$$G_c(s) = \begin{bmatrix} A - BK - HC & B \\ -K & I \end{bmatrix} \quad (15)$$

The controller $G_c(s)$ in Equation (15) is called the observer-based controller, since the structural reference of the observer is reflected within the controller.

Where the state space model of the plant, G , the state feedback gain vector K , and the observer gain vector H are then returned, respectively.

We select the weighting matrix Q and R as

$$Q = \begin{bmatrix} 3 & 0 & 0 & 0 \\ 0 & 3 & 0 & 0 \\ 0 & 0 & 3 & 0 \\ 0 & 0 & 0 & 3 \end{bmatrix} \text{ and } R = 5$$

And we select the observer gain vector as

$$H = \begin{bmatrix} 1.5 & -0.3 \\ 0.4 & 1.2 \\ 0.7 & 0 \\ 0.9 & -0.5 \end{bmatrix}$$

And we obtain the state feedback gain vector K as

$$K = [0.7746 \quad 86.0062 \quad 70.8594 \quad 212.6783]$$

The observer-based controller state space representation become

$$\dot{x}_o = \begin{bmatrix} -1.5 & 1 & 0 & 0 \\ -0.42 & -2.8 & 22.87 & -6.38 \\ -0.7 & 0 & 0 & 1 \\ -0.9 & 1 & -9.362 & 1.9 \end{bmatrix} x_o + \begin{bmatrix} 1.5 \\ 0.4 \\ 0.7 \\ 0.9 \end{bmatrix} u_o$$

$$y_o = (0.77 \quad 86 \quad 71 \quad 212.7)x_o$$

— Augmentations of the Model with Weighting Functions

In this section, we will center on the weighted control system shown in Figure 3, where $W1(s)$, $W2(s)$, and $W3(s)$ are weighting functions or weighting filters. We assume that $G(s)$ (gantry crane system), $W1(s)$, and $W3(s)$ $G(s)$ are all proper; i.e., they are bounded when $s \rightarrow \infty$. It can be seen that the weighting function $W3(s)$ is not required to be proper. In the two-port system, the output vector $y1 = [yla, ylb, ylc]$ T is not used directly to construct the vector $u2$. Understand that $y1$ is actually for the control outline attainment measurement. So, it is not strange to include the filtered "input signal" $u(t)$ in the "output signal" $y1$ because one may indispensability to quantities the control energy to assess

whether the designed controller is perfect or not. Clearly, Figure 2 represents a more general diagram of optimal and robust control systems. We can design an optimal H 2 controller by using the thought of the augmented system model.

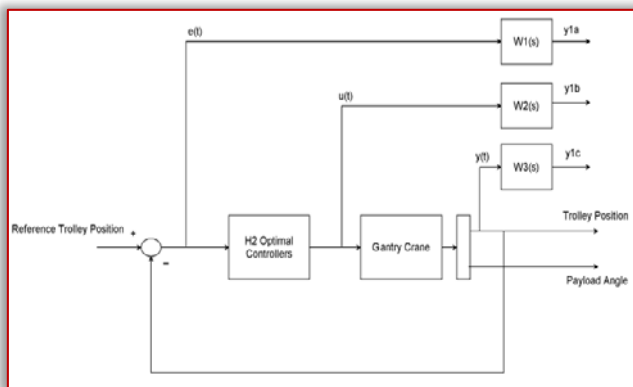


Figure 3. Weighted control structure of the gantry crane system with the H 2 optimal controller
The weighting function $W_1(s)$, $W_2(s)$, and $W_3(s)$ are chosen as

$$W_1(s) = \frac{s+1}{s^2+6s+12} \quad W_2(s) = \frac{s+4}{s^2+16s+42}$$

$$W_3(s) = \frac{s+8}{s^2+21s+55}$$

The H 2 optimal controller state space representation become

$$\begin{bmatrix} \dot{z}_1 \\ \dot{z}_2 \\ \dot{z}_3 \\ \dot{z}_4 \end{bmatrix} = \begin{bmatrix} 0.43 & 1.27 & 2.05 & 23 \\ 20 & 32 & 45 & 10 \\ 0.9 & -0.35 & 12 & 1 \\ 34 & 22 & -0.45 & 0 \end{bmatrix} \begin{bmatrix} z_1 \\ z_2 \\ z_3 \\ z_4 \end{bmatrix} + \begin{bmatrix} 20 \\ 13 \\ 0.54 \\ -5 \end{bmatrix} u$$

$$w = [27.98 \quad 0 \quad 0.936 \quad 0] \begin{bmatrix} \dot{z}_1 \\ \dot{z}_2 \\ \dot{z}_3 \\ \dot{z}_4 \end{bmatrix}$$

RESULT AND DISCUSSION

— Comparison of the Gantry Crane System using Augmentation Based H 2 Optimal & Observer Based Controllers for a Step Input Trolley Position Signal

The Simulink model of the gantry crane system using augmentation based H 2 optimal & observer based controllers using step input desired trolley position signal is shown in Figure 4 below.

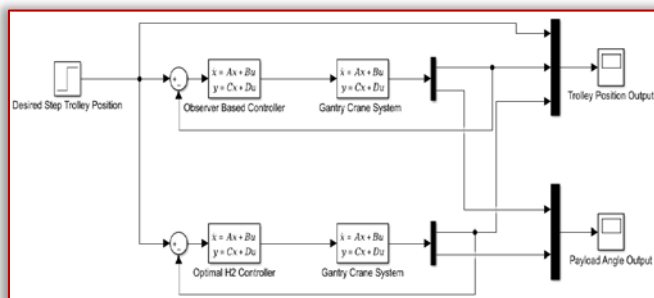


Figure 4. Simulink model of the gantry crane system using augmentation based H 2 optimal & observer based controllers using step input desired trolley position signal

The simulation result of the trolley and payload comparison for the proposed controllers and the input force to the gantry crane system are shown in Figure 5, Figure 6, Figure 7 and Figure 8 respectively.

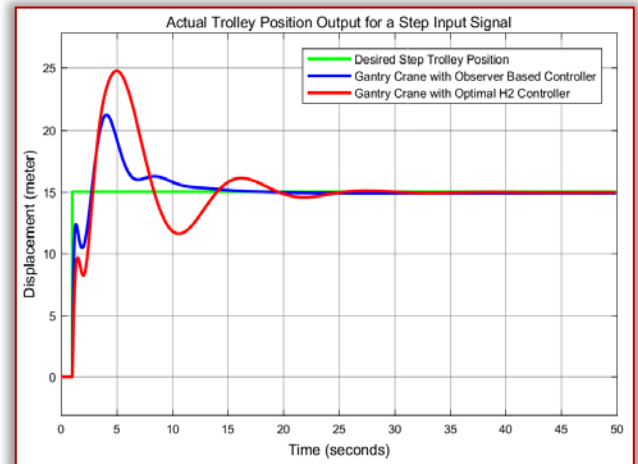


Figure 5. Step response of the trolley position comparison

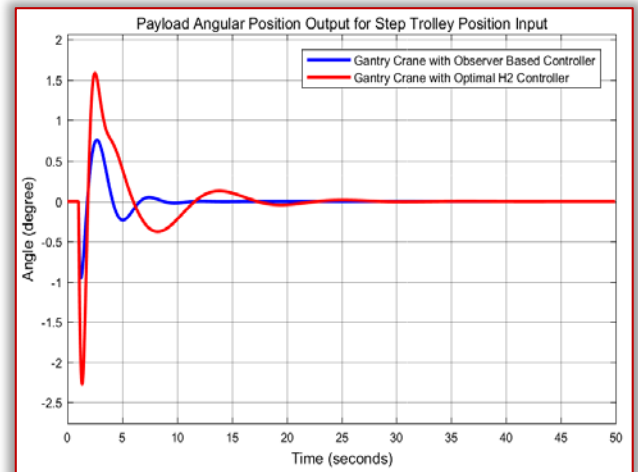


Figure 6. Step response of the trolley position comparison

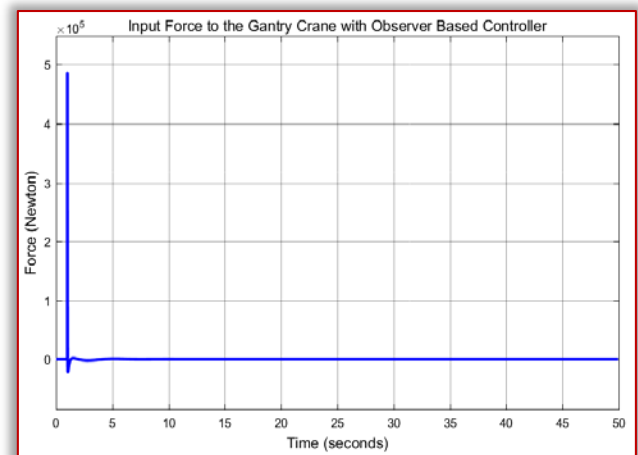


Figure 7. Input Force to the system with observer based controller

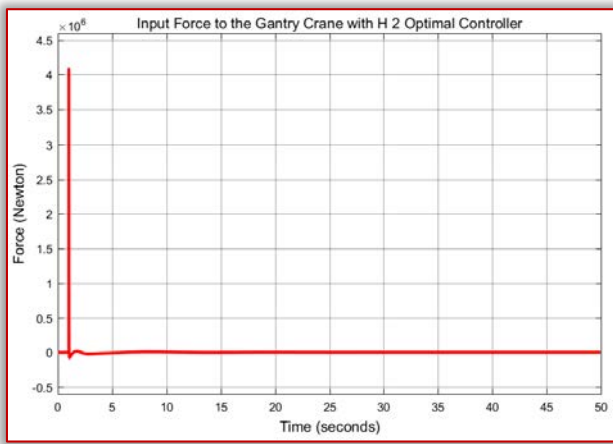


Figure 8. Input Force to the system with H 2 optimal controller

The input force of the gantry crane system with the observer based controller shows improvement in reducing the force amplitude. The data of the rise time, percentage overshoot and settling time of the trolley is shown in Table 2.

Table 2. Trolley step response data

| No | Performance Data | Observer based controller | H 2 optimal controller |
|----|------------------|---------------------------|------------------------|
| 1 | Rise time | 1 sec | 1.1 sec |
| 2 | Per. overshoot | 26.6 % | 46.6 % |
| 3 | Settling time | 15 sec | 30 sec |

As Table 2 shows that the gantry crane system with the observer based controller improves the performance of the Trolley position by minimizing the percentage overshoot and settling time.

The data of the rise time, percentage overshoot and settling time of the payload is shown in Table 3.

Table 3. Payload step response data

| No | Performance Data | Observer based controller | H 2 optimal controller |
|----|------------------|---------------------------|------------------------|
| 1 | Rise time | 1 sec | 1 sec |
| 2 | Per. overshoot | 18.6 % | 35.6 % |
| 3 | Settling time | 10 sec | 28 sec |

As Table 3 shows that the gantry crane system with the observer based controller improves the performance of the payload angle by minimizing the percentage overshoot and settling time.

— Comparison of the Gantry Crane System using Augmentation Based H 2 Optimal & Observer Based Controllers for a Sine Wave Input Trolley Position Signal

The Simulink model of the gantry crane system using augmentation based H 2 optimal & observer based controllers using sine wave input desired trolley position signal is shown in Figure 9 below.

The simulation result of the trolley and payload comparison for the proposed controllers and the input force to the gantry crane system are shown in Figure 10, Figure 11, Figure 12 and Figure 13 respectively.

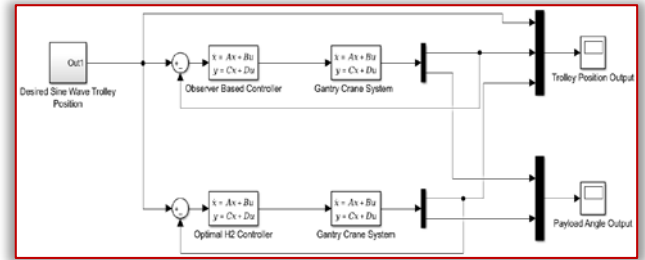


Figure 9 Simulink model of the gantry crane system using augmentation based H 2 optimal & observer based controllers using sine wave input desired trolley position signal

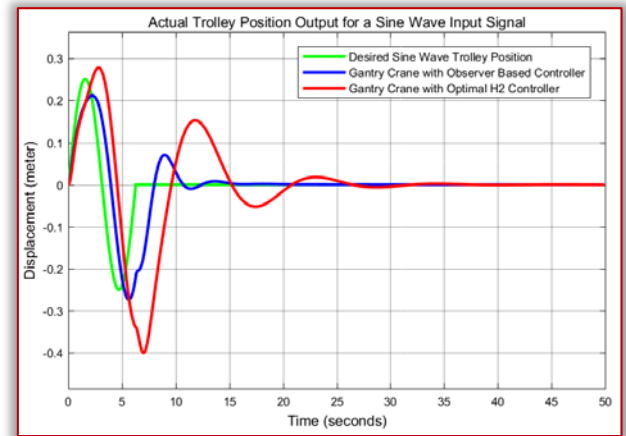


Figure 10. Sine wave response of the trolley position comparison

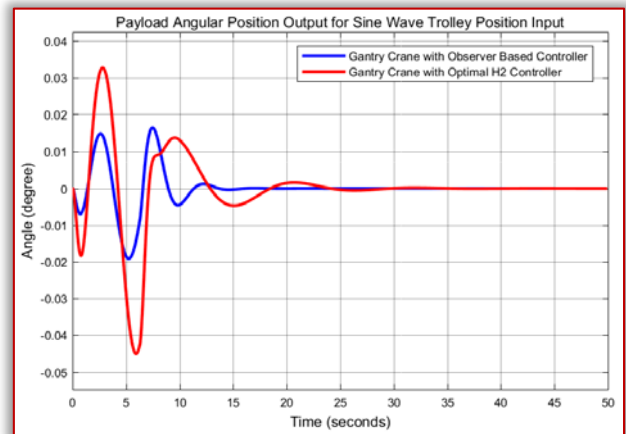


Figure 11. Sine wave response of the trolley position comparison

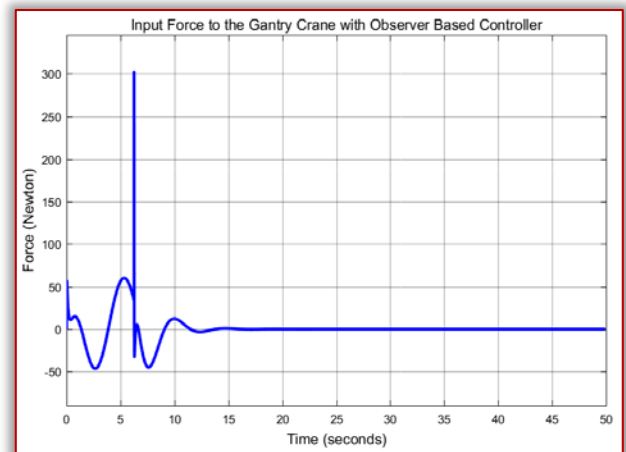


Figure 12. Input Force to the system with observer based controller

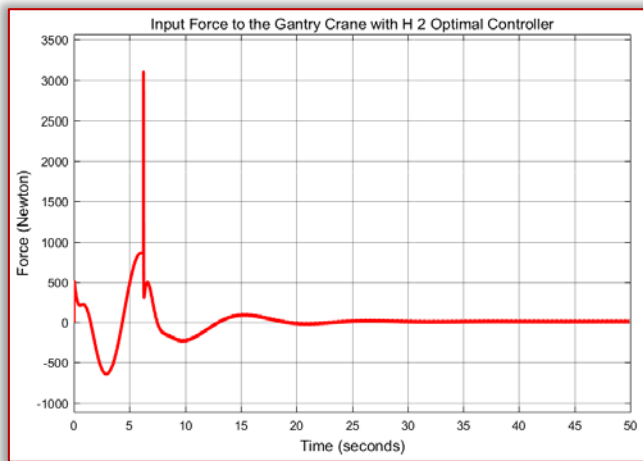


Figure 13. Input Force to the system with H 2 optimal controller

The input force of the gantry crane system with the observer based controller shows improvement in reducing the force amplitude.

Figure 10 and Figure 11 shows that the gantry crane system with the observer based controller improves the performance of the trolley position and payload angle by minimizing the percentage overshoot and settling time.

CONCLUSION

In this paper, a minimum payload angular deflection has been achieved for a gantry crane using a feedback controller. This achievement has been done by controlling the trolley position instead. Comparison of the system with the proposed controllers shows that the system with observer based controller improves the payload deflection and vibration better than the proposed H 2 optimal controller with a minimum force input to the system.

Reference

- [1] Nguyen H. H et al. "Nonlinear Control of a Gantry Crane System with Limited Payload Angle" International Journal of Electrical and Electronics Engineering, Vol. 5, Issue 8, 2018.
- [2] Ayodeji O. et al. "Vision Based Control of Gantry Crane System" Eskisehir Technical University Journal of Science and Technology A-Applied Sciences and Engineering, Vol. 19, Issue 4, pp. 1023-1032, 2018.
- [3] Sturzer D. et al. "A Closed Loop Stability Analysis of a Gantry Crane with Heavy Chain and Payload" International Journal of Control, 7179: pp. 1-13, 2017.
- [4] Ospina Henao PA. et al. "Dynamic Analysis and Control PID Path of a Model Type Gantry Crane" J Phys Conf Series, 850:12004, 2017.
- [5] Ashwani K. et al. "Automated Control and Optimization of Overhead Cranes" International Journal of Manufacturing, Vol. 7, Issue 3, pp. 41-68, 2017.
- [6] Da-peng Z. et al. "Variational Analysis of Mid Span Deflection of Gantry Cranes" Journal of Central South University, Vol. 24, Issue 1, pp. 2705-2716, 2017.
- [7] Tuan LA. "Design of Sliding Mode Controller for the 2D Motion of an Overhead Crane with Varying Cable Length" Journal of Automotive Control Engineering, Vol. 4, Issue 8, 2016.



ISSN: 2067-3809

copyright © University POLITEHNICA Timisoara,
Faculty of Engineering Hunedoara,
5, Revolutiei, 331128, Hunedoara, ROMANIA
<http://acta.fih.upt.ro>

Fascicule 4

[October – December]

t o m e

XIV

[2021]

ACTA Technica CORVINIENSIS
BULLETIN OF ENGINEERING



ISSN: 2067-3809

copyright © University POLITEHNICA Timisoara,
Faculty of Engineering Hunedoara,
5, Revolutiei, 331128, Hunedoara, ROMANIA
<http://acta.fih.upt.ro>

MANUSCRIPT PREPARATION

– GENERAL GUIDELINES

Manuscripts submitted for consideration to **ACTA TECHNICA CORVINIENSIS – Bulletin of Engineering** must conform to the following requirements that will facilitate preparation of the article for publication. These instructions are written in a form that satisfies all of the formatting requirements for the author manuscript. Please use them as a template in preparing your manuscript. Authors must take special care to follow these instructions concerning margins.

INVITATION

We are looking forward to a fruitful collaboration and we welcome you to publish in our **ACTA TECHNICA CORVINIENSIS – Bulletin of Engineering**. You are invited to contribute review or research papers as well as opinion in the fields of science and technology including engineering. We accept contributions (full papers) in the fields of applied sciences and technology including all branches of engineering and management.

ACTA TECHNICA CORVINIENSIS – Bulletin of Engineering publishes invited review papers covering the full spectrum of engineering and management. The reviews, both experimental and theoretical, provide general background information as well as a critical assessment on topics in a state of flux. We are primarily interested in those contributions which bring new insights, and papers will be selected on the basis of the importance of the new knowledge they provide.

Submission of a paper implies that the work described has not been published previously (except in the form of an abstract or as part of a published lecture or academic thesis) that it is not under consideration for publication elsewhere. It is not accepted to submit materials which in any way violate copyrights of third persons or law rights. An author is fully responsible ethically and legally for breaking given conditions or misleading the Editor or the Publisher.

ACTA TECHNICA CORVINIENSIS – Bulletin of Engineering is an international and interdisciplinary journal which reports on scientific and technical contributions. Every year, in four online issues (**fascicules 1–4**), **ACTA TECHNICA CORVINIENSIS – Bulletin of Engineering** [e-ISSN: 2067-3809] publishes a series of reviews covering the most exciting and developing areas of engineering. Each issue contains papers reviewed by international researchers who are experts in their fields. The result is a journal that gives the scientists and engineers the opportunity to keep informed of all the current developments in their own, and related, areas of research, ensuring the new ideas across an increasingly the interdisciplinary field. Topical reviews in materials science and engineering, each including:

- surveys of work accomplished to date
- current trends in research and applications
- future prospects.

As an open-access journal **ACTA TECHNICA CORVINIENSIS – Bulletin of Engineering** will serve the

whole engineering research community, offering a stimulating combination of the following:

- Research Papers – concise, high impact original research articles,
- Scientific Papers – concise, high impact original theoretical articles,
- Perspectives – commissioned commentaries highlighting the impact and wider implications of research appearing in the journal.

ACTA TECHNICA CORVINIENSIS – Bulletin of Engineering encourages the submission of comments on papers published particularly in our journal. The journal publishes articles focused on topics of current interest within the scope of the journal and coordinated by invited guest editors. Interested authors are invited to contact one of the Editors for further details.

BASIC MANUSCRIPT REQUIREMENTS

The basic instructions and manuscript requirements are simple:

- Manuscript shall be formatted for an A4 size page.
- The all margins of page (top, bottom, left, and right) shall be 20 mm.
- The text shall have both the left and right margins justified.
- Single-spaced text, tables, and references, written with 11 or 12-point Georgia or Times New Roman typeface.
- No Line numbering on any pages and no page numbers.
- Manuscript length must not exceed 15 pages (including text and references).
- Number of the figures and tables combined must not exceed 20.
- Manuscripts that exceed these guidelines will be subject to reductions in length.

The original of the technical paper will be sent through e-mail as attached document (*.doc, Windows 95 or higher). Manuscripts should be submitted to e-mail: redactie@fih.upt.ro, with mention “for **ACTA TECHNICA CORVINIENSIS**”.

STRUCTURE

The manuscript should be organized in the following order: Title of the paper, Authors' names and affiliation, Abstract, Key Words, Introduction, Body of the paper (in sequential headings), Discussion & Results, Conclusion or Concluding Remarks, Acknowledgements (where applicable), References, and Appendices (where applicable).

THE TITLE

The title is centered on the page and is CAPITALIZED AND SET IN BOLDFACE (font size 14 pt). It should adequately describe the content of the paper. An abbreviated title of less than 60 characters (including spaces) should also be suggested. Maximum length of title: 20 words.

AUTHOR'S NAME AND AFFILIATION

The author's name(s) follows the title and is also centered on the page (font size 11 pt). A blank line is required between the title and the author's name(s). Last names should be spelled out in full and succeeded by author's initials. The author's affiliation (in font size 11 pt) is provided below. Phone and fax numbers do not appear.

ABSTRACT

State the paper's purpose, methods or procedures presentation, new results, and conclusions are presented. A nonmathematical abstract, not exceeding 200 words, is required for all papers. It should be an abbreviated, accurate presentation of the contents of the paper. It should contain sufficient information to enable readers to decide whether they should obtain and read the entire paper. Do not cite references in the abstract.

KEY WORDS

The author should provide a list of three to five key words that clearly describe the subject matter of the paper.

TEXT LAYOUT

The manuscript must be typed single spacing. Use extra line spacing between equations, illustrations, figures and tables. The body of the text should be prepared using Georgia or Times New Roman. The font size used for preparation of the manuscript must be 11 or 12 points. The first paragraph following a heading should not be indented. The following paragraphs must be indented 10 mm. Note that there is no line spacing between paragraphs unless a subheading is used. Symbols for physical quantities in the text should be written in italics. Conclude the text with a summary or conclusion section. Spell out all initials, acronyms, or abbreviations (not units of measure) at first use. Put the initials or abbreviation in parentheses after the spelled-out version. The manuscript must be writing in the third person (“the author concludes...”).

FIGURES AND TABLES

Figures (diagrams and photographs) should be numbered consecutively using Arabic numbers. They should be placed in the text soon after the point where they are referenced. Figures should be centered in a column and should have a figure caption placed underneath. Captions should be centered in the column, in the format “Figure 1” and are in upper and lower case letters.

When referring to a figure in the body of the text, the abbreviation “Figure” is used. Illustrations must be submitted in digital format, with a good resolution. Table captions appear centered above the table in upper and lower case letters.

When referring to a table in the text, “Table” with the proper number is used. Captions should be centered in the column,

in the format “Table 1” and are in upper and lower case letters. Tables are numbered consecutively and independently of any figures. All figures and tables must be incorporated into the text.

EQUATIONS & MATHEMATICAL EXPRESSIONS

Place equations on separate lines, centered, and numbered in parentheses at the right margin. Equation numbers should appear in parentheses and be numbered consecutively. All equation numbers must appear on the right-hand side of the equation and should be referred to within the text.

CONCLUSIONS

A conclusion section must be included and should indicate clearly the advantages, limitations and possible applications of the paper. Discuss about future work.

Acknowledgements

An acknowledgement section may be presented after the conclusion, if desired. Individuals or units other than authors who were of direct help in the work could be acknowledged by a brief statement following the text. The acknowledgment should give essential credits, but its length should be kept to a minimum; word count should be <100 words.

References

References should be listed together at the end of the paper in alphabetical order by author's surname. List of references indent 10 mm from the second line of each references. Personal communications and unpublished data are not acceptable references.

— *Journal Papers*: Surname 1, Initials; Surname 2, Initials and Surname 3, Initials: Title, Journal Name, volume (number), pages, year.

— *Books*: Surname 1, Initials and Surname 2, Initials: Title, Edition (if existent), Place of publication, Publisher, year.

Proceedings Papers: Surname 1, Initials; Surname 2, Initials and Surname 3, Initials: Paper title, Proceedings title, pages, year.



ISSN: 2067-3809

copyright © University POLITEHNICA Timisoara,
Faculty of Engineering Hunedoara,
5, Revolutiei, 331128, Hunedoara, ROMANIA
<http://acta.fih.upt.ro>

INDEXES & DATABASES

We are very pleased to inform that our international scientific journal **ACTA TECHNICA CORVINIENSIS – Bulletin of Engineering** completed its 13 years of publication successfully [2008–2020, Tome I–XIII].

In a very short period the **ACTA TECHNICA CORVINIENSIS – Bulletin of Engineering** has acquired global presence and scholars from all over the world have taken it with great enthusiasm.

We are extremely grateful and heartily acknowledge the kind of support and encouragement from all contributors and all collaborators!

ACTA TECHNICA CORVINIENSIS – Bulletin of Engineering is accredited and ranked in the “B+” CATEGORY Journal by CNCIS – The National University Research Council’s Classification of Romanian Journals, position no. 940 (<http://cncis.gov.ro/>).

ACTA TECHNICA CORVINIENSIS – Bulletin of Engineering is a part of the ROAD, the Directory of Open Access scholarly Resources (<http://road.issn.org/>).

ACTA TECHNICA CORVINIENSIS – Bulletin of Engineering is also indexed in the digital libraries of the following world's universities and research centers:

WorldCat – the world's largest library catalog

<https://www.worldcat.org/>

National Library of Australia

<http://trove.nla.gov.au/>

University Library of Regensburg – GIGA German Institute of Global and Area Studies

<http://opac.giga-hamburg.de/ezb/>

Simon Fraser University – Electronic Journals Library

<http://cufts2.lib.sfu.ca/>

University of Wisconsin – Madison Libraries

<http://library.wisc.edu/>

University of Toronto Libraries

<http://search.library.utoronto.ca/>

The University of Queensland

<https://www.library.uq.edu.au/>

The New York Public Library

<http://nypl.bibliocommons.com/>

State Library of New South Wales

<http://library.sl.nsw.gov.au/>

University of Alberta Libraries – University of Alberta

<http://www.library.ualberta.ca/>

The University of Hong Kong Libraries

<http://sunzi.lib.hku.hk/>

The University Library – The University of California

<http://harvest.lib.ucdavis.edu/>

ACTA TECHNICA CORVINIENSIS – Bulletin of Engineering is indexed, abstracted and covered in the world-known bibliographical databases and directories including:

INDEX COPERNICUS – JOURNAL MASTER LIST

<http://journals.indexcopernicus.com/>

GENAMICSJOURNALSEEK Database

<http://journalseek.net/>

DOAJ – Directory of Open Access Journals

<http://www.doaj.org/>

EVISA Database

<http://www.speciation.net/>

CHEMICAL ABSTRACTS SERVICE (CAS)

<http://www.cas.org/>

EBSCO Publishing

<http://www.ebscohost.com/>

GOOGLE SCHOLAR

<http://scholar.google.com>

SCIRUS – Elsevier

<http://www.scirus.com/>

ULRICHWeb – Global serials directory

<http://ulrichweb.serialssolutions.com>

getCITED

<http://www.getcited.org>

BASE – Bielefeld Academic Search Engine

<http://www.base-search.net>

Electronic Journals Library

<http://rzblx1.uni-regensburg.de>

Open J-Gate

<http://www.openj-gate.com>

ProQUEST Research Library

<http://www.proquest.com>

Directory of Research Journals Indexing

<http://www.drji.org/>

Directory Indexing of International Research Journals

<http://www.citefactor.org/>



ACTA TECHNICA CORVINIENSIS – Bulletin of Engineering

ISSN: 2067-3809

copyright © University POLITEHNICA Timisoara,

Faculty of Engineering Hunedoara,

5, Revolutiei, 331128, Hunedoara, ROMANIA

<http://acta.fih.upt.ro>



copyright © University POLITEHNICA Timisoara,
Faculty of Engineering Hunedoara,
5, Revolutiei, 331128, Hunedoara, ROMANIA
<http://acta.fih.upt.ro>